CM Aprvd ISSUED 2009/09/18

911168
Revision 0

ENGINEERING SERVICES FOR THE NEXT GENERATION NUCLEAR PLANT (NGNP) WITH HYDROGEN PRODUCTION

Technical Basis for NGNP Fuel Performance and Quality Requirements

Prepared by General Atomics
For the Battelle Energy Alliance, LLC

Subcontract No. 00075309
Uniform Filing Code UFC:8201.3.1.2

GA Project 30302

GENERAL ATOMICS

Rolls-Royce

URS Washington Division

TOSHIBA Leading Innovation

FE

OKBM

Korea Atomic Energy Research Institute

GENERAL ATOMICS

GA 1485 (REV. 08/06E)

ISSUE/RELEASE SUMMARY

☐ R & D ☐ DV&S ☒ DESIGN ☐ T&E ☐ NA	APPVL LEVEL	DISC	QA LEVEL	SYS	DOC. TYPE	PROJECT	DOCUMENT NO.	REV
	5	N	I	N/A	RGE	30302	911168	0

TITLE:
Technical Basis for NGNP Fuel Performance and Quality Requirements

CM APPROVAL/ DATE	REV	PREPARED BY	APPROVAL(S) ENGINEERING	APPROVAL(S) QA	APPROVAL(S) PROJECT	REVISION DESCRIPTION/ W.O. NO.
7 ISSUED SEP 1 8 2009	0	D. Hanson	W. Scheffel for A. Shenoy	K. Partain	J. Saurwein	Initial Issue A30302.0516

CONTINUE ON GA FORM 1485-1

NEXT INDENTURED DOCUMENT(S)

N/A

COMPUTER PROGRAM PIN(S)

N/A

☐ GA PROPRIETARY INFORMATION

☒ NO GA PROPRIETARY INFORMATION

LIST OF CONTRIBUTORS

Name	Organization
David Hanson	GA
Chuck Charman	C Squared, LLC
Jessie Crozier	GA
Bill McTigue	URS-WD
Paul Reichert	URS-WD

TABLE OF CONTENTS

LIST OF FIGURES

LIST OF TABLES

ACRONYMS AND ABBREVIATIONS

ALARA	as low as reasonably achievable [radiation exposure][1]
AOO	Anticipated Operational Occurrence
BEA	Battelle Energy Alliance
CEDE	committed effective dose equivalent
CFR	Code of Federal Regulations
COT	core outlet temperature
CPA	core performance analysis
D&D	decontamination and decommissioning
DBA	design basis accident
DBE	Design Basis Event
DCF	dose conversion factor
DDN	Design Data Need
DOE	[United States] Department of Energy
EAB	Exclusion Area Boundary
EFPD	effective full-power days
EJ	engineering judgment
EPA	Environmental Protection Agency
EPRI	Electric Power Research Institute
EPZ	Emergency Planning Zone
FAW	Functional Analysis Worksheet
FDDM/F	Fuel Design Data Manual, Issue F [GA Proprietary Information]
FIMA	fissions per initial metal atom
FOAK	first-of-a-kind
FRG	Federal Republic of Germany
FSV	Fort St. Vrain [US prismatic HTGR]
GA	General Atomics

[1] In this report, text in [square brackets] is explanatory; numbers in [square brackets] are tentative values that are likely to change as the design matures.

GT-MHR	Gas Turbine – Modular Helium Reactor
HEU	high enriched uranium [typically 93% U-235]
HHT	Hochtemperaturreaktor mit Helium Turbine [German direct-cycle HTR]
HM	heavy metal [contamination]
HPCC	High Pressure Conduction Cooldown
HPS	helium purification system
HTA	High Temperature Absorber
HTE	High temperature electrolysis
HTGR	High Temperature Gas-Cooled Reactor
HTR	High Temperature Reactor [pebble bed HTGR]
HTTR	[Japanese] High Temperature Test Reactor
IAEA	International Atomic Energy Agency
IHX	intermediate heat exchanger
INL	Idaho National Laboratory
ISI	in-service inspection
JAEA	Japan Atomic Energy Agency [formerly JAERI]
KAERI	Korean Atomic Energy Research Institute
KFA	Kernforschungsanlage - Juelich [now renamed FZJ]
LBE	Licensing Basis Event
LEU	low enriched uranium [<20% U-235]
LPCC	Low Pressure Conduction Cooldown
LTA	Low Temperature Absorber
LWR	light water reactor
MB	missing-buffer [fuel particles]
MHR	Modular Helium Reactor
MHTGR	[steam-cycle] Modular High Temperature Gas-cooled Reactor
NFI	Nuclear Fuel Industries
NGNP	Next Generation Nuclear Plant
NP-MHTGR	New Production-Modular Helium Reactor
NRC	[United States] Nuclear Regulatory Commission
O&M	operation and maintenance

ORNL	Oak Ridge National Laboratory
PAG	Protective Action Guide
PBMR	Pebble Bed Modular Reactor [South Africa]
PC-MHR	Plutonium Consumption-Modular Helium Reactor
PCS	power-conversion system
PCDSR	pre-conceptual design studies report
PCRV	prestressed concrete reactor vessel
PNP	Prototype Nuclear Process [Heat Project – FRG]
PV	pressure-vessel [failure]
PyC	pyrolytic carbon
QA	quality assurance
QC	quality control
R/B	release rate-to-birth rate ratio
RB	Reactor building
RCCS	Reactor Cavity Cooling System
RCPB	Reactor Coolant Pressure Boundary
RN	radionuclide
RPV	Reactor Pressure Vessel
SCS	Shutdown Cooling System
SG	steam generator
SRDC	Safety Related Design Condition
SRM	System Requirements Manual
TBD	to be determined
TEDE	Total Effective Dose Equivalent
TRISO	TRI-material, ISOtropic with the materials being low-density PyC (buffer), high-density IPyC and OPyC, and SiC.
UCNI	Unclassified Controlled Nuclear Information
U/U	user/utility [requirements]
VHTR	Very High Temperature Reactor
VLPC	Vented Low-Pressure Containment

1 SUMMARY

The Battelle Energy Alliance (BEA) has subcontracted with three industrial teams, including a team led by General Atomics (GA), for engineering studies in support of Next Generation Nuclear Plant (NGNP) technology development and licensing. As part of the contractual work scope, GA used a top-down functional analysis methodology to establish a defensible basis for the in-core fuel performance criteria and the as-manufactured fuel quality specifications for a steam-cycle, prismatic Modular Helium Reactor (MHR) with a 750 ^{o}C core outlet temperature.

The programmatic benefits of performing the subject study during conceptual design are threefold: (1) to assure that the radionuclide (RN) source terms used for NGNP plant design and licensing are consistent with the top-level RN control requirements applicable to the NGNP Project; (2) to provide a logical basis to refine, or to revise as necessary, the fuel/fission product Design Data Needs (DDNs) that have been identified for the NGNP Project; and (3) to provide direction to the NGNP/AGR Fuel Development and Qualification Program [AGR Plan/2 2008] to assure that its goals are responsive to the needs of the NGNP Project. The scope of this study includes the following subtasks:

1. Determination of the RN control requirements and corresponding RN release limits for a steam-cycle MHR with a 750 ^{o}C core outlet temperature (Section 3).
2. Allocation of target decontamination factors to Individual RN release barriers (Section 4).
3. Estimation of RN source terms for the GA “reference” steam-cycle MHR Design (Section 6).
4. Comparison of predicted and target decontamination factors (Section 7).
5. Impact of higher core outlet temperatures on RN source terms and barrier performance (Section 8).

1.1 Radionuclide Control Requirements

Stringent, top-level radionuclide control requirements are anticipated for MHRs. Limits on RN release from the core that are consistent with these top-level RN control requirements are needed in order to derive allowable in-service fuel failure and as-manufactured fuel quality requirements (e.g., allowable heavy-metal contamination, SiC coating defects, etc). The top-level RN control requirements are defined in several programmatic documents, including the NGNP System Requirements Manual [NGNP SRM 2009]. In addition, the Statement of Work for this task [SOW-6795 2009] invokes the GA System Requirements Manual [GA SRM 2007]. The most constraining RN control requirements included in these documents are listed in Table 1-1 and elaborated in Section 3.

Table 1-1. Key Top-Level RN Control Requirements

Top-Level Regulatory Requirements	
1	10CFR50, Appendix I, Limits for Radionuclides in Plant Effluents (Goals 1 & 2): a. Whole Body Dose ≤ 5 mrem/yr b. Thyroid Dose ≤ 15 mrem/yr
2	10CFR20 Occupational Dose Limits (Goals 1 & 2): a. Whole Body Dose ≤ 5 rem b. Thyroid Dose ≤15 rem
3	10CFR100 Offsite Dose Limits (Construction Permit) for Licensing Basis Events (Goal 3): a. Whole Body Dose ≤ 20 rem b. Thyroid Dose ≤ 150 rem
4	EPA-520 PAGs for Radioactive Release for Public Sheltering and Evacuation: a. Whole Body Dose ≤ 1 rem b. Thyroid Dose ≤ 5 rem
5	NRC Safety Risk Limits.
Utility/User Requirements	
1	Occupational Exposures ≤ 10% of 10CFR20 Limits (Goals 1 & 2) a. Whole Body Dose ≤ 0.5 rem/yr b. Thyroid Dose ≤ 1.5 rem/yr
2	Top Level Regulatory Criteria, including PAGs at the Exclusion Area Boundary for all events with a frequency $\leq 5 \times 10^{-7}$/yr (Goal 3)

The radionuclide containment system for an MHR is comprised of multiple barriers to limit RN release from the core to the environment to insignificant levels during normal operation and a spectrum of postulated accidents. The five principal release barriers are: (1) the fuel kernel; (2) the particle coatings, particularly the SiC coating; (3) the fuel-compact matrix and fuel-element graphite collectively; (4) the primary coolant pressure boundary; and (5) the Vented Low-Pressure Containment (VLPC) building.

As part of the design process, performance requirements must be derived for each of the above release barriers. Of these barriers, the particle coatings are the most important. Moreover, the in-reactor performance characteristics of the coated-particle fuel can be strongly influenced by its as-manufactured attributes. Consequently, the fuel performance requirements and fuel quality requirements must be systematically defined and controlled.

After review of the top-level radionuclide control requirements, it was determined that meeting the EPA Protective Action Guidelines (PAG) limits at a 425-m Exclusion Area Boundary (EAB)[2] will likely be the most restrictive requirement for setting fuel performance and quality requirements for a steam-cycle MHR. This circumstance should not be surprising since meeting the PAGs at a 425-m EAB was determined to be the bounding RN control requirement for the earlier 350 MW(t) steam-cycle MHTGR. In the 1992 version of the PAGs, the Total Effective Dose Equivalent (TEDE) dose protocol[3] was used instead of the earlier whole-body dose protocol. The 1992 PAG also includes a 5-rem thyroid dose limit to preclude the need for public sheltering, and this 5-rem thyroid dose limit proved more constraining than 1-rem TEDE limit.

The protocol to be used to convert these PAG dose limits to corresponding limits on the release of specific radionuclides from the plant to the environment proved to be a complex issue. Such RN release limits are a prerequisite to establishing fuel performance and quality requirements. Previously, when the rem-to-Curie conversion was made for the 350 MW(t) MHTGR and for the NP-MHTGR, atmospheric dispersion factors (χ/Q) and breathing rates were taken from USNRC Regulatory Guide 1.4, and the effectivities (rem/Ci) were taken from NRC Regulatory Guide 1.109. More recently, the TEDE dose conversion protocol has been adopted. After considerable internal discussion within GA, discussion with licensing experts at URS-WD (a member of the GA team) and dialogue with BEA, a conservative approach for making the rem-to-Curie conversion which roughly parallels the earlier approach was agreed upon for this study. The PAG thyroid limit was then used to derive limits on the I-131 release from the plant during postulated accidents.

The second, most constraining, top-level RN control requirement is to limit the occupational exposure to ≤ 10% of 10CFR20. Typically, occupational exposures result primarily from O&M activities, especially ISI, during normal plant operation. Plateout activity throughout the primary coolant circuit, especially on the steam generator of a steam-cycle MHR, is expected to be a dominant source of occupational exposure. A detailed occupational exposure assessment has not yet been performed for a steam-cycle MHR. Hence, in deriving limits on plateout activity consistent with the subject goal, it was necessary to rely heavily upon previous occupational exposure assessments and upon engineering judgment. On that basis, it was projected that the ≤ 10% of 10CFR20 goal would be met if the gamma radiation fields around the primary circuit due to fission product plateout were limited to ≤ 10 mR/hr for scheduled maintenance activities (e.g., circulator ISI) and to ≤ 100 mR/hr for unscheduled maintenance activities (e.g., steam-

[2] The NGNP System Requirements Manual [2009] specifies “approximately 400 meters,” and Statement-of-Work-6795 [2009] specifies a 400-m EAB. The dose/dispersion calculations that are currently available from the safety analyses for the 350 MW(t) MHTGR [PSID 1992] and for the 450 MW(t) MHTGR [Dilling 1993] were done for a 425-m EAB; consequently, a 425-m EAB was assumed here.

[3] The TEDE dose is the sum of the deep-dose equivalent for external exposures and the committed effective dose equivalent (CEDE) for internal exposures.

generator tube plugging). These limits on gamma dose rates were in turn used to set limits on primary circuit plateout (in particular, limits on Cs-137 and Ag-110m plateout).

1.2 Target Decontamination Factors

When the fuel requirements presented herein were derived, credit was taken for RN retention by each of the release barriers. Barrier performance requirements are specified such that only the particle coatings are needed to meet 10CFR100 off-site dose limits; however, credit for the additional barriers is taken to meet the PAG dose limits. The alternative would be to set fuel failure limits sufficiently low that the PAG dose limits could be met even if it were assumed that 100% of the fission product inventories of failed particles were released to the environment. This approach is considered impractical. For perspective, for the 350 MW(t) steam-cycle MHTGR with a 425-m EAB, the allowable I-131 release limits to meet the PAG thyroid dose limit of 5 rem were 2.6 Ci for short-term events, such a rapid depressurization, and 29 Ci for long-term events, such as a depressurized core conduction cooldown. Converting these Curie limits to allowable fuel failure fractions for a 600 MW(t) MHR gives failure limits of ~10^{-7} during normal operation and ~10^{-6} during core heatup events, respectively.

The near-term NGNP Project emphasis has shifted to process heat/process-steam applications with reactor core outlet temperatures of 750 to 800 ^{o}C, and the GA team has proposed a conceptual design of a steam-cycle MHR with a core outlet temperature of 750 ^{o}C.[4] However, the power level has yet to be chosen with powers from 350 to 600 MW(t) under consideration for prismatic designs. Given the lack of an approved conceptual plant design and the lack of a detailed safety analysis for such a design, the decontamination factors derived for the 350 MW(t) steam-cycle MHTGR were adopted here as the targets for a “reference” steam-cycle MHR as a necessary expedient. The MHTGR design and safety analysis, which included the submittal of a Preliminary Safety Information Document (PSID) to the Nuclear Regulatory Commission (NRC), were far more advanced than the aforementioned GA conceptual design at this writing.

If a 600 MW(t) steam-cycle MHR were selected, the target RN decontamination factors would result in predicted source terms that nearly satisfy the requirement in [NGNP SRM 2009] to meet the lower limit PAGs at a 425-m EAB. In general, the thyroid doses are <2x higher than the 5-rem PAG limit which is to be expected because the power level, hence the RN inventories, would increase by 1.7x (600/350) and the target decontamination factors were chosen to just satisfy the 5-rem PAG limit for a 350 MW(t) plant.

---

[4] Based upon past optimization studies for steam-cycle MHRs, the optimal core outlet temperature for a steam-cycle MHR may ultimately prove to be closer to 700 ^{o}C, depending upon the specific application.

The target RN decontamination factors for a steam-cycle MHR are summarized in Table 1-2 and elaborated in the Section 4.

Table 1-2. Summary of Target Decontamination Factors for Steam-Cycle MHR

	Parameter	Key Radionuclides determining Fuel Requirements (release timing)						Comments
		I-131 (short-term)	I-131 (long-term)	Xe-133 (long-term)	Cs-137 (long-term)	Sr-90 (long-term)	Ag-110m (long-term)	
Plant Limits	Accident Release Limits	2.6	29	2300	TBD	1.2	TBD	Appendix A
600 MW "Design" Activities (Normal)	Core (Ci)	$2.0 \times 10^{+7}$	$2.0 \times 10^{+7}$	$3.6 \times 10^{+7}$	$1.7 \times 10^{+6}$	$1.5 \times 10^{+6}$	$2.8 \times 10^{+4}$	[Hanson 2008a]
	Circulating (Ci)	1.8×10^{-1}	1.8×10^{-1}	$2.0 \times 10^{+1}$	3.3×10^{-3}	1.6×10^{-5}	7.2×10^{-3}	
	Plateout (Ci)	$1.5 \times 10^{+2}$	$1.5 \times 10^{+2}$	0	$2.4 \times 10^{+3}$	$1.2 \times 10^{+1}$	$1.7 \times 10^{+2}$	
Fuel Attributes	"Design" HM Contamination	$\leq 2 \times 10^{-5}$	$\leq 2 \times 10^{-5}$	$\leq 2 \times 10^{-5}$	$\leq 2 \times 10^{-5}$	$\leq 2 \times 10^{-5}$	$\leq 2 \times 10^{-5}$	
	"Max. Exp." HM Contamination	$\leq 1 \times 10^{-5}$	$\leq 1 \times 10^{-5}$	$\leq 1 \times 10^{-5}$	$\leq 1 \times 10^{-5}$	$\leq 1 \times 10^{-5}$	$\leq 1 \times 10^{-5}$	
	"Design" SiC Defects	$\leq 1 \times 10^{-4}$	$\leq 1 \times 10^{-4}$	$\leq 1 \times 10^{-4}$	$\leq 1 \times 10^{-4}$	$\leq 1 \times 10^{-4}$	$\leq 1 \times 10^{-4}$	
	"Max. Exp." SiC Defects	$\leq 5 \times 10^{-5}$	$\leq 5 \times 10^{-5}$	$\leq 5 \times 10^{-5}$	$\leq 5 \times 10^{-5}$	$\leq 5 \times 10^{-5}$	$\leq 5 \times 10^{-5}$	
	"Design" Failure – Normal	$\leq 2 \times 10^{-4}$	$\leq 2 \times 10^{-4}$	$\leq 2 \times 10^{-4}$	$\leq 2 \times 10^{-4}$	$\leq 2 \times 10^{-4}$	$\leq 2 \times 10^{-4}$	
	"Max. Exp." Failure – Normal	$\leq 5 \times 10^{-5}$	$\leq 5 \times 10^{-5}$	$\leq 5 \times 10^{-5}$	$\leq 5 \times 10^{-5}$	$\leq 5 \times 10^{-5}$	$\leq 5 \times 10^{-5}$	
	"Design" ΔFailure - Accidents	0	$\leq 6 \times 10^{-4}$	$\leq 6 \times 10^{-4}$	$\leq 6 \times 10^{-4}$	$\leq 6 \times 10^{-4}$	$\leq 6 \times 10^{-4}$	
	"Max. Exp." ΔFailure - Accidents	0	$\leq 1.5 \times 10^{-4}$	$\leq 1.5 \times 10^{-4}$	$\leq 1.5 \times 10^{-4}$	$\leq 1.5 \times 10^{-4}$	$\leq 1.5 \times 10^{-4}$	
RN Transport in Core	Kernel Retention	50	8	8	TBD	TBD	TBD	
	Matrix/graphite Retention	1	1	1	10	100	1	
RN Transport in PCS	Plateout Retention – Depressurization	20	20	1	20	20	20	DBE-10
	Depressurized Core Conduction Cooldown	-	30	1	30	30	30	SRDC-11

	Parameter	Key Radionuclides determining Fuel Requirements (release timing)						Comments
		I-131 (short-term)	I-131 (long-term)	Xe-133 (long-term)	Cs-137 (long-term)	Sr-90 (long-term)	Ag-110m (long-term)	
	Plateout Retention – H_2O Ingress + Pressure Relief	2 x 7	2 x 7	7	2 x 7	2 x 7	2 x 7	SRDC-6
RN Transport in VLPC	VLPC Retention Factor	1	[10][5]	1	[10]	[10]	[10]	SRDC-11
	Wake Retention Factor	1.5	1.5	1.5	1.5	1.5	1.5	Impacts Prompt Release
Plant Release	RN Transport to EAB	5.0	50	2700	TBD	0.3	TBD	
Plant Limits	Accident Release Limits	2.6	29	2300	TBD	1.2	TBD	
Additional Retention Needed		1.9	1.7	1.2	TBD	1	TBD	

[5] Numbers in [square brackets] throughout the report are provisional and subject to change as the design matures.

1.3 Recommended Fuel Requirements for a Steam-Cycle MHR

The recommended fuel performance and quality requirements for a steam-cycle MHR with a 750 °C core outlet temperature are summarized in Table 1-3, and the recommended fission gas and metal release limits for key radionuclides are shown in Tables 1-4 and 1-5, respectively. The recommended limits are the same for the earlier steam-cycle MHTGR except that the allowable Ag-110m release is reduced by 2.5x to match the limit adopted for the direct-cycle GT-MHR with a 850 °C core outlet temperature. The corresponding limits for the earlier 350 MW(t) steam-cycle MHTGR (note its significantly lower core outlet temperature) and the provisional limits for a process-heat MHR with a 900 °C core outlet temperature are also shown in the Tables 1-4 and 1-5.

Table 1-3. Recommended Fuel Requirements for a Steam-Cycle MHR

Parameter	Steam-Cycle MHTGR		Steam-Cycle MHR	
	"Maximum Expected"	"Design"	"Maximum Expected"	"Design"
As-Manufactured Fuel Quality[6]				
HM contamination	$\leq 1.0 \times 10^{-5}$	$\leq 2.0 \times 10^{-5}$	$\leq 1.0 \times 10^{-5}$	$\leq 2.0 \times 10^{-5}$
Missing or defective buffer	$\leq 5.0 \times 10^{-5}$	$\leq 1.0 \times 10^{-4}$	$\leq 1.0 \times 10^{-5}$	$\leq 2.0 \times 10^{-5}$
Missing or defective IPyC	$\leq 4.0 \times 10^{-5}$	$\leq 1.0 \times 10^{-4}$	$\leq 4.0 \times 10^{-5}$	$\leq 1.0 \times 10^{-4}$
Defective SiC	$\leq 5.0 \times 10^{-5}$	$\leq 1.0 \times 10^{-4}$	$\leq 5.0 \times 10^{-5}$	$\leq 1.0 \times 10^{-4}$
Missing or defective OPyC	$\leq 1.0 \times 10^{-4}$	$\leq 2.0 \times 10^{-4}$	[0.01]	[0.02]
In-Service Fuel Performance[7]				
Normal operation	$\leq 5.0 \times 10^{-5}$	$\leq 2.0 \times 10^{-4}$	$\leq 5.0 \times 10^{-5}$	$\leq 2.0 \times 10^{-4}$
Core heatup accidents	[$\leq 1.5 \times 10^{-4}$]	[$\leq 6.0 \times 10^{-4}$]	[$\leq 1.5 \times 10^{-4}$]	[$\leq 6.0 \times 10^{-4}$]

[6] ≥ 95% confidence that the mean value for a fuel segment will be ≤ "Maximum Expected" value, and ≥ 95% confidence that ≤ 5% of fuel compacts will be > "Design" value.

[7] ≥ 50% probability that the fuel failure and fission product release will be ≤ "Maximum Expected" criteria and ≥ 95% probability that the failure and release will be ≤ "Design" criteria (see Section 2.4.6).

Table 1-4. Recommended Fission Gas Release Limits for a Steam-Cycle MHR

Reactor Plant	Type	COT (°C)	Allowable Core Fractional Release			
			Kr-88		I-131	
			"Maximum Expected"	"Design"	"Maximum Expected"	"Design"
MHTGR	Steam-cycle	687	$\leq 8.3 \times 10^{-7}$	$\leq 3.3 \times 10^{-6}$	$\leq 2.0 \times 10^{-6}$	$\leq 8.0 \times 10^{-6}$
MHR	**Steam-cycle**	**750**	**$\leq 8.3 \times 10^{-7}$**	**$\leq 3.3 \times 10^{-6}$**	**$\leq 2.0 \times 10^{-6}$**	**$\leq 8.0 \times 10^{-6}$**
GT-MHR	Direct-cycle	850	$\leq 8.3 \times 10^{-7}$	$\leq 3.3 \times 10^{-6}$	$\leq 2.0 \times 10^{-6}$	$\leq 8.0 \times 10^{-6}$
MHR	Process heat	900	$\leq [8.3 \times 10^{-7}]$	$\leq [3.3 \times 10^{-6}]$	$\leq [2.0 \times 10^{-6}]$	$\leq [8.0 \times 10^{-6}]$

Table 1-5. Recommended Fission Metal Release Limits for a Steam-Cycle MHR

Plant	Type	COT (°C)	Allowable Core Fractional Release					
			Cs-137		Ag-110m		Sr-90	
			"Maximum Expected"	"Design"	"Maximum Expected"	"Design"	"Maximum Expected"	"Design"
MHTGR	Steam-cycle	687	$\leq 7.0 \times 10^{-6}$	$\leq 7.0 \times 10^{-5}$	$\leq 5.0 \times 10^{-4}$	$\leq 5.0 \times 10^{-3}$	$\leq 3.0 \times 10^{-8}$	$\leq 3.0 \times 10^{-7}$
MHR	**Steam-cycle**	**750**	**$\leq 7.0 \times 10^{-6}$**	**$\leq 7.0 \times 10^{-5}$**	**$\leq 2.0 \times 10^{-4}$**	**$\leq 2.0 \times 10^{-3}$**	**$\leq 3.0 \times 10^{-8}$**	**$\leq 3.0 \times 10^{-7}$**
GT-MHR	Direct-cycle	850	$\leq 1.0 \times 10^{-5}$	$\leq 1.0 \times 10^{-4}$	$\leq 2.0 \times 10^{-4}$	$\leq 2.0 \times 10^{-3}$	$\leq 3.0 \times 10^{-8}$	$\leq 3.0 \times 10^{-7}$
MHR	Process heat	900	$\leq [1.0 \times 10^{-5}]$	$\leq [1.0 \times 10^{-4}]$	$\leq [5.0 \times 10^{-4}]$	$\leq [5.0 \times 10^{-3}]$	TBD	TBD

1.4 Estimated RN Source Terms for a Steam-Cycle MHR

This task is closely coupled to a parallel NGNP core performance analysis (CPA) task to determine if an acceptable core design can be achieved using a single fissile fuel particle or whether a binary fuel particle system (i.e., including a fissile particle and a fertile particle) is necessary to meet requirements. The coupling of these two tasks results from the necessity to perform a quantitative assessment of the fuel performance and fission product release from a "reference" steam-cycle core with a 750 °C core outlet temperature and to assess the effects of higher core outlet temperatures. The core physics design and the calculational performance analysis tools developed as part of the CPA task were utilized here as well.

Radionuclide source terms were estimated for the GA "reference" steam-cycle plant with core inlet and outlet temperatures of 322 and 750 °C, respectively. Best estimate RN source terms were predicted for normal plant operation using the final binary-particle core design (Case 7.9SC) and the final single-particle core design (Case 8.9.3SC) from the CPA task where the

suffix “SC” designates the above steam-cycle gas temperatures that are different from the core inlet and outlet temperatures of 540 and 900 °C, respectively, used for the CPA). The results are compared with the recommended fuel performance and fission product release criteria (Section 1.3) in Table 1-6.

Table 1-6. Comparison of Predicted Core Performance with Recommended Criteria

Parameter	“Maximum Expected” Limit	Case 7.9SC (Binary Particle)	Case 8.9.3SC (Single Particle)
Fuel failure during normal operation (exposed kernel fraction)	$\leq 5.0 \times 10^{-5}$	1.2×10^{-5} (fissile) 2.3×10^{-6} (fertile)	9.2×10^{-6}
In-service SiC failure fraction	N/A	8.3×10^{-6}	2.2×10^{-5}
Total SiC failure fraction	N/A	6.6×10^{-5}	7.9×10^{-5}
Kr-88 R/B (fractional release)	$\leq 8.3 \times 10^{-7}$	5.8×10^{-7}	6.8×10^{-7}
I-131 R/B (fractional release)	$\leq 2.0 \times 10^{-6}$	1.6×10^{-6}	1.9×10^{-6}
Ag-110m cumulative fractional release	$\leq 2.0 \times 10^{-4}$	3.2×10^{-4}	1.9×10^{-3}
Cs-137 cumulative fractional release	$\leq 7.0 \times 10^{-6}$	8.7×10^{-6}	1.8×10^{-5}
Sr-90 cumulative fractional release	$\leq 3.0 \times 10^{-8}$	3.4×10^{-8}	2.4×10^{-7}

The predicted exposed kernel fractions for both cases are well below the limit because of the tight specification on the as-manufactured, missing-buffer particle fraction. The exposed kernel fraction for the single-particle design is slightly lower than that for the fissile particle of the binary-particle design because of the lower burnup of the former results in the survival of some of the missing-buffer particles (the fraction for the single-particle design is close to the weighted average for the fissile/fertile design). The predicted SiC failure fraction is modest and dominated by the as-manufactured SiC defect fraction of $\leq 5 \times 10^{-5}$ in both cases. The predicted Kr-88 and I-131 fractional releases are near the limits and completely dominated by the release from as-manufactured heavy-metal (HM) contamination. Reduction in the predicted fission gas release (and, thus, in the iodine plateout inventory) would necessarily require a tighter specification on HM contamination.

The predicted fractional releases of the three volatile metals are significantly higher for the single-particle design because of the higher fuel and graphite temperatures for that design. While the temperature differences may seem relatively modest, they are in a regime where nominally small incremental temperature increases result in significantly more diffusive Ag release from intact TRISO particles and significantly less matrix/graphite retention of Cs and especially of Sr. For this reason, the differences between the two cases are somewhat less pronounced for the CPA base case of T_{out} = 900 ^{o}C and ΔT_{core} = 360 ^{o}C.

For the binary-particle case, the predicted releases of the three metals slightly exceed the recommended criteria because of excessively high predicted fuel temperatures during the second irradiation cycle; the metal releases during the remaining three cycles are below the limits (it is anticipated that the high fuel temperatures in Cycle 2 can be reduced by further optimization of the nuclear design and/or the analytical methods). However, the predicted releases of Ag and Sr for the single-particle design exceed "Maximum Expected" criteria by an order of magnitude. It will be more difficult to reduce these predicted releases to that degree. A reduced core outlet temperature and/or a reduced core temperature rise would certainly help, but such design changes have their own disadvantages. Perhaps, a fuel shuffling scheme can be identified that provides the required reductions in fuel and graphite temperatures.

In summary, a binary-fuel-particle system provides an inherent advantage relative to a single-particle system having a single U-235 enrichment because it allows U-235 enrichment zoning as well as uranium zoning and fixed burnable poison zoning [GA 2009b]. Thus, use of a binary-fuel-particle system should always result in improved RN retention in the core relative to that achievable with a single fuel particle having a single U-235 enrichment. This conclusion does not, however, mean that use of a single fuel particle is not feasible as discussed in greater detail in the CPA Phase 2 final report (GA report 911184).

1.5 Comparison of Predicted and Target Decontamination Factors

The target RN decontamination factors presented in Table 1-2 were reviewed considering the predicted behavior of steam-cycle cores operating at 750 ^{o}C COT analyzed herein and the behavior of the core designs analyzed as part of the CPA task. The emphasis was on the in-core RN retention barriers (kernels, coatings and graphite), but the predicted ex-core RN transport behavior under accident conditions was also reviewed.

The fuel performance and fission product release predictions are based upon component models and material property data that, in general, have very large uncertainties (hence, the large number of fuel/fission product DDNs that have been identified). A large number of variation cases were run with the SURVEY and TRAFIC-FD codes to determine how sensitive the predicted fuel performance and fission product release are to certain key material property data. These sensitivity studies were performed for core outlet temperatures of 750 ^{o}C and 900 ^{o}C. The implications for the NGNP/AGR fuel development program are summarized below (Section 1.8).

The NGNP Project is still in the conceptual design phase with major design selections yet to be made. While the GA team has made certain recommendations [Labar 2009], the NGNP Project has not officially chosen a plant power level, a core outlet temperature, or determined whether the steam generator will be located in the primary circuit. Given these circumstances, it appears premature to reallocate the RN decontamination factors simply because the thyroid doses are

<2x higher than the 5-rem PAG limit for a 600 MW(t) plant. If such a reallocation were done now, the most effective reallocation would be to reduce the allowable as-manufactured heavy-metal contamination and the in-service failure fractions by 1.7x to compensate for the increase in core power level and to leave the other decontamination factors unchanged.

While a reallocation of the RN decontamination factors is not recommended at the moment, it is appropriate to review the target decontamination factors in the context of the core performance analyses that have been done here and in the CPA task. Such a review has been done, and judgments were made as to which RN decontamination factors could be increased, decreased or left unchanged. The results are summarized in Table 1-7 and elaborated in Section 7.

Table 1-7. Potential for Reallocation of RN Decontamination Factors

RN Retention Barrier	RN	Reallocation of RN Decontamination Factors (- / 0 / +)[8]				Key DDNs
		Normal	SRDC-10	SRDC-6	SRDC-11	
Kernels	Xe^{9}	0	NA[10]	+	+	Effect of hydrolysis on Kr, Xe, Te & I release; I release during LPCC
	I	0	NA	+	+	
	Cs	+	NA	0	+	Kernel retention of Sr and Cs during normal operation and LPCC. Burnup dependence of diffusivity
	Ag	+	NA	-	-	
	Sr	++	NA	+	++	
Coatings	Xe	++	NA	++	++	Determine performance limits of TRISO particles. Determine feasibility of tighter limits on allowable coating failure during normal operation & HPCC/LPCC
	I	++	NA	++	++	
	Cs	++	NA	++	++	
	Ag	++	NA	++	++	
	Sr	++	NA	++	++	
Matrix/ Graphite	Xe	NA	NA	NA	NA	No significant graphite retention
	I	NA	NA	NA	NA	
	Cs	+	+	+	+	Characterize metal transport behavior in new fuel-block graphite. Determine metal behavior in graphite during H_2O ingress.
	Ag	-	-	-	-	
	Sr	++	++	++	++	

[8] Scale (- / 0 / +) denotes (smaller RN retention factor/no change/larger RN retention factor) to be assigned as required.
[9] Applies to Kr isotopes as well as Xe isotopes.
[10] NA = not applicable; barrier not effective under these circumstances.

RN Retention Barrier	RN	Reallocation of RN Decontamination Factors (- / 0 / +)[8]				Key DDNs
		Normal	SRDC-10	SRDC-6	SRDC-11	
Primary Coolant Pressure Boundary	Xe	0	NA	NA	NA	Improved sorption isotherms for condensables. Characterize liftoff during rapid depressurization and washoff during H_2O ingress + pressure relief.
	I	++	++	+	+	
	Cs	++	++	+	+	
	Ag	++	++	+	+	
	Sr	++	++	+	+	
Reactor Building	Xe	NA	NA	NA	NA	Characterize RN transport in VLPC during H_2O ingress + pressure relief and depressurized core conduction cooldown.
	I	NA	-	++	++	
	Cs	NA	-	++	++	
	Ag	NA	-	++	++	
	Sr	NA	-	++	++	
Design Mitigation Features		Improved control rod management to reduce power peaking	TBD	High efficiency filter in pressure relief train.	Purge system to minimize air ingress into core.	Characterize efficiencies of candidate filters, especially for I removal from He/steam mixtures.

1.6 Impact of higher Core Outlet Temperatures

The effect of higher core outlet temperatures on RN control was evaluated by performing a sensitivity study. This temperature sensitivity study complements the material property sensitivity study (Section 1.5).

The base case chosen for this sensitivity study was the VHTR core from the CPA task with T_{in} = 540 °C and T_{out} = 900 °C with a core ΔT = 360 C. The "reference" steam-cycle core (Section 1.4) has a relatively high core temperature rise of 428 °C which is typical of steam-cycle cores. However, the price of a large core temperature rise is higher peak fuel temperatures for a given core outlet temperature since the temperature rise in a given coolant channel is proportional to the product of the core-average temperature rise and the radial peaking factor. SURVEY and TRAFIC runs were made for core outlet temperatures of 700, 750, 800, 850 and 950 °C with a constant core ΔT = 360 C. The results are presented in Section 8.

The exposed kernel fraction increases only modestly up to an outlet temperature of 950 °C. Consequently, the fission gas release rates are still dominated by release from heavy-metal contamination even at 950 °C. The SiC failure fraction rises to 2×10^{-4} at 950 °C due to fission product corrosion which contributes to increasing fission metal release.

The cumulative fractional releases of Ag-110m, Cs-137, and Sr-90 are plotted as a function of core outlet temperature in Figure 1-1 (fission metal release is generally the most temperature sensitive metric). The Ag-110m fractional release increases rapidly with increasing outlet temperatures because the diffusive Ag release from intact TRISO particles is a strong function of temperature. The Cs-137 and Sr-90 fractional releases increase rapidly with increasing outlet temperatures primarily because retention by the matrix/graphite decreases as the average core temperatures rise.

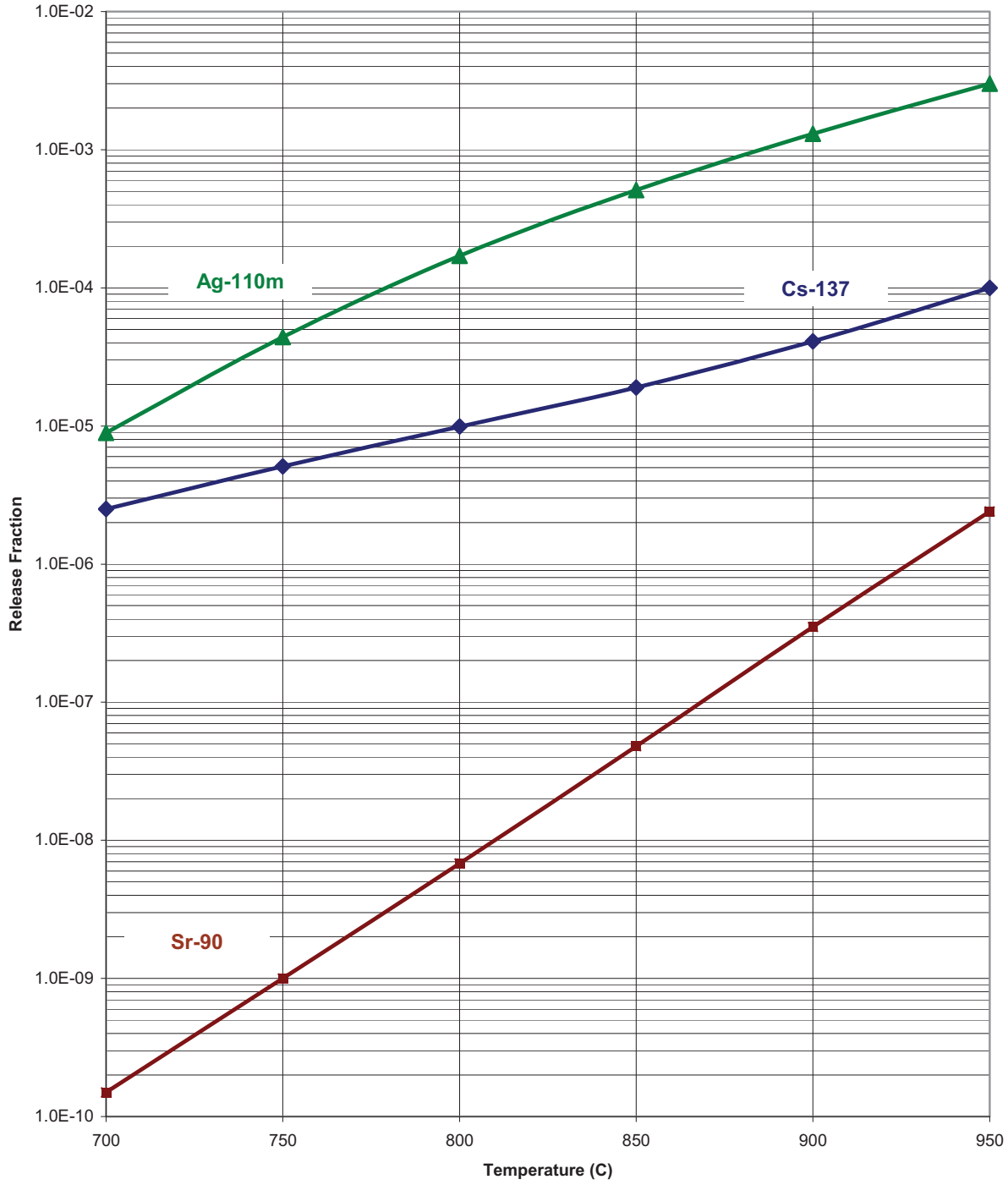

Figure 1-1. Fractional Release of Volatile Metals vs. Core Outlet Temperature

1.7 Plant Tritium Source Term and Limits

While tritium control would likely be an important issue for a VHTR producing hydrogen or other commercial feedstocks and/or products, it is of little or no practical consequence when defining fuel performance and quality requirements. Tritium is diffusively released from intact TRISO particles at high temperatures and is also produced by other external sources outside of the fuel

particles. Consequently, the as-manufactured defect fractions and in-service exposed kernel fractions have only a modest influence on the total concentration of tritium in the primary helium coolant. Given these circumstances, tritium control receives little attention in the present report.

1.8 Implications for NGNP Fuel/Fission Product Design Data Needs

The implications of this task, especially the sensitivity studies introduced above, for the NGNP fuel/fission product DDNs were evaluated and documented for each DDN (Section 9). No new fuel/fission product DDNs were identified in the process of performing this task. Several of the conclusions and recommendations are particularly noteworthy.

1.8.1 Fuel Development

1. The feasibility of tighter specifications on as-manufactured, heavy-metal contamination and on SiC coating defects should be investigated
2. The NGNP/AGR fuel development program should have the goal of developing and qualifying fuel manufacturing processes that can meet the “Maximum Expected” fuel quality requirements (rather than the “Design” values) in Table 1-3 on a core segment basis with 95% confidence. The “Design” fuel quality requirements in Table 1-3, which are less stringent, should be applicable to individual fuel compact lots and must also be met at the 95% confidence level.
3. Even under steam-cycle core conditions, a small fraction of the fuel may experience temperatures above 1400 ^{o}C, and there is significant uncertainty in the predicted fuel temperatures. Consequently, it is extremely important to perform a margin test as soon as possible (i.e., as is currently planned in one of the AGR-2 capsules). A more reliable fission product/SiC corrosion model is urgently needed, especially with regard to the time dependence.
4. Postirradiation heating tests need to be performed in atmospheres that are characteristic of air ingress and water ingress events rather than exclusively in pure dry helium.

1.8.2 Fission Product Transport

1. Based upon past experience with the 350 MW(t) steam-cycle MHTGR, large water ingress plus pressure relief will likely be the bounding accident for a future steam-cycle MHR. The effects of hydrolysis at high water partial pressures need to be better quantified, and the release rates of I-131 need to be measured directly. (Plans are currently being developed to include such testing in the NGNP/AGR Fuel Program.)
2. The release of I-131 from failed UCO particles under simulated core heatup conditions needs to be measured as is planned in the NGNP/AGR Fuel Program.
3. The diffusivities of volatile fission metals (Cs, Sr and, to a lesser extent, Ag) in UCO kernels need to be determined as a function of temperature and burnup. The GA Fuel Design Data Manual/Issue F [FDDM/F 1987] correlations, which are characterized by extremely large

burnup dependencies, are highly suspect. The planned AGR-3/-4 tests can, in principle, provide the requisite data.

4. The transport properties of volatile metals (Cs, Sr, and Ag) in the new fuel-element graphite selected to replace H-451 need to be characterized. The planned AGR-3/-4 tests can, in principle, provide the requisite data.

2 INTRODUCTION AND BACKGROUND

The Battelle Energy Alliance (BEA) has subcontracted with three industrial teams, including a team led by General Atomics (GA), for engineering studies in support of Next Generation Nuclear Plant (NGNP) technology development and licensing. As part of the contractual work scope [Work Plan 2009], GA used a top-down functional analysis methodology to establish a defensible basis for the in-core fuel performance criteria and the as-manufactured fuel quality specifications for a steam-cycle prismatic Modular Helium Reactor (MHR) with a 750 ^{o}C core outlet temperature.

2.1 Purpose

The primary purpose of this study is to establish a defensible basis for the in-core fuel performance criteria and the as-manufactured fuel quality specifications for the NGNP Project. The programmatic benefits are threefold: (1) to assure that the RN source terms used for a steam-cycle MHR design and licensing are consistent with the top-level RN control requirements applicable to an MHR; (2) to provide a logical basis to refine, and to revise as necessary, the fuel/fission product Design Data Needs (DDNs) that have been identified for the NGNP; and (3) to provide direction to NGNP/AGR Fuel Development and Qualification Program [AGR Plan/2 2008] to assure that its goals are responsive to the needs of the NGNP Project.

2.2 NGNP Design

At this writing, the NGNP Project is still in the conceptual design phase with major design selections yet to be made. Consistent with the EPAct, the early emphasis of the NGNP Project was on very high temperature process-heat applications for hydrogen production with reactor core outlet temperatures of 900 - 950 ^{o}C [e.g., GA PCDSR 2007]. After an extensive market survey of potential NGNP users, the near-term NGNP Project emphasis has shifted to process heat/process-steam applications with reactor core outlet temperatures of 750 to 800°C [NGNP SRM 2009].

Given this re-direction of the NGNP Project and consistent with [Work Plan 2009], the work reported herein was performed for a steam-cycle MHR having the following basic parameters (designated the “reference” design herein) [Labar 2009]:

Power Level:	≤ 600 MW(t)
Primary Application	Process heat/process steam
Exclusion Area Boundary (EAB)	425 m
Emergency Planning Zone (EPZ)[11]	425 m
Reactor Core Type	Prismatic core

[11] The requirement to meet the PAGs at the EAB allows the EPZ to be co-located at the EAB.

Power Conversion System	Steam cycle (steam generator in primary circuit)
Reactor Building	Vented Low-Pressure Containment (VLPC)
Core Power Density	≤ 6.6 w/cm^3
Fuel Cycle Length:	18 mo
Core He Inlet Temperature:	≤ 322 °C
Core He Outlet Temperature:	≤ 750 °C
System Pressure	7 MPa
Max. Time-averaged Fuel Temperature:	1250°C[12]
Fuel Particle Systems:	(1) Binary fuel particle system: UCO fissile particle (350-μm kernel and 19.9-wt% enrichment and a UCO (or UO_2) fertile particle (500-μm kernel and 0.72-wt% enrichment)[13]
	(2) Single fissile fuel particle: UCO TRISO, ~14-wt% U-235 enrichment, 425-μm kernel[14]

While the "reference" design has a core outlet temperature (COT) of 750 ^oC, higher core outlet temperatures (up to 950 ^oC) are also considered in this evaluation.

2.3 Interrelationship with NGNP Core Performance Analysis Task

This task is closely coupled to a parallel core performance analysis (CPA) task to determine if an acceptable core design can be achieved using a single fissile fuel particle or whether a binary fuel particle system (i.e., including a fissile particle and a fertile particle) is necessary. The CPA task was performed in two phases: the objectives of Phase 1 were to update and verify the computer codes to be used in the CPA, and to complete the first-cut of a binary-fuel-particle core physics design that would serve as the point of departure for the more detailed physics analyses to be performed during the second phase. Phase 2 evaluated both one- and binary-particle core designs and investigated numerous design options to optimize fuel performance, including fuel shuffling [GA 2009a, GA 2009b].

The coupling of these two tasks results from the necessity to perform a quantitative assessment of the fuel performance and fission product release from a "reference" steam-cycle core operating at 750 ^oC and to assess the effects of higher core outlet temperatures. The core physics design and the calculational performance analysis tools developed as part of the CPA task were utilized here as well. The fuel performance and fission product release rates from the core during normal operation were calculated for core outlet temperatures of 750, 800 and 950 ^oC using the final binary-particle core design from the CPA task.

---

[12] Historically, GA has used a maximum time-average fuel temperature of 1250°C only as a guideline (i.e., a rule-of-thumb) in assessing the initial suitability of a core physics design.
[13] The terms "binary," "2-particle," and "fissile/fertile" are used interchangeably to describe this fuel option.
[14] The terms "single" and "1-particle" are used interchangeably to describe this fuel option.

2.4 Background and Planned Approach

2.4.1 Radionuclide Control Philosophy

The most effective means of minimizing radioactive contamination in a nuclear power plant is source reduction. The dominant source of radionuclides in an MHR is the fission product inventory in the reactor core. For modular HTGR designs, a hallmark philosophy has been adopted since the early 1980s to design the plant such that the radionuclides would be retained in the core during normal operation and postulated accidents [e.g., PSID 1992]. The key to achieving this safety goal is the reliance on TRISO-coated fuel particles for primary fission product containment at their source, along with passive cooling to assure that the integrity of the coated particles is maintained even if the normal cooling systems were permanently disrupted.

2.4.2 Radionuclide Containment System

In response to the above goal, a RN containment system for an MHR, which reflects a defense-in-depth philosophy, has been designed to limit radionuclide release from the core to the environment to insignificant levels during normal operation and a spectrum of postulated accidents. Nevertheless, a small fraction of TRISO fuel particles have as-manufactured defects, and these particles may experience in-service coating failure [e.g., PSID 1992], resulting in fission product release from the core and attendant contamination of the primary coolant circuit. A fundamental design requirement is to establish allowable limits on core releases during normal operation and postulated accidents.

As shown schematically in Figure 2-1, the five principal release barriers in an MHR radionuclide containment system are: (1) the fuel kernel, (2) the particle coatings, particularly the SiC coating, (3) the fuel-compact matrix and fuel-element structural graphite, collectively, (4) the primary coolant pressure boundary; and (5) the VLPC. The effectiveness of these individual barriers for containing radionuclides depends upon a number of fundamental factors including the chemistry and half-lives of the various radionuclides, the service conditions, and irradiation effects. The effectiveness of these release barriers is also event specific.

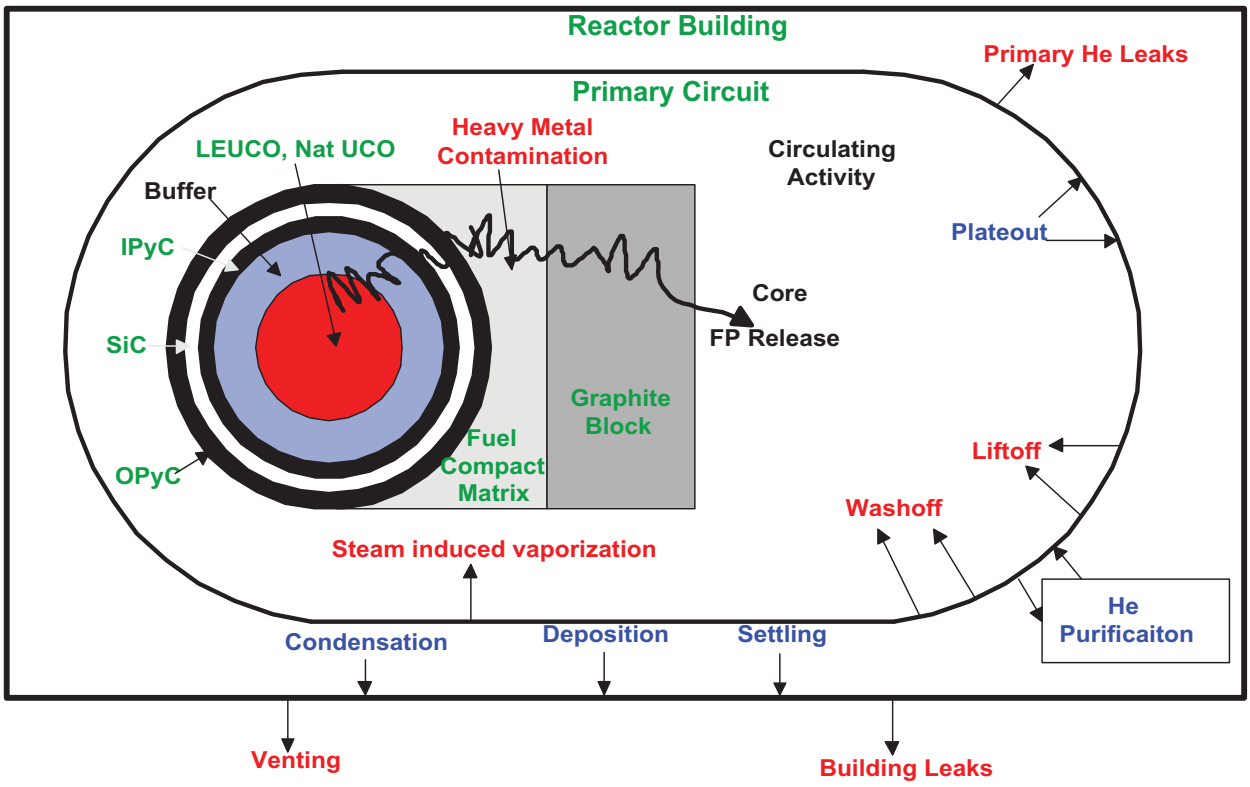

Figure 2-1. MHR Radionuclide Containment System

The first barrier to fission product release is the fuel kernel itself. Under normal operating conditions, the kernel retains >95% of the radiologically important, short-lived fission gases such as Kr-88 and I-131. However, the effectiveness of a UCO kernel for retaining gases can be reduced at elevated temperatures or if an exposed kernel is hydrolyzed by reaction with trace amounts of water vapor which may be present in the helium coolant (the UO_2 kernel used in PBMR fuel is somewhat less susceptible to hydrolysis effects than is UCO). The retentivity of oxidic fuel kernels for long-lived, volatile fission metals such as Cs, Ag, and Sr is strongly dependent upon the temperature and the burnup.

The second - and most important - barrier to fission product release from the core is the silicon carbide and pyrocarbon coatings of each fuel particle. Both the SiC and PyC coatings provide a barrier to the release of fission gases. The SiC coating acts as the primary barrier to the release of metallic fission products because of the low solubilities and diffusion coefficients of fission metals in SiC; the PyC coatings are also partially retentive of Cs at lower temperatures but provide little holdup of Ag and Sr.

With a prismatic core, the fuel-compact matrix and the fuel-block graphite collectively are the third release barrier (with a pebble-bed core, the analog is the pebble matrix, including the unfueled outer shell). The fuel-compact matrix is relatively porous and provides little holdup of the fission gases which are released from the fuel particles. However, the matrix is a composite

material which has a high content of amorphous carbon, and this constituent of the matrix is highly sorptive of metallic fission products, especially Sr. While the matrix is highly sorptive of metals, it provides little diffusional resistance to the release of fission metals because of its high interconnected porosity.

The fuel-element graphite, which is denser and has a more ordered structure than the fuel-compact matrix, is somewhat less sorptive of the fission metals than the matrix, but it is more effective as a diffusion barrier than the latter. The effectiveness of the graphite as a release barrier decreases as the temperature increases. Under typical steam-cycle core conditions, the fuel element graphite attenuates the release of Cs from the core by an order of magnitude, and the Sr is essentially completely retained. The extent to which the graphite attenuates Ag release is not nearly as well characterized, and there is some evidence that the retention of Ag by graphite increases as the total system pressure increases (implying gas-phase transport through the interconnected pore structure of the graphite).

The fourth release barrier is the primary coolant pressure boundary. Once the fission products have been released from the core into the coolant, they are transported throughout the primary circuit by the flowing helium coolant. The He purification system (HPS) efficiently removes both gaseous and metallic fission products from the primary coolant at a rate determined by the gas flow rate through the purification system (the primary purpose of the HPS is to control chemical impurities in the primary coolant). However, for the condensable fission products, the dominant removal mechanism is deposition (“plateout”) on the various helium-wetted surfaces in the primary circuit (i.e., the deposition rate far exceeds the He purification rate).

The plateout rate is determined by the mass transfer rates from the coolant to the fixed surfaces and by the sorptivities of the various materials of construction for the volatile fission products and by their service temperatures. Condensable radionuclides may also be transported throughout the primary circuit sorbed on particulates (“dust”) which may be present in the primary coolant; the plateout distribution of these contaminated particulates may be considerably different than the distribution of radionuclides transported as atomic species.

The circulating and plateout activities in the primary coolant circuit are potential sources of environmental release in the event of primary coolant leaks or as a result of the venting of primary coolant in response to overpressuring of the primary circuit (e.g., in response to significant water ingress in a steam-cycle plant). The fraction of the circulating activity lost during such events is essentially the same as the fraction of the primary coolant that is released, although the radionuclide release can be mitigated by pump down through the HPS if the leak rate is sufficiently slow.

A small fraction of the plateout may also be reentrained, or “lifted off,” if the rate of depressurization is sufficiently rapid. The amount of fission product liftoff is expected to be strongly influenced by the amount of dust in the primary circuit as well as by the presence of

friable surface films on primary circuit components which could possibly spall off during a rapid depressurization.

Other mechanisms which can potentially result in the removal and subsequent environmental release of primary circuit plateout activity are “steam-induced vaporization” and “washoff.” In both cases, the vehicle for radionuclide release from the primary circuit is water which has entered the primary circuit. In principle, both water vapor and liquid water could partially remove plateout activity. However, even if a fraction of the plateout activity were removed from the fixed surfaces, there would be an environmental release only in the case of venting of helium/steam from the primary circuit. For all but the largest water ingress events the pressure relief valve does not lift. Moreover, the radiologically important nuclides, such as iodine and cesium, are expected to remain preferentially in the liquid water which remains inside the primary circuit. (The probability of large water ingress with a gas-turbine plant or a plant with an IHX is much lower than for a conventional steam-cycle plant because with the former the secondary water pressures are lower than the primary He pressures.)

The vented low-pressure containment is the fifth barrier to the release of radionuclides to the environment. Its effectiveness as a release barrier is highly event-specific. The VLPC may be of limited value during rapid depressurization transients; however, it is of major importance during longer term, core conduction cool-down transients during which forced cooling is unavailable. Under such conditions, the natural removal mechanisms occurring in the VLPC, including condensation, fallout and plateout, serve to attenuate the release of condensable radionuclides, including radiologically important iodines, by at least an order of magnitude.

2.4.3 Radionuclide Source Terms

The most important consideration in predicting the radionuclide release rates from an MHR core is to predict the in-service performance of the TRISO-coated fuel particles. However, it is impractical to rely exclusively on the fuel particle coatings for radionuclide containment. Consequently, the effectiveness of the other radionuclide release barriers in the RN containment system must also be quantified.

2.4.3.1 Sources of Radioactive Contamination

The dominant source of radioactive contamination in an MHR will be relatively modest quantities of radionuclide release from the core [e.g., PSID 1992]. *In situ* activation of structural materials will be limited and the activation products will be fixed. There is no analog in an MHR to radioactive “crud” in water-cooled reactors since the helium coolant is chemically inert.

The two dominant sources of fission product release from the core are as-manufactured, heavy-metal contamination and failed particles. In addition, the volatile metals (e.g., Cs, Ag, Sr) can, at sufficiently high temperatures for sufficiently long times, diffuse through the SiC coating and be released from intact TRISO particles; however, diffusive release from intact particles during normal operation is only significant compared to other sources for silver and tritium release.

Fission products resulting from fissions in HM contamination outside of the particles are obviously not attenuated by the kernels or coatings, nor are the fission products produced in the kernels of failed particles appreciably attenuated by the failed coatings. In these cases, the fission products must be controlled by limiting the respective sources and by the fuel-element matrix/graphite in the case of the fission metals and actinides.

Expressed in the simplest terms, the fractional release of a radionuclide from the core is given by the following relationship:

$$(f.r.)_{core} = \frac{C(f.r.)_c + F(f.r.)_F + [1-C-F](f.r.)_D}{AF_{graphite}} \quad (2\text{-}1)$$

where:

- $(f.r.)_{core}$ = fractional release from core
- C = heavy-metal contamination fraction
- $(f.r.)_C$ = fractional release from contamination
- F = failure fraction
- $(f.r.)_F$ = fractional release from failed particles
- $(f.r.)_D$ = fractional diffusive release from intact particles
- $AF_{graphite}$ = graphite attenuation factor[15]

In reality, the problem of calculating the full-core fractional release is much more complicated than implied by Eqn. (2-1). For example, the fissile and fertile particle failure fractions are generally different and vary in space and time, the fractional releases from contamination and failed particles and graphite attenuation factors vary in space and time, and "partially" failed particles (i.e., particles with a failed SiC coating but with intact inner and/or outer pyrocarbon coatings) must also be considered. Full-core computer codes are needed to keep track of all these effects; nevertheless, the results given by Eqn. (2-1) are quite intuitive.

[15] Graphite attenuation factor = fission product release from fuel compact/release into coolant.

2.4.3.2 Fuel Failure Mechanisms

During the past four decades of coated-particle fuel development and demonstration, a number of mechanisms have been identified - and quantified – which can compromise the capability of the coated fuel particles to retain radionuclides (i.e., functional failure of the coated particle). A considerable number of documents have been prepared on the topic of coated particle failure mechanisms; IAEA TECDOC-978 [1997] provides a good summary along with an extensive bibliography.

The following failure mechanisms have been identified as capable of causing partial or total failure of the TRISO coating system under irradiation and during postulated accidents; these mechanisms are shown schematically in Figure 2-2. Phenomenological performance models, typically inspired by first principles and correlated with experimental data, have been developed to model each of these mechanisms. Design methods incorporating these models have been developed to predict fuel performance and fission product release from the reactor core into the primary coolant.

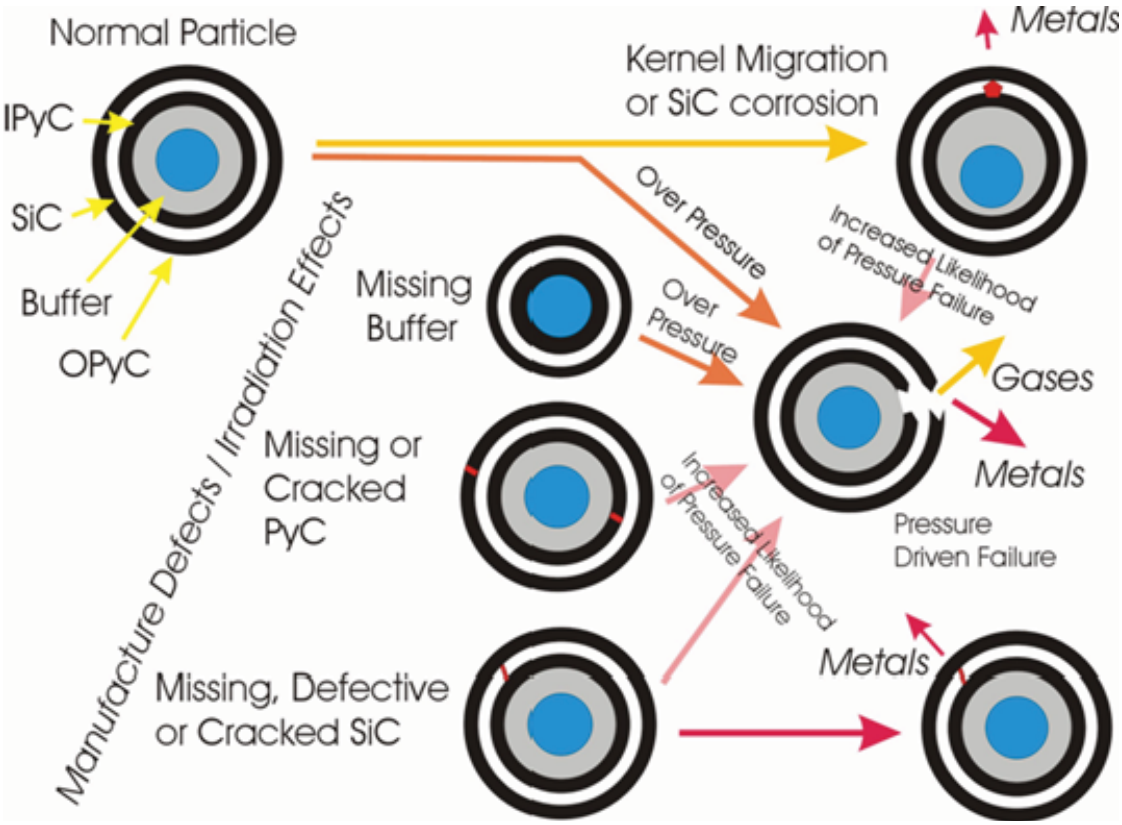

Figure 2-2. TRISO Particle Failure Mechanisms

1. Coating damage during fuel manufacture, resulting in HM contamination on coating surfaces and in the fuel compact matrix.
2. Pressure vessel failure in standard particles (i.e., particles without manufacturing defects).
3. Pressure vessel failure in particles with defective or missing coatings.
4. Irradiation induced failure of the OPyC coating;
5. Irradiation induced failure of the IPyC coating and potential SiC cracking;
6. Failure of the SiC coating due to kernel migration in the presence of a temperature gradient.
7. Failure of the SiC coating caused by fission product/SiC interactions.
8. Failure of the SiC coating by thermal decomposition.
9. Failure of the SiC coating due to heavy-metal dispersion in the IPyC coating.

These particle failure mechanisms will not be discussed in any detail here. The interested reader is encouraged to consult the large number of technical reports and journal articles on the topic. As stated previously, [TECDOC-978 1997] is a good point of departure.

2.4.3.3 Radionuclide Release Mechanisms

As with fuel particle failure, a number of mechanisms have been identified - and quantified – which govern the transport of radionuclides in HTGR core materials, and a large number of documents have been prepared on the topic. Especially notable is Dragon Project Report DP-828, Part III, which provides a comprehensive set of transport models along with analytical solutions for many bounding cases [Nabielek 1974]; this report remains as useful today as it was three decades ago despite the development of numerical methods for predicting fission product transport. Once again, [TECDOC-978 1997] provides a good summary of radionuclide transport phenomena in HTGR core materials along with an extensive bibliography.

The transport of radionuclides from the location of their birth through the various material regions of the core to their release into the helium coolant is a relatively complicated process [Haire 1974, Alberstein 1975]. The principal steps and pathways are shown schematically in Figure 2-3. For certain classes of radionuclides, some steps are eliminated (e.g., noble gases are not diffusively released from intact TRISO particles, and noble gases are not significantly retarded by the compact matrix or fuel-element graphite).

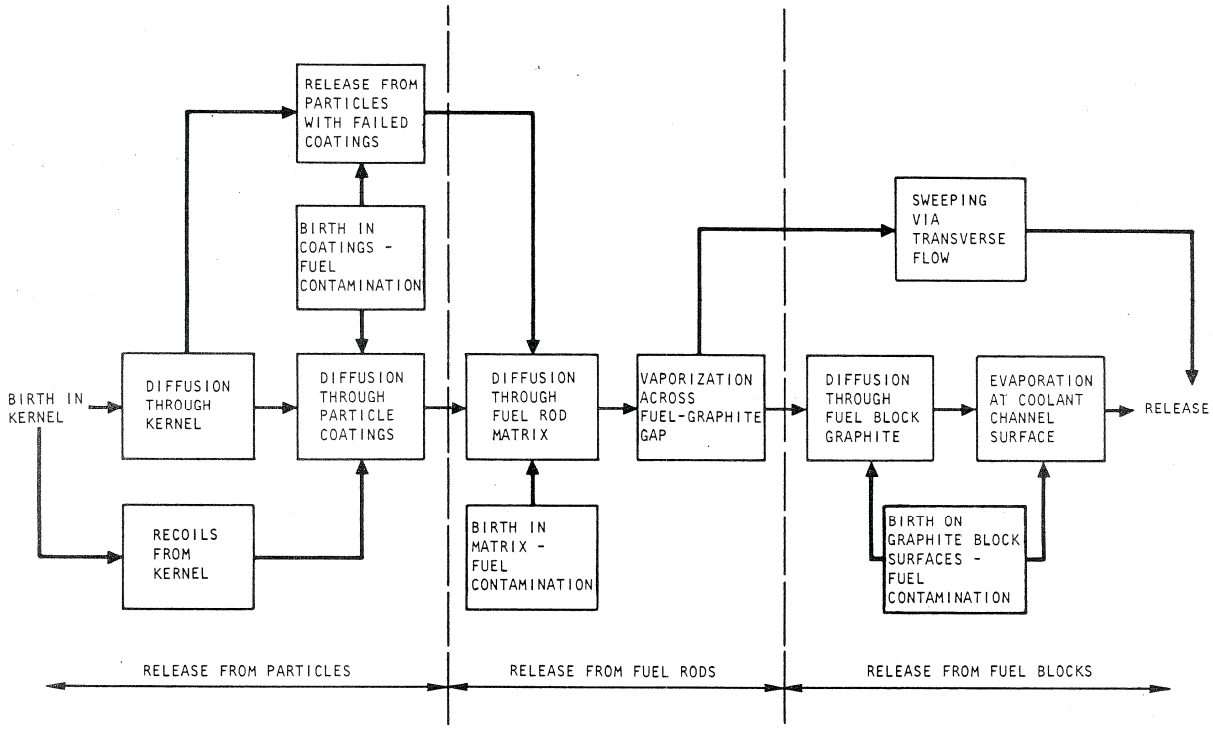

Figure 2-3. Principal Steps in Radionuclide Release from an HTGR Core

As implied by Eqn. (2-1), radionuclide transport must be modeled in the fuel kernel, in the particle coatings, in fuel-compact matrix, and fuel-element graphite. While the actual radionuclide transport phenomena in an HTGR core are complex and remain incompletely characterized after four decades of modeling efforts, the basic approach remains unchanged; radionuclide transport is essentially treated as a transient solid-state diffusion problem with various modifications and/or additions to account for the effects of irradiation and heterogeneities in the core materials. The transport of the various classes of radionuclides (Table 2-1) in the kernels, coatings, matrix and graphite are considered.

Table 2-1. Classes of Radionuclides of Interest for HTGR Design

RN Class	Key Nuclide	Breathing DCF (Sv/Bq)	Form in Fuel	In-Core Behavior
Tritium	H-3	4.3×10^{-11}	Element (gas)	Permeates intact SiC
Noble Gases	Xe-133	~ 0	Element (gas)	Retained by PyC/SiC
Halogens	I-131	2.3×10^{-7}	Element (gas)	Retained by PyC/SiC
Alkali Metals	Cs-134	1.2×10^{-8}	Oxide-Element	Retained by SiC
Tellurium Group	Te-132	6.0×10^{-8}	Complex	Retained by PyC/SiC
Alkaline Earths	Sr-90	7.3×10^{-7}	Oxide-Carbide	High graphite retention
Noble Metals	Ag-110m	1.2×10^{-7}	Element	Permeates intact SiC
Lanthanides	La-140	4.2×10^{-9}	Oxide	Retained by graphite
Actinides	Pu-239	3.2×10^{-4}	Oxide-Carbide	Retained by graphite

2.4.3.4 MHR Accident Source Term Characteristics

The overall MHR source term is a function of as-manufactured fuel quality, fuel performance during normal operation, the extent of fuel heatup during loss of forced cooling, and the extent of chemical attack during water or air ingress events. There are generally two distinct components to the MHR source term: (1) a prompt source term which can be released immediately and (2) a delayed source term whose timing is determined by the slow heatup of the core.

The prompt source term is comprised of the circulating activity and a fraction of the plateout activity. Circulating activity is comprised of mostly noble gases that can be released during a primary coolant depressurization event. Plateout activity is comprised of mostly condensable radionuclides (e.g., I-131, Cs-137, Ag-110m, etc.) that plateout on the He-wetted surfaces of the primary coolant circuit. Plateout activity can be released as the result of surface shear forces during a rapid depressurization event (large break of the primary coolant pressure boundary) and by wash-off or steam-induced vaporization during a water ingress event that causes the pressure relief valves to actuate. The time scale for the prompt source term ranges from seconds to minutes.

For an MHR, the delayed source term is typically much larger than the prompt source term. The combination of graphite with high heat capacity and a core with low power density results in limited fuel temperature transients that occur slowly over time periods of several days during loss of flow or loss of coolant accidents. The delayed source term develops over the course of the heatup portion of the transient and consists primarily of radioactivity released from heavy metal contamination, defective fuel particles that fail during normal operation, and the very small fraction of non-defective (“standard”) particles that fail during normal operation and during the

heatup.[16] During a water-ingress event, hydrolysis of the exposed heavy metal increases the release rate of radioactivity, but the hydrolysis reaction typically occurs over several hours. The time constant for the delayed source term ranges from several hours to days.

As discussed in [Dilling 1993], the delayed source term dominates the radiological source term and offsite doses for the more severe accidents. For these types of accidents, the radiological consequences are reduced by allowing the Reactor Building (RB) to vent at a low differential pressure, resulting in a slow, low-concentration release from the building. If the Reactor Building is designed to vent at a higher differential pressure, the delayed source term will build up within the RB until the relief setpoint is exceeded, resulting in a more rapid, higher-concentration release, which typically results in higher offsite doses.

2.4.3.5 Tritium Transport in MHRs

A radionuclide containment issue of special interest for the NGNP is the containment of tritium [e.g., Hanson 2006b]. Tritium will be produced in an HTGR by various nuclear reactions. Tritium is extremely mobile, especially at high temperature. It permeates and/or diffuses through most solid materials, including ceramics and metals. While tritium does permeate through most solid materials, the permeation rates can vary by many orders of magnitude as illustrated in Figure 2-4.

[16] In the highest temperature regions of the core, some radionuclides (typically noble metals, e.g., Ag-110m) can be released by diffusion through intact coatings.

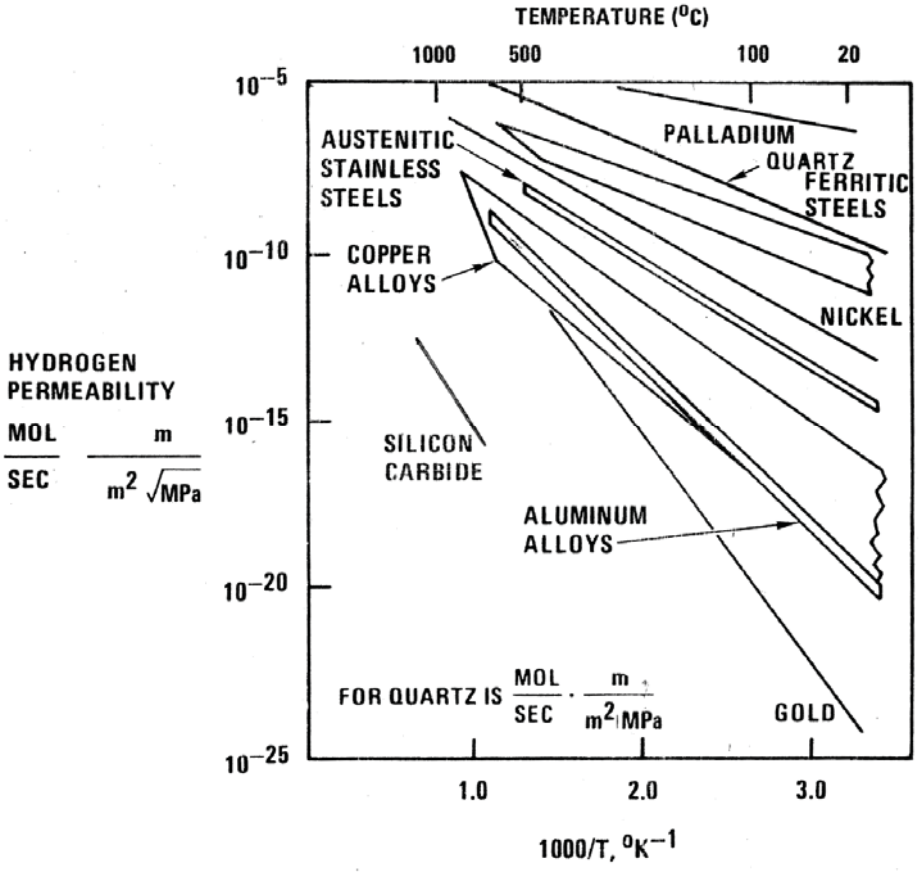

Figure 2-4. H-3 Permeabilities of Various Materials

Given its high mobility, especially at high temperatures, some tritium will permeate through the heat exchangers and process vessels, contaminating the process steam and, potentially, any commercial products. This tritium contamination will contribute to public and occupational radiation exposures; consequently, stringent limits on tritium contamination in commercial products are anticipated to be imposed by regulatory authorities. Design options are available to control tritium in an HTGR, but they can be expensive so an optimal combination of mitigating features must be implemented in the design.

The following sources of tritium production have been identified, primarily from early surveillance programs at operating HTGRs (steam-cycle plants), and they can be reasonably quantified for an MHR: (1) ternary fission, (2) neutron activation of He-3 in the primary He coolant, (3) neutron activation of lithium impurities in fuel-compact matrix and core graphite, and (4) neutron capture reactions in boron in control materials. Ternary fission will be the dominant source of tritium production, but this tritium will be largely retained in the TRISO-coated fuel particles. He-3 activation will generate a relatively modest fraction of the total tritium production in the reactor; however, since it is born in the primary coolant, it will likely be an important source of tritium in the primary helium and, hence, a major source of contamination as well.

Tritium strongly chemisorbs on irradiated nuclear graphite at elevated temperatures (the sorptivity of unirradiated graphite is much lower). Consequently, a large fraction of the tritium entering the primary helium will be sorbed on the huge mass graphite in the core. In operating HTGRs, including Fort St. Vrain, the core graphite was a far more important sink for tritium removal than the helium purification systems. However, a large fraction of this stored tritium can be released if water is introduced into the primary coolant.

Surface films will play a critically important role in establishing the in-reactor, tritium permeation rates. Oxide films can reduce H-3 permeability by orders of magnitude. However, normal plant operating transients (e.g., startup/shutdown, etc.) may compromise film integrity and result in increased H-3 permeation rates.

2.4.3.6 Codes for Predicting RN Source Terms

The US computer codes, component models, and material property data used in the prediction of RN source terms have been described previously [e.g., TECDOC 1997, Martin 1993, Hanson 2004, etc.]. The purpose of this section is not to provide another comprehensive description of these codes, component models, and material property data but rather to provide a summary description and relevant citations.

The prediction of RN source terms during normal plant operation and postulated accidents is part of a core performance analysis sequence that begins with the prediction of core power distributions. The major GA codes used for CPA and the analysis sequence are shown in Figure 2-5 (there are other auxiliary codes for pre-processing, post-processing, etc., that are not shown in the figure). The fuel performance and fission product transport codes are shown in **bold** in Figure 2-5, and their primary functions are summarized below. The aforementioned CPA reports provide additional details about these analytical methods [Ellis 2009a, GA 2009b].

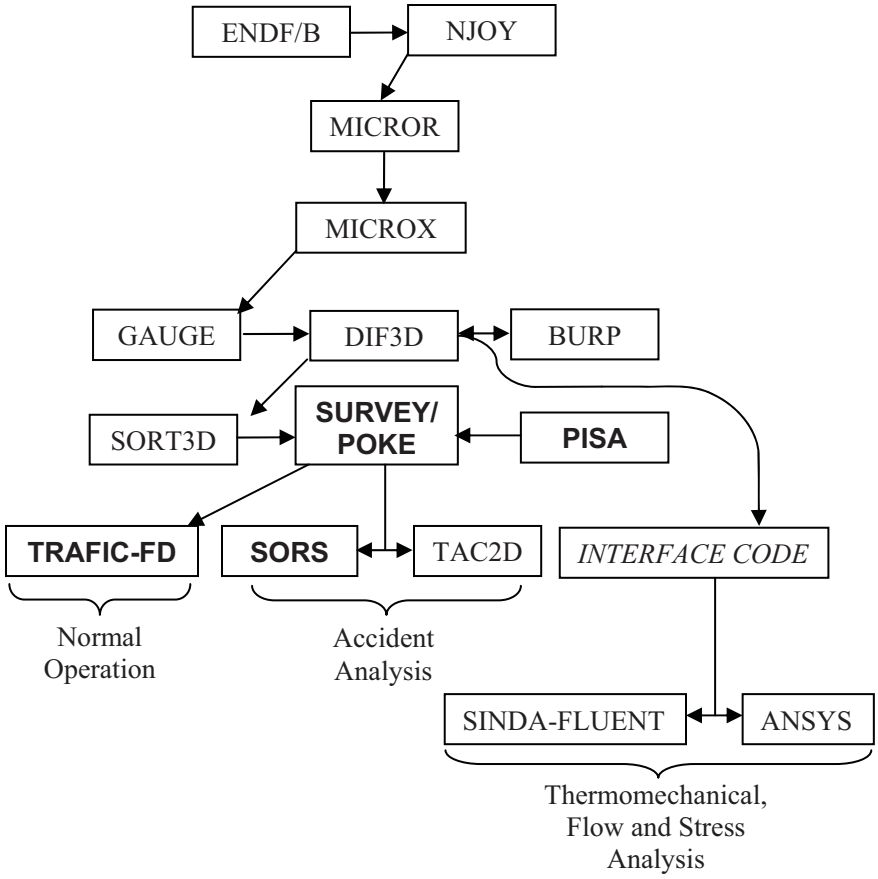

Figure 2-5. Code Flow Sequence for Core Performance Analysis

2.4.3.6.1 Fuel Particle Design

PISA [Pelessone 1993]: A one-dimensional, spherically symmetric, coupled, thermal-stress finite-element code used for fuel particle design, fuel specification development, and irradiation capsule analysis. PISA performs deterministic, non-linear stress analysis of fuel particle "pressure vessel" performance for arbitrary irradiation histories. PISA can also be used to perform Monte Carlo calculations.

SOLGASMIX-PV [Besman 1977]: A thermochemical code that calculates equilibrium relationships in complex chemical systems by minimizing the free energy while preserving the masses of each element present for either constant pressure or volume. The code can calculate equilibria in systems containing a gaseous phase, condensed phase solutions, and condensed phases of invariant and variable stoichiometry. It has been used extensively to model kernel chemistry. (Code was used previously to determine UCO kernel stoichiometry.)

2.4.3.6.2 Fission Product Release from Core

The computer codes currently available to predict fission product transport in prismatic cores during normal operation and core heatup accidents are listed below. (There are a number of related particle analysis codes and support codes that are not included here.)

2.4.3.6.2.1 Normal Operation

SURVEY [Pfremmer 2002]: an analytical/finite difference, core survey code that calculates the steady state, full core, fuel particle coating failure and the full core fission gas releases rates. An automatic interface with the core physics codes provides burnup, fast fluence and temperature distributions; likewise, the temperature and fuel failure distributions calculated by SURVEY are passed on to the metallic release code TRAFIC. SURVEY contains component models for each of the fuel failure mechanisms and fission gas release models for failed particles and HM contamination.

SURVEY/HYDROBURN [Pfremmer 2002]: an optional subroutine in SURVEY which calculates the corrosion of fuel element graphite and the hydrolysis of failed fuel particles by coolant impurities, particularly water vapor. Transport of water vapor through the graphite web of the fuel element is modeled as a combination of diffusion and convection due to cross block pressure gradients. The effects of catalysts and burnoff on the graphite corrosion kinetics are modeled. (Not used in this analysis which assumed all exposed kernels were hydrolyzed.)

TRAFIC-FD [Tzung 1992a]: a core survey code for calculating the full core release of metallic fission products and actinides. TRAFIC-FD is a finite difference solution to the transient diffusion equation for prismatic fuel element geometry with a convective boundary condition at the coolant hole surface. The effect of fluence on graphite sorptivity is modeled explicitly. The temperature and failure distributions required as input are supplied by an automatic interface with the SURVEY code. TRAFIC-FD contains component models for fission metal transport in kernels, coatings, compact matrix and fuel-element graphite.

COPAR-FD [Tzung 1992b]: a stand-alone code as well as a subroutine in the TRAFIC-FD code which calculates the transient fission product release from failed and intact coated particles with burnup dependent kernel diffusivities. COPAR-FD is a finite-difference solution to the transient diffusion equation for multi-region spherical geometry and arbitrary temperature and failure histories.

2.4.3.6.2.2 Accident Conditions

OXIDE-4 [Tangirala 1993]: a computer code for analyzing the transient response following inleakage of steam and/or air into the primary circuit. Based on defined (input) primary system transients and oxidant ingress rates, mass continuity and state equations are solved for all gaseous species. This code also computes fuel hydrolysis and subsequent radionuclide releases from failed fuel particles. Plant protection system actions of moisture detection and

reactor trip, steam generator isolation and dump, and safety valve pressure relief to the reactor building can be simulated. (OXIDE-4 was used to analyze SRDC-6 for the PSID.)

SORS/NP1 [Cadwallader 1993]: a core-survey code for calculating the transient releases of gaseous and metallic fission products; the code is used extensively for the analysis of core conduction cooldown transients. The transient core temperature distributions required as input are supplied by an automatic interface with a suitable, transient thermal analysis code, such as SINDA/FLUENT. SORS/NP1 uses the same material property correlations that are used by the SURVEY code for normal operation but uses a fuel performance model that was specifically developed for core conduction cooldown conditions.

2.4.3.6.2.3 Plant Mass Balance

TRITGO [Hanson 2006a]: a pseudo one-dimensional compartment code which calculates an overall plant mass balance for tritium. TRITGO calculates the production of tritium due to ternary fission of the fuel and neutron reactions with graphite impurities, boron materials, and He-3 in the primary coolant of an HTGR. The code also calculates the tritium permeation through heat exchanger tubes.

RADC [Eichenberg 1993]: A zero-dimensional, steady-state, mass balance code that calculates an overall radionuclide mass balance for the plant: radionuclide inventories in the fuel elements, circulating activity in the primary coolant, plateout on surfaces exposed to the primary coolant, and inventories in the purification system from user-supplied input data defining radionuclide birth rates, decay rates, release rates, plateout (deposition) rates, and coolant purification rates.

2.4.3.7 Component Models and Material Property Data

The reference GA component models and material property correlations are contained in [FDDM/F 1987]. The FDDM/F has several notable limitations; in particular, it presents models and correlations along with extensive references, but it does not include the experimental data from which they were derived. In recognition of the above limitations, Martin of ORNL prepared a compilation in 1993 which collected the GA models and the supporting data base under a single cover [Martin 1993].

2.4.4 Radionuclide Control Requirements

Top-level radionuclide control requirements, such as offsite dose limits and occupational exposure limits, are defined by both plant regulators and (potential) users. Lower-level requirements are then systematically derived using a top-down functional analysis methodology. Previous MHR designs were developed according to the principles of the Integrated Approach [HTGR-85-022 1985]; it is anticipated that the same (or similar) protocol will be utilized for the NGNP Project once the mission has been defined. Since it is anticipated that the design will be similar to the steam-cycle MHTGR (although the power level may be larger), the protocol used

for the MHTGR was employed here. This protocol has been described in detail in [PSID 1992] and elsewhere. The functional analysis for the steam-cycle MHTGR as it relates to the definition of RN control requirements and the attendant fuel performance and quality requirements is described in Appendix A.

The logic for deriving the fuel quality specifications is illustrated in Figure 2-6. Top-level requirements for the plant are defined by both the regulators and the user as described above. Lower-level requirements are then systematically derived using a top-down functional analysis methodology described in [HTGR-85-022 1985]. With this approach, the RN control requirements for each of the release barriers can be defined.[17] For example, starting with the allowable doses at the site boundary, limits on RN releases from the plant, from the reactor vessel, and from the reactor core are successively derived. Fuel performance criteria are in turn derived from the allowable core release limits. Finally, the required, as-manufactured fuel attributes are derived from the in-core fuel performance criteria, thus providing a logical basis for the as-manufactured fuel quality specifications (a key component of the Fuel Product Specification). The logic of the process is illustrated in Figure 2-6.

[17] Referred to as “decontamination factors” in BEA SOW-6795 [Work Plan 2009]. The terms “decontamination factor,” “attenuation factor,” and “retention factor” are used interchangeably throughout this report.

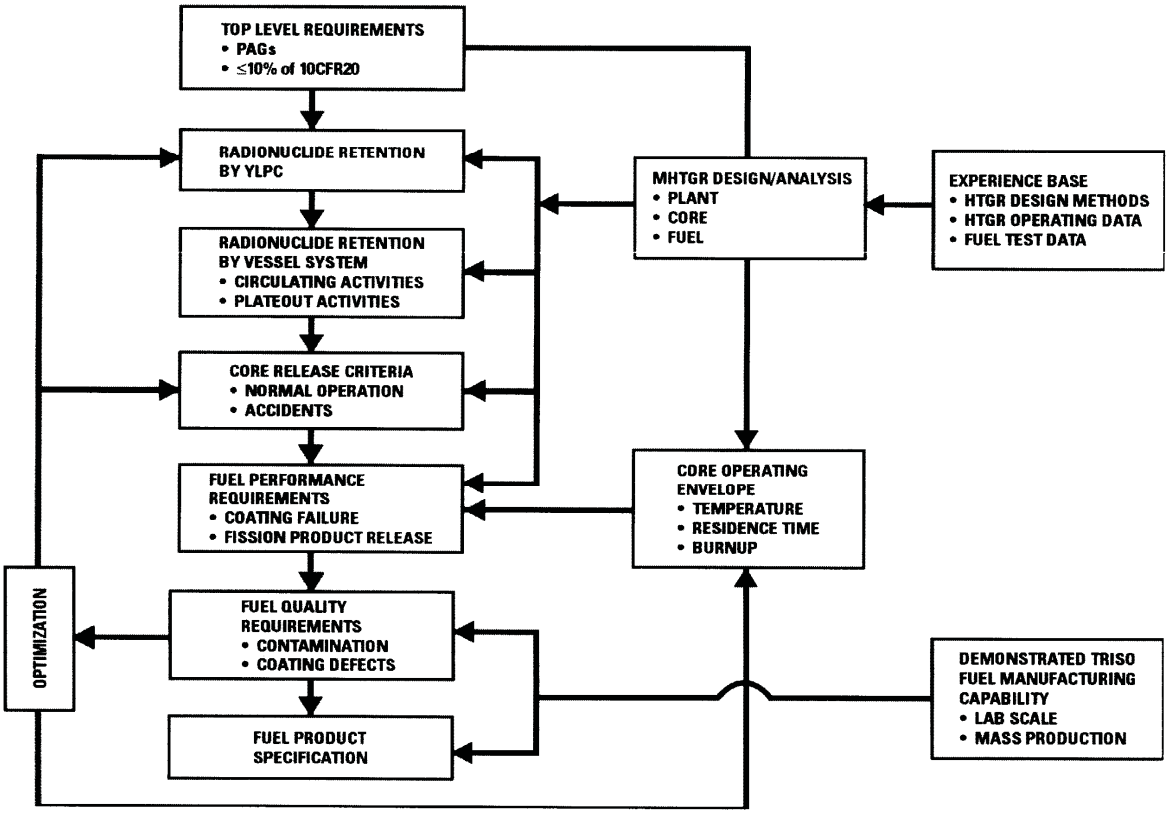

Figure 2-6. Logic for Derivation of As-Manufactured Fuel Quality Requirements

As illustrated in Figure 2-6, this process is necessarily iterative. The primary purpose of performing the functional analysis was to define an estimate of the required fuel quality at the start of preliminary design phase to be used in the detailed fuel performance assessments and safety analyses.

2.4.5 Design Data Needs

In the above process, the reactor designer must make certain assumptions about coated-particle fuel performance and RN transport behavior, especially during the conceptual and preliminary design phases. In some cases, the assumption simply anticipates the expected results of a future trade study or of a more detailed analysis. In this case, the assumption is reviewed after the trade study or analysis has been completed. If the assumption is confirmed, it is replaced by the trade study, and the design is verified; if the assumption is incorrect, then the design must be modified accordingly.

In other cases, the current technology may not be sufficient to judge the correctness of the assumption at the required confidence level, and this leads to a need for improved technology; conducting an R&D program typically satisfies this technology development need [“Design Data Needs” (DDNs)]. Once the test program has been completed, the assumptions are reevaluated

and their correctness assessed. In effect, this second type of assumption is reduced to the first type of assumption described in the preceding paragraph. This iterative procedure is repeated until all the assumptions have been eliminated through either analysis or technology development.

As an adjunct to the functional analysis protocol, a formal methodology was developed for identifying Design Data Needs [DDN Procedure 1986]; the essence of the methodology is illustrated in Figure 2-7.

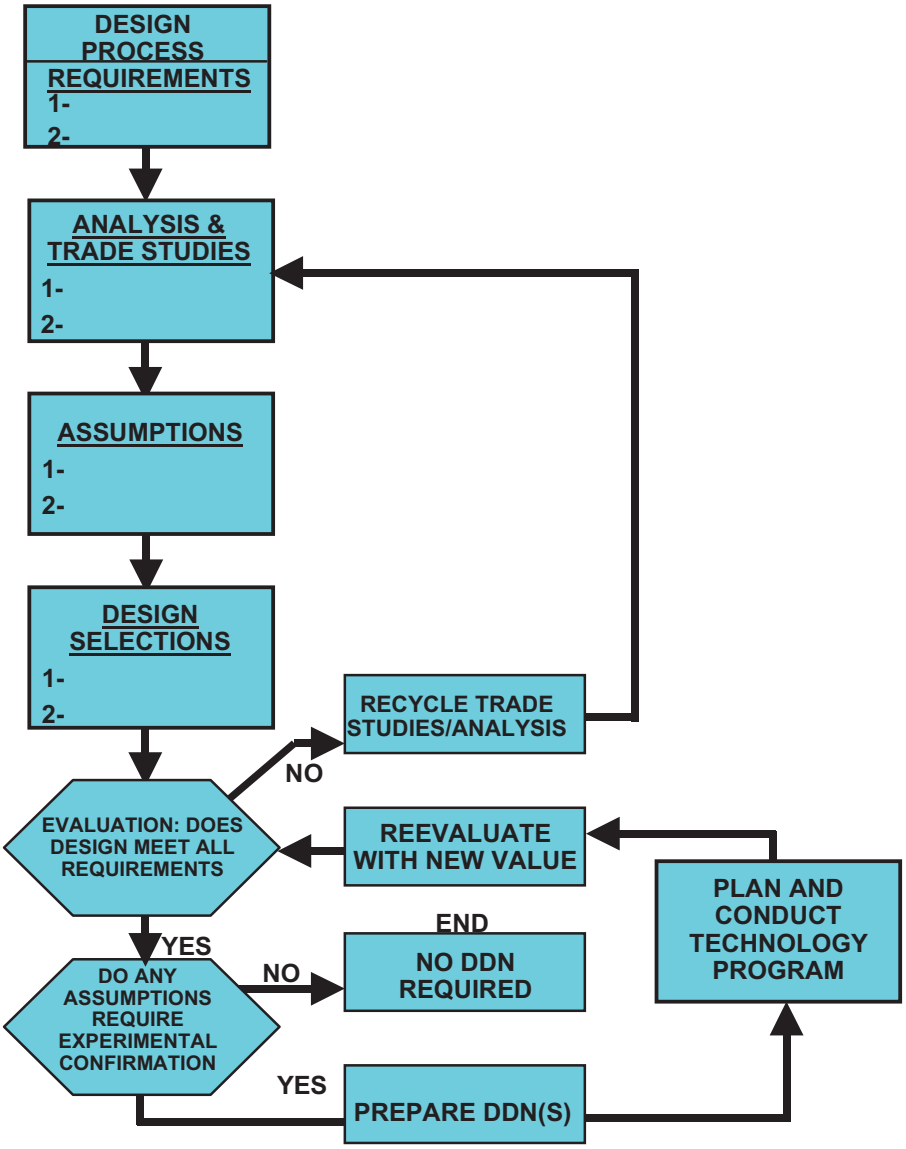

Figure 2-7. Process for Identifying DDNs

2.4.6 Radionuclide Design Criteria

Standard GA design practice is to define a two-tier set of radionuclide design criteria, - referred to as “Maximum Expected” and “Design” criteria, - (or allowable core releases for normal

operation and Anticipated Operational Occurrences); this practice has been followed since the design of the Peach Bottom 1 prototype U.S. HTGR up through the commercial GT-MHR [e.g., Hanson 2002b]. The "Design" criteria are derived from externally imposed requirements, such as site-boundary dose limits, occupational exposure limits, etc.; in principle, any of these radionuclide control requirements could be the most constraining for a given reactor design. The off-site PAG dose limits proved to be the most constraining for the 350 MW(t) steam-cycle MHTGR, and they will probably be the most constraining for future MHRs as well.

Once the "Design" criteria have been derived from the radionuclide control requirements, the corresponding "Maximum Expected," criteria are derived by dividing the "Design" criteria by an uncertainty factor, or design margin, to account for uncertainties in the design methods. This uncertainty factor is typically a factor of four for the release of fission gases from the core and a factor of 10 for the release of fission metals. The fuel and core are to be designed such that there is at least a 50% probability that the fission product release will be less than the "Maximum Expected" criteria and at least a 95% probability that the release will be less than the "Design" criteria. The GA approach to implementing such radionuclide design criteria is illustrated in Figure 2-8. (No particular scale is implied in this figure; it is simply a conceptual illustration of the approach.)

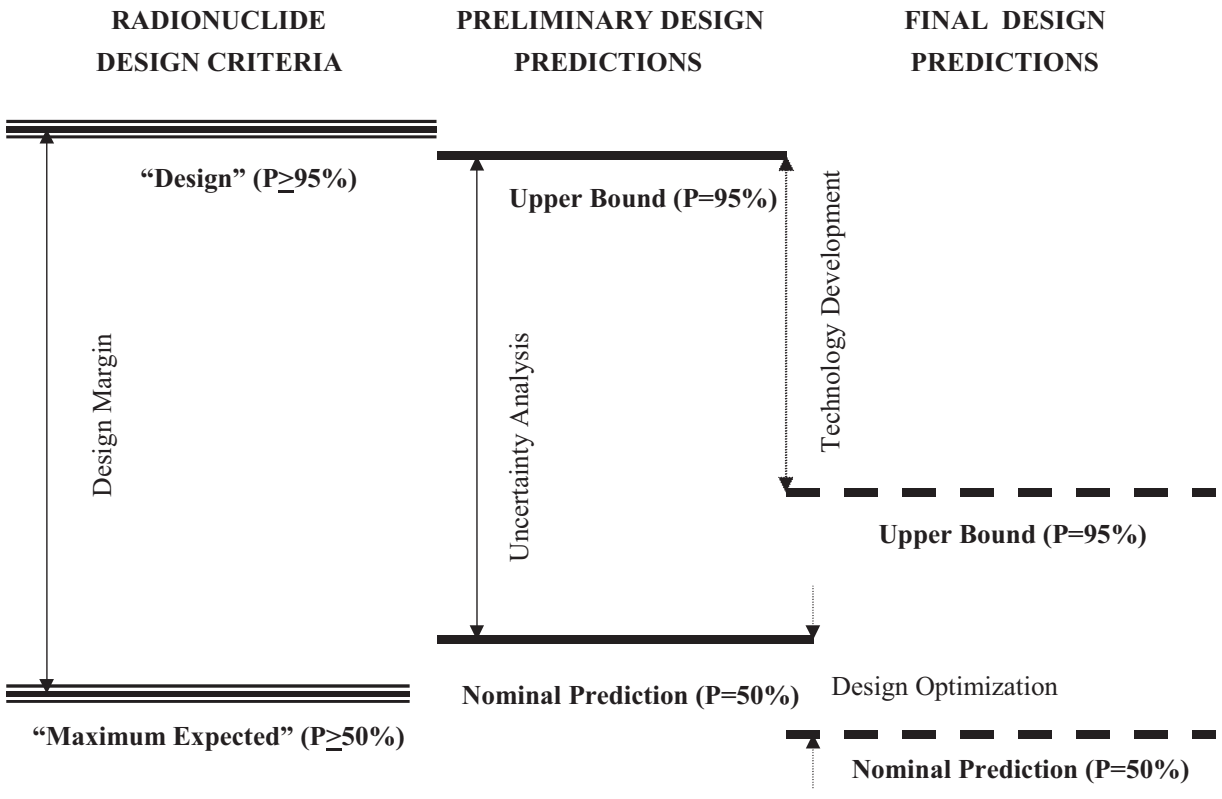

Figure 2-8. Radionuclide Design Criteria

In the example given in Figure 2-8, the Preliminary Design predictions (solid lines) slightly exceed the criteria (triple lines) at the 50% confidence level: i.e., the nominal (50% confidence) prediction is slightly higher than the "Maximum Expected" criterion, but 95% confidence prediction meets the "Design" criterion, primarily because a large design margin was chosen to accommodate the considerable uncertainties in the current design methods at the Preliminary Design stage. This example was chosen because it is anticipated to roughly reflect the current prediction of Ag-110m release from a GT-MHR core, based upon previous GA analysis of the PC-MHR operating with a 850 ^{o}C core outlet temperature. Silver release is of particular concern for a direct-cycle MHR because it can be diffusively released from intact TRISO particles at high temperatures and preferentially deposit on the turbine, where it is predicted to be a dominant contributor to operation and maintenance (O&M) dose rates; it is expected to be a minor contributor to off-site accident doses based upon the safety analysis performed for the 350 MW(t) steam-cycle MHTGR [PSID 1992].

2.4.7 Helium Purification System

In order to avoid deleterious effects on structural materials, undesirable chemical impurities present in the primary coolant must be controlled; consequently, all HTGR designs, including modern VHTR designs, include a helium purification system. Principally, the chemical impurities involved are:

1. H_2O, N_2, and O_2 from graphite outgassing;
2. H_2O, CO, CH_4, CO_2 and H_2 from water ingress and its subsequent reaction with graphite;
3. H_2 and CH_4 from reaction of oil contaminants with graphite;
4. N_2 and O_2 from air ingress during maintenance and venting operations.

Source #2 will be of much less importance for direct-cycle GT-MHRs and for hydrogen-producing VHTRs with an intermediate heat exchanger because of the absence of a steam-generator in the primary circuit which is typically the primary source of water ingress for a steam-cycle HTGR (FSV with its water-bearing circulators was an exception). Source #3 has been practically eliminated for modern MHR designs wherein magnetic bearings have replaced oil-lubricated bearings.

While the primary purpose of the HPS is to control chemical impurities, it also serves to remove radionuclides from the circulating helium coolant, including noble gases and tritium. The HPS also removes condensable radionuclides, including iodine isotopes and volatile fission metals (Ag, Cs, Sr, etc.), but these condensable radionuclides typically deposit on the He-wetted surfaces in the primary coolant circuit much more rapidly than they are removed by the HPS.

Typically, the HPS consists of a number of unit operations to efficiently control the chemical and radioactive impurities in the primary coolant, including tritium. The HPS for the commercial GT-MHR is briefly described below as the most recent example of an HPS conceptual design

[Shenoy 1996]. It is anticipated that the HPS design for future MHRs will be quite similar to that for the GT-MHR although the mass flow rates for the two plant designs may be different.

The GT-MHR HPS operates to remove helium from the primary coolant loop, process it to remove chemical and radioactive impurities, and return the purified helium to the primary coolant loop as purge helium for turbomachinery seals, vessel seals, and vessel pressure relief piping (and possible use for reactor pressure vessel cooing). In addition, the HPS operates in conjunction with the helium transfer and storage train to pressurize, depressurize, and control the primary coolant inventory consistent with plant load.

For a four-module, commercial GT-MHR, the HPS consists of four helium purification sections and two shared regeneration sections [Shenoy 1996]. Each helium purification section purifies a side stream of primary coolant helium at a maximum rate of 0.567 kg/sec (4500 lb/hr), and the regeneration section regenerates spent absorber beds within the helium purification section. One He purification section is provided for each reactor module, while one regeneration section is shared by two reactor modules. A block diagram of the helium purification section is shown in Figure 2-9. The system is a He processing train consisting of filters, dryers, packed beds, and heat exchangers. With the exception of the He compressors and He isolation valves, there are no moving parts which assures that the system that has high reliability and availability.

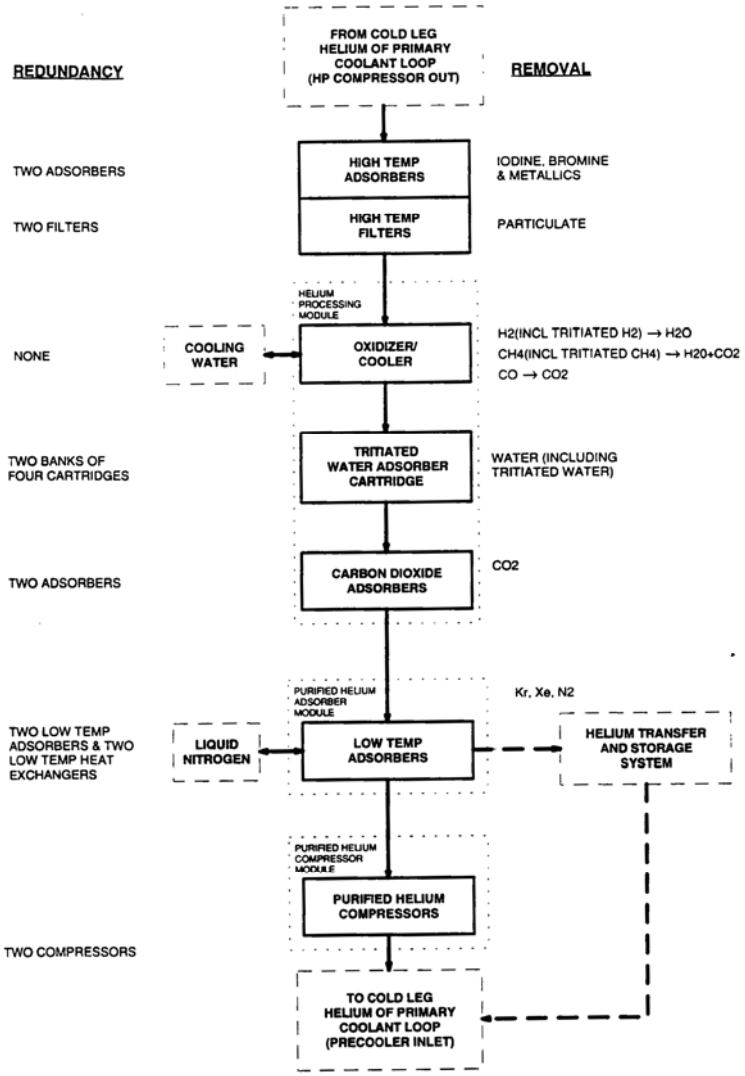

Figure 2-9. Block Diagram of HPS for GT-MHR

With such a design, control of hydrogen and tritium is accomplished by the use of copper oxide beds to oxidize the H_2 and HT to H_2O and HTO, respectively. The tritiated water is subsequently removed by molecular sieve dryers downstream of the oxidizers. Any trace amounts of HT or HTO remaining in the helium will be completely removed by the liquid nitrogen-cooled charcoal beds which are included in the train primarily to remove noble gases.

2.5 Scope of Work

As defined in [Work Plan 2009], the scope of this study includes the following subtasks:

1. Determination of the RN control requirements and corresponding RN release limits for a steam-cycle MHR with a 750 ^{o}C core outlet temperature (Section 3).
2. Allocation of target decontamination factors to Individual RN release barriers (Section 4).
3. Estimation of RN source terms for the "reference" steam-cycle MHR Design (Section 6).
4. Comparison of predicted and target decontamination factors (Section 7).
5. Impact of higher core outlet temperatures on RN source terms and barrier performance (Section 8).

2.6 Assumptions

A number of key assumptions had to be made before the study could be performed; these assumptions are summarized here and repeated throughout the body of the report as they apply.

1. The "reference" steam-cycle MHR will have the characteristics listed in Section 2.2.
2. This MHR will be used to supply process heat/process steam and will be co-located with a chemical plant or petroleum refinery.
3. The Exclusion Area Boundary (EAB) will ultimately be set at 425 m.[18]

2.7 Report Organization

After the introductory and background information presented here in Section 2, the report organization closely follows the Work Plan subtasks (Section 2.5). Conclusions and recommendations are presented in Section 9.

[18] The NGNP System Requirements Manual [2009] specifies "approximately 400 meters," and Statement-of-Work-6795 [2009] specifies a 400-m EAB. The dose/dispersion calculations that are currently available from the safety analyses for the 350 MW(t) MHTGR [PSID 1992] and for the 450 MW(t) MHTGR [Dilling 1993] were done for a 425-m EAB; consequently, a 425-m EAB was assumed here.

3 RADIONUCLIDE CONTROL REQUIREMENTS

The bounding, top-level radionuclide control requirements are established in this section. Top-level radionuclide control requirements are reviewed and their applicability to a future MHR assessed. The primary points of departure for this review are the User/Utility Requirements and the Preliminary Safety Information Document (PSID) for the earlier 350 MW(t) steam-cycle MHTGR along with the NGNP System Requirements Manual (SRM) [2009] and the GA SRM prepared for the GA NGNP pre-conceptual design (GA Document 911102).[19] Once the bounding RN control requirements are determined, the corresponding allowable radionuclide release rates for a future MHR are calculated.

Based upon past experience with steam-cycle MHRs, it is anticipated that the radionuclide release limits presented in this section will provide the appropriate basis for defining the fuel requirements that are summarized in Section 5.

3.1 Top-Level Radionuclide Control Requirements

3.1.1 NGNP SRM Requirements

The plant-level RN control requirements are defined in the NGNP System Requirements Manual [NGNP SRM 2009] Consistent with EPAct 2005, the NGNP SRM defines "…the requirements hierarchy for the NGNP with hydrogen production and electricity production and includes initial requirements based on the current maturity state of the NGNP Project." However, it also states that the near-term NGNP Project emphasis has shifted to process heat/process-steam applications with reactor core outlet temperatures of 750 – 800 ^{o}C for a first-of-kind (FOAK) application. The NGNP SRM includes the following requirements that are directly relevant here (obviously, all of the requirements are applicable to the overall MHR design):[20]

Selection of requirements from the NGNP SRM [2009] for inclusion here became somewhat arbitrary in certain cases. For example, Section 4.3.1, Reactor System, and Section 4.3.3.7, Radioactive Waste and Decontamination System, contain a large number of requirements that could conceivably impact fuel performance or quality requirements or at least serve to establish fuel service conditions. However, since these requirements were typically not quantified (e.g., they were [TBD] or included operators such as "minimize," "reduce," etc.), they were not reproduced herein. As stated above, the NGNP design will ultimately have satisfy (or be granted a waiver) for all of the requirements in the final version of the NGNP SRM.

---

[19] The latter document was prepared for a hydrogen-production MHR operating with a 950 ^{o}C core outlet temperature so that there was considerable emphasis on controlling tritium contamination of the product hydrogen. Tritium contamination of the process steam in a steam-cycle MHR with a 750 ^{o}C core outlet temperature is anticipated to be less of a design issue.

[20] The numbering and nomenclature appearing in this subsection are reproduced verbatim from [NGNP SRM 2009].

3.2.2. HTGR Fundamental Requirements

1. The Nuclear Heat Supply System shall be design certified for a broad range of applications and sites.

2. The NHSS shall be licensed independent of the application.

4. Reactor gas outlet temperature in the range of 750 to 800°C.

6. Capable of controlling the transport of radionuclides to the end products at levels below the concentration or exposure requirements for the product (e.g., tritium in steam, gas, hydrogen). (Initial acceptable tritium levels will be set at a fraction of the U.S. Environmental Protection Agency [EPA] limits for drinking water and air.)

7. Can be collocated with the process; Protective Action Guidelines limits at site boundary of approximately 400 meters.

10. Normal maintenance exposure target limit of no more than 50 person-REM/year per module in a refueling year.

12. Target plant design lifetime of 60 years (calendar).

3.3.1 NRC/EPA/DOE Regulatory Documents

5. 51 CFR 28044, Policy Statement on Safety Goals for the Operation of Nuclear Power Plants

6. 10 CFR 20, Standards for Protection Against Radiation, (Permissible dose levels and activity concentrations in restricted and unrestricted areas).

6. 10 CFR 50, Appendix I – Numerical Guides for Design Objectives and Limiting Conditions for Operation to Meet the Criterion “as Low as is Reasonably Achievable” for Radioactive Material…

11. 10 CFR 100, Reactor Site Criteria, (Numerical dose guidelines for determining the exclusion area boundary, low population zone, and population center distances)

12. 10 CFR 835, Occupational Radiation Protection

16. 40 CFR 190, Environmental Radiation Protection Standards for Nuclear Power Operations

18. EPA, 520/1-75-001, Protective Action Guide Doses for Protective Actions for Nuclear Incidents

4.1.1 System Configuration and Essential Features Requirements

1. The NGNP design will be such that the HTGR can be collocated with the process; PAG limits met at the site boundary of approximately 400 meters.

7. For the NGNP (FOAK), the designed reactor gas outlet temperature shall be in the range of 750 to 800°C.

4.1.2 Operational Requirements

1. The NGNP NHS shall have an operational lifetime of 60 years (calendar).

3. The NGNP shall be designed to use low-enriched uranium (LEU) TRISO-coated particle fuel.

6. The NGNP shall be designed so as to support the anticipated NOAK design to have a normal maintenance exposure target limit of no more than 50 person-REM/year per module in a refueling year.

4.1.4 Environmental Requirements

5. The NGNP and NOAK plant will be capable of controlling the transport of radionuclides to the end products at levels below the concentration of exposure requirements for the product (e.g., tritium in steam, gas hydrogen). (Initial acceptable tritium levels will be set at a fraction of the EPA limits for drinking water and air)

4.1.9 Safety Requirements

2. Protection Criteria for the Worker and the Public are as follows:

    a. Upper bound offsite doses during design basis events shall meet 10 CFR 50.34 with margin.

    b. There shall be a technical basis for eliminating or minimizing the need for offsite emergency planning. This technical basis shall consider a risk-informed, realistic assessment of design basis and beyond design basis accidents and shall demonstrate high confidence that the EPA Protection Action Guidelines are met. The NGNP design shall effectively demonstrate that emergency plan requirements may be minimized (e.g., eliminate requirements for emergency drills, sirens, etc.).

    c. Exposure to the Worker and the Public under normal operation shall meet 10 CFR 20 and ALARA (as low as reasonably achievable) as quantified in Appendix I of 10 CFR 50.

4.1.14 Decommissioning Requirements

1. Upon completion of its useful life, the NGNP nuclear heat source shall be put into a condition of safe storage for 10 years and then decommissioned and dismantled to allow continued use of the land as a power plant or industrial site.

4.2 Requirements Applicable to Fuel

The fuel performance shall allow for a source term calculation capable of obtaining an NRC license with an exclusion zone of no more than 400 meters (approximately) for the design power level.

The fuel shall be designed with the following requirements:[21]

As-manufactured Quality Requirements, at a 95% confidence level:

1. Heavy metal contamination: ≤2 x 10^{-5} (Prismatic Block); ≤6.0 x 10^{-5} (Pebble Bed)

2. SiC Defect Fraction: ≤1 x 10^{-4} (Prismatic Block); ≤6.0 x 10^{-5} (Pebble Bed)

In-service Fuel Performances Requirements, at a 95% confidence level:

1. Fuel failure during normal operations: ≤2 x 10^{-4} (Prismatic Block); ≤4.6 x 10^{-5} (Pebble Bed)

2. Incremental fuel failures during accident conditions: ≤6.0 x 10^{-4} (Prismatic Block); ≤5.0 x 10^{-4} (Pebble Bed)

4.3.1.1 Reactor Core

5. Reference fuel shall be LEU-based (UCO or UO2) with an enrichment limited to <20.0% (in mass)and with a peak burnup limited to 20% fissions per initial metal atom (FIMA).

4.6.2 Hydrogen Production Plant Configuration

12. The total concentration of radioactive contaminants in the hydrogen product gas and associated hydrogen production systems shall be minimized to ensure that worker and public dose limits do not exceed NRC regulatory limits.

[21] In fact, the purpose of the work reported herein is to determine these fuel requirements and a defensible basis for such. These fuel requirements from Section 4.2 of the NGNP SRM [2009] are included largely for completeness.

3.1.2 Bounding Radionuclide Control Requirements

The top-level RN control requirements for the NGNP are listed in Section 3.1.1, and those *quantitative* requirements that could dictate fuel performance and quality requirements are summarized in Table 3-2.

Table 3-1. Key Top Level Requirements that Define Radionuclide Control

Top-Level Regulatory Requirements	
1	10CFR50, Appendix I, Limits for Radionuclides in Plant Effluents (Goals 1 & 2): a. Whole Body Dose ≤ 5 mrem/yr b. Thyroid Dose ≤ 15 mrem/yr
2	10CFR20 Occupational Dose Limits (Goals 1 & 2): a. Whole Body Dose ≤ 5 rem b. Thyroid Dose ≤ 15 rem
3	10CFR100 Offsite Dose Limits (Construction Permit) for Licensing Basis Events (Goal 3): a. Whole Body Dose ≤ 20 rem b. Thyroid Dose ≤ 150 rem
4	EPA-520 PAGs for Radioactive Release for Public Sheltering and Evacuation: a. Whole Body Dose ≤ 1 rem b. Thyroid Dose ≤ 5 rem
5	NRC Safety Risk Limits.
Utility/User Requirements	
1	Occupational Exposures ≤ 10% of 10CFR20 Limits (Goals 1 & 2) a. Whole Body Dose ≤ 0.5 rem/yr b. Thyroid Dose ≤ 1.5 rem/yr
2	Top Level Regulatory Criteria, including PAGs at the Exclusion Area Boundary for all events with a frequency, 5 X 10^{-7}/yr (Goal 3)

3.1.2.1 PAG Dose Limits

From inspection of Table 3-1, meeting "Protective Action Guidelines limits at site boundary of approximately 400 meters" (NGNP SRM, Section 3.2.2 HTGR Fundamental Requirements, Requirement 7) will likely be the most restrictive requirement as far as setting fuel performance and quality requirements for the NGNP. This circumstance should not be surprising since meeting the PAGs at a 425-m EAB was determined to be the bounding RN control requirement for the 350 MW(t) steam-cycle MHTGR [PSID 1992, Hanson 2001] and for the 600 MW(t) direct-cycle GT-MHR [Hanson 1994, Bolin 1994].

However, the exact quantitative dose limits invoked by the programmatic requirement to "…meet the PAG dose limits at the EAB…" is a complex issue. In fact, the various versions of the EPA Protective Action Guides are complicated (and, occasionally, ambiguous) regulatory documents that are subject to a spectrum of logical interpretations. In general, they contain

broad regulatory "guidance" regarding preventive actions to be taken in the event of nuclear incidents that may lead to significant radiation exposure of the public. This guidance is given for a particular timeline: (1) Early Phase (from hours to days until the release has stopped), (2) Intermediate Phase (from a week to months) and (3) Late Phase (from months to years). The guidance addresses not only radiation exposure as a result of immersion and ingestion of radionuclides but also includes limits on contamination of drinking water and foodstuffs as well as decontamination criteria.

In the early versions of the PAGs (the first was in 1975, and there was an update in 1980 that GA cited in the MHTGR PSID), there were both a whole body dose limit (1 rem) and a thyroid dose limit (5 rem) to preclude the need for public sheltering. These PAG limits were the basis for the fuel performance and quality requirements adopted for the 350 MW(t) MHTGR [PSID 1992, Hanson 2001].

In the 1992 version of the PAGs [1992 PAG], the Total Effective Dose Equivalent (TEDE) dose protocol[22] was used instead of the earlier whole-body dose protocol, and the thyroid dose is clearly to be included in the TEDE dose calculations. In addition, [1992 PAG] strongly implies a 5 rem thyroid dose limit to preclude the need for public sheltering (i.e., the lower early phase PAG limit).[23] There is another thyroid dose limit in the 1992 PAGs as well: an anticipated >25-rem thyroid dose requires the administration of potassium iodide to children (<18 years old). Moreover, in the draft 2007 PAGs, it is proposed to reduce this thyroid dose limit for KI administration to 5 rem (i.e., back to the 1980 thyroid PAG dose limit) based upon Food and Drug Administration (FDA) analyses of Chernobyl thyroid dose/cancer data. In fact, there are a multitude of dose limits given in the PAGs, including a 5-rem dose limit to the maximally exposed organ from foodstuff contamination in the draft 2007 PAGs.

[22] The sum of the deep-dose equivalent for external exposures and the committed effective dose equivalent (CEDE) for internal exposures.
[23] Footnote b to Table 2-1 and Section 2.3.2 of [1992 PAG].

A pertinent question is whether or not an MHR should be designed and licensed to preclude the need for KI distribution/administration to children. From its inception, the MHR design and licensing basis has been to avoid public sheltering and evacuation even with the EPZ at a 425-m EAB. Consequently, GA concludes that if the NGNP Project is determined to avoid having to tell the affected public to stay indoors, it would not want to have to tell them to give KI tablets to their children. Further, it seems that the draft 2007 PAG or its equivalent is likely adopted during the next decade and will include an explicit 5 rem thyroid dose limit as well as a 1-rem TEDE dose limit.

Based upon GA's review of the relevant NRC and EPA documents and with input from licensing specialists at URS-WD, GA recommends that the NGNP Project include a 5-rem thyroid dose limit as part of the design and licensing basis for the NGNP. [1992 PAG] strongly implies a 5-rem thyroid dose limit to preclude the need for public sheltering. Moreover, it seems highly likely that the draft 2007 PAG or its equivalent will be adopted during the next decade and that it will include an explicit 5 rem thyroid dose limit as well as a 1-rem TEDE dose limit.[24]

3.1.2.2 Occupational Exposure Limits

The second, most constraining, top-level RN control requirement is to limit the occupational exposure to ≤ 10% of 10CFR20 [GA SRM, PLT 3.1.9, NGNP SRM 2009]. Typically, occupational exposures result primarily from O&M activities, especially ISI, during normal plant operation. The dominant sources of radiation in an MHR which can contribute to worker doses are: (1) direct radiation from the reactor core, (2) neutron activation of structural components, e.g., control rod drives, (3) neutron activation of Ar-40 in the air-cooled Reactor Cavity Cooling System (RCCS), and (4) plateout activity throughout the primary coolant circuit. All of these sources must be controlled to limit occupational exposure; of these, only the limits on plateout activity impose performance criteria on the fuel.

Several occupational exposure assessments have been performed for various MHR designs. For steam-cycle MHRs, the most detailed assessment was done by Bechtel for the 350 MW(t) MHTGR [DOE-HTGR-86809 1989]. The results of this assessment and others for the MHTGR are summarized in Chapter 12 of the PSID [1992]. For direct-cycle GT-MHRs, O&M dose rates are considered to be a greater issue than for a steam-cycle MHR because of the higher core outlet temperatures, and the need to change out the turbine about every seven years [Shenoy 1996]. A maintainability assessment was done for the 600 MW(t) International (Russian) GT-MHR design by Electric Power Research Institute (EPRI) which did not identify any severe O&M issues [EPRI 2001]; however, this assessment provided little insight on expected occupational exposures. The same EPRI team later performed a similar assessment of the

[24] Westinghouse/PBMR also invoked a 5-rem thyroid limit in their reactor building alternatives study [Wells 2008].

South African PBMR and reached essentially the same conclusions [EPRI 2002]; occupational exposures again were not emphasized.[25] The available information on expected occupational exposure for the 600 MW(t) commercial GT-MHR is summarized in Section 8.15 of the GT-MHR Closeout Report [Silady 1996].

Unfortunately, none of the MHR O&M dose assessments cited above included a systematic investigation of the quantitative relationships between the level of primary circuit contamination, the corresponding gamma dose rates, and the attendant occupational exposure. Hence, in deriving limits on plateout activity consistent with the subject goal, it was necessary to rely heavily upon previous occupational exposure assessments, particularly the one for the 2240 MW(t) HTGR-SC/C [Hanson 1983], and upon engineering judgment. On that basis, it was projected that the ≤ 10% of 10CFR20 goal would be met if the gamma radiation fields around the primary circuit due to fission product plateout were limited to ≤ 10 mR/hr for scheduled maintenance activities (e.g., circulator ISI) and to ≤ 100 mR/hr for unscheduled maintenance activities (e.g., SG tube plugging) [Section 4.1.3, PSID 1992].

These limits on gamma dose rates were in turn used to set limits on plateout in the primary circuit. The greatest limitation with the approach is that these earlier HTGR designs had pre-stressed concrete reactor vessels (PCRV) rather than the steel vessels used for all MHR designs, and for certain O&M activities the PCRV would serve as an effective biological shield which could lead to the gamma dose rates being under estimated for comparable activities for an MHR. Once a comprehensive occupational exposure assessment for a steam-cycle MHR is available, these plateout criteria will be reviewed.

The quantitative performance criteria imposed upon the MHTGR radionuclide containment system in order to satisfy the above top-level requirements are summarized below. It should be emphasized that the following description relates to the functional analysis performed to derive the required as-manufactured fuel attributes to provide a basis for the fuel quality specifications. The validity of the many assumptions made in this derivation need to be assessed by detailed design and safety analyses and revised as required.

[25] The EPRI report did indicate that a PBMR design goal was to limit gamma dose rates for planned O&M activities to ≤100 mrem/hr.

3.1.3 Corresponding Limits on Radionuclide Release

3.1.3.1 Dose Conversion Protocol

In addition to the above issue of what quantitative dose limits are invoked by the programmatic requirement to "…meet the PAG dose limits at the EAB…," there is another equally complex issue regarding the protocol to be used to convert these PAG dose limits to corresponding limits on the release of specific radionuclides from the plant to the environment. Such RN release limits are a prerequisite to establishing fuel performance and quality requirements.

Previously, when the rem-to-Curie conversion was made for the steam-cycle MHTGR and for the NP-MHTGR, atmospheric dispersion factors (χ/Q) and breathing rates were taken from USNRC Regulatory Guide 1.4, and the effectivities (rem/Ci) were taken from NRC Regulatory Guide 1.109. More recently, TEDE dose conversion protocol has been adopted.

After considerable internal discussion within GA, discussion with licensing experts at URS-WD and dialogue with BEA, the following approach for making rem-to-Curie conversion was agreed upon for this study:

1. The NGNP Project should include a 5-rem thyroid dose limit as part of the design and licensing basis for the NGNP.

2. Dispersion factors (χ/Q) should be taken from NRC Reg. Guide 1.4. For simplicity (and modest conservatism), a bounding breathing rate of 3.5×10^{-4} m^3/sec should be used. NRC Reg. Guide 1.183 gives the following breathing rates: 3.5×10^{-4} m^3/sec for 0-8 hours, 1.8×10^{-4} m^3/sec for 8-24 hours and 2.3×10^{-4} m^3/sec for >24 hours. The GA-recommended rate is nearly equal to the EPA rate of 3.3×10^{-4} m^3/sec given in [1992 PAG].

3. The dose conversion factors (DCFs) should be taken from Federal Guidance Reports FGR-11 and FGR-12 as explicitly recommended in FGR-13 [Eckerman 1999].

4. The 1-rem whole body TEDE does not permit derivation of a unique set of RN release limits. In contrast, a thyroid dose limit effectively sets a unique limit on iodine release. The RN design criteria given in [Hanson 2008a] – which are largely consistent with those in the MHTGR PSID after adjusting for core power – should be used for normal operation, and the core release rates given in [Richards 2008] should be used for core heatup and water ingress accidents (identified as SRDC-11 and SRDC-6, respectively).

5. Credit should be taken for RN holdup by all of the release barriers as appropriate for a given accident scenario. In particular, credit should be taken for holdup in the PCS during rapid depressurization accidents and by the VLPC during core heatup accidents.

In general, offsite doses are calculated by the following simple formulae, depending upon on whether the dose pathway is due external irradiation due to submersion in a cloud containing disperse radionuclides or due to inhalation of this cloud [Reichert 2009].[26]

Air Submersion Pathway

$$Dose[rem] = \mathrm{Re}lease[Curies] * \frac{\mathrm{X}}{Q}\left[\frac{\sec}{m^3}\right] * Dose\,Conversion\,Factor\left[\frac{rem - m^3}{Ci - \sec}\right] \qquad (3\text{-}1)$$

Inhalation Pathway

$$Dose[rem] = \mathrm{Re}lease[Curies] * \frac{\mathrm{X}}{Q}\left[\frac{\sec}{m^3}\right] * Inhalation\,Rate\left[\frac{m^3}{\sec}\right] Dose\,Conversion\,Factor\left[\frac{rem}{Ci}\right] \qquad (3\text{-}2)$$

The "Dose" of primary interest here is the short-term PAGs; these PAGs are with respect to the effect of airborne releases and the doses resulting from exposure in and to the plume.

3.1.3.2 Radionuclide Retention by Plant Site

The offsite dose limits given in Table 3-1 provide a basis for deriving limits on environmental radionuclide releases from an MHR during Licensing Basis Events (LBEs). Several key assumptions were made in the derivation. Atmospheric dispersion factors and breathing rates were taken from USNRC Regulatory Guide 1.4, and the effectivities (rem/Ci) were taken from NRC Regulatory Guide 1.109. A building wake factor of 1.5x was included.

In calculating the I-131 release limit from the thyroid dose limit, it was assumed, on the basis of analyses supporting preparation of [PSID 1992], that I-131 would be responsible for 50% of the total thyroid dose. In calculating the noble gas release limits from the whole body dose limit, it was assumed, again on the basis of the PSID analyses, that 2.8-hr Kr-88 is the dominant nuclide for short-term events (0-2 hr) and that 5.2-day Xe-133 is dominant for long-term (0-30 day) events. In calculating the Sr-90 release limit, it was assumed that a practiced PAG limit for bone dose would ultimately be defined which is a factor of 30 lower than the practiced 10CFR100 (Construction Permit) dose limit of 75 rem (which is the case for the thyroid dose

[26] The SI units of Sieverts and Becquerels can be used in place of rems and Curies as long as the usage is consistent.

limit).[27] Insufficient information was available to define limits on the offsite releases of volatile fission metals (e.g., Cs and Ag). The resulting limits on radionuclide releases from the plant are summarized below.

The MHR plant shall be designed such that the releases of the following key radionuclides from the plant during short-term (0 to 2-hr) and long-term (0 to 30-day) accidents are limited to values given in Table 3-2.

Table 3-2. Limits on Off-Site RN Releases during LBEs

	PAG (User) Limits (Ci)		10CFR100 (Reg) Limits (Ci)	
Nuclide	**Short-Term**	**Long-Term**	**Short-Term**	**Long-Term**
Kr88	≤ 170	≤ TBD	≤ 3400	≤ TBD
Xe-133	≤ TBD	≤ 2300	≤ TBD	≤ 46,000
I-131	≤ 2.6	≤ 29	≤ 78	≤ 870
Sr-90	≤ 0.1	≤ 1.2	≤ 3	≤ 36
Ag-110m	≤ TBD	≤ TBD	≤ TBD	≤ TBD
Cs-137	≤ TBD	≤ TBD	≤ TBD	≤ TBD

3.2 Requirements Mandating Tritium Control

The 10CFR20 limits for occupational exposure, including a factor of 10 ALARA margin, will have to be met for all pathways that expose plant workers to tritium-contaminated products and to tritium-contaminated process steam and secondary coolant water. The 10CFR50, Appendix I, dose limits for off-site releases from nuclear power plants during normal operation will have to met, including the contributions from tritium releases via liquid, gaseous, and solid pathways. These regulatory limits will be the basis for deriving quantitative tritium release limits once a conceptual MHR plant design is defined.

3.3 Limits on Tritium Contamination in Products

A perplexing challenge at this stage of the NGNP Project is to set a provisional limit on the allowable tritium contamination in commercial products and/or process steam when the plant mission still being determined. The international regulatory standards for allowable tritium contamination in air and drinking water vary remarkably (see Table 3-3). For example, the regulatory limits on tritium in drinking water (Table 3-4) vary from a low of 2.7 pCi/g in France to

[27] In fact, no such anticipated bone-dose limits were included in the 1992 PAG or in the draft 2007 PAG. Consequently, it may be possible to relax the PSID limit on Sr-90 release. However, 29-yr Sr-90 concentrates in the food chain and may be an important contributor to foodstuff contamination.

2057 pCi/g in Australia to no tritium-specific regulatory limits in Japan and Korea (although the public exposure from all sources of artificial radiation is obviously controlled); the US EPA standard is 20 pCi/g (0.74 Bq/g) [CNSC 2008]. Traditional exposure pathway analysis for specific assumed release and transport scenarios appears inappropriate for this stage of NGNP design definition. Consequently, it is recommended that the US EPA drinking water standard of 20 pCi/g be provisionally adopted as the goal for allowable tritium contamination in the product hydrogen and/or process steam for MHR conceptual design [Hanson 2008a].

Table 3-3. International Limits on Tritium Contamination in Various Media

Organization	H-3 Limit	Value
Regulatory Limits		
US NRC	Air	**84 pCi/g** (100 pCi/l)
US EPA	Drinking Water	**20 pCi/g** (20,000 pCi/l)
France, Germany, UK	Drinking Water	**2.7 pCi/g** (100 Bq/l)
Canada (Ontario)	Drinking Water	**189 pCi/g** (7000 Bq/l)
Australia	Drinking Water	**2057 pCi/g** (76,103 Bq/l)
IAEA	Exemption Limits	**27 x 10^6 pCi/g** (10^6 Bq/g)
Programmatic Limits		
PNP (FRG)	H-3 in syn gas	**10 pCi/g**
KINS (Korean "ACRS")	H-3 in hydrogen (IAEA limit)	**27 x 10^6 pCi/g**
KAERI (Korea)	Air	**6284 pCi/g** (232.5 Bq/g)
KAERI (Korea)	Water	**1081 pCi/g** (40 Bq/g)
JAERI (Japan)	H-3 in hydrogen	**1510 pCi/g**
MHR	H-3 in hydrogen/steam	[**20**] **pCi/g** (EPA H_2O)

This recommendation can be compared with the previous German goal of ≤ 10 pCi/g of tritium in synthetic natural gas produced by coal gasification with a pebble-bed HTR (the so-called PNP Project). It is fully expected that as the NGNP Project conceptual design progresses and a traditional exposure pathway analysis is performed, it will be demonstrated that this 20 pCi/g limit on tritium contamination is excessively conservative and that it can be relaxed by at least two orders of magnitude (as was the case for the PNP Project). Consequently, this recommended limit should not be considered a formal requirement for the NGNP Project but an early and ambitious figure-of-merit for use until the conceptual design is defined.

While tritium control would likely be an important issue for a VHTR producing hydrogen or other commercial feedstocks and/or products, it is of little or no practical consequence when defining fuel performance and quality requirements. Tritium is diffusively released from intact TRISO

particles at high temperatures and is also produced by other external sources outside of the fuel particles. Consequently, the as-manufactured defect fractions and in-service exposed kernel fractions have only a modest influence on the total concentration of tritium in the primary helium coolant. Fortunately, other design solutions are available to control tritium in a VHTR [e.g., Hanson 2008a]. Given these circumstances, tritium control will receive no further attention in the present report.

Table 3-4. International Limits for Tritium in Drinking Water

TABLE A1.
SUMMARY TABLE OF INTERNATIONAL LIMITS FOR TRITIUM IN DRINKING WATER

		Power reactors*		Information Obtained	Tritium Limit (Bq/L)
		CANDU	Total		
CANDU OWNERS	Canada	18	18	yes	7,000
	- Alberta	0	0	yes	7,000
	- Manitoba	0	0	yes	7,000
	- N. Brunswick	1	1	yes	none
	- Ontario	16	16	yes	7,000
	- Quebec	1	1	yes	7,000
	India	15	17	no	n/a
	Republic of Korea	4	20	partly	none
	Romania	2	2	yes	100
	China	2	10	yes	none
	Argentina	1	12	partly	none
	Pakistan	1	2	no	n/a
EU	Total	2	126	yes	100
	Belgium	0	7	yes	100
	Finland	0	4	yes	30,000
	France	0	59	yes	100
	Germany	0	17	yes	100
	Italy	0	0	yes	100
	Northern Ireland	0	0	yes	100
	Scotland	0	2	yes	100
	Spain	0	8	yes	100
	Sweden	0	10	yes	100
	United Kingdom	0	19	yes	100
OTHER	Australia	0	0	yes	76,103
	Japan	0	53	partly	none
	Norway	0	0	yes	100
	Russia	0	31	partly	7,700
	Switzerland	0	5	yes	10,000
	United States	0	103	yes	740
	- California	0	4	yes	740
	WHO	n/a	n/a	yes	10,000

* Sources:
World Nuclear Association reactor database
http://www.world-nuclear.org/reference/reactorsdb_index.php
CANDU Owners Group website
http://www.candu.org

4 TARGET DECONTAMINATION FACTORS

Using a top-down functional analysis methodology, the goal is to assign target "decontamination factors" to the multiple RN release barriers in the MHR radionuclide containment system such that the top-level RN control requirements applicable to the MHR are satisfied during normal plant operation and a broad spectrum of postulated accidents. As described in Section 2.4.2, the principal release barriers are: (1) the fuel kernel, (2) the particle coatings, particularly the SiC coating, (3) the fuel-compact matrix/fuel-element graphite collectively, (4) the primary coolant pressure boundary; and (5) the reactor building/containment structure.

4.1 Target Decontamination Factors by RN Release Barrier

The near-term NGNP Project emphasis has shifted to process heat/process-steam applications with reactor core outlet temperatures of approximately 750 - 800 ^{o}C [NGNP SRM 2009], and the GA team has proposed a conceptual design of a 600 MW(t) steam-cycle MHR with a core outlet temperature of 750 ^{o}C [Labar 2009].[28] Given the lack of an approved conceptual plant design and the lack of a detailed safety analysis for such a design, the decontamination factors derived for the 350 MW(t) steam-cycle MHTGR [PSID 1992] were adopted here as the targets for the steam-cycle MHR as a necessary expedient. (The MHTGR design and safety analysis were far more advanced than the aforementioned GA conceptual design at this writing.)

4.1.1 RN Retention by VLPC

As introduced above, the safety risk for a steam-cycle MHR is dominated by three classes of events: (1) rapid depressurization, (2) depressurized core conduction cooldown, and (3) steam ingress plus pressure relief. Because the VLPC is not designed for high pressure, it was assumed to provide no radionuclide retention during a rapid depressurization event. However, during the other two dominant classes of events, it was assumed that the building will attenuate release of condensable radionuclides, including iodines, to the environment by [10x] because of plateout and settling and also by washout in the case of steam ingress plus pressure relief.

No direct measurements have been made of RN removal from contaminated helium by condensation, settling, and plateout under the conditions expected in the VLPC during a core heatup event. There is an extensive LWR and CANDU database on the behavior of radionuclides in water-reactor containment buildings. Some of these LWR data, especially those that relate to RN partitioning between steam and liquid phases in steam-water mixtures, may be applicable to RN behavior in VLPCs. After an extensive review, the water-reactor database was judged to be of limited value for refining and independently validating the design methods used to predict RN transport in VLPCs [Hanson 2007a]. An experimental program has

[28] Based upon past optimization studies for steam-cycle MHRs, the optimal core outlet temperature for a steam-cycle MHR may ultimately prove to be closer to 700 ^{o}C, depending upon the specific application.

been proposed to characterize RN transport under the conditions predicted for the VLPC during specific MHR accident scenarios [Hanson 2008c].

4.1.2 RN Retention by Primary Coolant Pressure Boundary

As in the case of the VLPC, the effectiveness of the primary coolant pressure boundary as a radionuclide release barrier is strongly dependent upon the nature of the event. During a rapid depressurization, it was conservatively assumed that 100% of circulating activity and ≤ 5% of plateout activity will be released from reactor vessel to the VLPC and, ultimately, to the environment. During depressurized core conduction cooldown events, it was assumed that releases of condensables will be attenuated by ≥ [30x] by primary circuit removal mechanisms including in-vessel plateout and thermal contraction of the gas mixture in the vessel.

For steam ingress plus pressure relief, it was assumed that initially 100% of circulating activity will be released and that ≤ 50%] of the plateout activity will be removed from fixed surfaces by steam induced vaporization and/or washoff. However, the pressure relief valve will reset after ~15% of gaseous volume is released; consequently, radionuclides in coolant as a result of washoff and incremental core releases, including iodines, will be attenuated by [7x (1/0.15)].

The extensive international data base regarding radionuclide transport behavior in the primary coolant circuit has been summarized in several reports [e.g., TECDOC-978 1997, Hanson 2002, Hanson 2005]. However, the uncertainties in the transport models are excessively large, especially regarding the plateout and liftoff behavior of iodine and volatile metals. The major reasons for these uncertainties are: (1) large uncertainties in the transport models (e.g., the effects of particulate matter in the primary circuit on plateout behavior); and (2) very large uncertainties in the material property data (e.g., sorption isotherms used as input to the models).

Test programs have been proposed to develop and validate design methods for predicting design methods for predicting RN transport in the primary circuit. First, out-of-pile, single-effects tests would be performed to generate the test data needed to upgrade the component models (e.g., sorption isotherms) [Hanson 2005]. Then independent integral tests in an in-pile loop would be performed to confirm the validity of these upgraded design methods [Hanson 2004].

4.1.3 RN Retention by the Reactor Core

Three of the primary RN retention barriers are in the reactor core: (1) fuel-element graphite/fuel-compact matrix collectively; (2) particle coatings, especially the SiC coating; and (3) fuel kernels. The target decontamination factors for each is described below.

Given the above limits on radionuclide releases from the plant (Section 3.1.3.2) and the assumed attenuation factors for the VLPC (Section 4.1.1) and for the reactor vessel (Section 4.1.2), limits on RN release from the reactor core can be derived for normal operation and for LBEs.

During normal operation, radionuclide release from core is limited such that a ≤ 5% liftoff of I-131 and Sr-90 can be accommodated during rapid depressurization events (Goal 3). Limits on Cs and Ag release were derived from Goals 1 and 2 considerations; specifically, plateout activities are limited such that expected gamma dose rates for tube plugging after 40 yr of operation will be ≤ 100 mR/hr.

As discussed in Section 3.1.2.2, none of the MHR O&M dose assessments performed to date has included a systematic investigation of the relationships between the level of primary circuit contamination, the corresponding gamma dose rates, and the attendant occupational exposure. Hence, in deriving limits on plateout activity consistent with the subject goal, it was necessary to rely heavily upon previous occupational exposure assessments, particularly the one for the 2240 MW(t) HTGR-SC/C [Hanson 1983], and upon engineering judgment.

For the 2240 the “Maximum Expected” gamma dose rate was 300 mR/hr or factor of three higher than the steam-cycle MHTGR criterion; consequently, the Cs and Ag plateout limits for the MHTGR were obtained by scaling the 2240 plateout limits [Jovanovic 1984] by thermal power and then reducing the results by an additional factor of three.

As described in Section 2.4.6, a two-tier set of radionuclide design criteria, referred to as "Maximum Expected" and "Design" criteria, are defined for normal operation. To reiterate, the "Design" criteria are derived from externally imposed requirements, such as the site-boundary dose limits discussed above. The "Maximum Expected," criteria are then derived by dividing the "Design" criteria by an uncertainty factor, or design margin, to account for uncertainties in the design methods. This uncertainty factor is a factor of four for the release of fission gases from the core and a factor of 10 for the release of fission metals. The fuel and core are to be designed such that there is at least a 50% probability that the fission product release will be less than the "Maximum Expected" criteria and at least a 95% probability that the release will be less than the "Design" criteria.

These limits on circulating and plateout activity in the primary circuit during normal operation are summarized in Table 4-1 [Hanson 2001; PSID 1992, Section 4.2.3]; it should be noted that this is only a representative listing of key radionuclides. Core release limits are actually specified for some 250 radionuclides in [PSID 1992, Section 11.)].

Table 4-1. Limits on Primary Circuit Activity during Normal Operation

Nuclide	Primary Circuit Activity (Ci)			
	Circulating Activity		Plateout Activity	
	P ≥ 50%	P ≥ 95%	P ≥ 50%	≥ 95%
H-3	0.2	0.7	-	-
Kr-88	5.5	22	-	-
Xe-133	2.5	10	-	-
I-131	0.02	0.08	20	80
Sr-90	-	-	0.32	3.2
Ag-110m	-	-	7.3	73
Cs-137	-	-	70	700
Cs-134	-	-	13	132

Limits on radionuclide release from the core are also specified for the dominant LBEs. For depressurized core conduction cooldown events, core release limits are calculated from the long-term plant release limits given in Table 4-2; for the condensable radionuclides, including iodines, attenuation factors of 30 and 10 are assumed for the reactor vessel and VLPC, respectively.[29] It should be noted that since this is a design-basis event, compliance is required at the 95% confidence level. Results for key radionuclides are summarized in Table 4-2:

[29] In [PSID 1992] no credit was taken was taken for holdup in the VLPC during core conduction cooldown events.

Table 4-2. Core Release Limits during Core Conduction Cooldown Events

Nuclide	Core Release Limits during Core Conduction Cooldown Events (Ci)	
	PAG (User) Limits P ≥ 95%	10CFR100 (Reg) Limits P ≥ 95%
Kr-88	≤ TBD	≤ TBD
Xe-133	≤ 2300	≤ 46,000
I-131[30]	≤ [13,050]	≤ [3.9 x 10^5]
Sr-90[31]	≤ [540]	≤ [16,200]
Ag-110m	≤ TBD	≤ TBD
Cs-137	≤ TBD	≤ TBD

Limits on incremental radionuclide release from the core during short-term design basis events, such as steam ingress with pressure relief, are calculated from the short-term plant release limits given in Table 4-2. In this event, 50% of the plateout activity is initially reentrained as a result of the water ingress, but the pressure relief valve reseats after 15% of the gaseous inventory is released from the vessel providing a factor of 7 attenuation. For condensable radionuclides, including iodines, an attenuation factor of 10 is also assumed for the VLPC. It should be noted that since this is also a design-basis event, compliance is again required at the 95% confidence level. Results for key radionuclides are summarized in Table 4-3.

[30] In [Section 4.2.3, PSID 1992] the allowable limits for I-131 are < 870 and < 26,000, respectively; the basis for these lower limits has not been identified at this writing.
[31] In [Section 4.2.3, PSID 1992] the allowable limits for Sr-90 are < 36 and < 1080, respectively; the basis for these lower limits has not been identified at this writing.

Table 4-3. Core Release Limits during Water Ingress plus Pressure Relief Events

	Incremental Core Release Limits during Steam Ingress plus Pressure Relief (Ci)			
	PAG (User) Limits		10CFR100 (Reg) Limits	
Nuclide	P ≥ 50%	P ≥ 95%	P ≥ 50%	P ≥ 95%
Kr-88[32]	≤ TBD	≤ [1168]	≤ TBD	≤ [23,780]
I-131[33]	≤ TBD	≤ [233]	≤ TBD	≤ [8150]

For the 350 MW(t) steam-cycle MHTGR, the Curie release limits given in this subsection were easily converted to fractional release limits using the total core inventories given in [Jovanovic 1987] with appropriate consideration of effects of radioactive buildup and decay. The results are summarized in Table 4-4.[34]

[32] In [Section 4.2.3, PSID 1992] the allowable limits for Kr-88 are < TBD < 148 < TBD < 3378, respectively.

[33] In [Section 4.2.3, PSID 1992] the allowable limits for I-131 are < TBD < 260 < TBD < 7800, respectively.

[34] Everything being equal, the corresponding fractional release limits for the 600 MW(t) would be lower by the ratio of the thermal powers (a factor of 1.7).

Table 4-4. Summary of Allowable Core Release Fractions for MHTGR

Normal Operation		
	Allowable Core Fractional Release	
Nuclide	**≥ 50% Confidence**	**≥ 95% Confidence**
H-3	≤ [TBD]	≤ [TBD]
Kr-88	≤ [7.5×10^{-7}]	≤ [3×10^{-6}]
Xe-133	≤ [1.5×10^{-6}]	≤ [6×10^{-6}]
I-131	≤ [1.9×10^{-6}]	≤ [7.4×10^{-6}]
Sr-90	≤ [5×10^{-8}]	≤ [5×10^{-7}]
Ag-110m	≤ [5×10^{-4}]	≤ [5×10^{-3}]
Cs-137	≤ [7×10^{-6}]	≤ [7×10^{-5}]
Cs-134	≤ [7×10^{-6}]	≤ [7×10^{-5}]
Depressurized Core Conduction Cooldown Events		
	Allowable Core Fractional Release	
Nuclide	**PAG (User) Limits P ≥ 95%**	**10CFR100 (Reg) Limits P ≥ 95%**
Kr-88	≤ TBD	≤ TBD
Xe-133	≤ [1.1×10^{-4}]	≤ [2.3×10^{-3}]
I-131	≤ [1.4×10^{-3}]	≤ [0.04]
Sr-90	≤ [7.3×10^{-4}]	≤ [0.02]
Ag-110m	≤ TBD	≤ TBD
Cs-137	≤ TBD	≤ TBD

Water Ingress plus Pressure Relief Events				
	Allowable Core Fractional Release			
	PAG (User) Limits		**10CFR100 (Reg) Limits**	
Nuclide	**P ≥ 50%**	**P ≥ 95%**	**P ≥ 50%**	**P≥ 95%**
Kr-88	≤ TBD	≤ [1.2×10^{-4}]	≤ TBD	≤ [2.4×10^{-3}]
I-131	≤ TBD	≤ [2.5×10^{-5}]	≤ TBD	≤ [8.7×10^{-4}]

4.1.4 RN Retention by Fuel Element Graphite

For the MHTGR, large graphite attenuation factors were specified In the Goal 1 functional analysis as indicated in Table 4-5. The primary reason that these target graphite attenuation factors are so large is that for Goal 1, the allowable fuel fraction for normal operation was 5×10^{-4}, or 10x the limit on fuel failure adopted in Goal 3 to meet PAG dose limits during depressurization accidents. Logically, one might have expected a corresponding relaxation in

the required graphite attenuation, but no such relaxation was included in the Goal 3 functional analysis.

Table 4-5. Graphite Attenuation Factors for Normal Operation (MHTGR)

Nuclide	Required Attenuation Factor	
	≥ 50% Confidence	≥ 95% Confidence
Sr	≥ [1200]	≥ [200]
Ag	≥ TBD	≥ TBD
Cs	≥ [70]	≥ [14]

Subsequent full-core analysis for the MHTGR indicated that the above graphite attenuation factor for cesium, would be difficult to achieve even with core inlet and outlet temperatures of 257 and 687 ^{o}C, respectively [Jovanovic 1989]. Based upon those results, a graphite attenuation factor for cesium of ~10x appears to be more realistic. For strontium, a graphite attenuation factor >10^3 may be attainable. The graphite attenuation factor for silver is not readily deduced from the reported data, but the predicted fractional release of Ag-110m exceeded the "Maximum Expected" criterion of ≤ 5 x 10^{-4} by factor of ~11.[35] Consequently, the target graphite attenuation factors shown in Table 4-6 are adopted for a steam-cycle MHR with a core outlet temperature of 750 ^{o}C.

Table 4-6. Target MHR Graphite Attenuation Factors for Normal Operation

Nuclide	Required Attenuation Factor	
	≥ 50% Confidence	≥ 95% Confidence
Sr	≥ [1000]	≥ [100]
Ag	≥ [2]	≥ TBD
Cs	≥ [10]	≥ TBD

No graphite attenuation factors are specified in the Goal 3 functional analysis (only a place holder with all entries "TBD"). The Goal 2 functional analysis contains the following required graphite attenuation factors for depressurized conduction cooldown events. However, the requirement to meet PAGs had not yet been invoked in Goal 2; consequently, the allowable fuel

[35] Section 4.2.3 of [PSID 1992] states that no credit was taken for Ag retention by the matrix and graphite. The results presented in [PSID 1992] are not identical to those in [Jovanovic 1989], but the differences are <2x.

failure fraction was 10x higher than ultimately required in Goal 3. As a result, the graphite attenuation factors given in Table 4-7 are not particularly meaningful.

Table 4-7. Graphite Attenuation Factors for LBEs (MHTGR)

Nuclide	Required Attenuation Factor	
	≥50% Confidence	≥95% Confidence
Sr	≥[16]	≥[100]
Ag	≥[11]	≥TBD
Cs	≥[6]	≥TBD

4.1.5 RN Retention by Particle Coatings

As discussed in Section 2.4.3.1, the two dominant sources of fission product release from the core are as-manufactured, heavy metal contamination and particles whose coatings fail in service. The latter source can be subdivided into (1) coating failure during normal operation and (2) incremental coating failure during LBEs. In addition, certain volatile fission metals, notably Ag, can at sufficiently high temperatures and long times, diffuse through the SiC coatings of intact TRISO particles.

To achieve the fractional release limits specified above, each of the above sources must be limited; in principle, any number of combinations could give the required degree of radionuclide retention as illustrated by the simplified relationship given in Eqn (4-1).

To illustrate how the above relationship is used in deriving limits on heavy-metal contamination and fuel failure, consider the core release limit for I-131 during normal operation (Table 4-4) which is the most constraining radionuclide control criterion for normal operation. For iodine, diffusive release from intact TRISO particles and graphite attenuation are both negligible so Eqn. (4-1) simplifies to

$$(f.r.)_{I\text{-}131} = C(f.r.)_C + F(f.r.)_F \qquad (4\text{-}1)$$

Using representative values for I-131 during normal operation,

$$(f.r.)_{I\text{-}131} = C\cdot(0.10) + F\cdot(0.02)_F = 1.9 \times 10^{-6} \qquad (4\text{-}2)$$

At this point, an allocation must be made because any number of combinations of allowable contamination fraction (C) and failure fraction (F) could, in principle, give the required I-131 retention. Assuming that the allowable iodine fractional release were allocated equally to contamination and failed particles, one can readily calculate that

$$C = (1.9 \times 10^{-6}/2)/0.10 = 9.5 \times 10^{-6} \sim 1 \times 10^{-5} \quad (4\text{-}3)$$

$$F = (1.9 \times 10^{-6}/2)/0.02 = 4.8 \times 10^{-5} \sim 5 \times 10^{-5} \quad (4\text{-}4)$$

Similar calculations must be made for the release of other key nuclides during normal operation, including Cs and Ag, but the above limits on contamination and fuel failure are, in fact, the most constraining and are the present design criteria. Naturally, it must be confirmed that these limits are also adequate to meet Goals 2 and 3 requirements. On the basis of the safety analyses done for the PSID, they appear to be adequate to meet Goal 3 radionuclide control requirements [PSID 1992, Chapter 15]. Their adequacy for meeting investment risk-related requirements (Goal 2) is less certain because relatively little analysis has been done.

The controlling assumption in defining Goal 2 radionuclide control requirements is that the allowable incremental core releases and fuel failures are calculated as the difference between "Design" and "Maximum Expected" limits for normal operation. In other words, since events with significant potential for fuel damage are rare, it is acceptable to use up the design margin specified for normal operation during such events. This rationale implies that the plant could be restarted after such events without replacing the core, but that the core release limits after restart would be, for limiting cases, near the technical specification limits on primary circuit contamination.

Given the above considerations, design criteria for heavy-metal contamination and fuel failure were derived which are consistent with core release limits. It should be noted that these criteria are dependent upon the fission product transport models used to predict the release fractions from contamination and failed fuel and are further dependent upon the environmental conditions in the core during normal operation and LBEs. The results are summarized in Section 5.

4.1.6 RN Retention by Fuel Kernels

Given the limits on heavy-metal contamination and coating failure derived above, the required radionuclide retention by fuel kernels can be addressed. Both contamination and the exposed kernels of particles with failed coatings still retain radionuclides to a degree. In fact, the degree of retention by fuel kernels is strongly dependent upon its physical (e.g., density) and chemical properties (e.g., resistance to hydrolysis); consequently, the amount of kernel retention can, to a degree, be specified. In contrast, the inherent release characteristics of heavy-metal contamination in the fuel-compact matrix which have been determined experimentally are, for practical purposes, beyond the control of the designer. Consequently, retention requirements are only defined for the fuel kernel; these are summarized below.

During normal operation, the kernel composition and attributes shall be specified such that the attenuation factors provided by the kernels in failed fuel particles at 1100 °C and full burnup after exposure to water are given in Table 4-8.

Table 4-8. Required Kernel Retention during Normal Operation

Nuclide	Allowable Fractional Release	
	≥50% Confidence	≥95% Confidence
Kr-88	≤[0.012]	≤TBD
Xe-133	≤[0.028]	≤TBD
I-131	≤[0.034]	≤TBD

No retention limits for fission metals during normal operation (Goal 1) have been specified to date because the limits on fuel failure and contamination that were derived from iodine release limits are so stringent that the metal release limits can be met without taking credit for kernel retention in failed particles. The exception to this conclusion is Ag-110m for which the dominant release mechanism is diffusive release from intact TRISO particles. However, at the elevated temperatures necessary for significant diffusive release, retention of Ag in candidate fuel kernels is likely modest.

Kernel retention requirements also must be evaluated for LBEs. Again, because of the stringent limits on fuel failure and contamination derived from iodine release limits for normal operation, core release limits for long-term LBEs, such as depressurized core conduction cooldowns, can be met without taking credit for kernel retention in failed particles. However, for short-term LBEs, such as water ingress plus pressure relief, credit for kernel retention in failed particles must be taken to meet PAGs at 95% confidence. The required, core-average, kernel attenuation factors can be computed from Eqn. (4-1); the results for short-term events, such as water ingress plus pressure relief (SRDC-6), are summarized in Table 4-9.

Table 4-9. Required Kernel Retention during Short-Term LBEs

Nuclide	Allowable Fractional Release			
	PAG (User) Limits		10CFR100 (Reg) Limits	
	P ≥50%	P ≥95%	P ≥50%	P ≥95%
Kr-88	≤TBD	≤[0.59]	≤TBD	≤[1.0]
I-131	≤TBD	≤[0.12]	≤TBD	≤[1.0]

4.2 Summary of Target Decontamination Factors

The FA/PSID decontamination factors described above for the individual RN release barriers are collected in Table 4-10. The multitude of assumptions that were necessarily made when

deriving these decontamination factors are summarized in the preceding subsections and illustrated in Appendix A. When considering this summary table, it is important to recall that some the target decontamination factors apply to best-estimate (≥ 50% confident) calculations and others to conservative (≥ 95% confident) calculations. For that level of detail, the reader should consult the preceding subsections and [Olsen 1988].

In general, the target decontamination factors are sufficient to within of ~2x to meet off-site Curie release limits which reflects the larger RN inventories that would result from increasing the plant power level from 350 to 600 MW(t).

Table 4-10. Summary of Target Decontamination Factors for Steam-Cycle MHR

	Parameter	Key Radionuclides determining Fuel Requirements (release timing)						Comments
		I-131 (short-term)	I-131 (long-term)	Xe-133 (long-term)	Cs-137 (long-term)	Sr-90 (long-term)	Ag-110m (long-term)	
Plant Limits	Accident Release Limits[36]	2.6	29	2300	TBD	1.2	TBD	Appendix A
600 MW "Design" Activities (Normal)	Core (Ci)	$2.0 \times 10^{+7}$	$2.0 \times 10^{+7}$	$3.6 \times 10^{+7}$	$1.7 \times 10^{+6}$	$1.5 \times 10^{+6}$	$2.8 \times 10^{+4}$	[Hanson 2008a]
	Circulating (Ci)	1.8×10^{-1}	1.8×10^{-1}	$2.0 \times 10^{+1}$	3.3×10^{-3}	1.6×10^{-5}	7.2×10^{-3}	
	Plateout (Ci)	$1.5 \times 10^{+2}$	$1.5 \times 10^{+2}$	0	$2.4 \times 10^{+3}$	$1.2 \times 10^{+1}$	$1.7 \times 10^{+2}$	
Fuel Attributes	"Design" HM Contamination	$\leq 2 \times 10^{-5}$	$\leq 2 \times 10^{-5}$	$\leq 2 \times 10^{-5}$	$\leq 2 \times 10^{-5}$	$\leq 2 \times 10^{-5}$	$\leq 2 \times 10^{-5}$	
	"Max. Exp." Contamination	$\leq 1 \times 10^{-5}$	$\leq 1 \times 10^{-5}$	$\leq 1 \times 10^{-5}$	$\leq 1 \times 10^{-5}$	$\leq 1 \times 10^{-5}$	$\leq 1 \times 10^{-5}$	
	"Design" SiC Defects	$\leq 1 \times 10^{-4}$	$\leq 1 \times 10^{-4}$	$\leq 1 \times 10^{-4}$	$\leq 1 \times 10^{-4}$	$\leq 1 \times 10^{-4}$	$\leq 1 \times 10^{-4}$	
	"Max. Exp." SiC Defects	$\leq 5 \times 10^{-5}$	$\leq 5 \times 10^{-5}$	$\leq 5 \times 10^{-5}$	$\leq 5 \times 10^{-5}$	$\leq 5 \times 10^{-5}$	$\leq 5 \times 10^{-5}$	
	"Design" Failure – Normal	$\leq 2 \times 10^{-4}$	$\leq 2 \times 10^{-4}$	$\leq 2 \times 10^{-4}$	$\leq 2 \times 10^{-4}$	$\leq 2 \times 10^{-4}$	$\leq 2 \times 10^{-4}$	
	"Max. Exp." Failure – Normal	$\leq 5 \times 10^{-5}$	$\leq 5 \times 10^{-5}$	$\leq 5 \times 10^{-5}$	$\leq 5 \times 10^{-5}$	$\leq 5 \times 10^{-5}$	$\leq 5 \times 10^{-5}$	
	"Design" ΔFailure - Accidents	0	$\leq 6 \times 10^{-4}$	$\leq 6 \times 10^{-4}$	$\leq 6 \times 10^{-4}$	$\leq 6 \times 10^{-4}$	$\leq 6 \times 10^{-4}$	
	"Max. Exp." ΔFailure - Accidents	0	$\leq 1.5 \times 10^{-4}$	$\leq 1.5 \times 10^{-4}$	$\leq 1.5 \times 10^{-4}$	$\leq 1.5 \times 10^{-4}$	$\leq 1.5 \times 10^{-4}$	
RN Transport in Core	Kernel Retention	50	8	8	TBD	TBD	TBD	
	Matrix/graphite Retention	1	1	1	10	100	1	
RN Transport in PCS	Plateout Retention – Depressurization	20	20	1	20	20	20	DBE-10
	Depressurized Core Conduction Cooldown	-	30	1	30	30	30	SRDC-11

[36] These environmental release limits are taken from the Functional Analysis (Appendix A).

	Parameter	Key Radionuclides determining Fuel Requirements (release timing)						Comments
		I-131 (short-term)	I-131 (long-term)	Xe-133 (long-term)	Cs-137 (long-term)	Sr-90 (long-term)	Ag-110m (long-term)	
	Plateout Retention – H_2O Ingress + Pressure Relief	2 x 7	2 x 7	7	2 x 7	2 x 7	2 x 7	SRDC-6
RN Transport in VLPC	VLPC Retention Factor	1	[10][37]	1	[10]	[10]	[10]	SRDC-11
	Wake Retention Factor	1.5	1.5	1.5	1.5	1.5	1.5	Impacts Prompt Release
Plant Release	RN Transport to EAB	5.0	50	2700	TBD	0.3	TBD	
Plant Limits	Accident Release Limits	2.6	29	2300	TBD	1.2	TBD	
Additional Retention Needed		1.9	1.7	1.2	TBD	1	TBD	

[37] No credit taken for retention in VLPC in [PSID 1992].

5 RESULTING FUEL DESIGN REQUIREMENTS

When the fuel requirements presented herein were derived, credit was taken for RN retention by each of the release barriers. Barrier performance requirements are specified such that only the particle coatings are needed to meet 10CFR100 off-site dose limits; however, credit for the additional barriers is taken to meet the PAG dose limits. The alternative would be to set fuel failure limits sufficiently low that the PAG dose limits could be met even if it were assumed that 100% of the fission product inventories of failed particles were released to the environment. This approach is considered impractical. For perspective, for the 350 MW(t) steam-cycle MHTGR with a 425-m EAB, the allowable I-131 release limits to meet the PAG thyroid dose limit of 5 rem were 2.6 Ci for short-term events, such a rapid depressurization, and 29 Ci for long-term events, such as a depressurized core conduction cooldown. Converting these Curie limits to allowable fuel failure fractions for a 600 MW(t) MHR gives failure limits of ~10^{-7} during normal operation and ~10^{-6} during core heatup events, respectively.

Based upon the target RN decontamination factors adopted in Section 4, the following fuel requirements are recommended for a steam-cycle MHR with a 750 ^{o}C core outlet temperature. The fuel performance and quality requirements are summarized in Table 5-1, and the fission gas and metal release limits for key radionuclides are shown in Tables 5-2 and 5-3, respectively. For perspective, the fission product release limits adopted by previous HTGR programs are also shown in Tables 5-2 and 5-3 [Hanson 1994, Hanson 2003, Hanson 2008a].

5.1 In-Service Fuel Performance Requirements

The recommended, in-service fuel failure limits for a steam-cycle MHR for normal operation and accidents are summarized in Table 5-1. These recommended failure limits are the same as those adopted for the 350 MW(t) steam-cycle MHTGR [PSID 1992]. The limits on fission gas release are given in Table 5-2. These R/B limits are also the same as for the MHTGR [PSID 1992]. Since the thermal power may be increased by 600 MW/350 MW, the Curie release rates from the core would be 1.7x higher for a larger MHR. The limits on fission metal release are given in Table 5-3. These cumulative fractional limits are almost the same as for the MHTGR [PSID 1992] except that the limit on Ag-110m has been reduced from 5 x 10^{-4} to 2 x 10^{-4}; the latter was the limit adopted previously for the commercial GT-MHR with a core outlet temperature of 850 ^{o}C.

For a process-heat MHR with a 900 ^{o}C core outlet temperature, the limits on fuel failure and fission gas release would be retained at the above steam-cycle values; however, the limits on fission metal fractional release would be increased from 7 x 10^{-6} to 1 x 10^{-5} for Cs-137 and from 2 x 10^{-4} to 5 x 10^{-4} for Ag-110m because of the higher fuel and graphite temperatures resulting from the higher core outlet temperature. These higher allowable metal release fractions were adopted as the provisional limits for the CPA task wherein a core outlet temperature of 900 ^{o}C was imposed. More investigation will be required to determine if the allowable limit on Sr-90

release can also be increased; specifically, the contribution of Sr-90 to the off-site TEDE doses during postulated accidents will need to be better quantified.

5.2 As-Manufactured Fuel Attributes

The recommended, as-manufactured fuel quality requirements for a future steam-cycle MHR are also summarized in Table 5-1. These recommended fuel quality are the same as those adopted for the 350 MW(t) steam-cycle MHTGR [PSID 1992] except that allowable missing-buffer fraction is reduced from 5×10^{-5} to 1×10^{-5} and the allowable missing or defective OPyC fraction was relaxed from 1×10^{-4} to 0.01; these changes were first introduced in the fuel product specification for the commercial GT-MHR [Munoz 1994]. It is anticipated that the fuel product specification for a steam-cycle MHR would closely parallel the product specification for the commercial GT-MHR [Munoz 1994]. (The fuel product specification controls many as-manufactured fuel attributes beyond allowable coating defects.)

The rationale for relaxing the allowable OPyC defect fraction was twofold. First, the quality control (QC) technique for determining the OPyC defect fraction is a visual inspection, and a 1×10^{-4} defect fraction is difficult to determine by visual inspection. Secondly, the FDDM/F model for irradiation-induced OPyC failure predicts that 3% of the OPyC coatings will fail at a fast fluence of 2×10^{25} n/m^2 so that a tight as-manufactured defect limit of 1×10^{-4} is of little practical benefit. The latter rationale was logical for fuel compacts manufactured with a matrix material derived from petroleum pitch because irradiation testing of such fuel compacts consistently demonstrated irradiated-induced OPyC failure. However, now that the NGNP/AGR fuel program has adopted a matrix material derived from phenolic resin, irradiation-induced OPyC failure is expected to be much reduced or even effectively eliminated, based upon the extensive German experience with similar matrix materials. With this new matrix material, a tighter specification on missing or defective OPyC layers may again be appropriate. However, the practical issue of qualifying a reliable QC technique to enforce it remains.

For a process-heat MHR with a 900 ^{o}C core outlet temperature, the above as-manufactured quality requirements would be the logical point of departure. Indeed, these quality attributes were assumed in the CPA task. However, given the inevitably higher fuel and graphite temperatures with a 900 ^{o}C COT, there would be an incentive to consider the feasibility of adopting tighter limits on as-manufactured HM contamination (to reduce the fission gas release) and on SiC coating defects (to compensate for less Cs and Sr retention by the hotter graphite).

Table 5-1. Recommended Coating Integrity for MHR Fuel

Parameter	Steam-Cycle MHTGR		Steam-Cycle MHR	
	"Maximum Expected"	"Design"	"Maximum Expected"	"Design"
As-Manufactured Fuel Quality[38]				
HM contamination	$\leq 1.0 \times 10^{-5}$	$\leq 2.0 \times 10^{-5}$	$\leq 1.0 \times 10^{-5}$	$\leq 2.0 \times 10^{-5}$
Missing or defective buffer[39]	$\leq 5.0 \times 10^{-5}$	$\leq 1.0 \times 10^{-4}$	$\leq 1.0 \times 10^{-5}$	$\leq 2.0 \times 10^{-5}$
Missing or defective IPyC	$\leq 4.0 \times 10^{-5}$	$\leq 1.0 \times 10^{-4}$	$\leq 4.0 \times 10^{-5}$	$\leq 1.0 \times 10^{-4}$
Defective SiC	$\leq 5.0 \times 10^{-5}$	$\leq 1.0 \times 10^{-4}$	$\leq 5.0 \times 10^{-5}$	$\leq 1.0 \times 10^{-4}$
Missing or defective OPyC	$\leq 1.0 \times 10^{-4}$	$\leq 2.0 \times 10^{-4}$	[0.01]	[0.02][40]
In-Service Fuel Performance[41]				
Normal operation	$\leq 5.0 \times 10^{-5}$	$\leq 2.0 \times 10^{-4}$	$\leq 5.0 \times 10^{-5}$	$\leq 2.0 \times 10^{-4}$
Core heatup accidents	[$\leq 1.5 \times 10^{-4}$]	[$\leq 6.0 \times 10^{-4}$]	[$\leq 1.5 \times 10^{-4}$]	[$\leq 6.0 \times 10^{-4}$]

Table 5-2. Recommended Fission Gas Release Limits for MHRs

Reactor Plant	Type	COT[5] (°C)	Allowable Core Fractional Release			
			Kr-88		I-131	
			"Expected"	"Design"	"Expected"	"Design"
MHTGR	Steam-cycle	700	$\leq 8.3 \times 10^{-7}$	$\leq 3.3 \times 10^{-6}$	$\leq 2.0 \times 10^{-6}$	$\leq 8.0 \times 10^{-6}$
MHR	**Steam-cycle**	**750**	$\mathbf{\leq 8.3 \times 10^{-7}}$	$\mathbf{\leq 3.3 \times 10^{-6}}$	$\mathbf{\leq 2.0 \times 10^{-6}}$	$\mathbf{\leq 8.0 \times 10^{-6}}$
GT-MHR	Direct-cycle	850	$\leq 8.3 \times 10^{-7}$	$\leq 3.3 \times 10^{-6}$	$\leq 2.0 \times 10^{-6}$	$\leq 8.0 \times 10^{-6}$
VHTR	Process heat	950	TBD	TBD	TBD	TBD
MHR	Process heat	900	$\leq [8.3 \times 10^{-7}]$	$\leq [3.3 \times 10^{-6}]$	$\leq [2.0 \times 10^{-6}]$	$\leq [8.0 \times 10^{-6}]$

[38] ≥ 95% confidence that the mean value for a fuel segment will be ≤ "Maximum Expected" value, and ≥ 95% confidence that ≤ 5% of fuel compacts will be > "Design" value.
[39] The missing-buffer specification was tightened in the GT-MHR fuel product specification [Munoz 1994].
[40] The GT-MHR fuel product specification [Munoz 1994] has two OPyC defect specs: missing OPyC = $\leq 1.0 \times 10^{-4}$, and defective OPyC = [0.02].
[41] ≥ 50% probability that the fuel failure and fission product release will be ≤ "Maximum Expected" criteria and ≥ 95% probability that the failure and release will be ≤ "Design" criteria (see Section 2.4.6).

Table 5-3. Recommended Fission Metal Release Limits for MHRs

Plant	Type	COT (°C)	Allowable Core Fractional Release					
			Cs-137		Ag-110m		Sr-90	
			"Max. Expected"	"Design"	"Max. Expected"	"Design"	"Max. Expected"	"Design"
MHTGR	Steam-cycle	687	$\leq 7.0 \times 10^{-6}$	$\leq 7.0 \times 10^{-5}$	$\leq 5.0 \times 10^{-4}$	$\leq 5.0 \times 10^{-3}$	$\leq 3.0 \times 10^{-8}$	$\leq 3.0 \times 10^{-7}$
MHR	**Steam-cycle**	**750**	**$\leq 7.0 \times 10^{-6}$**	**$\leq 7.0 \times 10^{-5}$**	**$\leq 2.0 \times 10^{-4}$**	**$\leq 2.0 \times 10^{-3}$**	**$\leq 3.0 \times 10^{-8}$**	**$\leq 3.0 \times 10^{-7}$**
HHT	Direct-cycle	850	$\leq 2.0 \times 10^{-5}$	$\leq 1.0 \times 10^{-4}$	$\leq 8.6 \times 10^{-5}$	$\leq 6.5 \times 10^{-4}$	?	?
GT-MHR	Direct-cycle	850	$\leq 1.0 \times 10^{-5}$	$\leq 1.0 \times 10^{-4}$	$\leq 2.0 \times 10^{-4}$	$\leq 2.0 \times 10^{-3}$	$\leq 3.0 \times 10^{-8}$	$\leq 3.0 \times 10^{-7}$
VHTR	Process heat	950	$\leq [1.0 \times 10^{-5}]$	$\leq [1.0 \times 10^{-4}]$	$\leq [2.0 \times 10^{-4}]$	$\leq [2.0 \times 10^{-3}]$	TBD	TBD
MHR	Process heat	900	$\leq [1.0 \times 10^{-5}]$	$\leq [1.0 \times 10^{-4}]$	$\leq [5.0 \times 10^{-4}]$	$\leq [5.0 \times 10^{-3}]$	TBD	TBD

6 ESTIMATED RN SOURCE TERMS FOR THE "REFERENCE" MHR DESIGN

Radionuclide source terms were estimated for the GA "reference" steam-cycle MHR design with core inlet and outlet temperatures of 322 and 750 °C, respectively [Labar 2009]. Best estimate RN source terms were predicted for normal plant operation using the final Phase 2 designs for a binary-particle core design (Case 7.9SC) and a single-particle core design (Case 8.9.3SC) developed on the CPA task [GA 2009b] where the "SC" suffix here denotes "steam-cycle" gas temperatures that are different from the core inlet and outlet temperatures of 540 and 900 °C, respectively, for the CPA. These results provide the first indication whether or not the allowable core releases for normal operation that were derived from the top-level RN control requirements (Section 5) can be met with margin with a core outlet temperature of 750 °C.

The best definition of accident source terms for a 600 MW(t) steam-cycle MHR available at this writing is from the NGNP containment options study [Richards 2008]. The results are reviewed in Section 6.2.

6.1 Normal Plant Operation

Fuel performance and fission product release analyses of two core designs developed under the CPA task were completed for a core outlet temperature of 750 °C with the SURVEY and TRAFIC-FD codes as modified for the CPA task [GA 2009a, GA 2009b].

6.1.1 Methodology and Assumptions

The SURVEY code was run using the SORT3D input files generated from the DIF3D output files for CPA core design Cases 7.9SC and 8.9.3SC [GA 2009b]. Using the SURVEY output results as input, the TRAFIC-FD code was used to calculate Cs-137, Ag-110m and Sr-90 releases from the two cores as well.

Case 7.9 is the final design from the Phase 2 binary-particle design study (without fuel shuffle). This design is described in detail in Sections 2.3 and 2.4 of [GA 2009a]. Case 7.9 is based on Case 7.3.2, but used the finer axial mesh geometric model (1/5th of a fuel block height per axial mesh point) and additional axial fuel zoning to further reduce the axial power factors. These fuel loading changes preserved the maximum packing fractions while steepening the axial power distribution over the initial cycle of each reload to further reduce peak fuel temperatures in the equilibrium fuel loads. The net result of these changes was a reduction in peak fuel temperatures and power peaking factors, and improved fuel performance relative to Case 7.3.2.

The focus of the single-particle core design work was to achieve an acceptable design for a single fissile fuel particle having a single U-235 enrichment. This work involved a series of design iterations that primarily investigated fuel zoning and fixed burnable poison zoning to achieve a design that meets the packing fraction and cycle length requirements. These iterations resulted in design Case 8.9.3, which is considered to be the best single-particle/single enrichment core design that was achieved within the time constraints of the CPA. Case 8.9.3 also did not include fuel shuffling.

The U-235 enrichment in the single-particle/single-enrichment core design was supposed to be ~14% would be consistent with the enrichment of the fuel particle that is currently being developed and qualified by the NGNP/AGR fuel program. However, it was determined during the binary-particle core design work that a U-235 enrichment of 14% is not compatible with the packing fraction limits and the cycle length goal adopted for the CPA. Consequently, a U-235 enrichment of 15.5% was selected for the fuel particle in the single-particle/single-enrichment design iterations based on the effective enrichment of the reloads in the two-particle design Case 7.9.

The core power distributions were assumed here to be identical to those calculated for Case 7.9 and Case 8.9.3 for the CPA cores. The base-case CPA design has core inlet and outlet temperatures of 540 and 900 ^{o}C, respectively, resulting in a 360 ^{o}C temperature rise across the core. For present purpose, the core operating parameters were adjusted to match the "reference" steam-cycle MHR design [Labar 2009]. The core inlet and outlet temperatures were reduced to 322 and 750 ^{o}C, respectively. Since the "reference" design has a core temperature rise of 428 ^{o}C that is 68 ^{o}C larger than for the base-case CPA design, the coolant mass flow rate was reduced to 84% of the CPA flow rate to maintain the same total core power.

As discussed in Section 4.1.1 of [GA 2009a] and elsewhere, the fuel temperatures at a given location in the core result from the addition of a number of temperature rises: (1) the temperature rise in the coolant from the sensible heat added as the coolant flow transverses the core; (2) the film temperature rise from the flowing helium coolant to the surface of the coolant channels in the graphite fuel blocks (forced convection); (3) the temperature rise across the graphite web separating the coolant holes from the adjacent fuel holes (conduction); (4) the temperature rise across the small gap between the fuel hole and fuel compacts (conduction and radiation), and (5) the temperature rise from the fuel compact surface to the compact centerline (conduction). The temperature rise in the coolant is proportional to the product of the column peaking factor and the core-average temperature rise. Consequently, part of the reduction in peak fuel temperatures resulting from reducing the core outlet temperature from 900 to 750 ^{o}C was offset by increasing the core temperature rise.

For this initial assessment, the as-manufactured fuel quality (e.g., heavy-metal contamination fraction, coating defect fractions, etc.,) was assumed to be consistent with the target allocations assigned in the "Target Decontamination Factors" task (Sections 4 and 5). The fuel performance models and fission product transport properties were taken from FDDM/F (see Section 2.4.3.7) with several important exceptions that are described below.

6.1.2 Core Performance of Binary-Particle Core Design (Case 7.9SC)

6.1.2.1 Fluence and Burnup

The volume fast fluence distribution calculated by SURVEY/THERM for Segment 2 is shown in Figure 6-1 (the distribution for Segment 1 is virtually identical with a slightly lower peak value).

The peak fast fluence is about 4.3 x 10^{25} n/m^2 (E >0.18 Mev) which is less than the practiced limit of ≤ 5 x 10^{25} n/m^2 (both the fuel and graphite are capable of operating to much higher fast fluence limits). The volume burnup distribution for fissile and fertile particles for Segment 2 is shown in Figures 6-2 and 6-3, respectively (the distributions for Segment 1 are slightly lower). The peak burnup is about 20% FIMA for the fissile particle and 6.4% FIMA for the fertile particle which are less than the design burnup limits of 26% and 7%, respectively [FDDM/F 1987].

With respect to the terminology used in these volume distribution figures, SURVEY uses a different terminology than that used in nuclear sections of [GA 2009a]. The correspondence is defined below.

Cycle	Segment A Fuel Load	Segment B Fuel Load
1	1	1
2	2	-
3	-	2
4	3	-
5	-	3

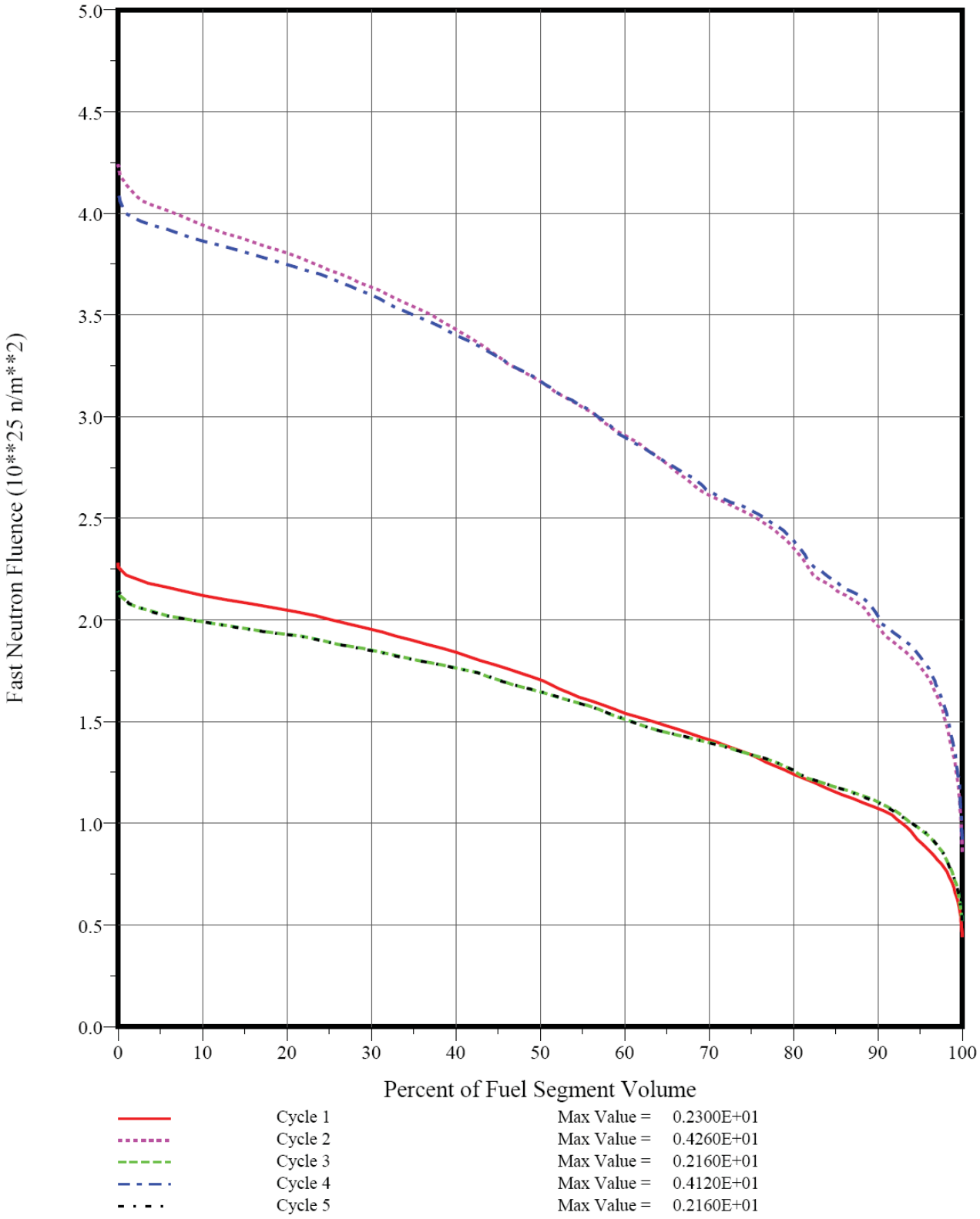

Figure 6-1. Fast Fluence Volume Distribution for Seg. 2 (Case 7.9SC)

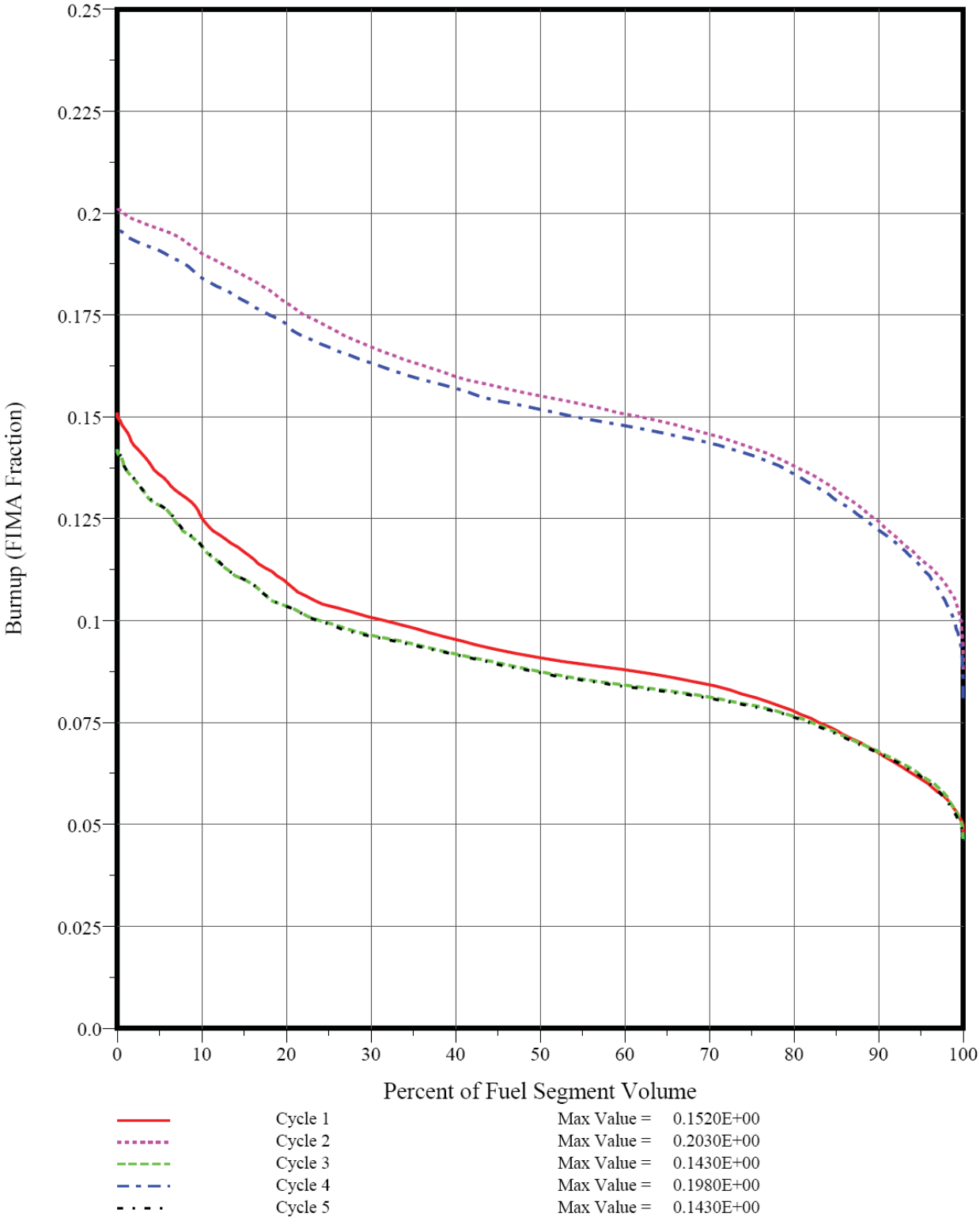

Figure 6-2. Fissile Particle Burnup Volume Distribution for Seg. 2 (Case 7.9SC)

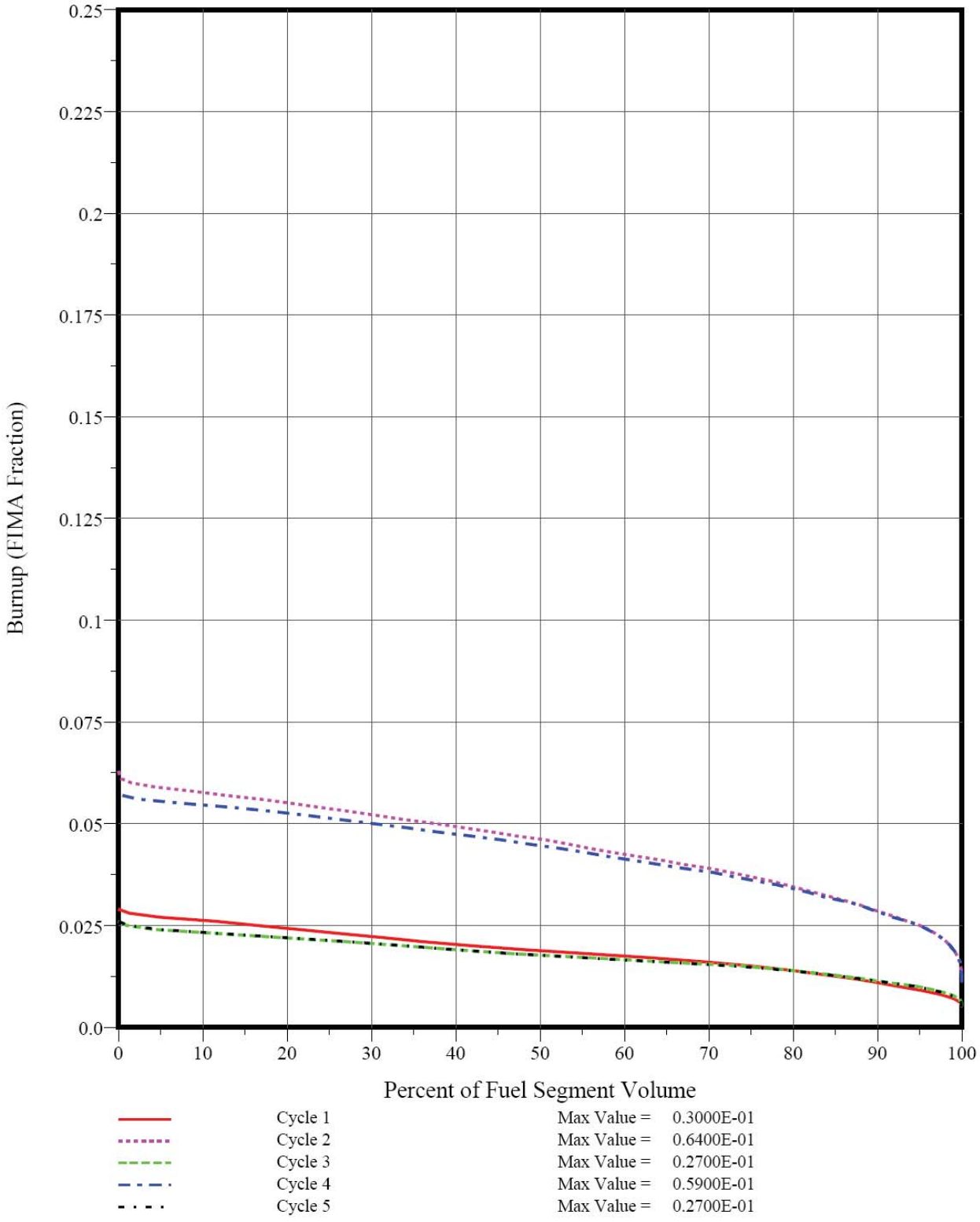

Figure 6-3. Fertile Particle Burnup Volume Distribution for Seg. 2 (Case 7.9SC)

6.1.2.2 Fuel and Graphite Temperature Distributions

Figures 6-4 and 6-5 give peak fuel temperature distributions for fuel Segment 1; the plots are given for both the full-core volume and hottest 5% of the core. The corresponding maximum temperature for Segment 2 is slightly lower (1433 versus 1460 ^{o}C). However, the maximum time-average temperature is slightly higher in Segment 2 (1171 versus 1134 ^{o}C); the full-core volume and hottest 5% of the core for Segment 2 are shown in Figures 6-6 and 6-7, respectively. Such volume-distribution plots have been generated for both Segments 1 and 2, but neither set of plots has any unique features so only the segment with the highest temperature is included here. The extreme peak fuel temperatures evident in Figures 6-4 and 6-5 are of concern, but they are limited to a relatively small fraction of the core and persist for only a short period of time (fuel temperatures >1400 ^{o}C in a core with a 750 ^{o} C outlet temperature can reasonably be characterized as “extreme.”). The maximum time-average fuel temperatures for Segment 1 and Segment 2 are all less than the design goal of <1250 °C.

Figure 6-8 gives the peak graphite volume distribution for Segment 1, and Figure 6-9 gives the time-average graphite volume distribution for Segment 2; the peak graphite temperature is 1364 ^{o}C, and the maximum time-average temperature is 1116 ^{o}C. The graphite temperature distributions are unremarkable and simply track on the fuel temperature distributions.

The highest fuel and graphite temperatures tend to occur in subcolumns in the bottom fuel elements of columns that are adjacent to the outer reflector and also adjacent to a control rod. These subcolumns are called buffered subcolumns. The high temperatures in these subcolumns suggest that it would be desirable to further reduce the radial power peaking in these areas. Reducing the heavy-metal loadings in the four fuel rows adjacent to fuel element-reflector interface in these buffered subcolumns, especially in the bottom axial fuel zone, should also have a beneficial effect in reducing maximum fuel temperatures. However, either of these changes would likely result in some increase in the maximum packing fractions. The results for Case 7.10 presented in [GA 2009a] suggest that the thermal and fuel performance of the physics design can likely be somewhat improved relative to Case 7.9 by pushing more power to the top of the core and allowing the maximum packing fraction to increase up to at least 45%

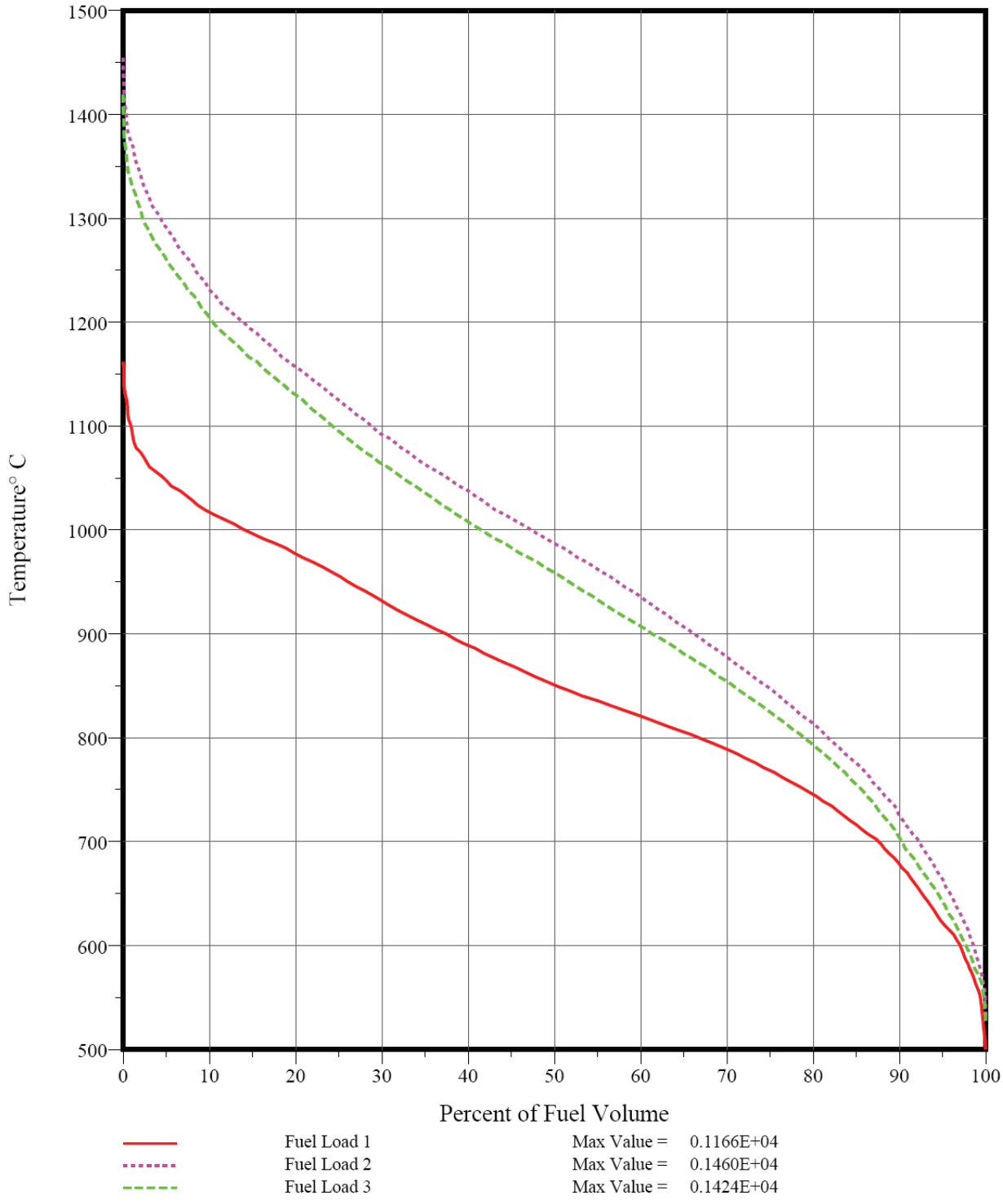

Figure 6-4. Peak Fuel Temperature Volume Distribution for Seg. 1 (Case 7.9SC)

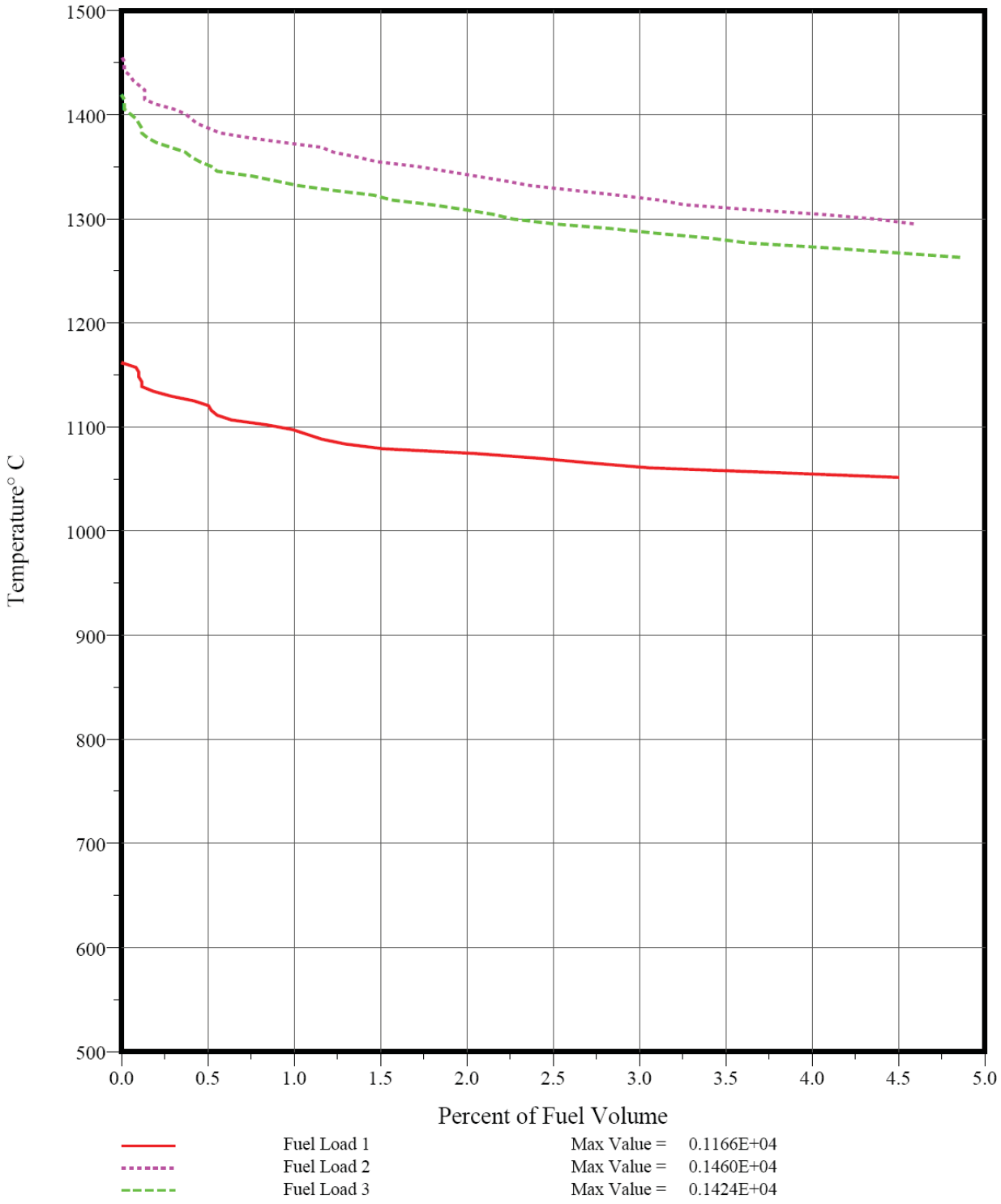

Figure 6-5. Peak Fuel Temperature Distribution for Seg. 1 (0-5%) (Case 7.9SC)

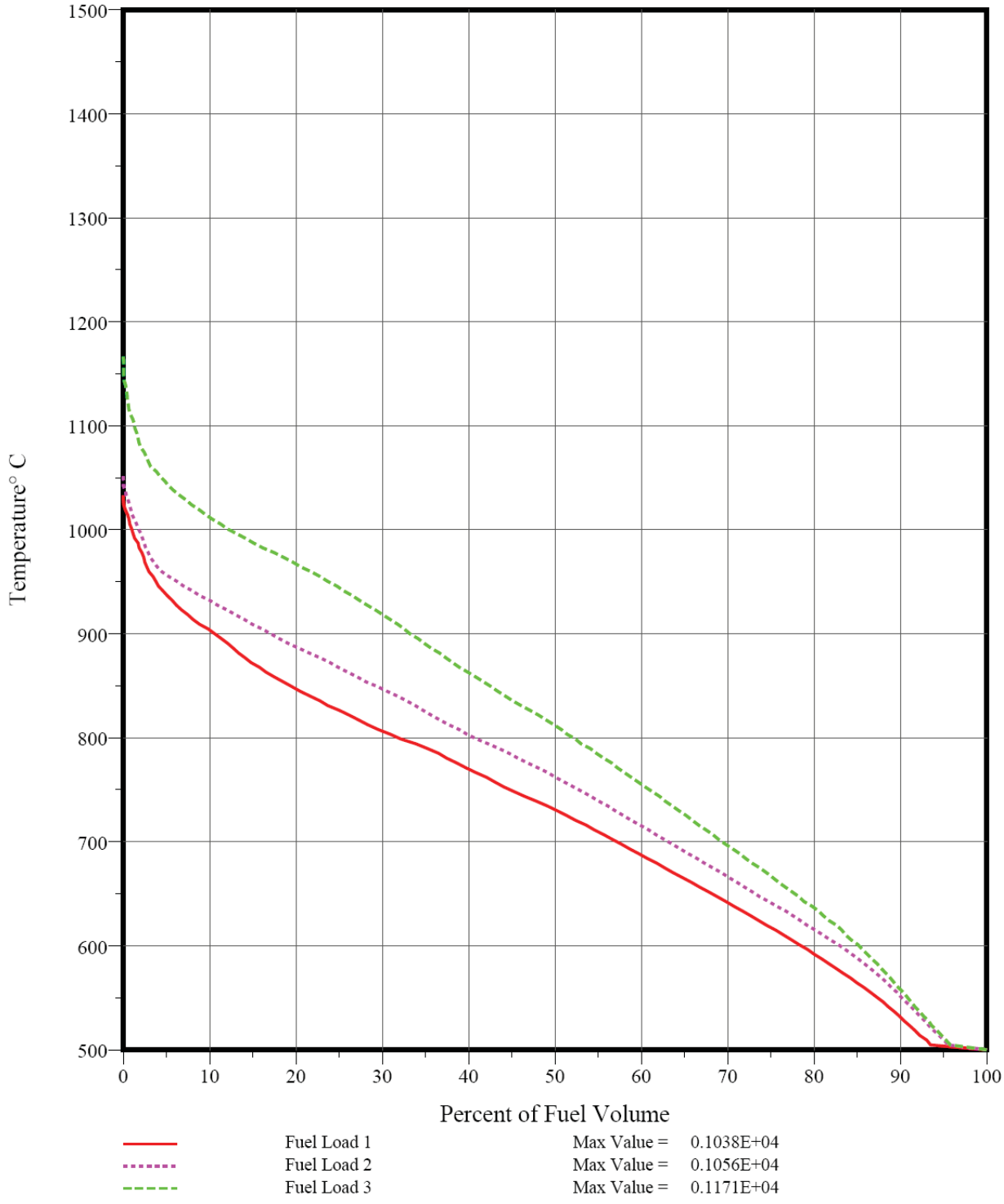

Figure 6-6. Time-Average Fuel Temperature Volume Distribution for Seg. 2 (Case 7.9SC)

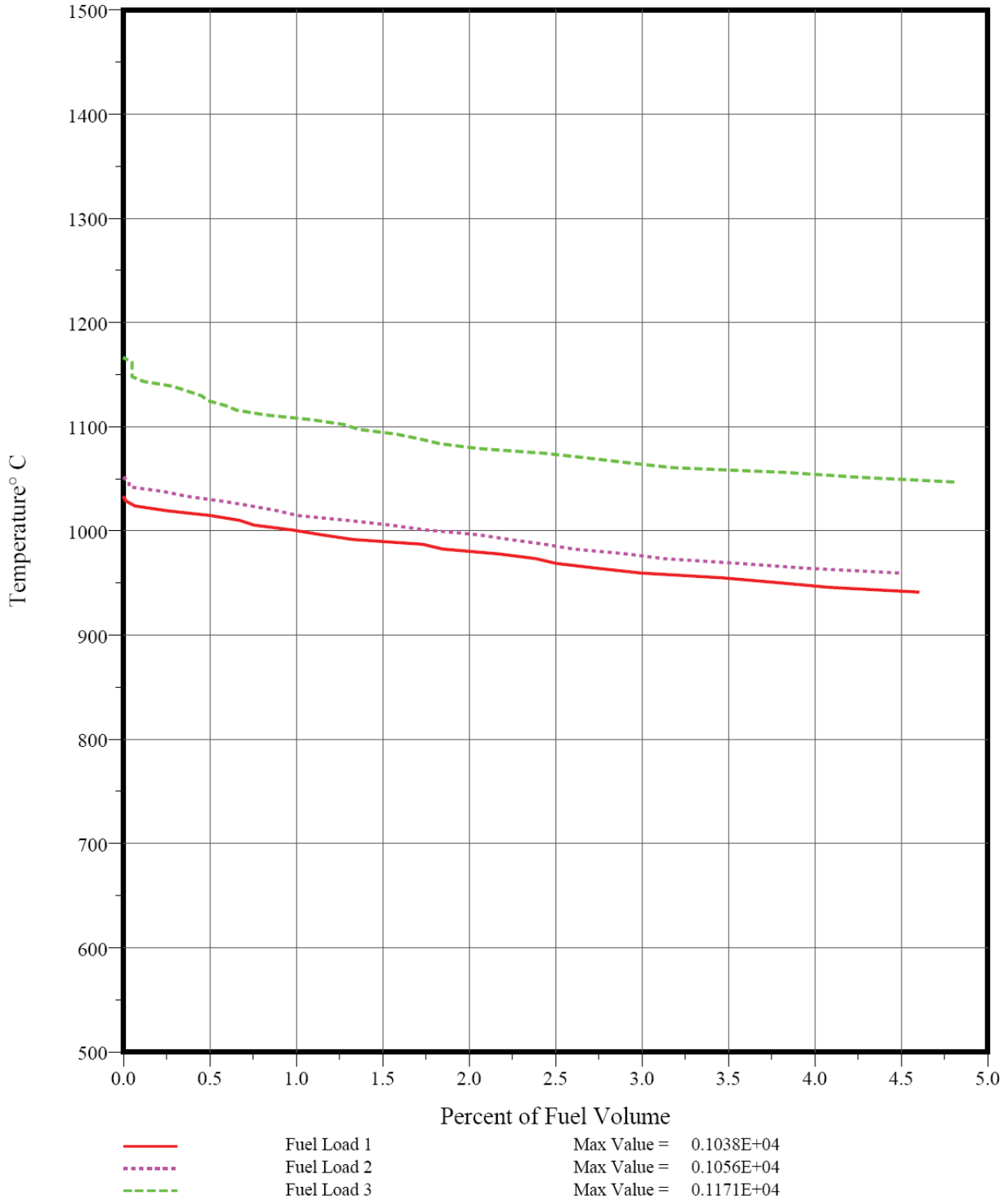

Figure 6-7. Time-Ave. Fuel Temperature Distribution for Seg. 2 (0-5%) (Case 7.9SC)

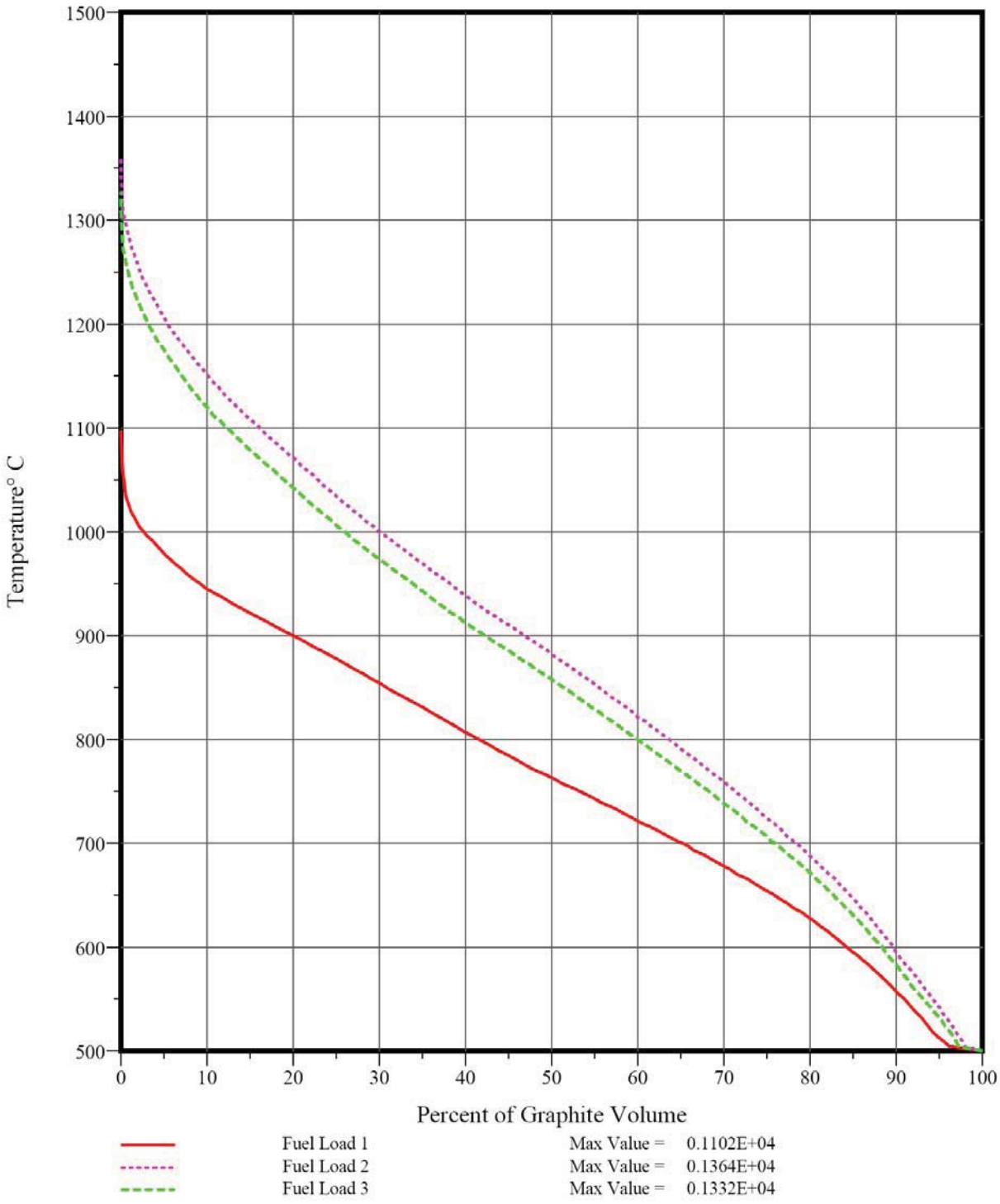

Figure 6-8. Peak Graphite Temperature Volume Distribution for Seg. 1 (Case 7.9SC)

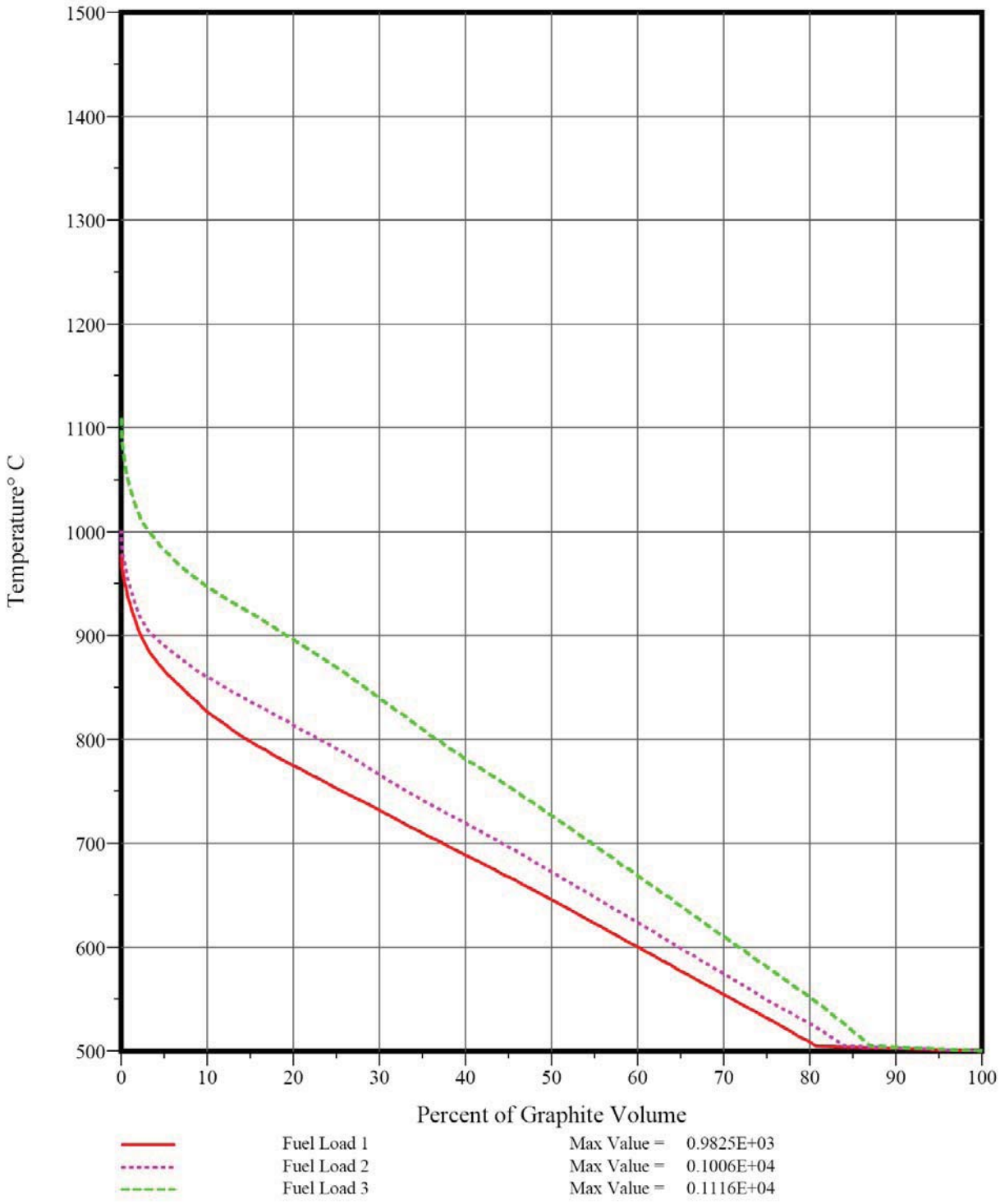

Figure 6-9. Time-Ave. Graphite Temperature Volume Distribution for Seg. 2 (Case 7.9SC)

6.1.2.3 Fuel Particle Failure

Based upon the burnups, fast fluences, and temperatures calculated by SURVEY/THERM, the fuel performance of core design Case 7.9SC was calculated by SURVEY/PERFOR using the component models and material property data from FDDM/F (Section 2.4.3.7).

The core-average SiC failure fractions as a function of operating time for the fissile and fertile particles are shown in Figures 6-10 and 6-11, respectively. The value plotted on the ordinates is the sum of the as-manufactured SiC defect fraction and the in-service SiC failure probability as a result of FP/SiC reactions plus kernel migration plus thermal decomposition plus heavy-metal dispersion as result of a defective IPyC layer.[42] The in-service SiC failure results from HM metal dispersion in the IPyC layer and FP/SiC reactions; kernel migration and SiC thermal decomposition are negligible. The predicted SiC failure fraction for the fissile particle is slightly higher than for the fertile particle since the FP/SiC corrosion failure is burnup dependent. The amount of in-service SiC failure peaks at the end of cycle 3 and is less than the as-manufactured SiC defect fraction in all cycles.

This SiC failure will primarily result in fission metal release. It will also contribute to a lesser degree to the exposed kernel fraction to the extent that OPyC layers are defective (the GT-MHR fuel product specification allows 1% defective OPyC layers) or fail in service (the FDDM/F model ramps up from zero to a constant 3% OPyC failure at a fast fluence of 2×10^{25} n/m^2).

[42] The variables in SURVEY/PERFOR have been renamed to correspond to the nomenclature used in FDDM/F and to facilitate SURVEY/PERFOR verification by comparison to the local-point CAPPER code. See the SURVEY/PERFOR verification description (Section 4.3) in [GA 2009a] for details.

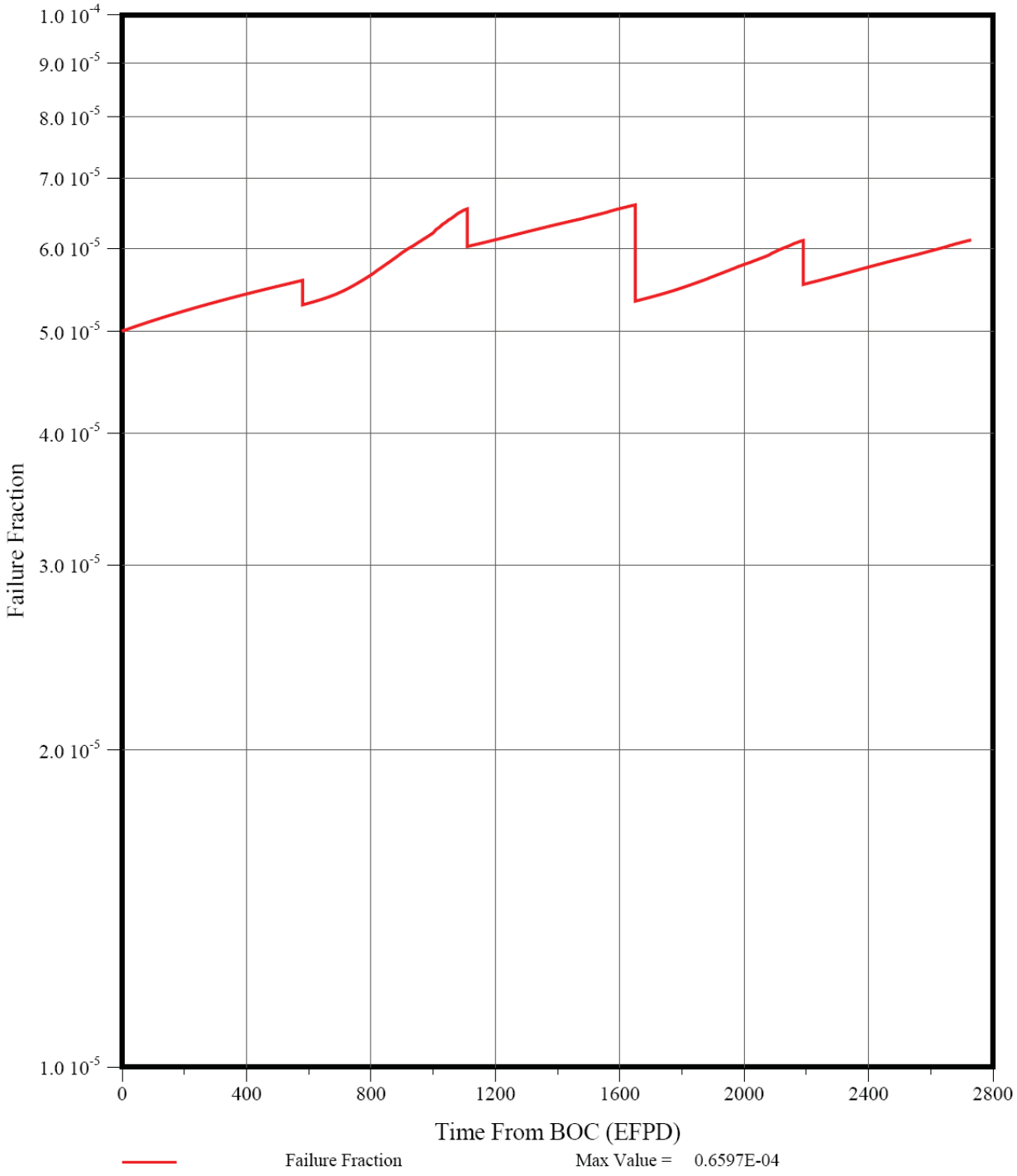

Figure 6-10. SiC Coating Failure Fraction for LEU UCO Fissile Particle (Case 7.9SC)

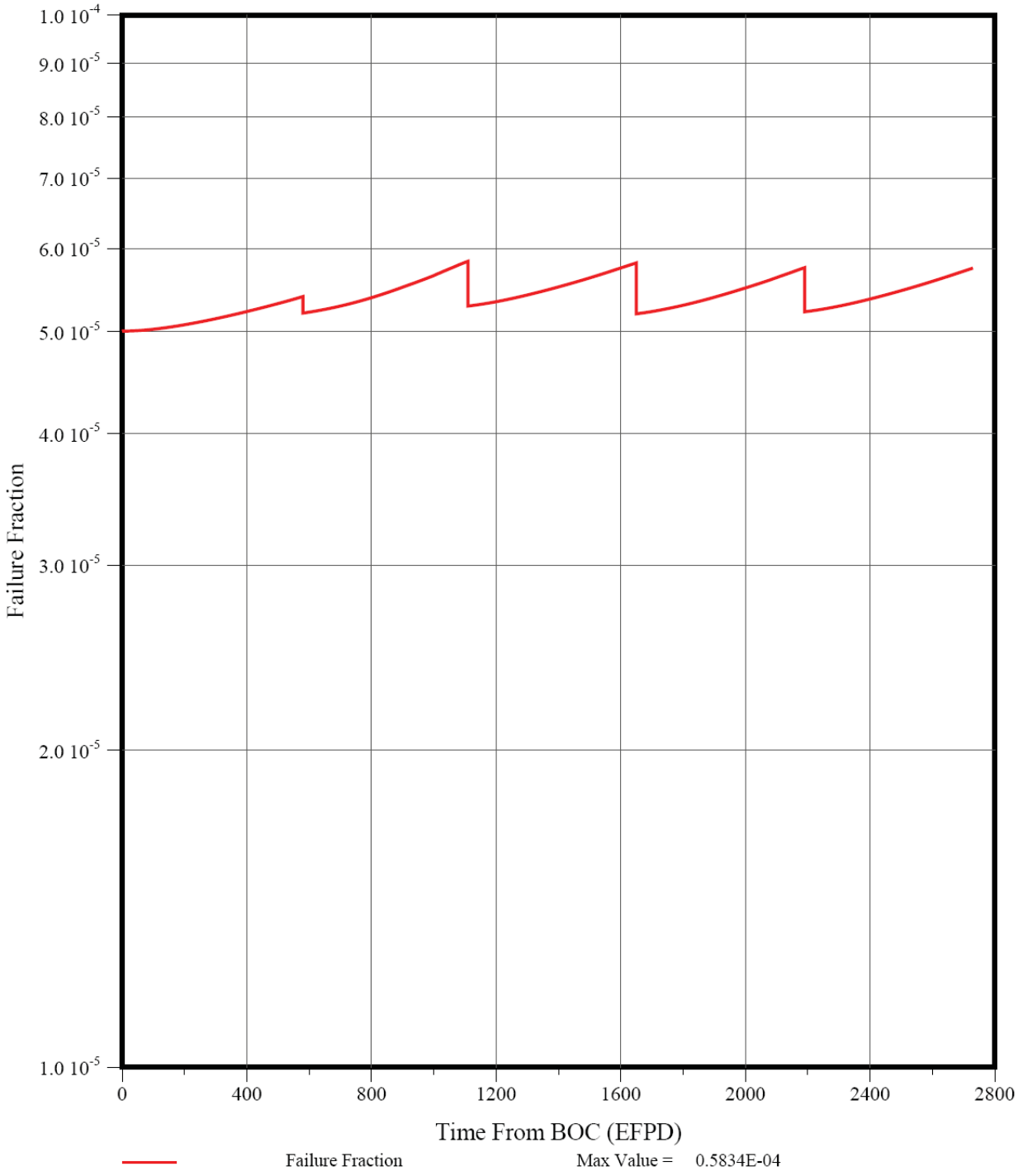

Figure 6-11. SiC Coating Failure Fraction for NUCO Fertile Particle (Case 7.9SC)

The maximum exposed kernel fractions calculated for the fissile and fertile fuel particles are about 1.2×10^{-5} and 2.3×10^{-6}, respectively, as shown in Figures 6-12 and 6-13. Exposed kernels may result from pressure-vessel (PV) failure of standard (intact) particles and particles with a variety of manufacturing defects. The initial value is very low because any exposed kernels in the as-manufactured fuel compacts would be counted as heavy-metal contamination. The contribution from PV failure of standard particles is insignificant because the failure probability is predicted to be negligible. The dominant sources of exposed kernels are therefore: (1) PV failure of particles with missing-buffer (MB) layers, (2) PV failure of particles with defective or failed OPyC layers, and (3) OPyC failure on particles with defective or failed SiC layers. As stated above, 3% OPyC failure is predicted at a fast fluence of 2×10^{25} n/m^2. On a core-average basis, most of the fissile particles with missing buffers (~90%) are predicted to fail; however, a significant fraction of the fertile particles with missing buffers are predicted to survive (>80%); see Figures 6-14 and 6-15. The contribution from OPyC failure on particles with defective or failed OPyC layers is about 0.03 times SiC failure fractions given in Figures 6-10 and 6-11, which is about 2×10^{-6}.

For earlier MHR designs, including the 350-MWt steam-cycle MHTGR, the predicted exposed kernel fraction was dominated by the PV failure of missing-buffer particles [Jovanovic 1989]. The reasons were that the MHTGR fuel product specification allowed a missing-buffer fraction of 5×10^{-5}, and minimal in-service FP/SiC corrosion failure was predicted (the MHGTR core outlet temperature was 687°C; hence, the fuel temperatures were significantly lower than predicted here). During the commercial GT-MHR program, the allowable missing-buffer fraction was reduced to 1×10^{-5} [Munoz 1994], and its contribution to in-service failure became less important.

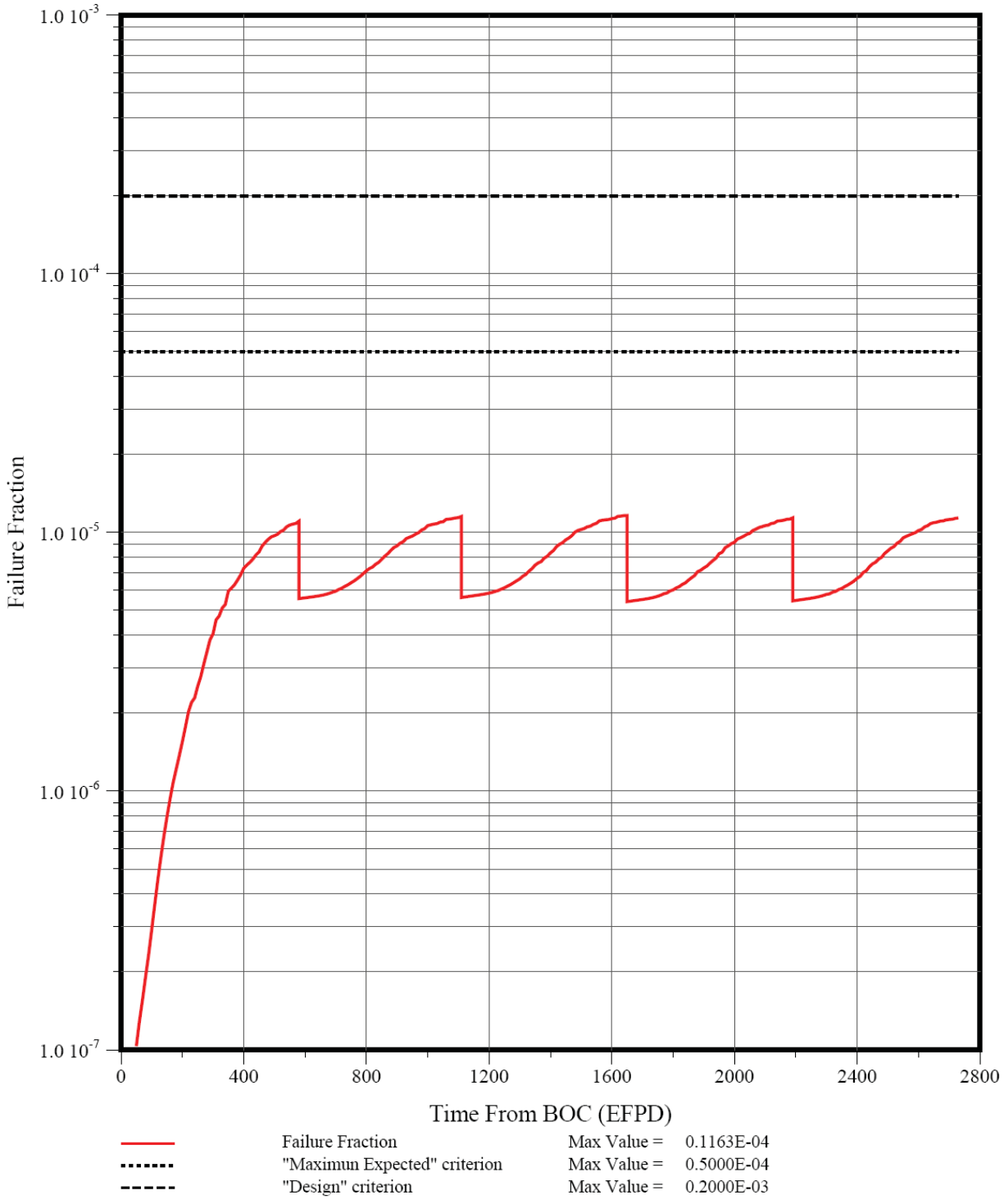

Figure 6-12. Exposed Kernel Fraction for LEU UCO Fissile Particle (Case 7.9SC)

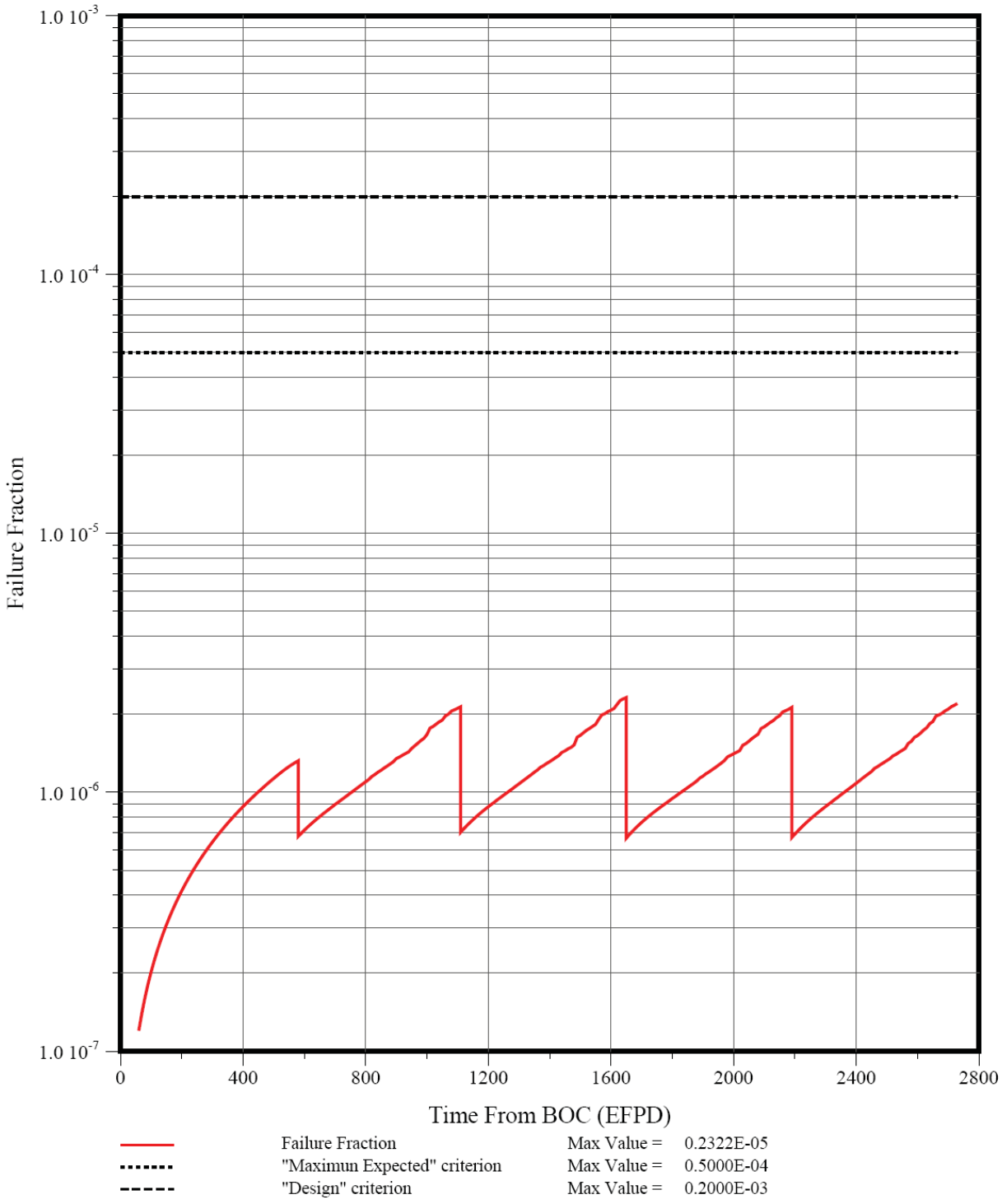

Figure 6-13. Exposed Kernel Fraction for NUCO Fertile Particle (Case 7.9SC)

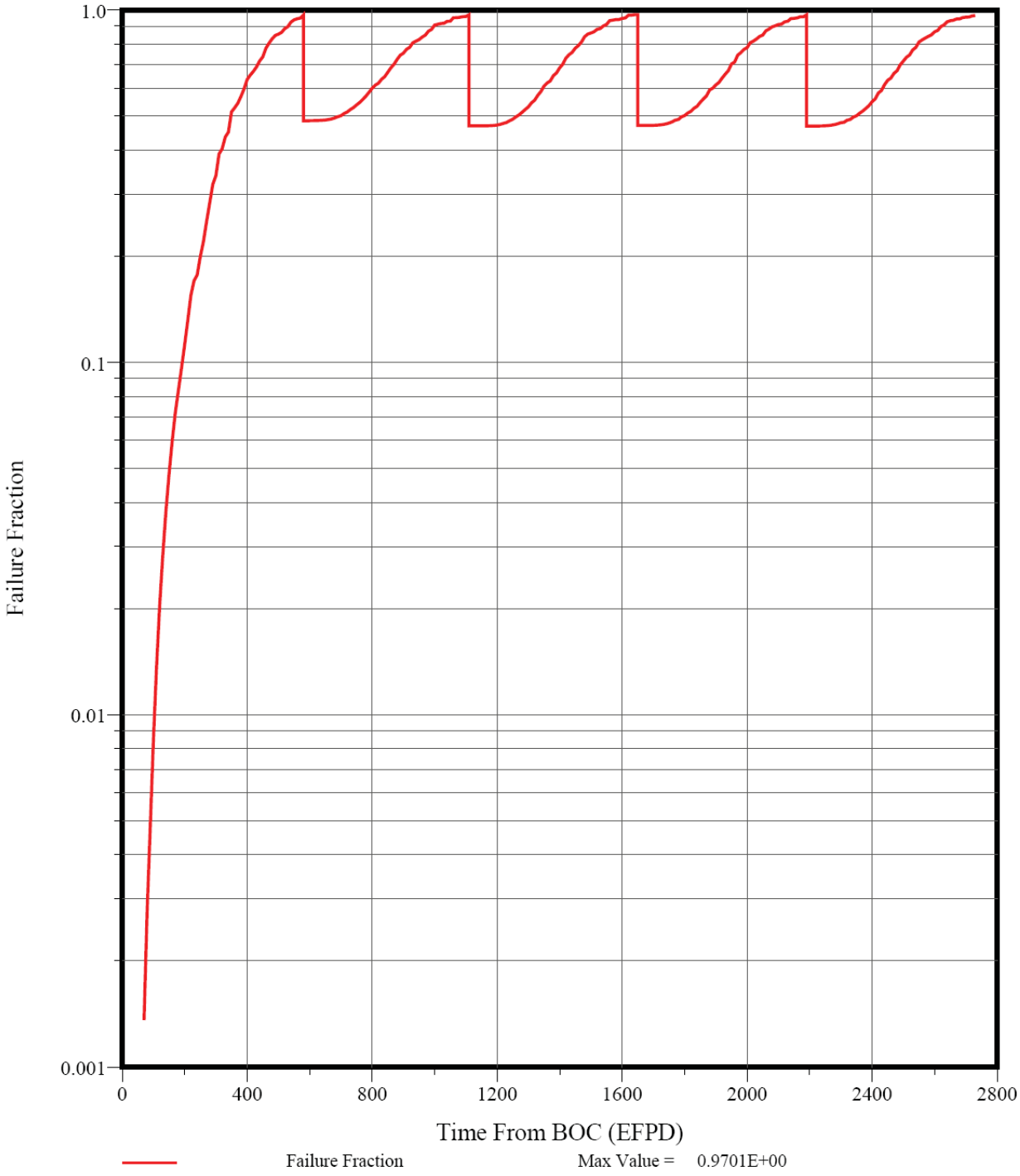

Figure 6-14. PV Failure Probability of Missing-Buffer Fissile Particles (Case 7.9SC)

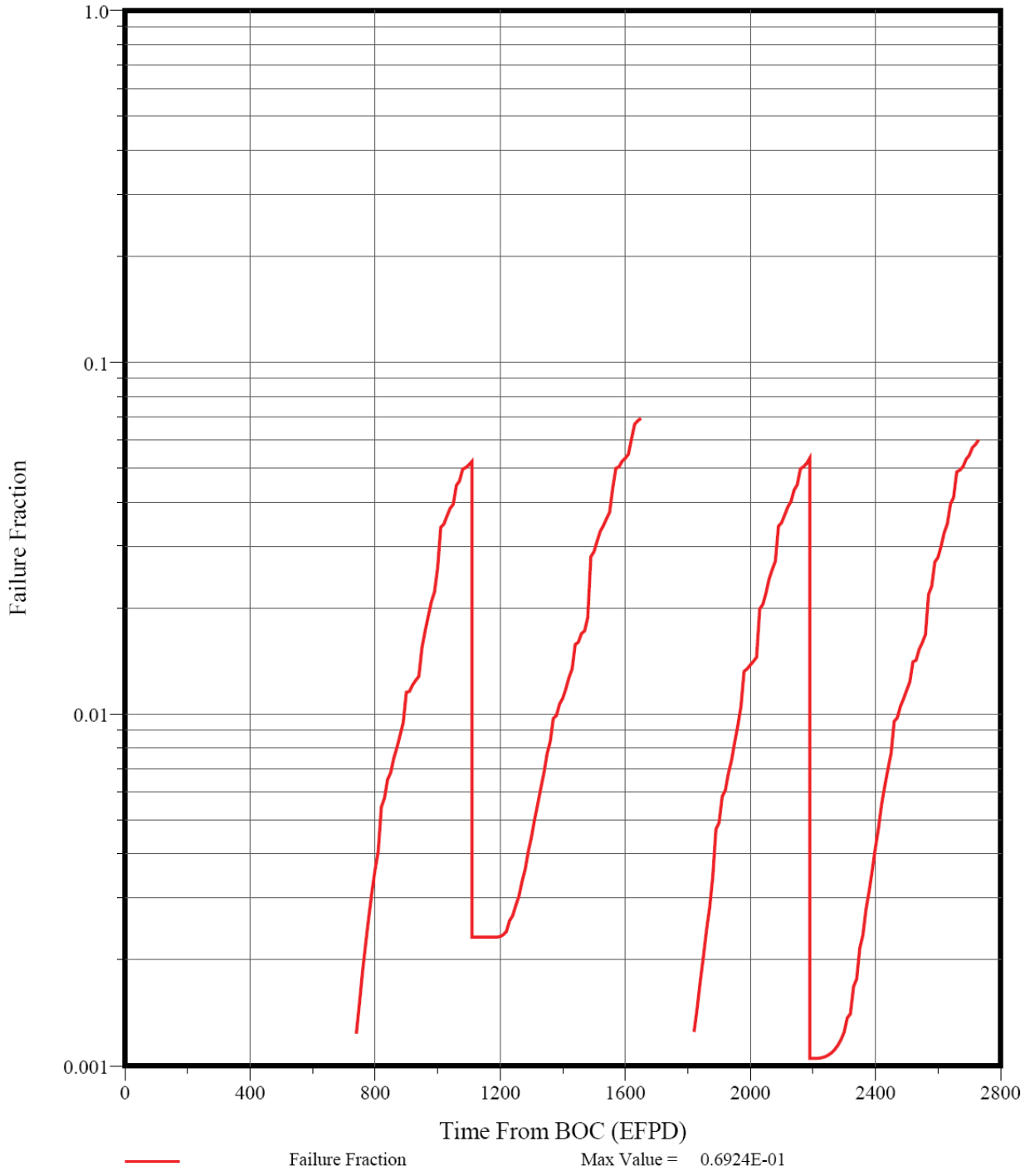

Figure 6-15. PV Failure Probability of Missing-Buffer Fertile Particles (Case 7.9SC)

6.1.2.4 Gaseous Fission Product Release

The release rate-to-birth rate (R/B) ratios (equivalent to the fractional release for steady-state calculations such as these) for 2.8-hr Kr-88 and 8-day I-131 were also calculated by SURVEY/PERFOR using the FDDM/F fission gas release models for hydrolyzed UCO fuel. These R/Bs as a function of time are shown in Figures 6-16 and 6-17. These two radionuclides were chosen because they are typically dominant contributors to off-site accident doses.

[FDDM/F 1987] contains fission gas release models for both unhydrolyzed and hydrolyzed UCO exposed kernels. The difference at steady-state is not particularly large (a factor of 1.7). The hydrolyzed model was chosen because the leading GA and AREVA candidate designs at the present time contain a steam generator in the primary circuit. Under the present circumstances, the choice of gas release model is of little practical consequence because the predicted fission gas release is dominated by the contribution from heavy-metal contamination. The contribution from failed particles is low because the predicted exposed kernel fraction is very low as discussed above (primarily a result of the tight specification on allowable missing-buffer particles). Nevertheless, the peak predicted R/Bs are near the “Maximum Expected” limits because of the high average fuel temperatures. The only effective way of reducing these R/Bs would be to tighten the specification on heavy-metal contamination.

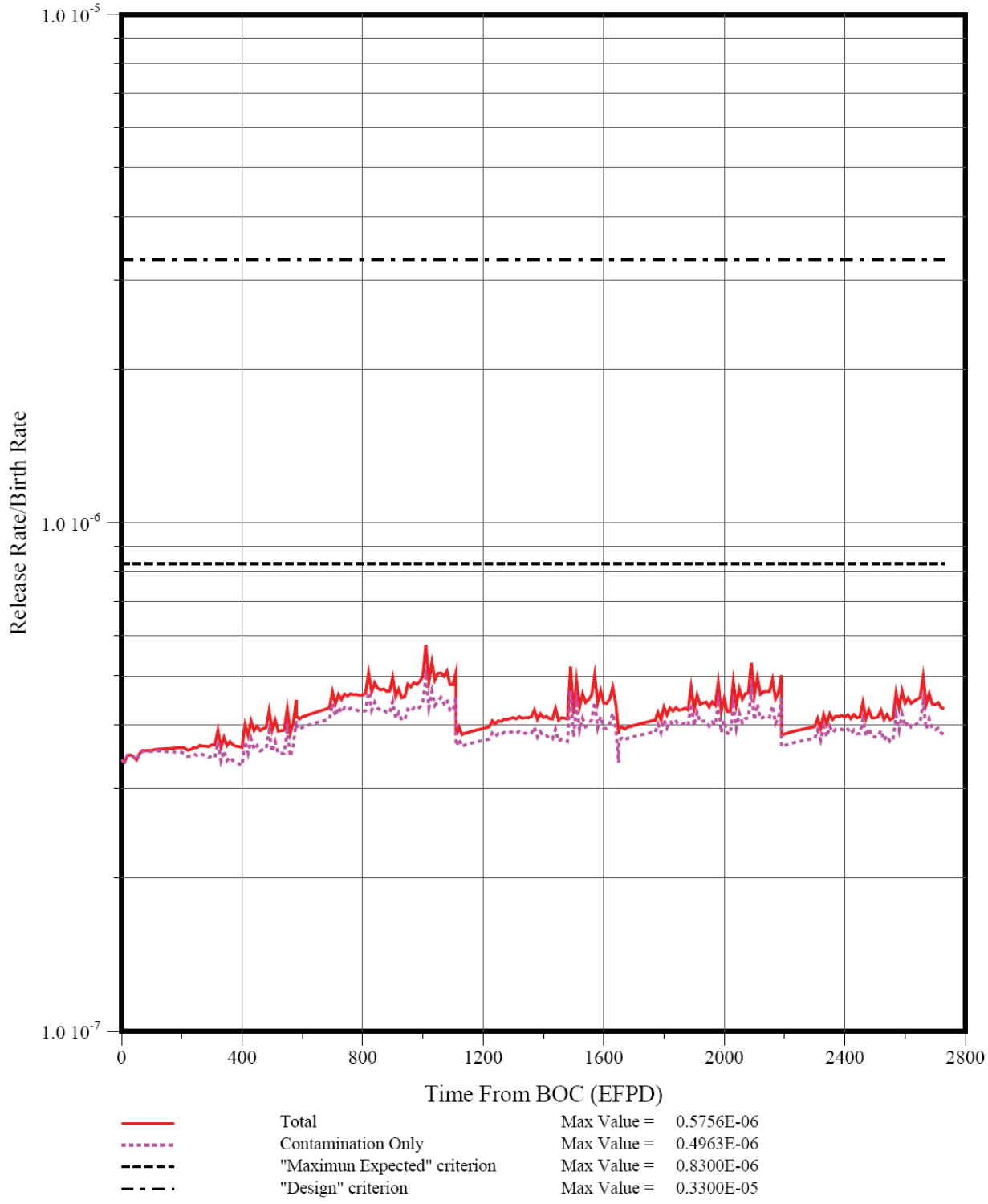

Figure 6-16. Core-Average R/B for Kr-88 (Case 7.9SC)

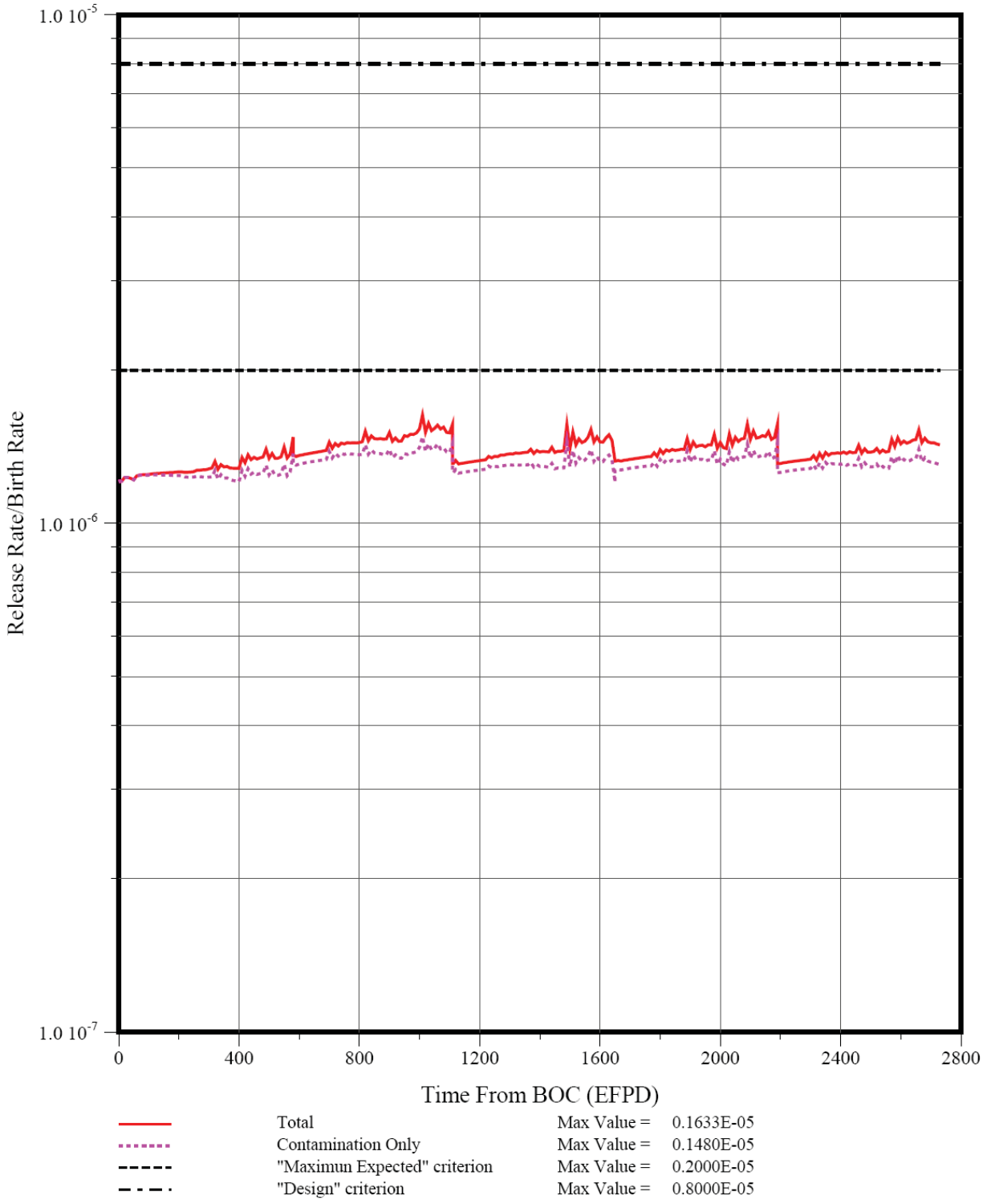

Figure 6-17. Core-Average R/B for I-131 (Case 7.9SC)

6.1.2.5 Metallic Fission Product Release

The SURVEY/PERFOR results summarized above were supplied as input to the TRAFIC-FD code which was used to predict the releases of Ag-110m, Cs-137, and Sr-90 from the core for Case 7.9SC.

The material property data (e.g., FP diffusivities in SiC coatings) required as input to TRAFIC-FD was taken from FDDM/F with two important exceptions. First, the KFA correlation for Ag diffusion in SiC coatings [Moormann 1987, TECDOC 1997] was used instead of the FDDM/F as recommended by a critical review of the Ag transport data in 1994 [Acharya 1994]. Use of the FDDM/F diffusivity correlation would likely increase the calculated Ag fractional release by a factor of five or more based upon previous core analysis [PC-MHR 1994]. Secondly, no credit was taken for Cs retention in exposed kernels. The FDDM/F correlation for Cs diffusion in UCO kernels has an extremely large burnup dependence [$D\ \alpha\ (FIMA)^4$]. This large burnup dependence for UCO kernels was inferred from the observed burnup dependence for Cs diffusion in ThO_2 kernels in the 1 - 6% FIMA range [Martin 1993]. This FDDM/F correlation was shown to grossly underpredict Cs release from UCO kernels at low burnups (2.5% FIMA) in the COMEDIE BD-1 test [Medwid 1993]; consequently, its use is not considered to be justified. An alternative would have been to use the German correlation for Cs diffusivity in LEU UO_2 which has no burnup dependence; however, this correlation would not necessarily be conservative for burnups >~10% FIMA.

The predicted overall core mass balance for 250-day Ag-110m is shown in Figure 6-18. The following "total" core (1/3 core because of symmetry) inventories are shown: (1) particle 1 (fissile), (2) particle 2 (fertile), (3) matrix, (4) graphite, and (5) cumulative release into the coolant.[43] These results are more easily interpreted by considering the corresponding inventories in each of the two core segments; the Ag-110m inventories in Segments 1 and 2 are shown in Figures 6-19 and 6-20, respectively. When Segment 1 is reloaded after Cycles 1 and 3, the Ag-110m inventories in the particles, matrix, and graphite are reduced to zero as the irradiated fuel is replaced by fresh fuel; however, the inventory released into the coolant continues to accumulate; for Segment 2 the in-core inventories are zeroed out after Cycles 2 and 4 when that segment is reloaded.

---

[43] Only the relative inventories reported in this section should be used directly (e.g., the ratio of the inventory in the graphite to that in the particles). The absolute core inventories of fission metals presented here are artificially high because a cumulative fission yield is used that is the sum of the yields for the stable and long-lived isotopes of a given chemical element (e.g., for Cs-137 which has an actual fission yield of ~0.06, a yield of 0.19 is used which is the cumulative yield of 30.1-yr Cs-137 + stable Cs-133 + 2.3 x 10^6-yr Cs-135. This practice is adopted because the sorption isotherms for fission metals on matrix and graphite are mass concentration dependent at high concentrations [FDDM/F 1987].

The cumulative fractional release of Ag-110m into the coolant is shown in Figure 6-21. The cumulative fractional release at any time point is defined as the cumulative release into the He coolant from time zero to that time point divided by the cumulative birth in the core from time zero to that time point with both release and birth inventories corrected for decay (the cumulative birth includes the birth in the fuel in the core at any given time plus the birth in any previously discharged fuel loads). This cumulative fractional release for long-lived fission metals can be contrasted to the use of an instantaneous release rate-to-birth rate (R/B) for short-lived fission gases, including iodines. For noble gases, the action of the He purification system results in an effective upper-limit half life of about 4.5 hours (depending upon the fractional purification rate) [Hanson 2008a]. Unlike the noble gases, the iodine and tellurium isotopes released from the core preferentially deposit ("plate out") in the primary circuit; however, the half lifes of the radiologically important I and Te isotopes are short compared to the length of an irradiation cycle such that their plateout inventories approach equilibrium values corresponding to their R/B values throughout plant operation.

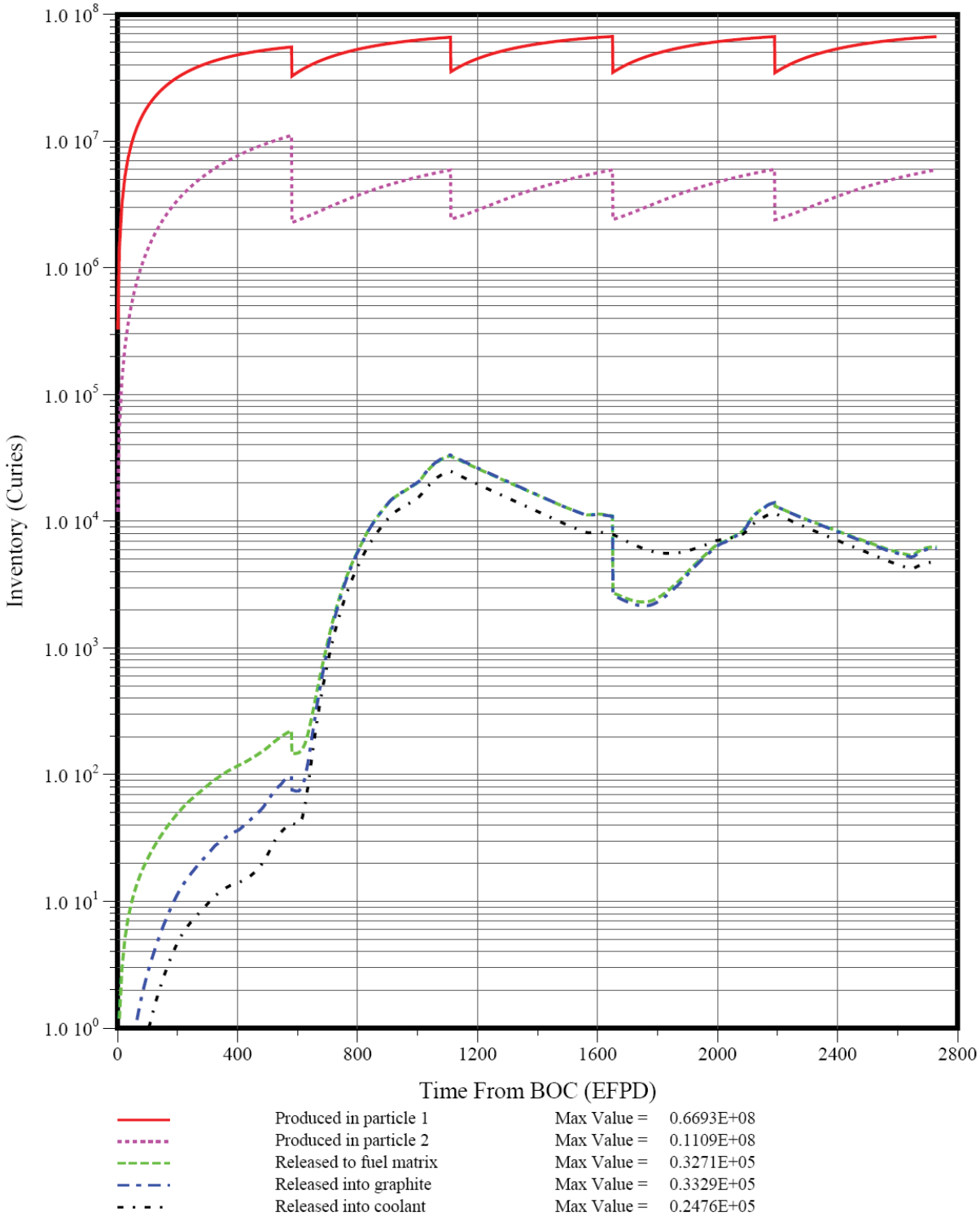

Figure 6-18. "'Full-core" Ag-110m Inventories by Core Material Region (Case 7.9SC)

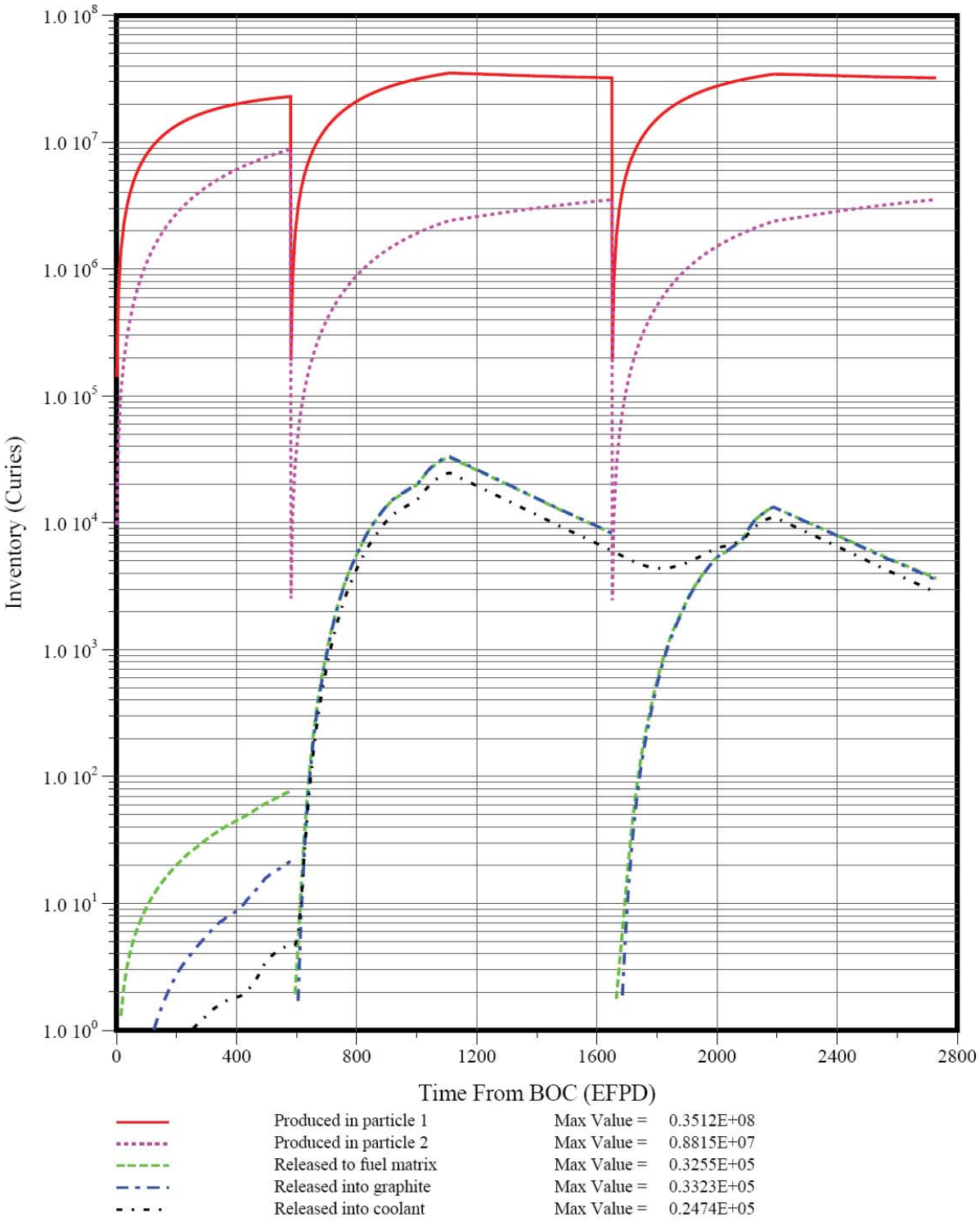

Figure 6-19. Ag-110m Inventories in Core Seg. 1 (Case 7.9SC)

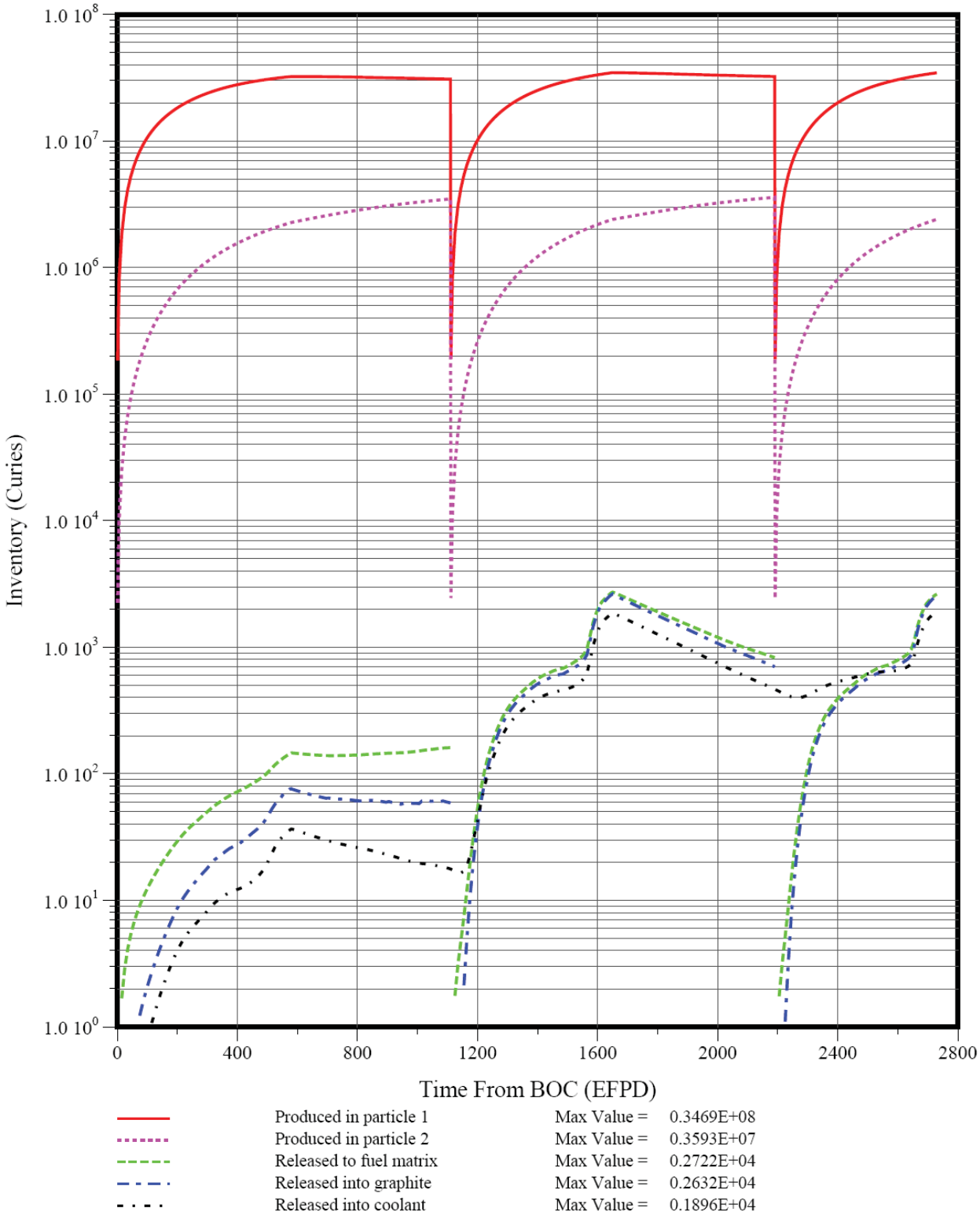

Figure 6-20. Ag-110m Inventories in Core Seg. 2 (Case 7.9SC)

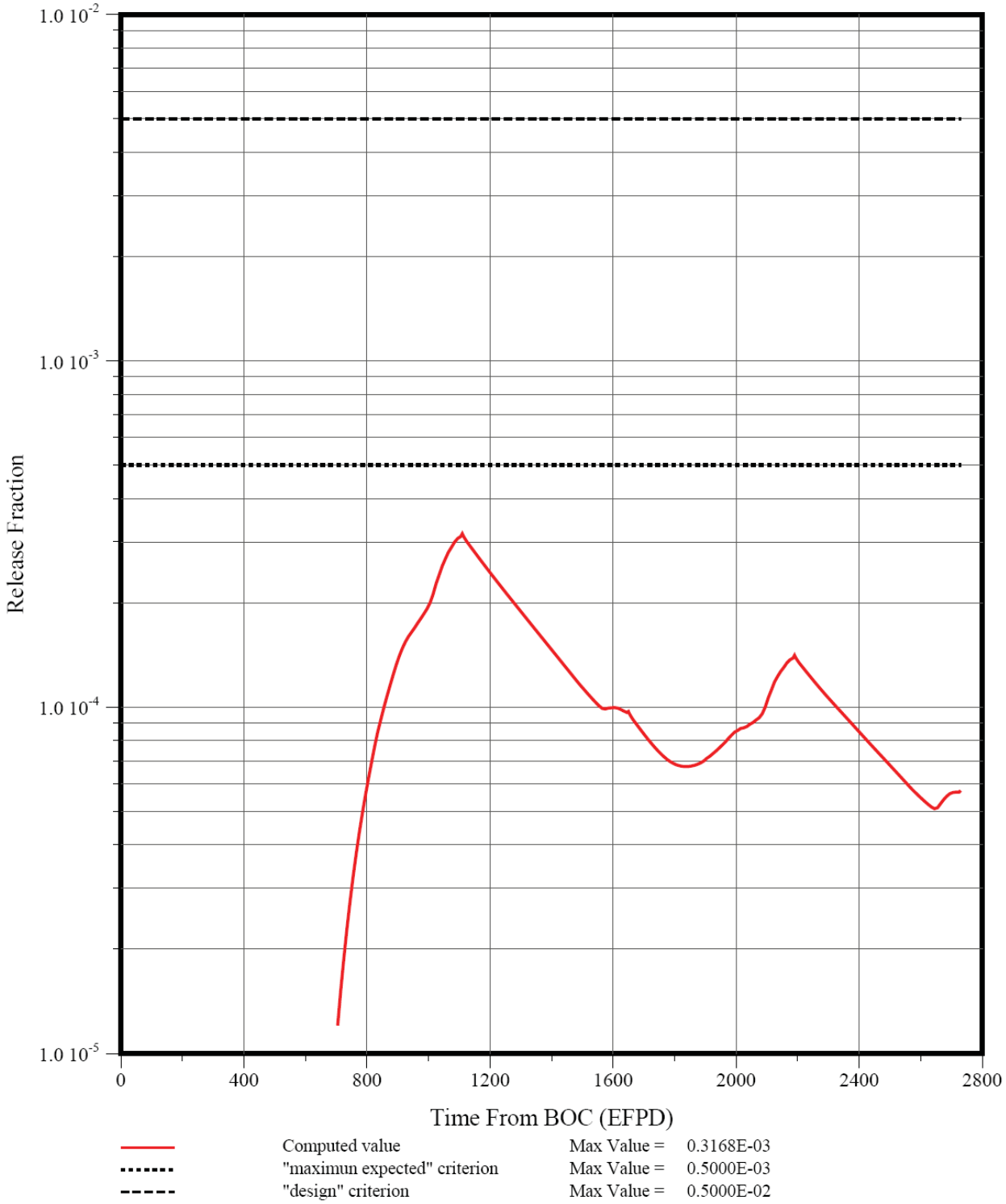

Figure 6-21. Cumulative Fractional Release of Ag-110m (Case 7.9SC)

Inspection of Figures 6-18 through 6-21 reveals a rather complex pattern wherein the initial cycle is unique and the behavior is approaching a repeating equilibrium cycle by the end of Cycle 5. The full-core inventory of Ag-110m (essentially the sum of the inventories in the two fuel particles) approaches an equilibrium value during each cycle since the cycle length of 540 EFPD is about two radioactive half lifes. Very little Ag is released from the particles during the first cycle because the SiC failure and exposed kernel fractions are low, and the Ag diffusing through the SiC layers of intact TRISO particles has not yet broken through. There is also significant holdup of Ag by the matrix and graphite during the first cycle.

However, diffusive Ag release from intact TRISO particles becomes dominant by the end of Cycle 2 but is significantly less by the end of Cycle 5 as is evident from Figure 6-19 where the fractional release of Ag is 3×10^{-4} at the end of Cycle 2 but the SiC failure fraction is only $\sim 6 \times 10^{-5}$ at that time (see Figure 6-10). During all cycles, the amount of Ag holdup by the matrix and graphite is modest because most of the Ag released from the particles is released into the coolant (see Figures 6-18 through 6-20). The core temperatures and, consequently, the SiC failure fractions and diffusive Ag release peak at the end of Cycle 2. Thus, during Cycle 3 and subsequent cycles, the cumulative fractional releases into the coolant actually decrease or go through minima during those time periods when the decay of the previously released Ag and the birth rate of "new" Ag exceed the release rate of "new" Ag from the core.

The corresponding predicted transport behavior of 30.1-yr Cs-137 is shown in Figures 6-22 through 6-25. The predicted behavior Cs-137 is generally similar though not identical to that of Ag-110m for two primary reasons. First, the half life of Cs-137 is much longer than that of Ag-110m (30.1 yr versus 0.68 yr) and much longer than an irradiation cycle; consequently, decay effects are insignificant during the five cycles analyzed. Secondly, there is no diffusive release from intact TRISO particles per the dictates of FDDM/F.[44]

[44] Per [FDDM/F 1987] and other GA documents of that vintage, Cs is not diffusively released from intact TRISO particles; rather Cs release from nominally intact TRISO particles at high temperatures (>~1600 ^{o}C) is an indication of SiC degradation from fission product corrosion and/or thermal decomposition. This interpretation is not universally accepted (e.g., see discussion in [Martin 1993]).

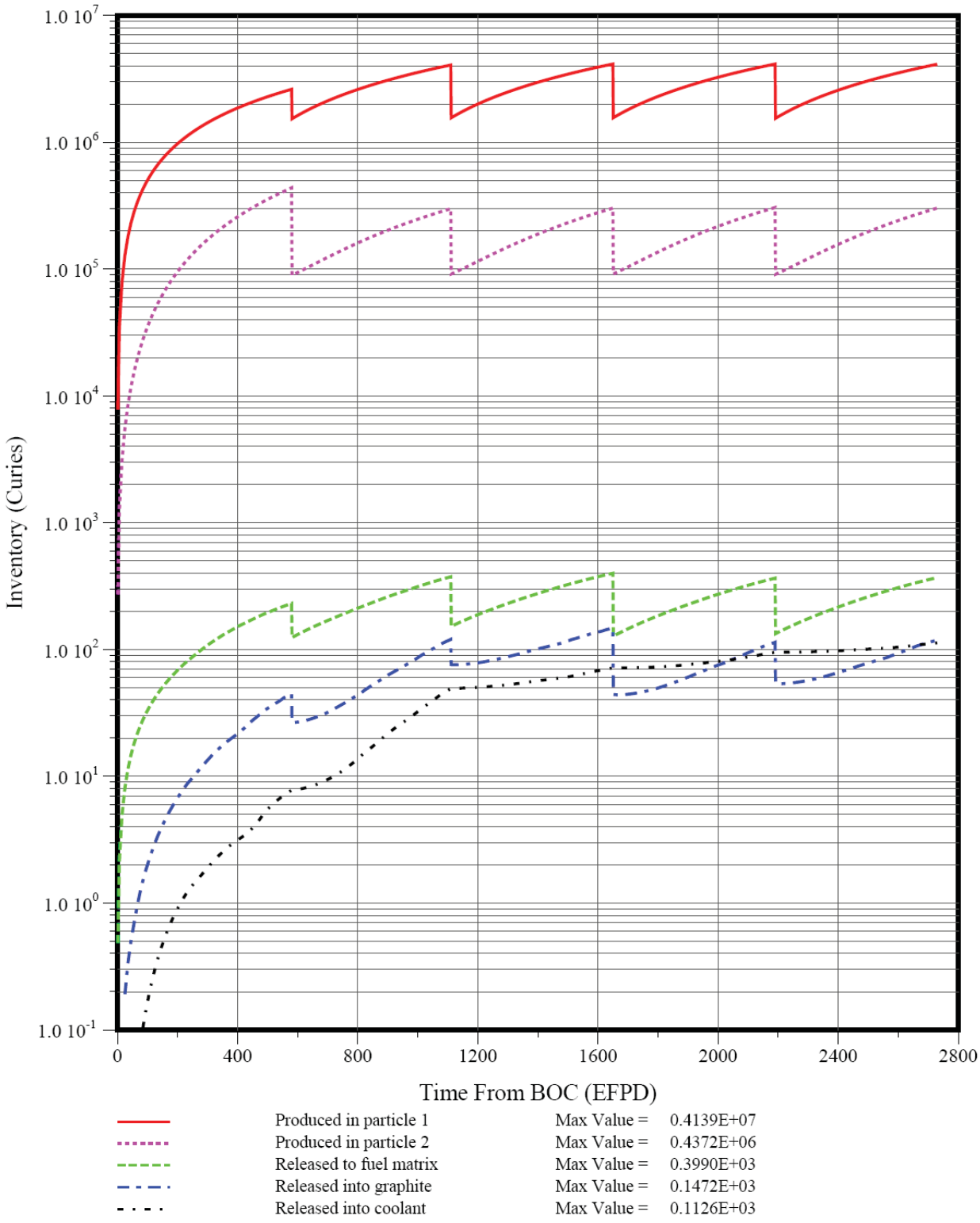

Figure 6-22. "'Full-core" Cs-137 Inventories by Core Material Region (Case 7.9SC)

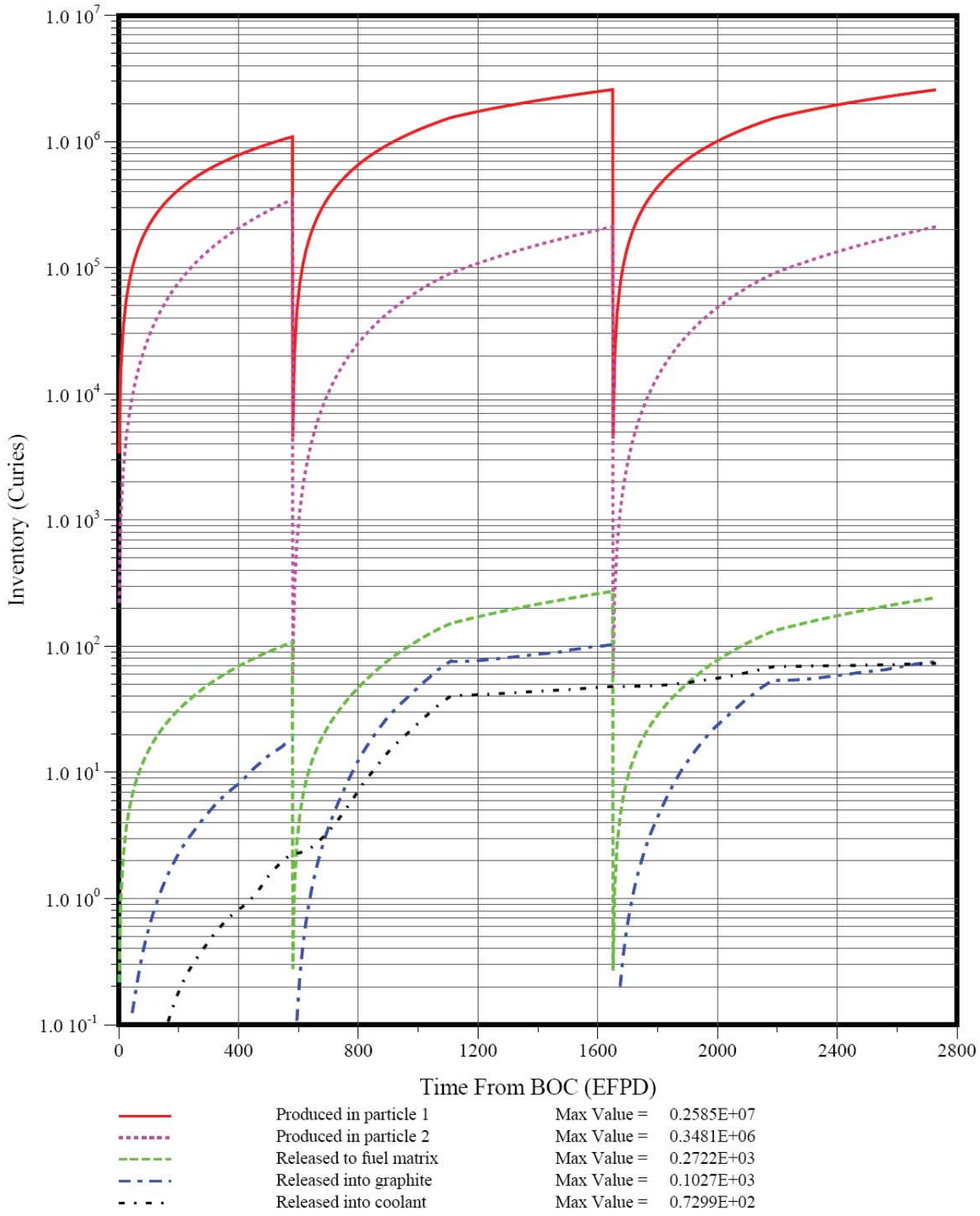

Figure 6-23. Cs-137 Inventories in Core Seg. 1 (Case 7.9SC)

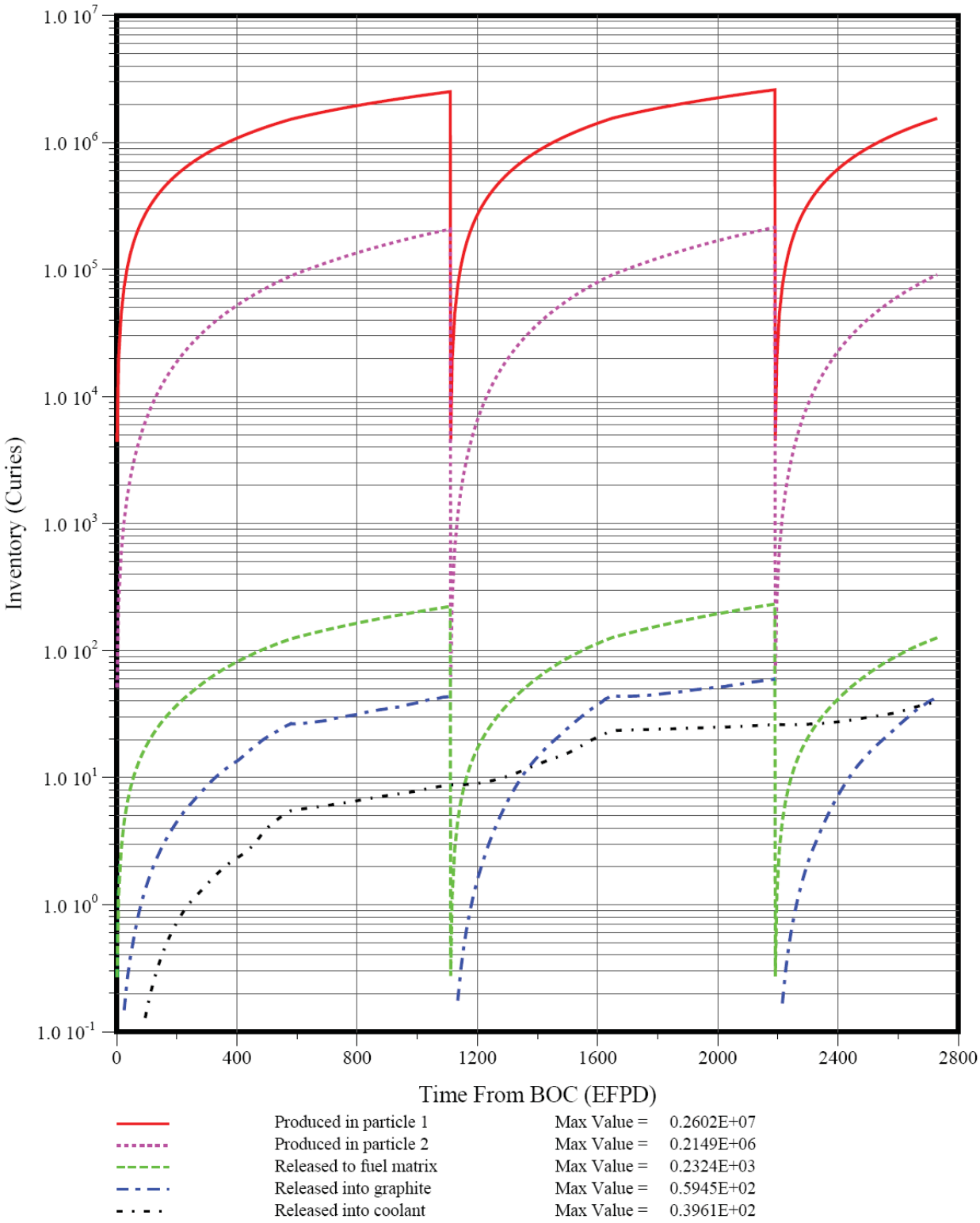

Figure 6-24. Cs-137 Inventories in Core Seg. 2 (Case 7.9SC)

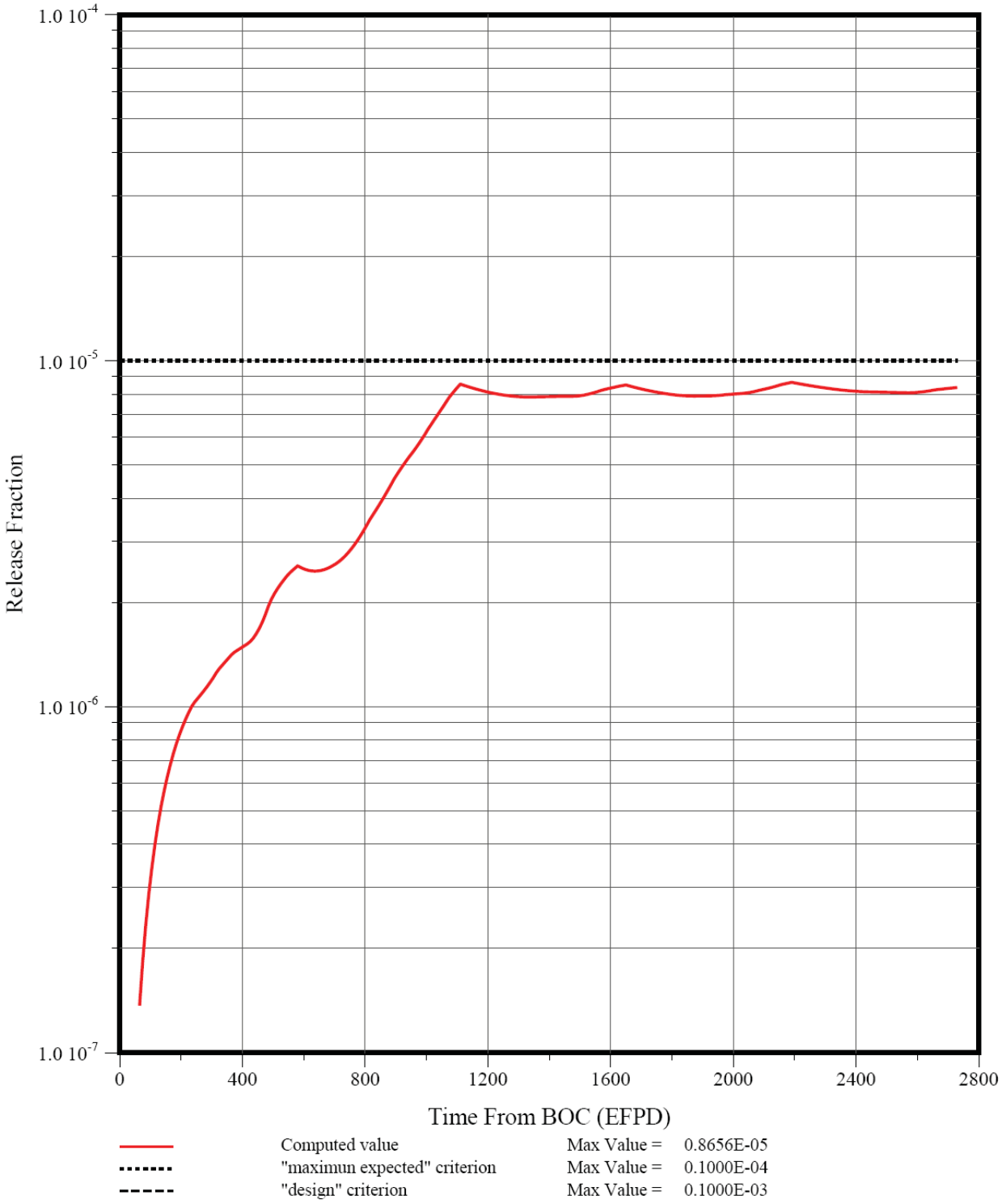

Figure 6-25. Cumulative Fractional Release of Cs-137 (Case 7.9SC)

Also, in contrast to the predicted Ag behavior, there is significant Cs holdup by the matrix and graphite; the effect is most obvious in the first cycle (see Figures 6-22 through 6-24). The core temperatures and, consequently, the SiC failure fractions and Cs release rates peak at the end of Cycle 2. Thus, during Cycle 3 and subsequent cycles, the fractional release of "new" Cs remains relatively constant, and the cumulative Cs release to the coolant is dominated by release during the first two cycles (in contrast to Ag-110m, this early Cs-137 release is not reduced because of its 30.1-yr half life).

As stated above, the predicted Cs release would likely be significantly reduced if the burnup-dependent FDDM/F correlation for Cs diffusion in UCO kernels were used; however, the use of that correlation is considered to be unjustified, given more recent experimental data [Medwid 1993].

The corresponding predicted transport behavior of 29-yr Sr-90 is shown in Figures 6-26 through 6-29. The predicted behavior of Sr-90 is distinctly different from Cs and Ag behavior in that there is massive holdup in the fuel-compact matrix and fuel-element graphite. The reason for this holdup is the FDDM/F isotherms for Sr sorption on matrix and graphite predict exceedingly low desorption pressures for typical steam-cycle core temperatures.[45] The desorption pressure over matrix and graphite rises rapidly with temperature; hence, the Sr release has a greater temperature sensitivity than even Ag release (as will be illustrated in Section 8.1).

In the base Case shown here, there is no diffusive Sr release from intact TRISO particles per the dictates of FDDM/F.[46] No credit is taken for Sr retention in the kernels of particles with failed SiC coatings or in exposed kernels for same reason that was explained for Cs earlier in this subsection. The sensitivity studies presented in Section 7.1 include the German modeling assumptions for Sr release from TRISO particles.

[45] In fact, these low desorption pressures resulted in persistent computational problems with TRAFIC-FD and required the conversion of much of the code to double precision for successful execution.

[46] Per [FDDM/F 1987] and other GA documents of that vintage, Sr is not diffusively released from intact TRISO particles; in marked contrast, the reference German diffusivity for Sr in SiC is almost the same as their diffusivity for Ag in SiC [Moormann 1987].

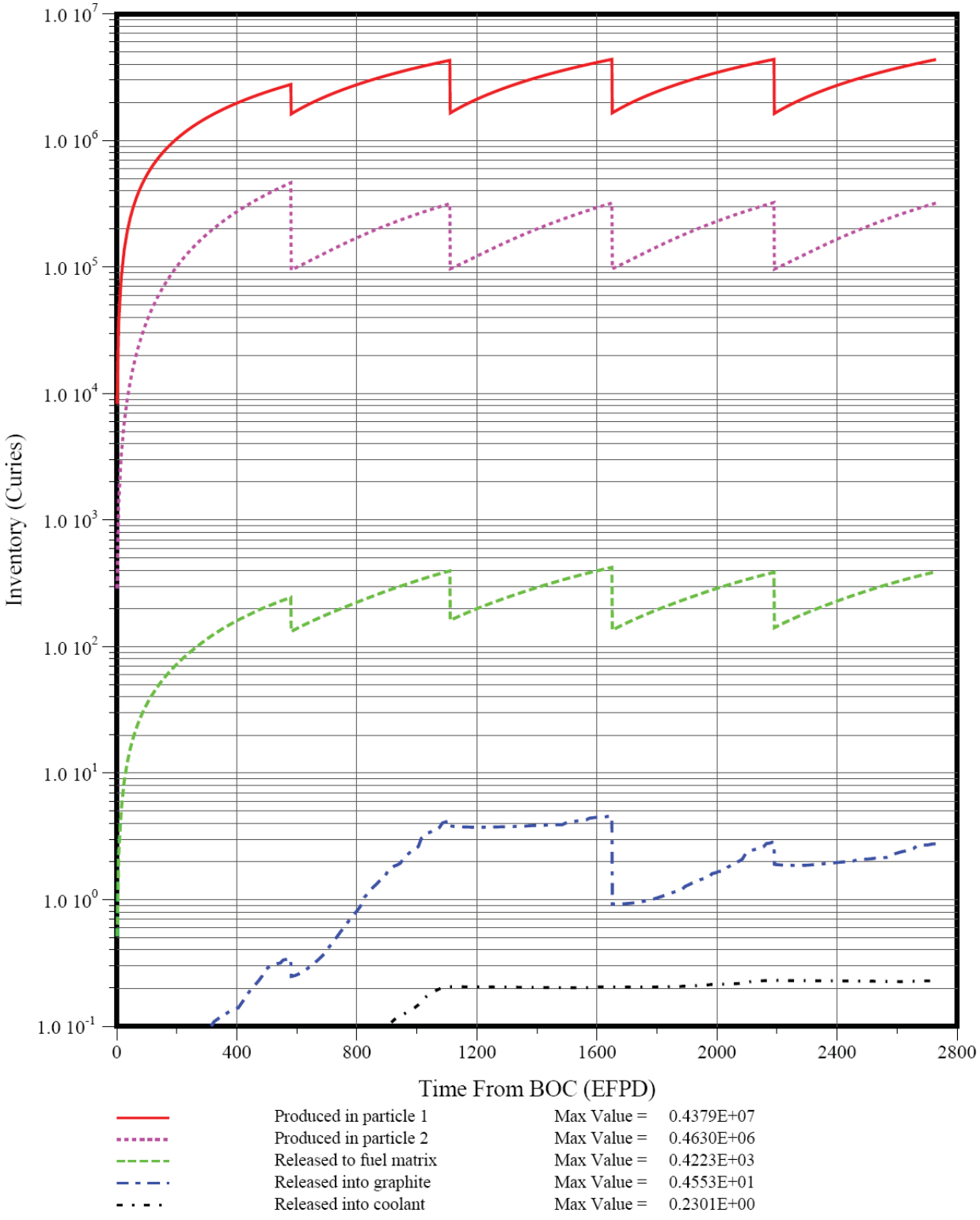

Figure 6-26. "'Full-core" Sr-90 Inventories by Core Material Region (Case 7.9SC)

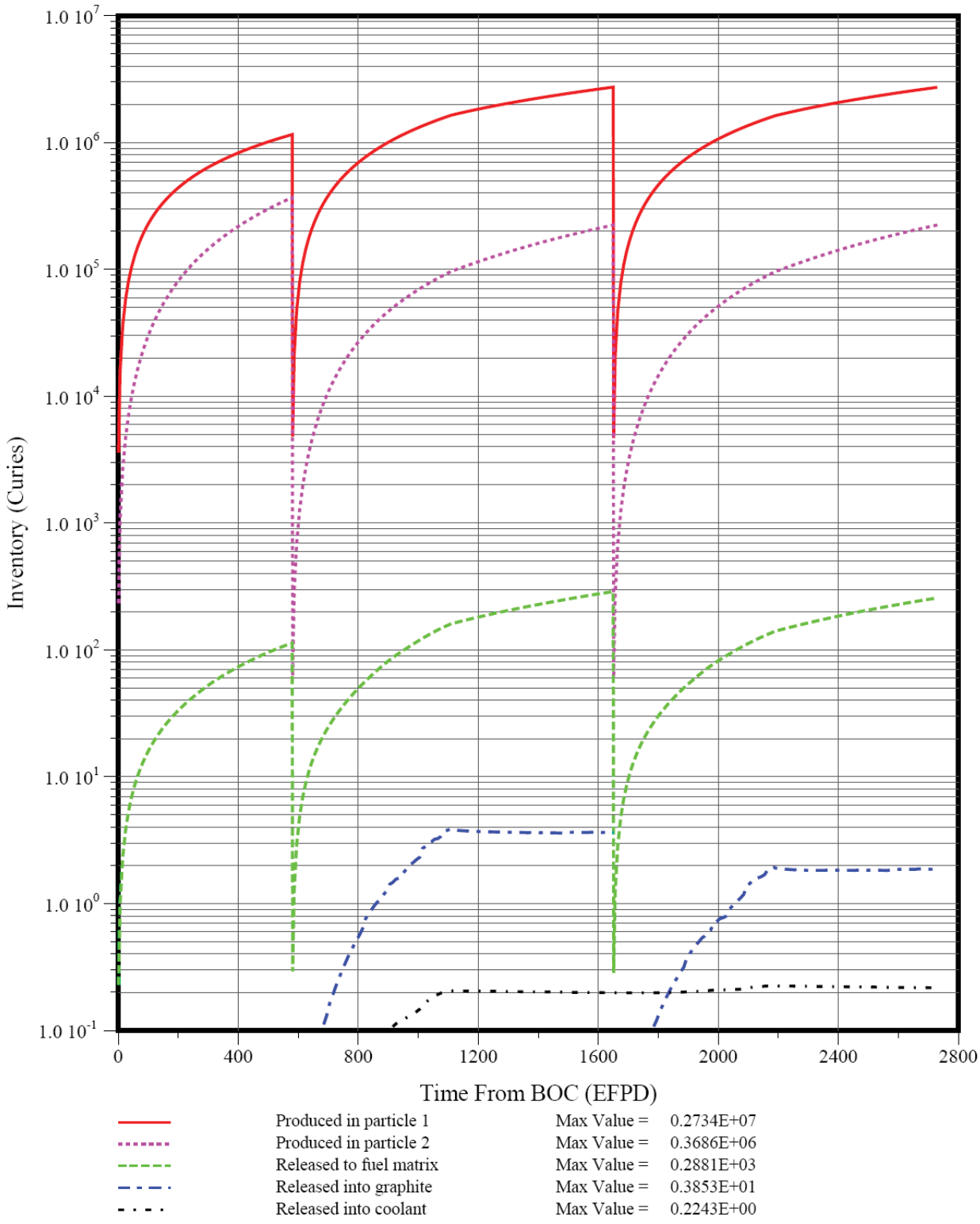

Figure 6-27. Sr-90 Inventories in Core Seg. 1 (Case 7.9SC)

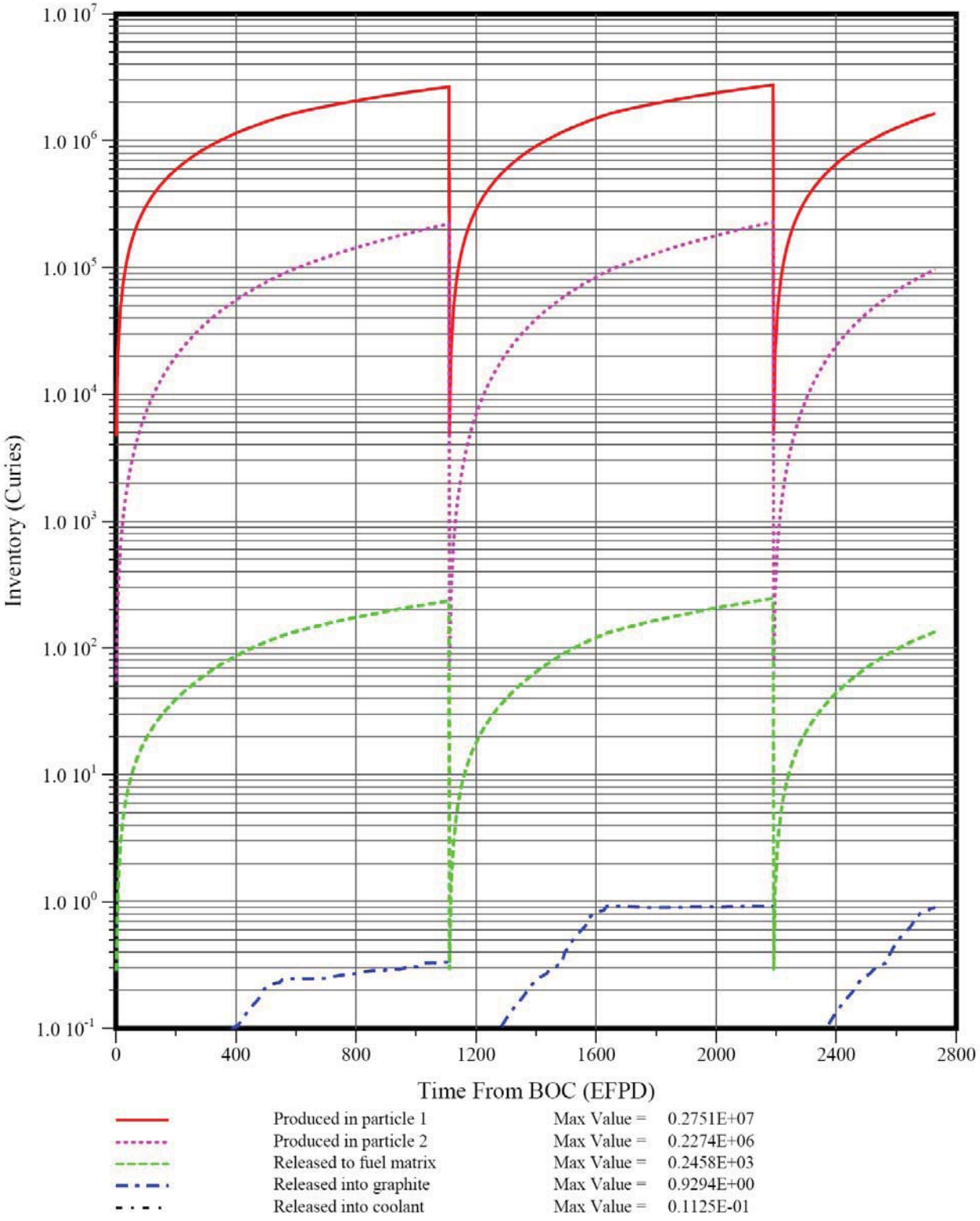

Figure 6-28. Sr-90 Inventories in Core Seg. 2 (Case 7.9SC)

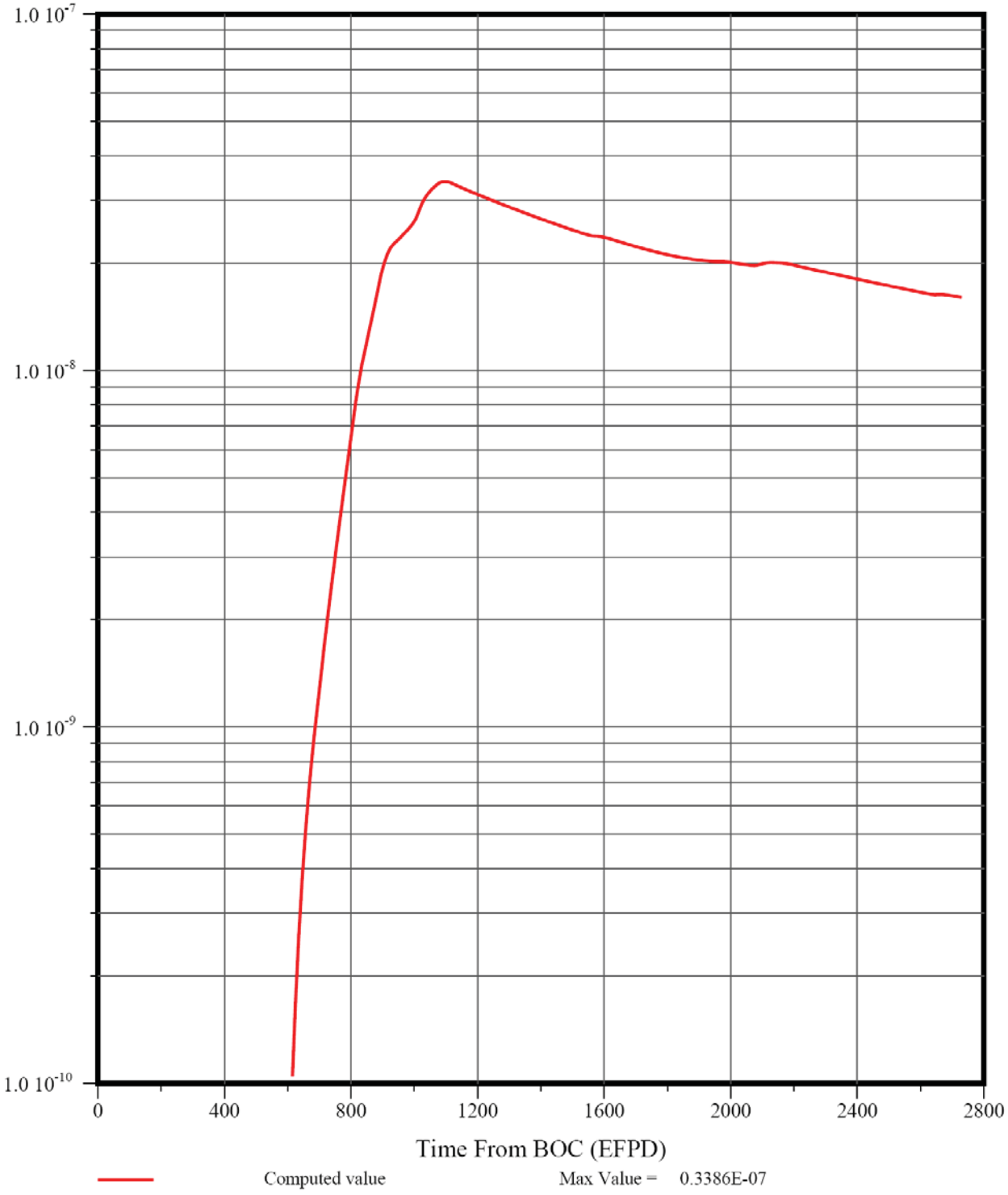

Figure 6-29. Cumulative Fractional Release of Sr-90 (Case 7.9SC)

6.1.3 Core Performance of Single-Particle Core Design (Case 8.9.3SC)

The above SURVEY and TRAFIC-FD analyses for the final binary-particle core design were repeated for the final single-particle core design (Case 8.9.3SC) with steam-cycle gas temperatures and coolant flow rates.

6.1.3.1 Fluence and Burnup

The volume fast fluence distribution calculated by SURVEY/THERM for Segment 2 is shown in Figure 6-30 (the distribution for Segment 2 is virtually identical with same peak value). The peak fast fluence is about 4.2×10^{25} n/m^2 (E >0.18 Mev) which is slightly less than the peak value for Case 7.9 (4.3×10^{25} n/m^2) and less than the practiced limit of $\leq 5 \times 10^{25}$ n/m^2 (both the fuel and graphite are capable of operating to much higher fast fluence limits). The volume burnup distribution for the single 425-µm, 15.5% enriched LEU UCO particle for Segment 2 is shown in Figure 6-31 (the distribution for Segment 1 is slightly lower). The peak burnups are 16.4% and 17.6% FIMA for Segments 1 and 2, respectively. The peak burnup for the 19.8% enriched fissile particle in Case 7.9 was 20.3% FIMA because its higher enrichment.

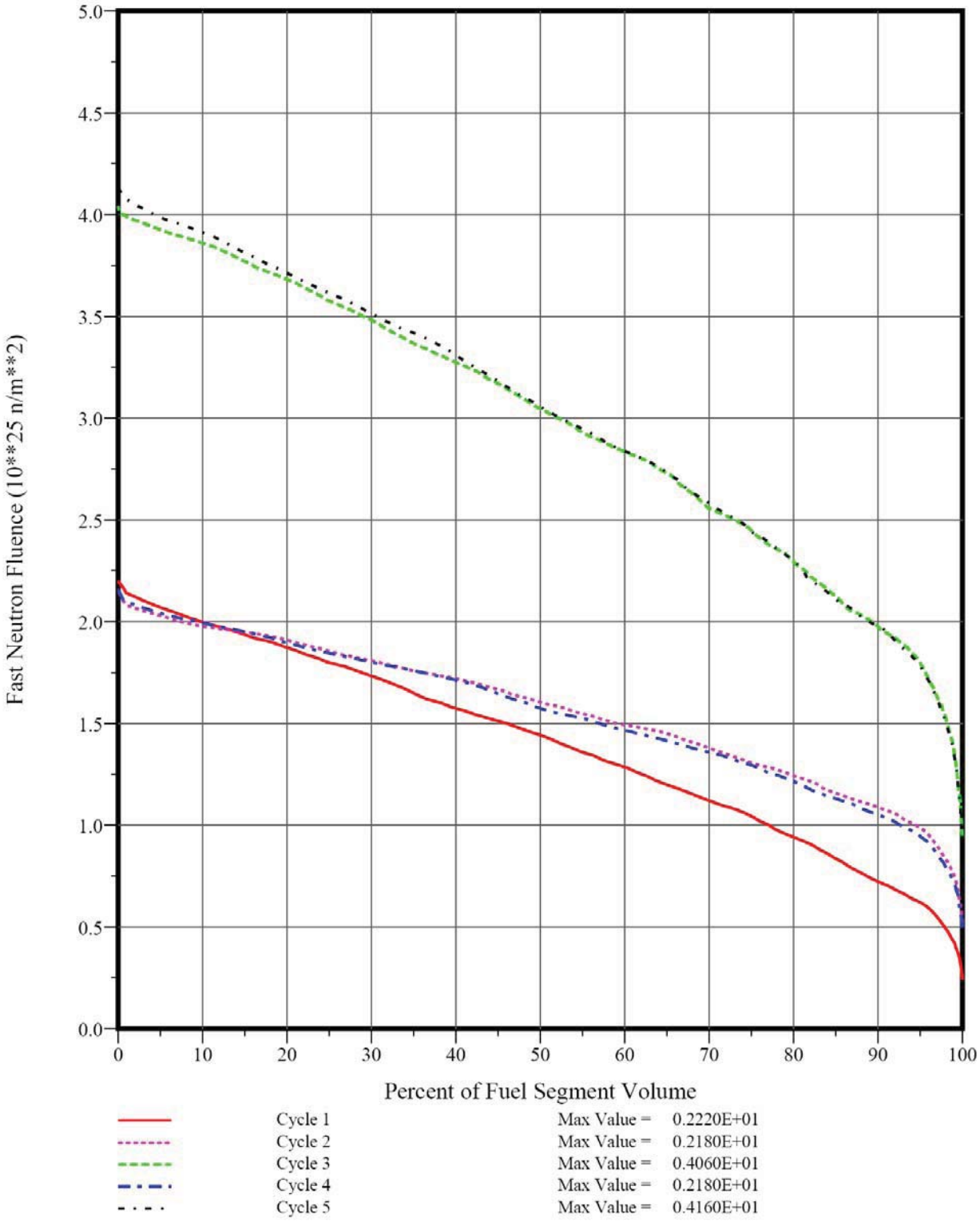

Figure 6-30. Fast Fluence Volume Distribution for Seg. 1 (Case 8.9.3SC)

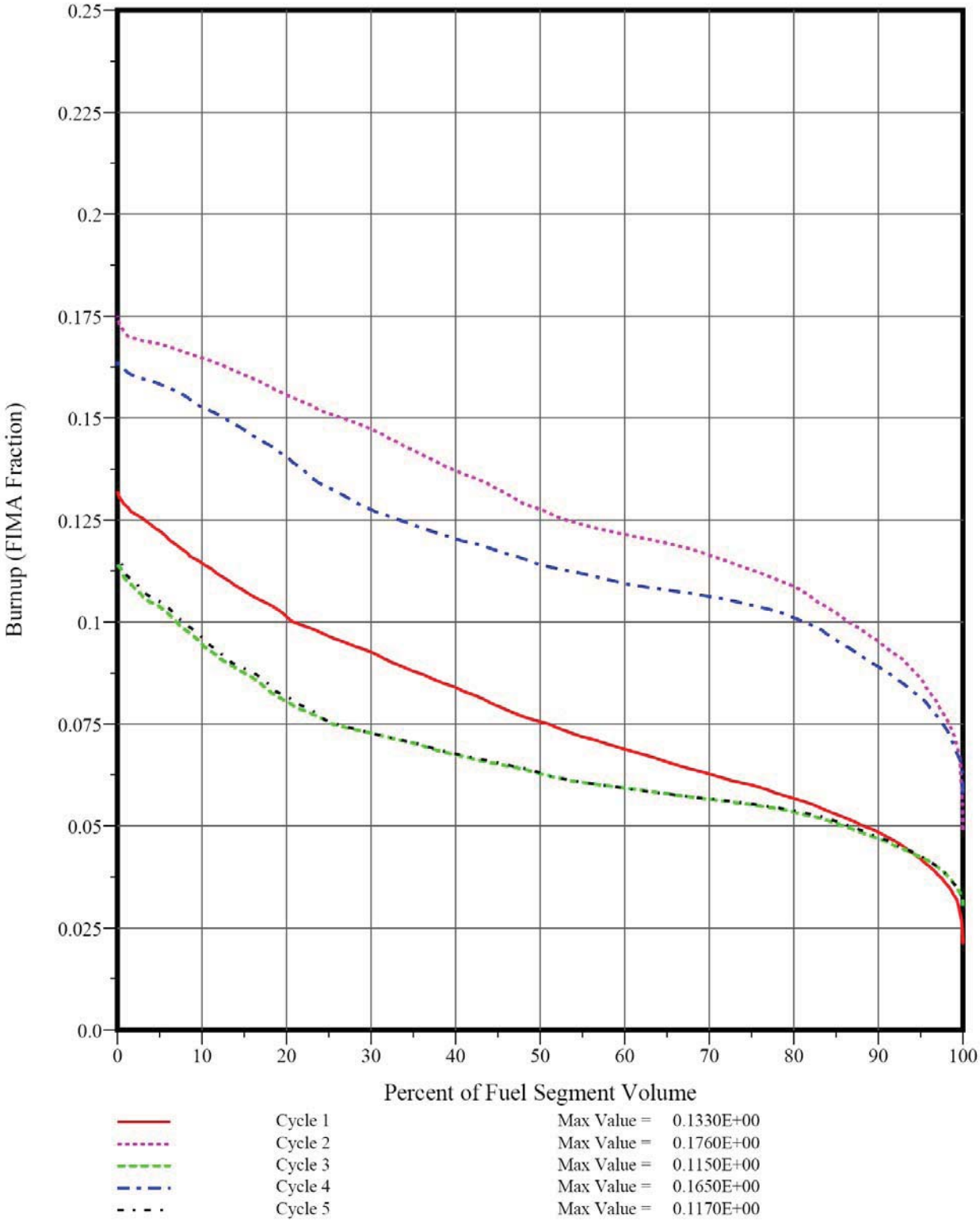

Figure 6-31. Particle Burnup Volume Distribution for Seg. 2 (Case 8.9.3SC)

6.1.3.2 Fuel and Graphite Temperature Distributions

Figures 6-32 and 6-33 give peak temperature distributions for fuel Segment 1; the plots are given for both the full-core volume and hottest 5% of the core. The corresponding maximum temperature for Segment 2 is slightly lower (1516 versus 1529 ^{o}C). However, the maximum time-average temperature is slightly higher in Segment 2 (1231 versus 1176 ^{o}C); the full-core volume and hottest 5% of the core for Segment 2 are shown in Figures 6-34 and 6-35, respectively. The maximum time-average fuel temperatures for Segment 1 and Segment 2 are all less than the design goal of <1250 °C.

The peak fuel temperatures for Case 8.9.3SC are higher than for Case 7.9SC (1529 vs. 1460 ^{o}C) as are the maximum time-average fuel temperatures (1231 vs. 1171 ^{o}C). For both designs, the highest fuel temperatures tend to occur in subcolumns in the bottom fuel elements of columns that are adjacent to the outer reflector and also adjacent to a control rod. The differences in the power distributions, hence, the fuel temperature distributions, between the single-particle and binary-particle core designs are discussed at greater length in [GA 2009b]. In general, the binary-particle core designs facilitate better power shaping than the single-particle designs and thus have somewhat lower peak fuel temperatures.

As illustrated for Case 7.9SC (Section 6.1.2.2), the graphite temperature distributions simply track the fuel temperature distributions; hence, they are not included here.

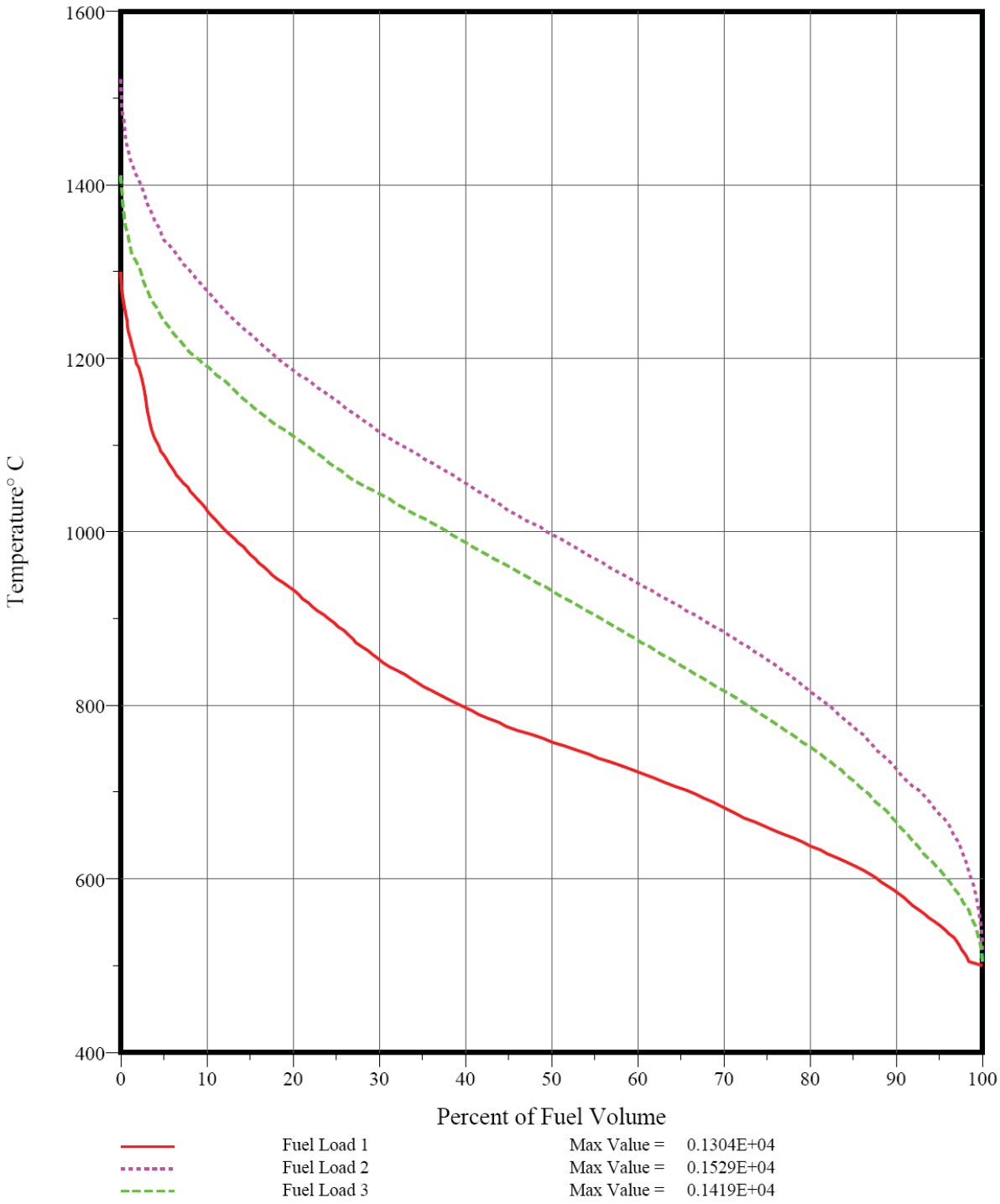

Figure 6-32. Peak Fuel Temperature Volume Distribution for Seg. 1 (Case 8.9.3SC)

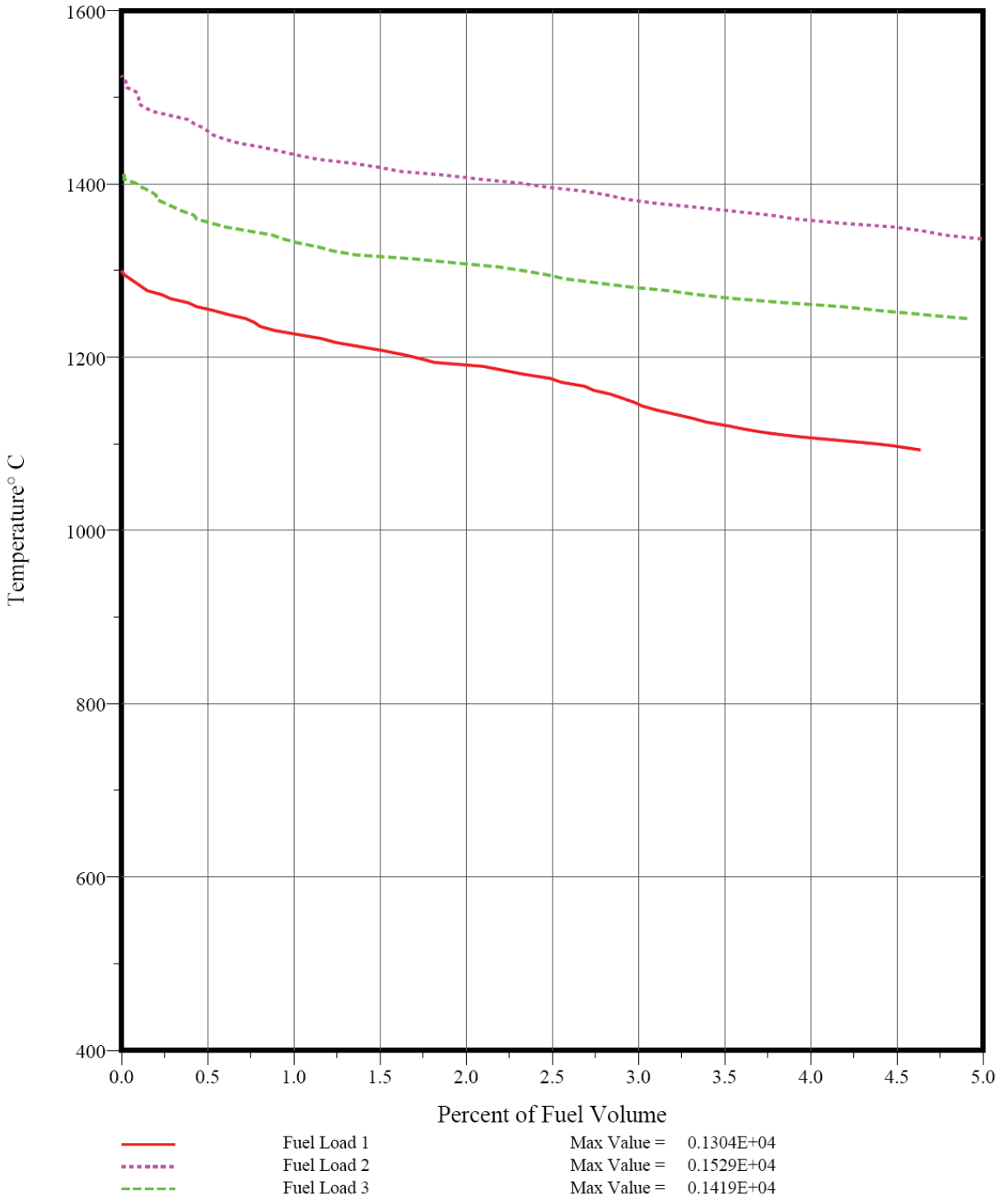

Figure 6-33. Peak Fuel Temperature Distribution for Seg. 1 (0-5%) (Case 8.9.3SC)

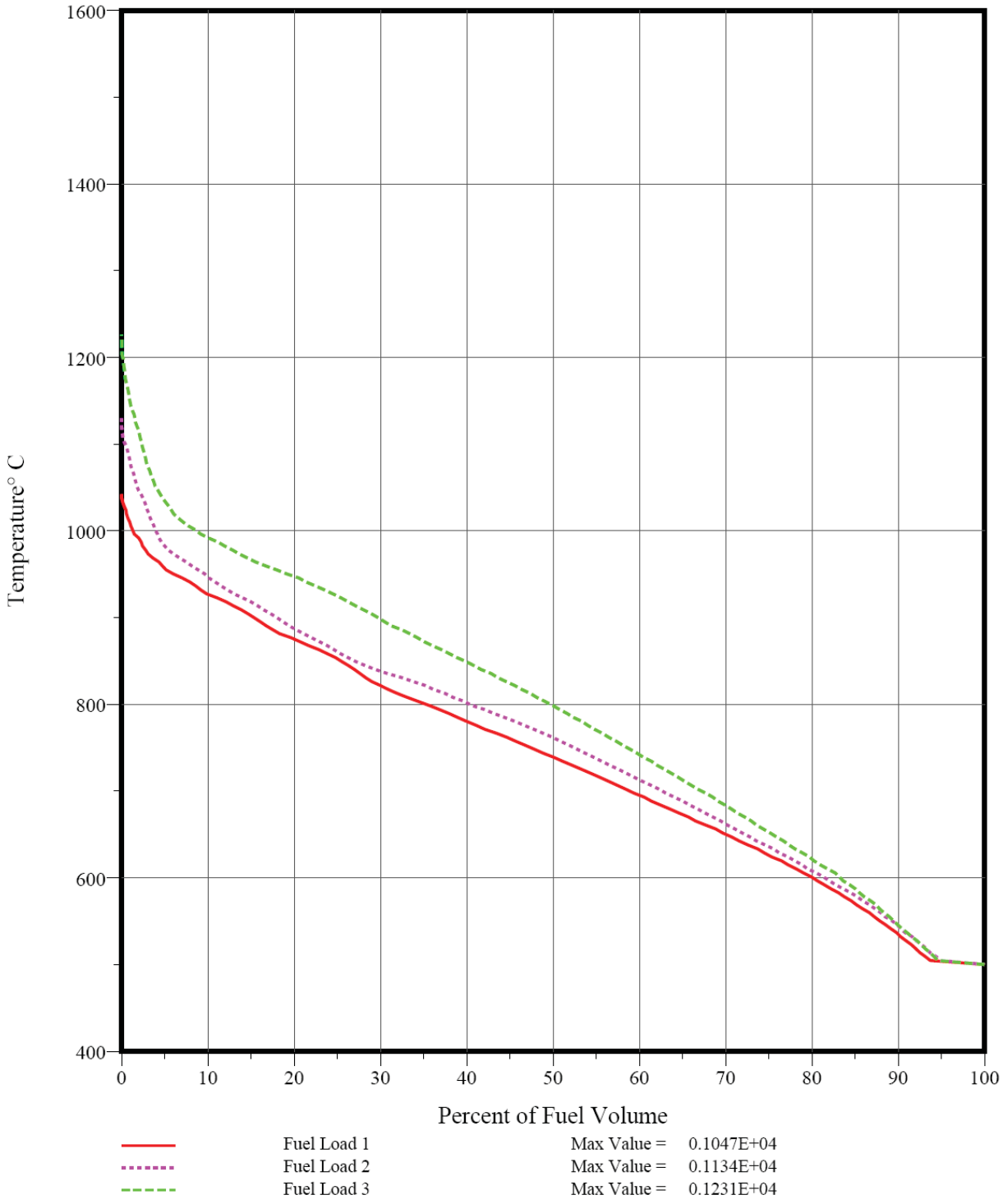

Figure 6-34. Time-Ave. Fuel Temperature Volume Distribution for Seg. 2 (Case 8.9.3SC)

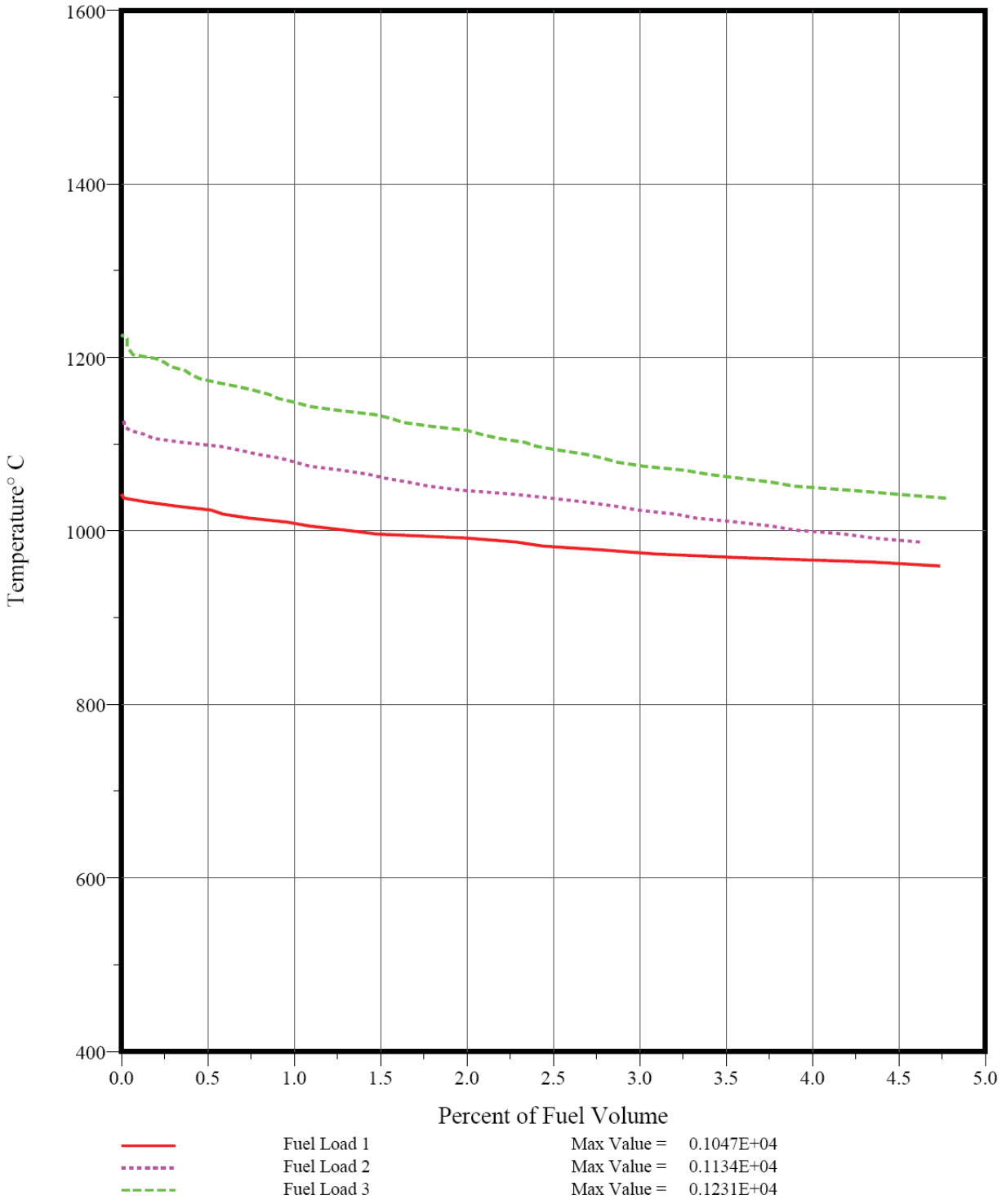

Figure 6-35. Time-Ave. Fuel Temperature Distribution for Seg. 2 (0-5%) (Case 8.9.3SC)

6.1.3.3 Fuel Particle Failure

Based upon the burnups, fast fluences, and temperatures calculated by SURVEY/THERM, the fuel performance of core design Case 8.9.3SC was calculated by SURVEY/PERFOR using the component models and material property data from FDDM/F.

The core-average SiC failure fraction as a function of operating time for the 425-μm 15.5%-enriched single particle is shown in Figures 6-36. The value plotted on the ordinates is the sum of the as-manufactured SiC defect fraction and the in-service SiC failure probability as a result of FP/SiC reactions plus kernel migration plus thermal decomposition plus heavy-metal dispersion as result of a defective IPyC layer. The in-service SiC failure results from HM metal dispersion in the IPyC layer and FP/SiC reactions; kernel migration and SiC thermal decomposition are negligible. The predicted SiC failure fraction for the 425-μm 15.5%-enriched particle is slightly higher than for the fissile particle in Case 7.9SC (7.9×10^{-5} vs. 6.6×10^{-5}) because the fuel temperatures are higher for Case 8.9.3SC. The amount of in-service SiC failure peaks at the end of cycle 2 and is less than the as-manufactured SiC defect fraction in all cycles.

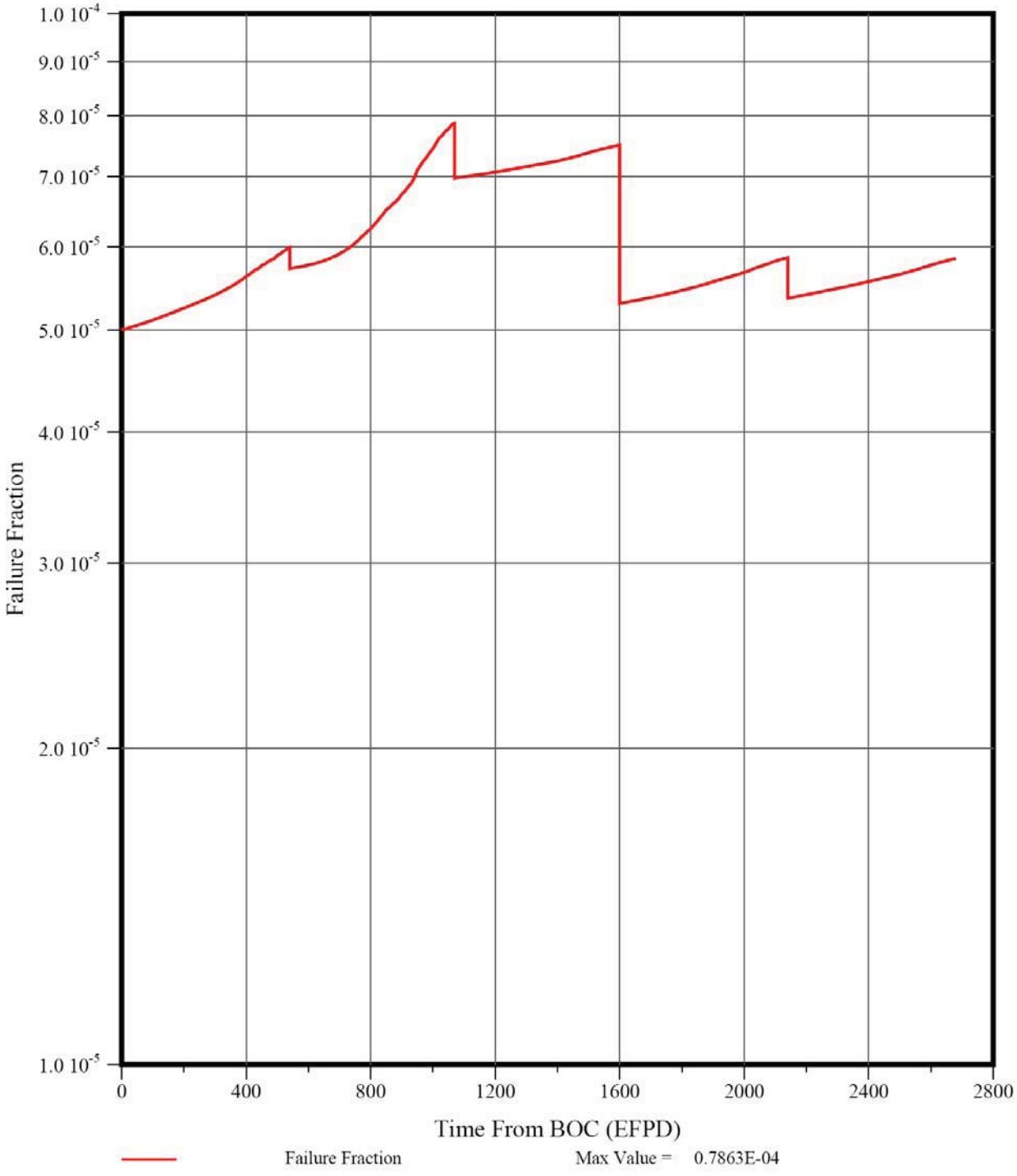

Figure 6-36. SiC Coating Failure Fraction for 425-µm UCO Particle (Case 8.9.3SC)

The maximum exposed kernel fraction is 9.2×10^{-6} as shown in Figure 6-37. Exposed kernels result from pressure-vessel (PV) failure of standard (intact) particles and particles with a variety of manufacturing defects. The initial value is very low because any exposed kernels in the as-manufactured fuel compacts would be counted as heavy-metal contamination. The contribution from PV failure of standard particles is insignificant because the failure probability is predicted to be negligible. The exposed kernel fraction for the 425 μm 15.5%-enriched single particle is slightly lower than for the 19.8%-enriched fissile particle in Case 7.9SC; a fraction of the missing-buffer particles are predicted to survive in the single-particle design because of the lower burnups (the MB fertile failure fraction in Case 7.9 was <7%); see Figure 6-38 for the single particle.

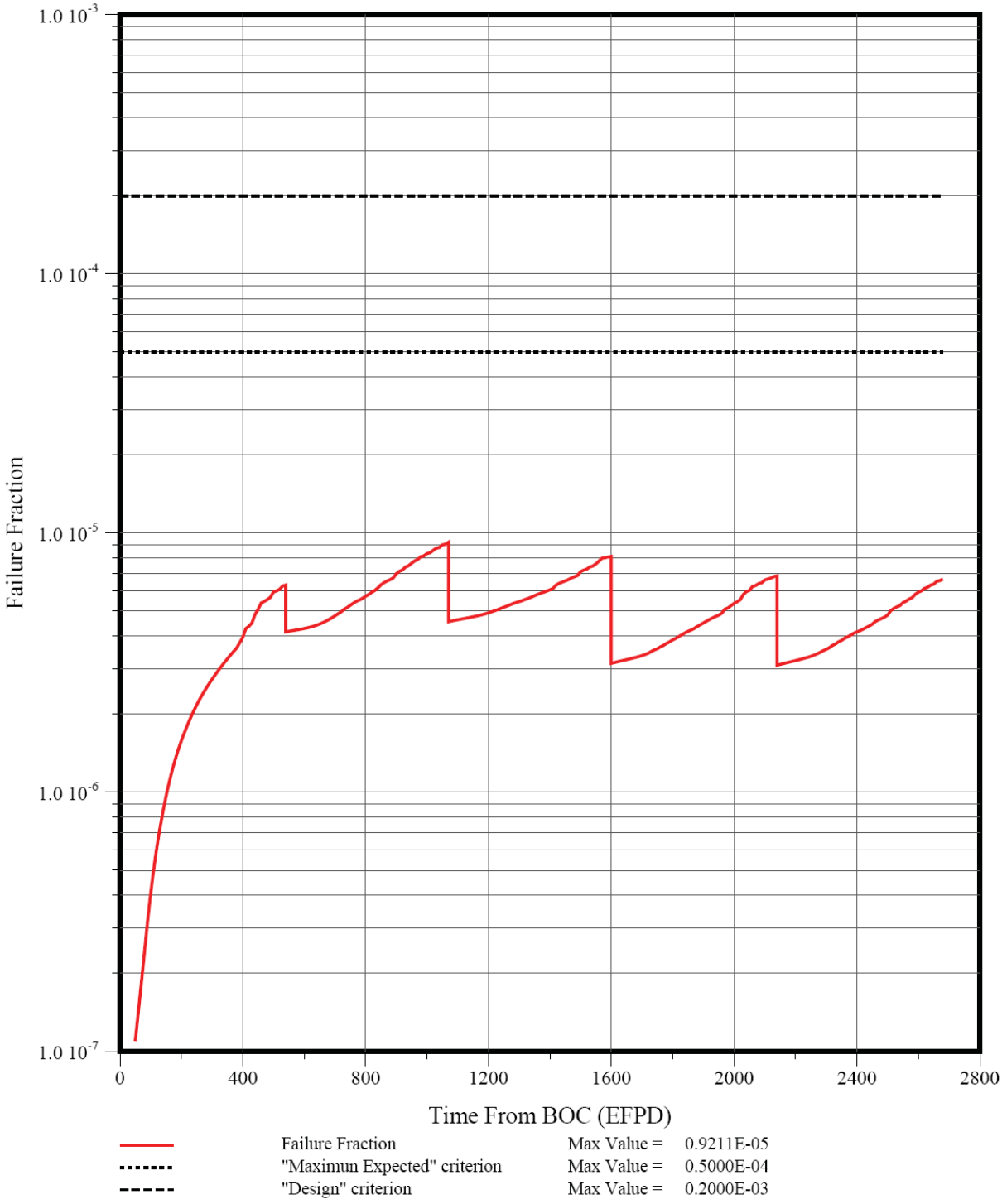

Figure 6-37. Exposed Kernel Fraction for 425-µm UCO Particle (Case 8.9.3SC)

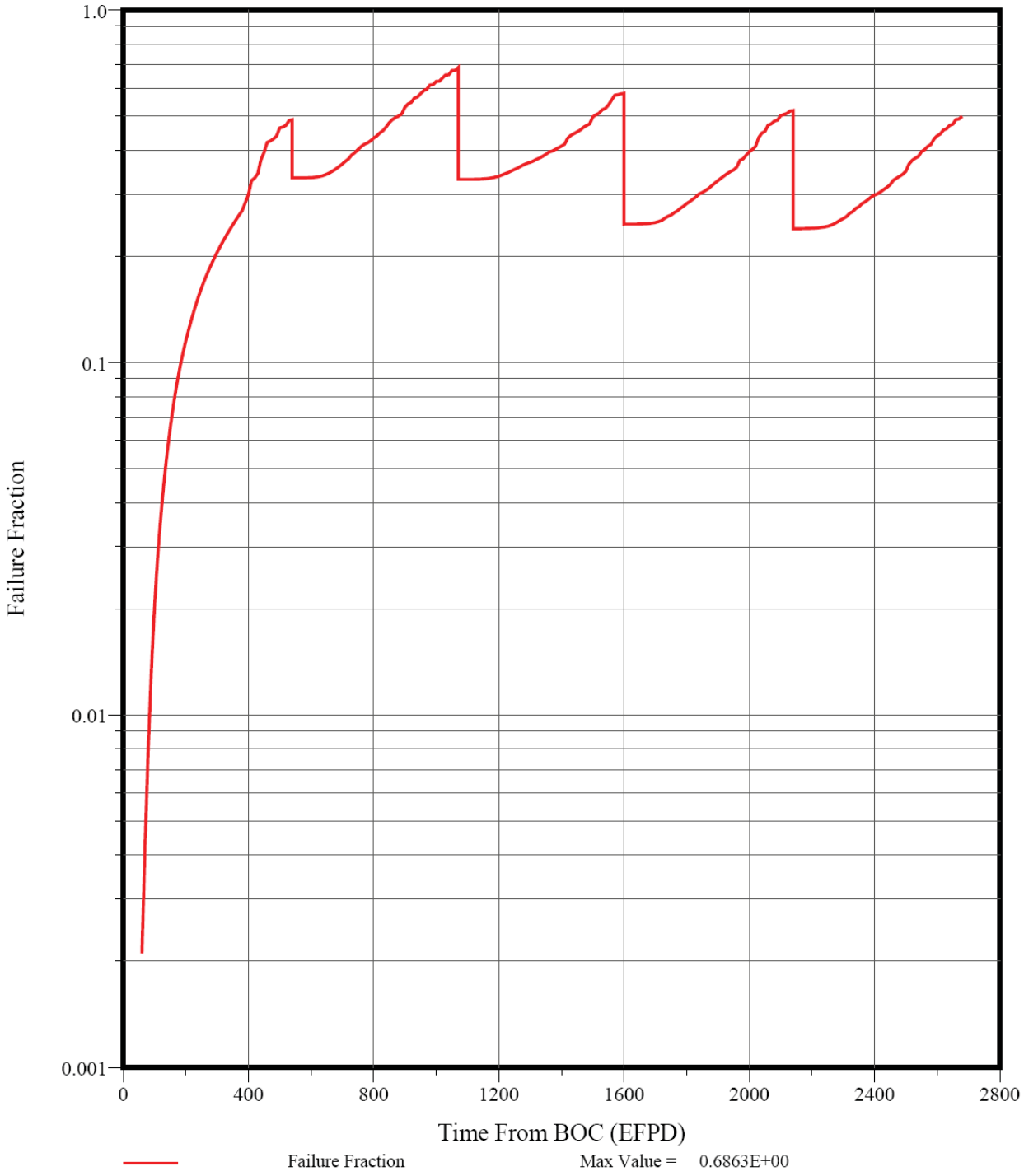

Figure 6-38. PV Failure Probability of Missing-Buffer Particles (Case 8.9.3SC)

6.1.3.4 Gaseous Fission Product Release

The release rate-to-birth rate (R/B) ratios for 2.8-hr Kr-88 and 8-day I-131 were also calculated by SURVEY/PERFOR using the FDDM/F fission gas release models for hydrolyzed UCO fuel. These R/Bs as a function of time are shown in Figures 6-39 and 6-40. The gas release is not significantly higher than for Case 7.9SC because the gas release for both designs is dominated by the release from HM contamination which is only weakly temperature dependent.

The contribution from failed particles is low because the predicted exposed kernel fraction is very low as discussed above (primarily a result of the tight specification on allowable missing-buffer particles). The peak predicted R/Bs are near the “Maximum Expected” limits because of the high average fuel temperatures. The only effective way of reducing these R/Bs would be to tighten the specification on HM contamination.

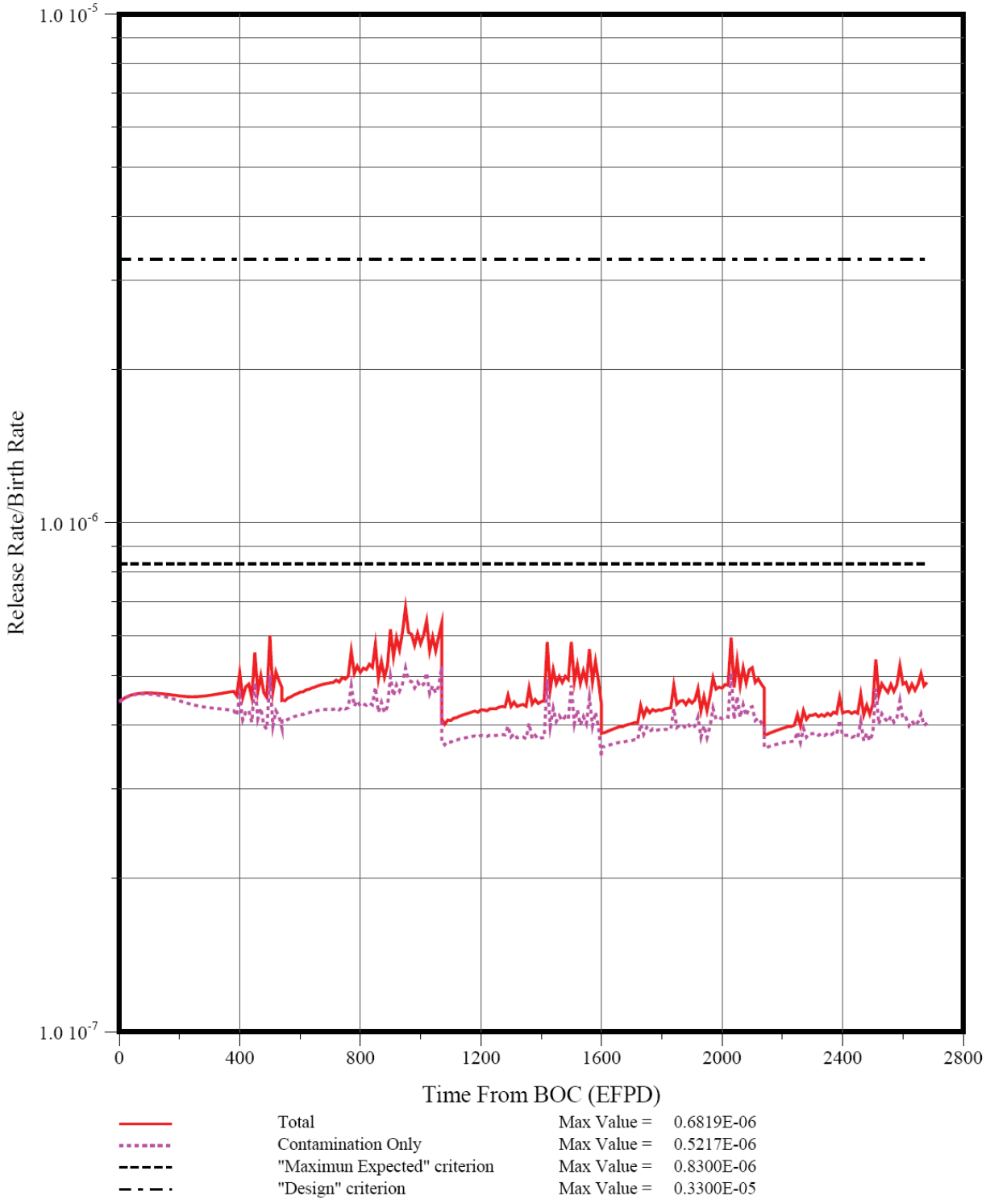

Figure 6-39. Core-Average R/B for Kr-88 (Case 8.9.3SC)

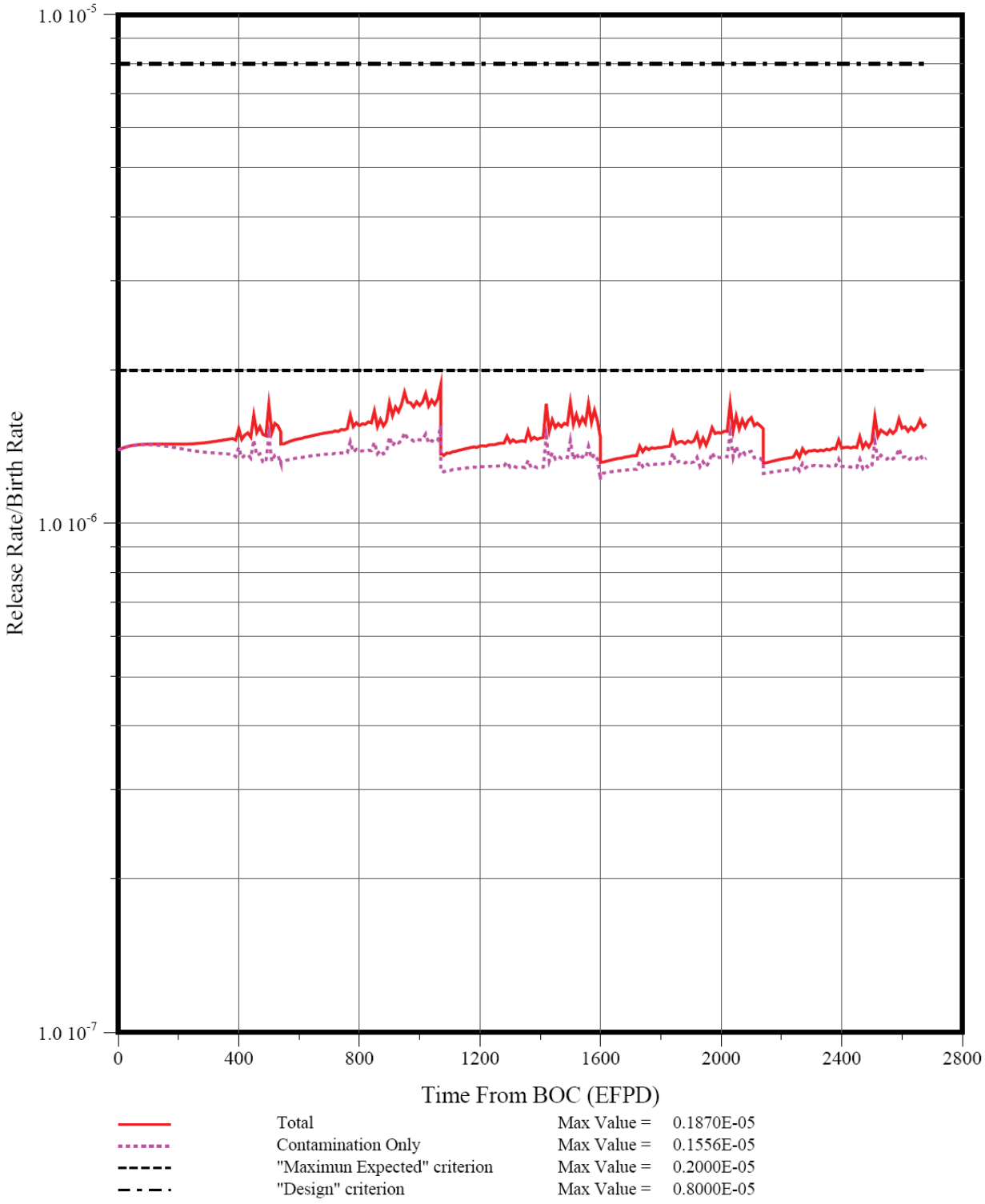

Figure 6-40. Core-Average R/B for I-131 (Case 8.9.3SC)

6.1.3.5 Metallic Fission Product Release

The SURVEY/PERFOR results summarized above were supplied as input to the TRAFIC-FD code which was used to predict the releases of Ag-110m, Cs-137 and Sr-90 from the core for Case 8.9. 3SC. The same modeling assumptions were used as for Case 7.9SC (Section 6.1.2.5).

The predicted overall core mass balance for 250-day Ag-110m is shown in Figure 6-41, and the cumulative fractional release into the coolant is shown in Figure 6-42. The predicted overall mass balance for 30.1-year Cs-137 is shown in Figure 6-43, and the cumulative fractional release into the coolant is shown in Figure 6-44. The predicted overall mass balance for 29-yr Sr-90 is shown in Figure 6-45, and the cumulative fractional release into the coolant is shown in Figure 6-46. The predicted metal transport behavior for Case 8.9.3SC is qualitatively the same as for Case 7.9SC. Because of the higher temperatures for Case 8.9.3SC, the cumulative fractional releases of the volatile metals all increase significantly: Ag-110m from 3.2×10^{-4} to 1.9×10^{-3}, Cs-137 from 8.7×10^{-6} to 1.8×10^{-5}, and Sr-90 from 3.4×10^{-8} to 2.4×10^{-7}.

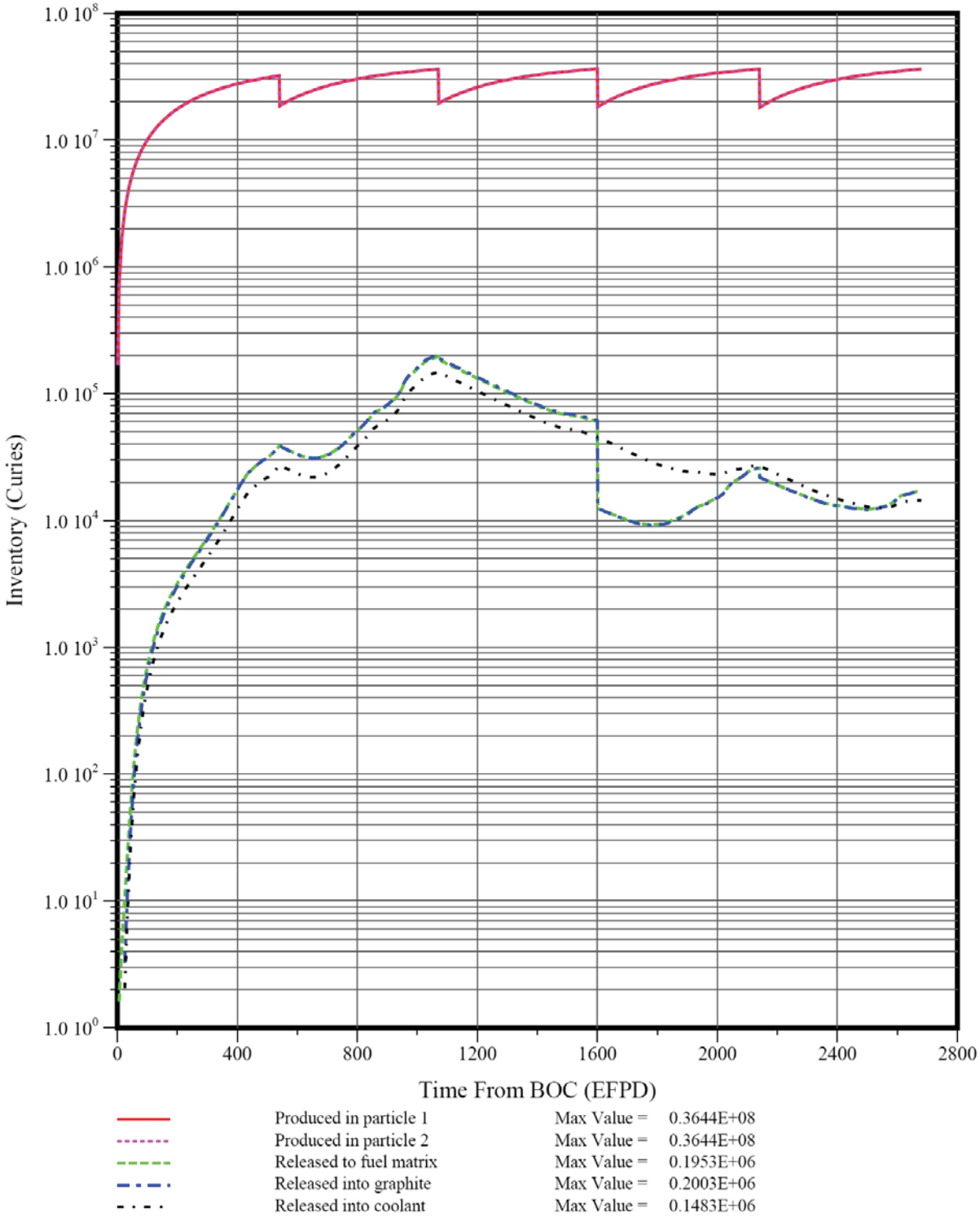

Figure 6-41. "'Full-core" Ag-110m Inventories by Core Material Region (Case 8.9.3SC)

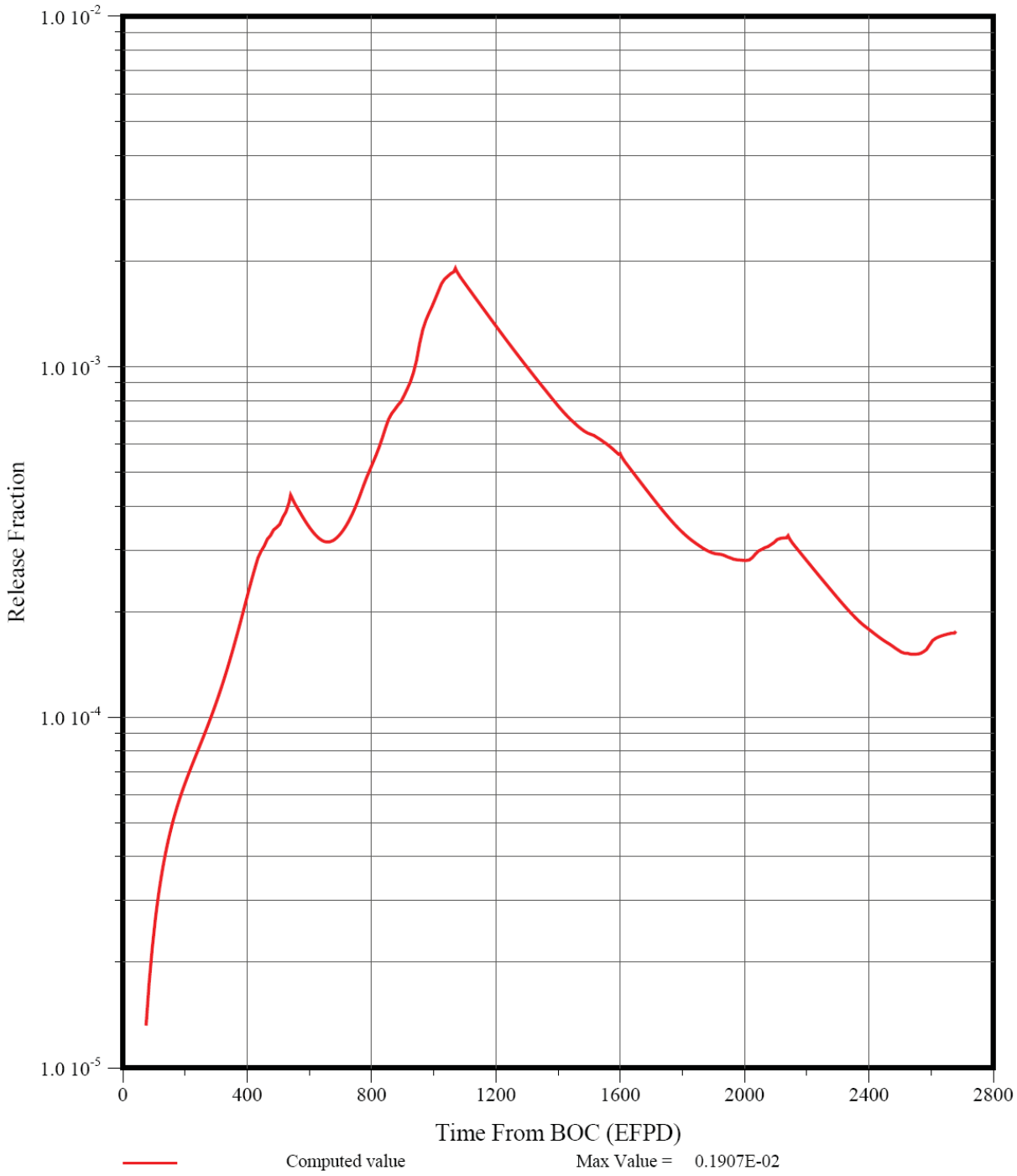

Figure 6-42. Cumulative Fractional Release of Ag-110m (Case 8.9.3SC

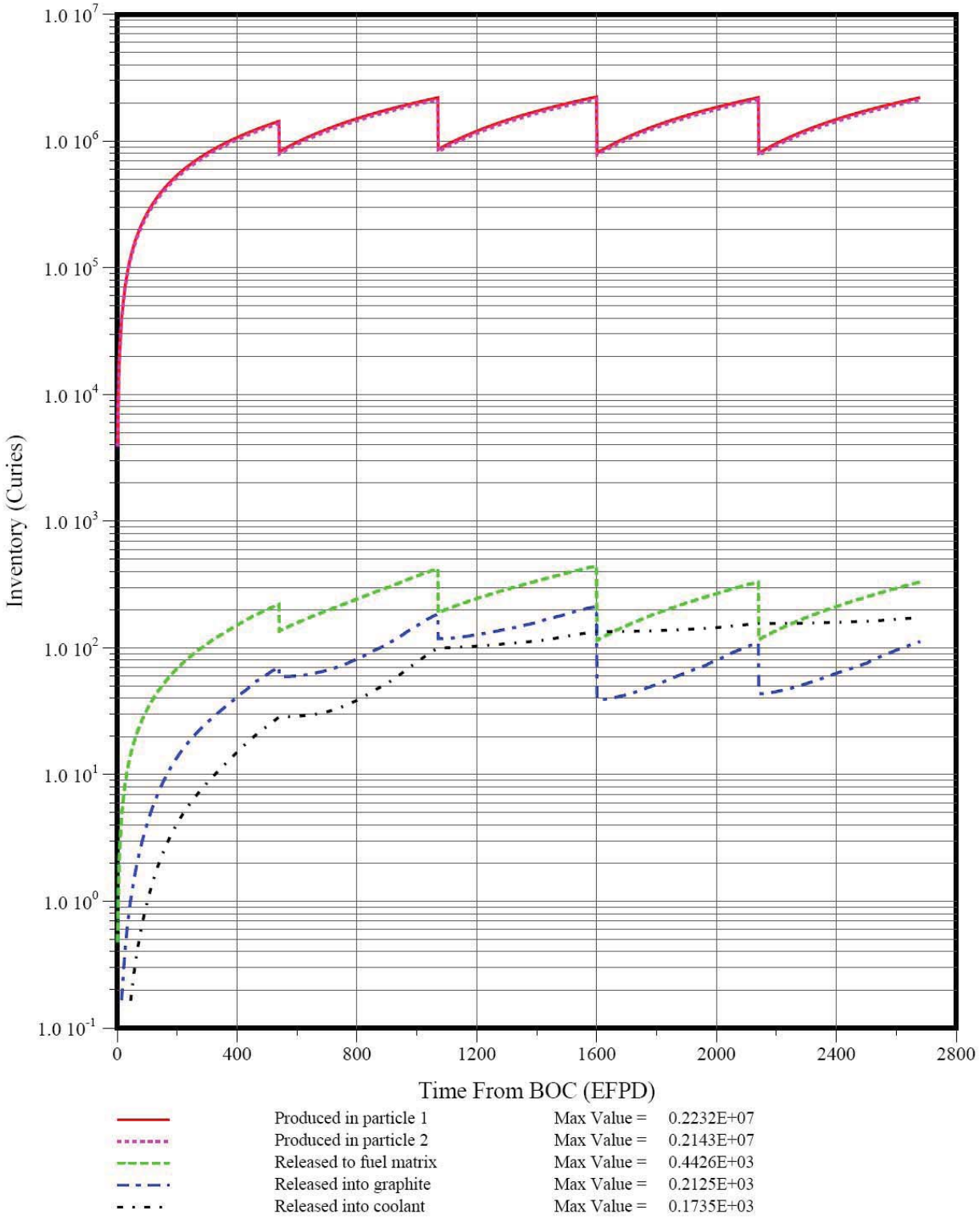

Figure 6-43. "'Full-core" Cs-137 Inventories by Core Material Region (Case 8.9.3SC)

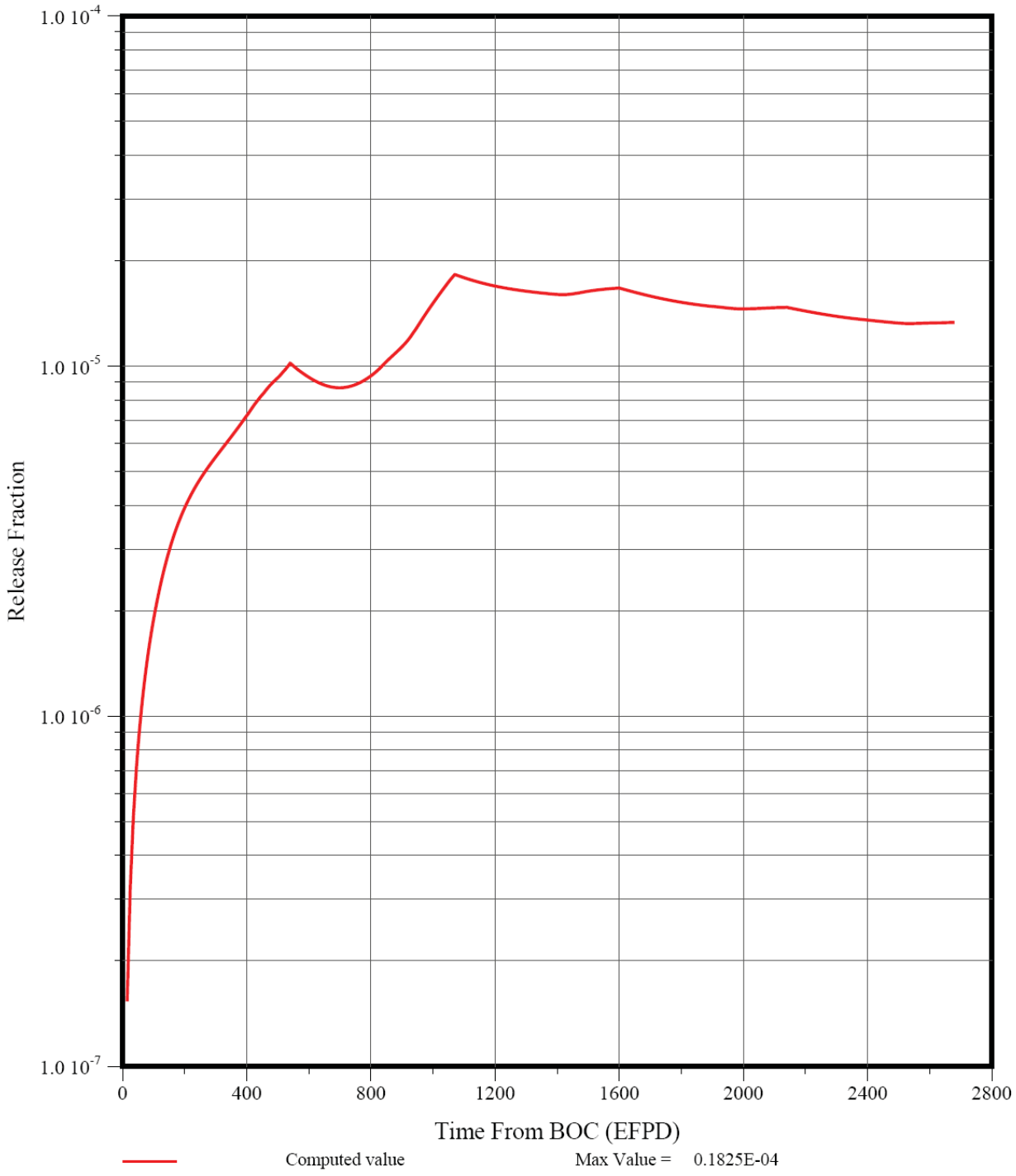

Figure 6-44. Cumulative Fractional Release of Cs-137 (Case 8.9.3SC)

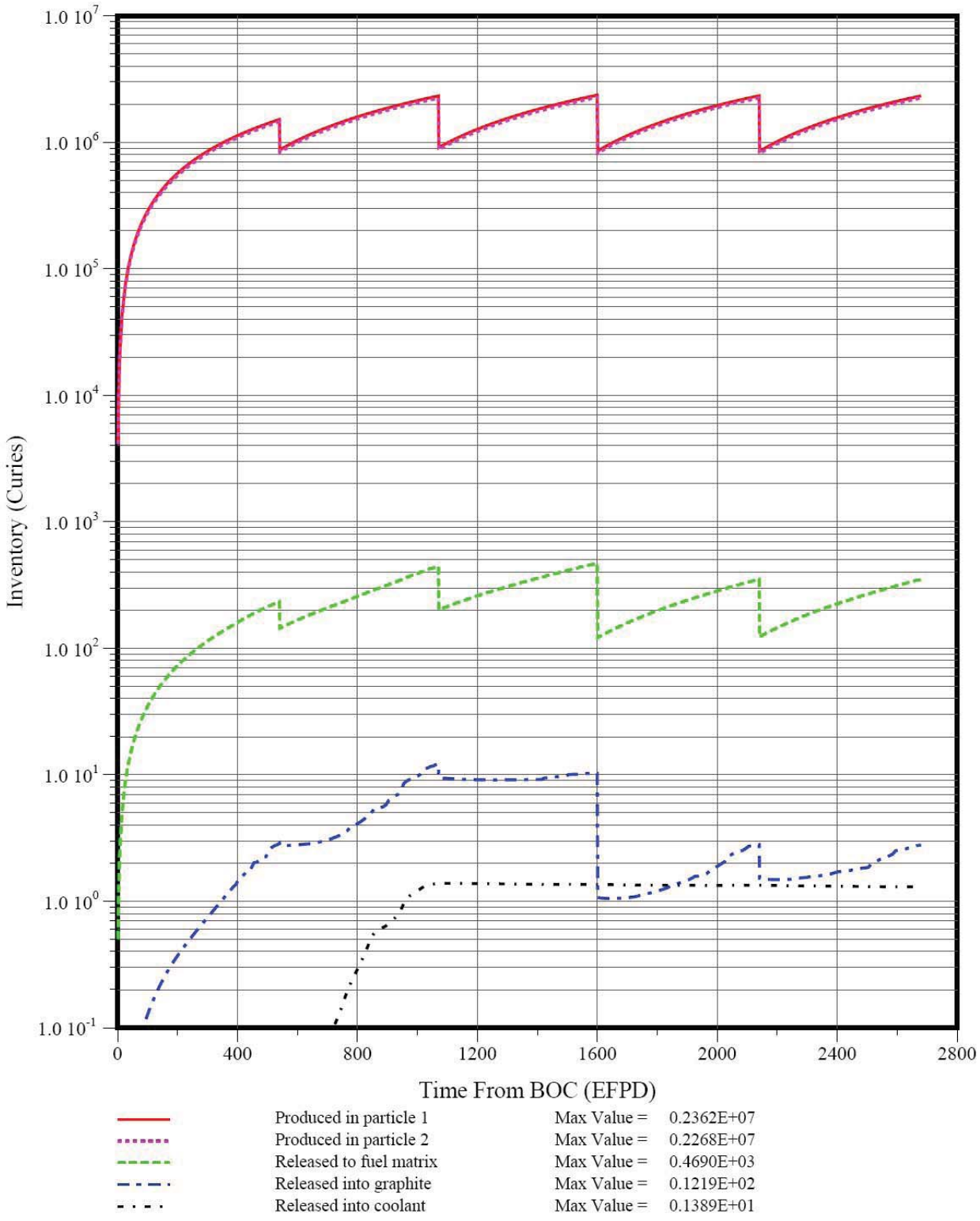

Figure 6-45. "'Full-core" Sr-90 Inventories by Core Material Region (Case 8.9.3SC)

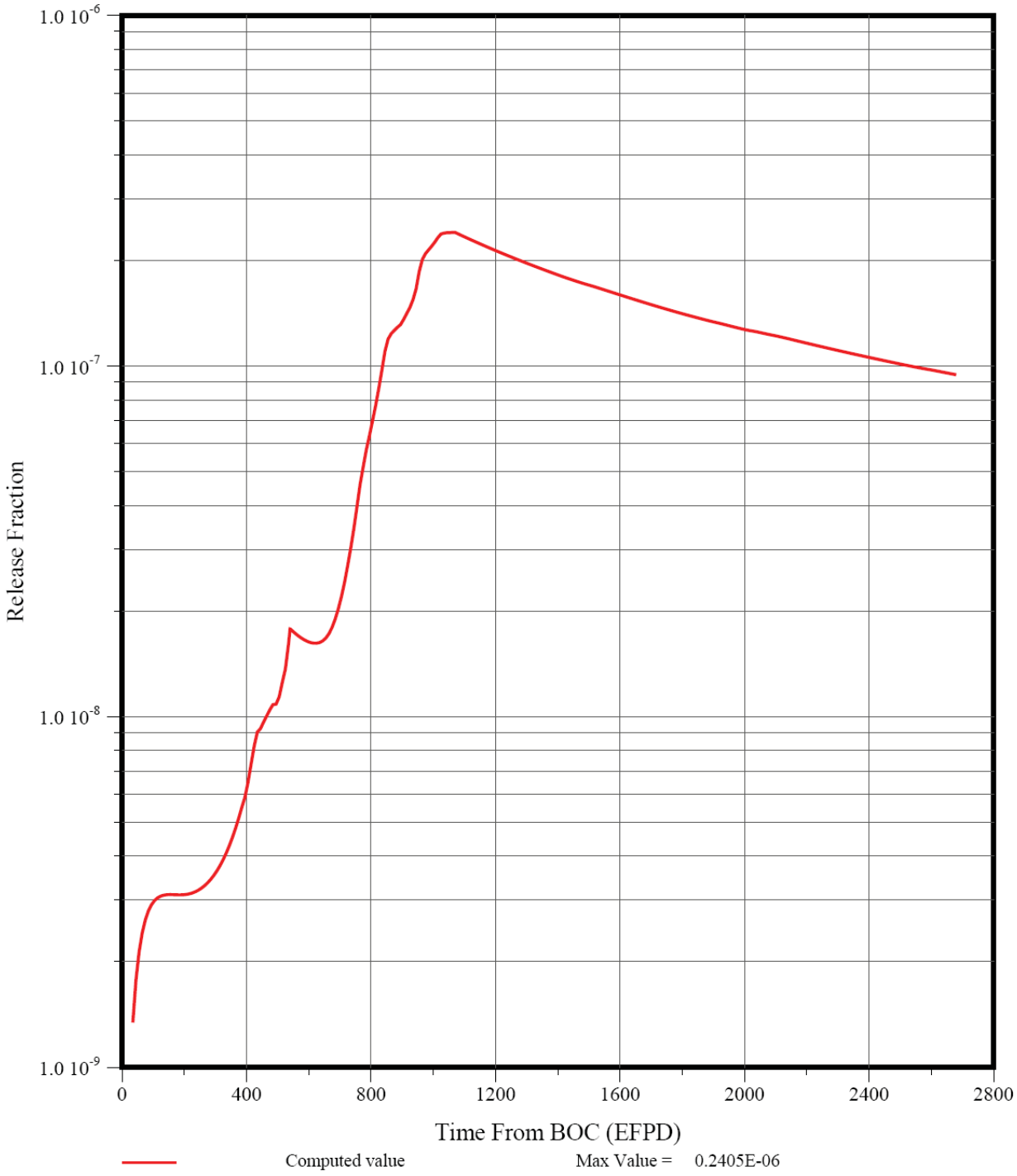

Figure 6-46. Cumulative Fractional Release of Sr-90 (Case 8.9.3SC)

As stated above, the predicted Cs release would likely be significantly reduced if the burnup-dependent FDDM/F correlation for Cs diffusion in UCO kernels were used; however, the use of that correlation is considered to be unjustified, given more recent experimental data [Medwid 1993].

6.1.4 Comparison of Predicted Core Performance with Requirements

The predicted core performance for the final binary-particle core (Case 7.9SC) and the for the final single-particle core (Case 8.9.3SC) from the CPA task is compared with the recommended fuel performance and fission product release criteria (Section 5.1) in Table 6-1.

Table 6-1. Comparison of Predicted Core Performance with Recommended Criteria

Parameter	"Maximum Expected" Limit	Case 7.9SC (Binary Particle)	Case 8.9.3SC (Single Particle)
Fuel failure during normal operation (exposed kernel fraction)	$\leq 5.0 \times 10^{-5}$	1.2×10^{-5} (fissile) 2.3×10^{-6} (fertile)	9.2×10^{-6}
In-service SiC failure fraction	N/A	8.3×10^{-6}	2.2×10^{-5}
Total SiC failure fraction	N/A	6.6×10^{-5}	7.9×10^{-5}
Kr-88 R/B (fractional release)	$\leq 8.3 \times 10^{-7}$	5.8×10^{-7}	6.8×10^{-7}
I-131 R/B (fractional release)	$\leq 2.0 \times 10^{-6}$	1.6×10^{-6}	1.9×10^{-6}
Ag-110m cumulative fractional release	$\leq 2.0 \times 10^{-4}$	3.2×10^{-4}	1.9×10^{-3}
Cs-137 cumulative fractional release	$\leq 7.0 \times 10^{-6}$	8.7×10^{-6}	1.8×10^{-5}
Sr-90 cumulative fractional release	$\leq 3.0 \times 10^{-8}$	3.4×10^{-8}	2.4×10^{-7}

The predicted exposed kernel fraction for both cases is well below the limit because the tight specification on the as-manufactured missing-buffer fraction. The exposed kernel fraction for the single-particle design is slightly lower than that for the fissile particle of the binary-particle design because of the lower burnup of the former results in the survival in some of the missing-buffer particles (the fraction for the single-particle design is close to the weighted average for the fissile/fertile design). The predicted SiC failure fraction is modest and dominated by the as-manufactured SiC defect fraction of $\leq 5 \times 10^{-5}$ in both cases. The predicted Kr-88 and I-131 releases are near the limits and completely dominated by the release from as-manufactured heavy-metal contamination. Reduction in the predicted fission gas release (and, thus, in the iodine plateout inventory) would necessarily require a tighter specification on HM contamination.

The predicted fractional releases of the three volatile metals are significantly higher for the single-particle design because of the higher fuel and graphite temperatures for that design. While the temperature differences seem relatively modest, they are evidently in a regime where nominally small temperature increases in temperature result in significantly more Ag release from intact TRISO particles and significantly less matrix/graphite retention of Cs and especially of Sr. For this reason, the differences between the two cases are somewhat less pronounced than for the CPA base case of T_{out} = 900 °C and ΔT_{core} = 360 °C.

For the binary-particle case, the predicted releases of the three metals slightly exceed the recommended criteria because of excessively high predicted fuel temperatures during the second irradiation cycle; the metal releases during the remaining three cycles are below the limits (it is anticipated the high fuel temperatures in Cycle 2 can be reduced by further optimization of the nuclear design). However, the predicted releases of Ag and Sr for the single-particle design exceed "Maximum Expected" criteria by an order of magnitude. It will be more difficult to reduce these predicted releases by an order of magnitude. A reduced core outlet temperature and/or reduced core temperature rise would certainly help, but such design changes have their own disadvantages. Perhaps, a fuel shuffling scheme can be identified that provides the required reductions in fuel and graphite temperatures.

In summary, a binary-fuel-particle system provides an inherent advantage relative to a single-fuel particle having a single U-235 enrichment because it allows U-235 enrichment zoning as well as uranium zoning and fixed burnable poison zoning [GA 2009b]. Thus, the use of a binary-fuel-particle system should always result in improved RN retention in the core relative to that achievable with a single fuel particle having a single U-235 enrichment. This conclusion does not, however, mean that use of a single fuel particle is not feasible as discussed in greater detail in the CPA Phase 2 final report [GA 2009b].

6.1.5 Effect of Lower Gas Temperatures for Steam-Cycle MHRs

The specification of T_{in} = 322 °C and T_{out} = 750 °C for a steam-cycle MHR core is high by historical standards although the core temperature rise is typical. Earlier steam-cycle HTGR designs, including Fort St. Vrain, did have core outlet temperatures in the 750 – 780 °C range because these plants had a gas reheater section in their steam generators. With the advent of MHRs in the early 1980s, gas reheat was eliminated and the optimal core outlet temperature decreased (e.g., for the 350 MW(t) steam-cycle MHTGR, T_{in} = 258 °C and T_{out} = 687 °C). Not surprisingly, there is a RN retention benefit associated with these lower temperatures as illustrated in Table 6-2 for the Case 7.9 core nuclear design with 350 MW(t) MHTGR core inlet and outlet temperatures.

Table 6-2. Effect of Lower Gas Temperatures on RN Release

Parameter	Steam-Cycle Base Case	Reduced Gas Temperatures	"Maximum Expected" Limit
Core inlet / outlet temperature (°C)	322 / 750	258 / 687	
Peak Fuel Temperature (°C)	1460	1415	
Max. Time-Ave. Fuel Temperature (°C)	1171	1116	[≤ 1250]
Exposed kernel fraction) Fissile Particle Fertile Particle	 1.2×10^{-5} 2.3×10^{-6}	 1.1×10^{-5} 1.9×10^{-6}	 $\leq 5.0 \times 10^{-5}$ $\leq 5.0 \times 10^{-5}$
In-service SiC failure fraction	8.3×10^{-6}	2.2×10^{-6}	N/A
Total SiC failure fraction	6.6×10^{-5}	6.0×10^{-5}	N/A
Kr-88 R/B	5.8×10^{-7}	4.7×10^{-7}	$\leq 8.3 \times 10^{-7}$
I-131 R/B	1.6×10^{-6}	1.4×10^{-6}	$\leq 2.0 \times 10^{-6}$
Ag-110m fractional release	3.2×10^{-4}	8.7×10^{-5}	$\leq 2.0 \times 10^{-4}$
Cs-137 fractional release	8.7×10^{-6}	3.8×10^{-6}	$\leq 7.0 \times 10^{-6}$
Sr-90 fractional release	3.4×10^{-8}	6.8×10^{-9}	$\leq 3.0 \times 10^{-8}$

The effects on the exposed kernel fractions and fission gas release are modest. However, the lower core temperatures associated with the lower gas temperatures effectively eliminate thermally activated SiC failure mechanisms and significantly reduce metal release.

6.2 Postulated Accidents

A number of safety assessments have been performed for various MHR designs with prismatic cores using both deterministic and probabilistic methodologies. The most comprehensive safety assessment to date was for the 350 MW(t) steam-cycle MHTGR [PSID 1992, etc.]. A broad spectrum of postulated accidents have been considered. Some of these postulated accidents have offsite dose consequences (IA, Goal 3); others do not result in offsite doses but pose significant investment risk (IA, Goal 2). Some of these accident scenarios, most obviously those resulting in public and/or occupational exposures, may serve to impose RN retention requirements on the fuel design.

In addition to [PSID 1992], two other MHR safety assessments are particularly relevant in the present context. In 1993, Bechtel and GA made an evaluation of the dose consequences for a 450 MW(t) steam-cycle MHTGR that would result with alternative source term assumptions for a range of VLPC designs [Dilling 1993]. The base-case source terms for this evaluation were the PSID source terms for the 350 MW(t) steam-cycle MHTGR scaled up by power level. A spectrum of alternative passive containment features were evaluated assuming: (1) a higher fuel failure fraction, (2) very rapid hydrolysis of failed fuel, (3) the possibility that the fuel could

suffer an undetected weakness (i.e., so-called “weak” fuel), and (4) a higher than expected release of plateout activity.

In 2008, various containment options for the GA steam-cycle MHR “reference” design were assessed [Richards 2008]. Like the previous GA commercial MHR designs, this design utilizes a Vented Low Pressure Containment building. The VLPC concept evaluated in this study is based on the Reactor Building (RB) design developed for the 450 MW(t) MHTGR steam-cycle plant [e.g., Dilling 1993, etc.].

Based on this study and studies performed for previous MHTGR concepts, the VLPC concept was endorsed for the “reference” MHR RB design. VLPC design alternatives that can reduce doses at the EAB were also identified: (1) filtered pathways on the RB and on the primary coolant pressure relief line, (2) an elevated stack, and (3) an extension of the EAB.

6.2.1 Bounding Classes of Accidents

As introduced above, US MHR programs have adopted a user/utility requirement - first applied to the 350 MW(t) steam-cycle MHTGR - to meet the lower EPA PAG dose limits at a 425-m EAB to preclude the need for public evacuation and sheltering for all credible accidents (expressed differently, the EPZ boundary would be set at the EAB)

To demonstrate compliance with this requirement, a wide spectrum of events have been evaluated down to a frequency of 5×10^{-7} per plant year to show that on a cumulative basis the PAGs are not exceeded at a 425-m EAB. Different classes of events are considered [PSID 1992]:

- Licensing Basis Events (LBE): full spectrum of events from anticipated operational occurrences (AOO) to events beyond the design basis with frequencies as low as 5 x 10-7 per plant year.
- Design Basis Events (DBE): events not expected in the plant lifetime but which might occur in the lifetime of a population of plants.
- Safety Related Design Conditions (SRDC): limiting conditions for the safety-related equipment which are derived from the DBEs by assuming that only safety related equipment is available to mitigate the consequences.

For steam-cycle MHRs, three classes of events are typically bounding. Using the nomenclature and event definitions developed for the 350 MW(t) MHTGR, the following events were determined to be bounding with regard to fuel performance requirements [PSID 1992, Dilling 1993]:

- **Large Water Ingress plus Pressure Relief (SRDC-6)**. These events encompass families of accidents that can potentially result in rapid combined releases of prompt and delayed source terms. Such events assume steam generator failure, large moisture ingress, opening of the Reactor Coolant Pressure Boundary (RCPB) relief valve and subsequent

loss of core cooling. Moisture ingress events without forced cooling can result in RCPB relief valve opening after about a day. These events result in releases of circulating activity, washoff of a portion of the plateout, and hydrolysis of failed fuel particles with an attendant release of a fraction of the fuel inventory. SRDC-6 is an extension of DBE-6 during which the steam generator dump system functions properly to preclude pressure relief such that there is no radionuclide release from the primary circuit.

- **Depressurized Core Conduction Cooldown (SRDC-11).** These events are limited to small RCPB leaks of less than 0.05 in^2 combined with subsequent core conduction cooldown events that provide a driving force for RN release from the vessel due to the slow depressurization of helium coolant (e.g., over several days). During the depressurization the circulating activity, a portion of the plateout activity, and a fraction of the RN inventory in fuel particles which might have failed during the core conduction cooldown are released. SRDC-11 is an extension of DBE-11 during which the Heat Transport System is assumed to function as a heat sink for the first 15 hours of the transient.

- **Rapid Helium Depressurization (SRDC-10).** These events are characterized by openings up to the design basis of 13 in^2 which result in a depressurized core conduction cooldown. In these events the helium leak size results in a rapid blowdown (e.g., the blowdown is complete within minutes) followed by a relatively slow transport from the vessel due to thermal expansion of the coolant as the core heats up mitigated by thermal contraction as the core cools down. SRDC-10 is an extension of DBE-10 during which the Shutdown Cooling System (SCS) is assumed to provide sufficient cooling to prevent significant RN release from the fuel.

This class of events typically has the most rapid release of the prompt source term. A smaller delayed source term results from large leaks than from small leaks because the helium coolant, which transports the fission products out of the RCPB, is essentially all released before the majority of the delayed source term is released from the fuel. Said differently, the prompt source term is greatest for this event, but the delayed source term is smaller than that for SRDC-11.

6.2.2 Predicted Accident Source Terms for a Steam-Cycle MHR

The best definition of accident source terms for a 600 MW(t) steam-cycle MHR available at this writing is from the NGNP containment options study [Richards 2008], and the fuel requirements implied by that study are summarized below. The original intent was to use the results of the accident assessment being performed under Phase 2 of the CPA task [Work Plan 2009]. This approach proved impractical for two reasons: (1) the results of the CPA accident analysis did not become available in a timely manner for use here; and (2) the scope of that analysis is limited to evaluation of depressurized core conduction cooldown events (SRDC-11). Based upon previous safety assessments for steam-cycle MHRs, events involving water ingress plus

pressure relief (SRDC-6) could well be more constraining with regard to fuel requirements than depressurized core conduction cooldown events (SRDC-11). Consequently, it was judged more appropriate to use a consistent set of predicted source terms from [Richards 2008].

6.2.2.1 Depressurized Core Conduction Cooldown (SRDC-11)

This event is assumed to be initiated by failure of one of the small instrument or service system lines that penetrate the reactor pressure vessel, resulting in a slow depressurization. The reactor trips automatically on low primary coolant pressure and only the safety-related RCCS is assumed to be available to remove decay heat. The reactor then undergoes a Low Pressure Conduction Cooldown (LPCC). Figure 6-47 shows the peak and average fuel temperature responses during this event for the 450 MW(t) steam-cycle MHTGR [Hoot 1991]. In terms of impact on the source term, the significance of the slow depressurization event is that the helium coolant is still exhausting from the Reactor Pressure Vessel (RPV) while core temperatures are rising.

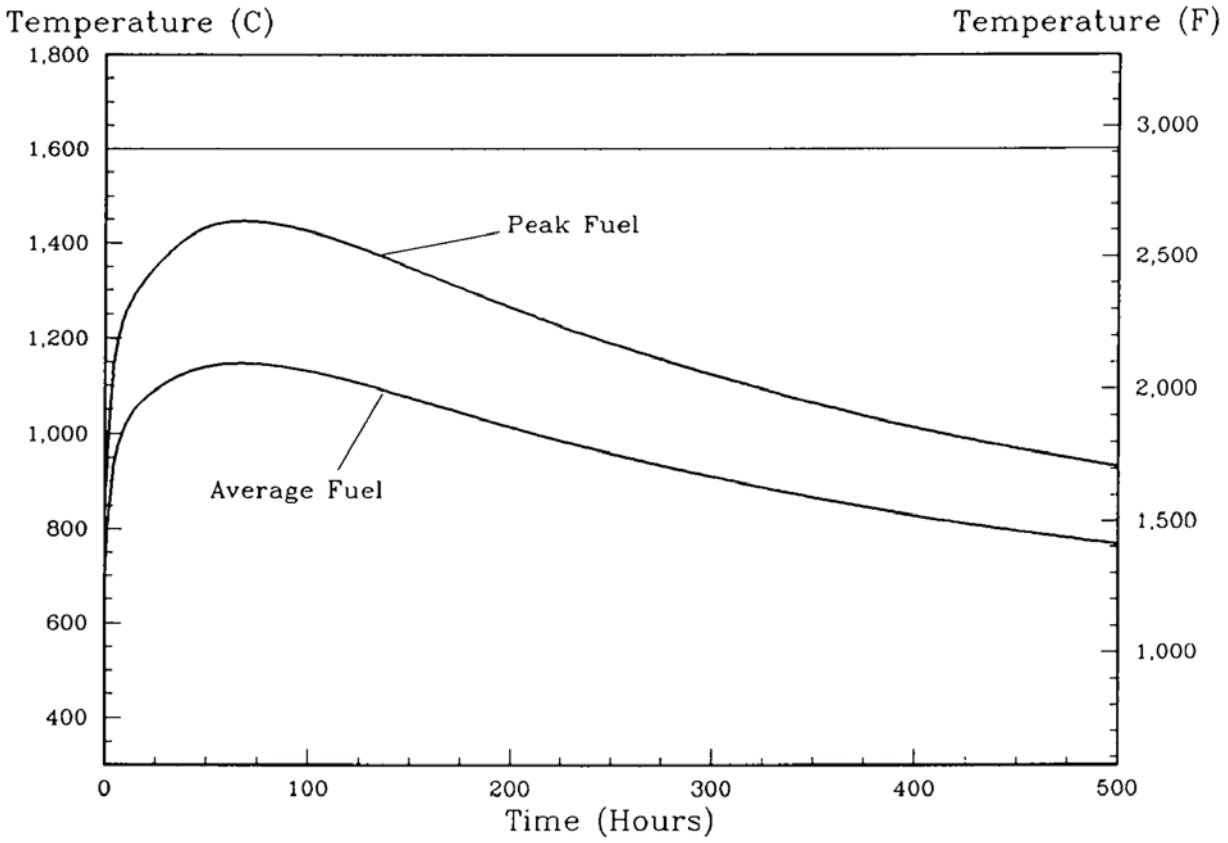

Figure 6-47. Fuel Temperatures during SRDC-11 for 450 MW(t) MHTGR

During the heatup period, radionuclides are released from exposed heavy metal, and the flow of helium transports some of these radionuclides into the RB and increases the source term available for release to the environment. For a larger break with rapid depressurization

(SRDC-10), there is no significant outflow of helium from the RPV during the core heatup period. The rapid depressurization events result in a greater release of plateout activity because of the higher shear forces on the He-wetted surfaces, but previous safety assessments have shown the slow depressurization events result in a greater overall release of radionuclides to the RB and the environment. Figure 6-48 shows the predicted release of I-131 from the core, vessel, and RB during this event for the 450 MW(t) MHTGR [Hoot 1991].

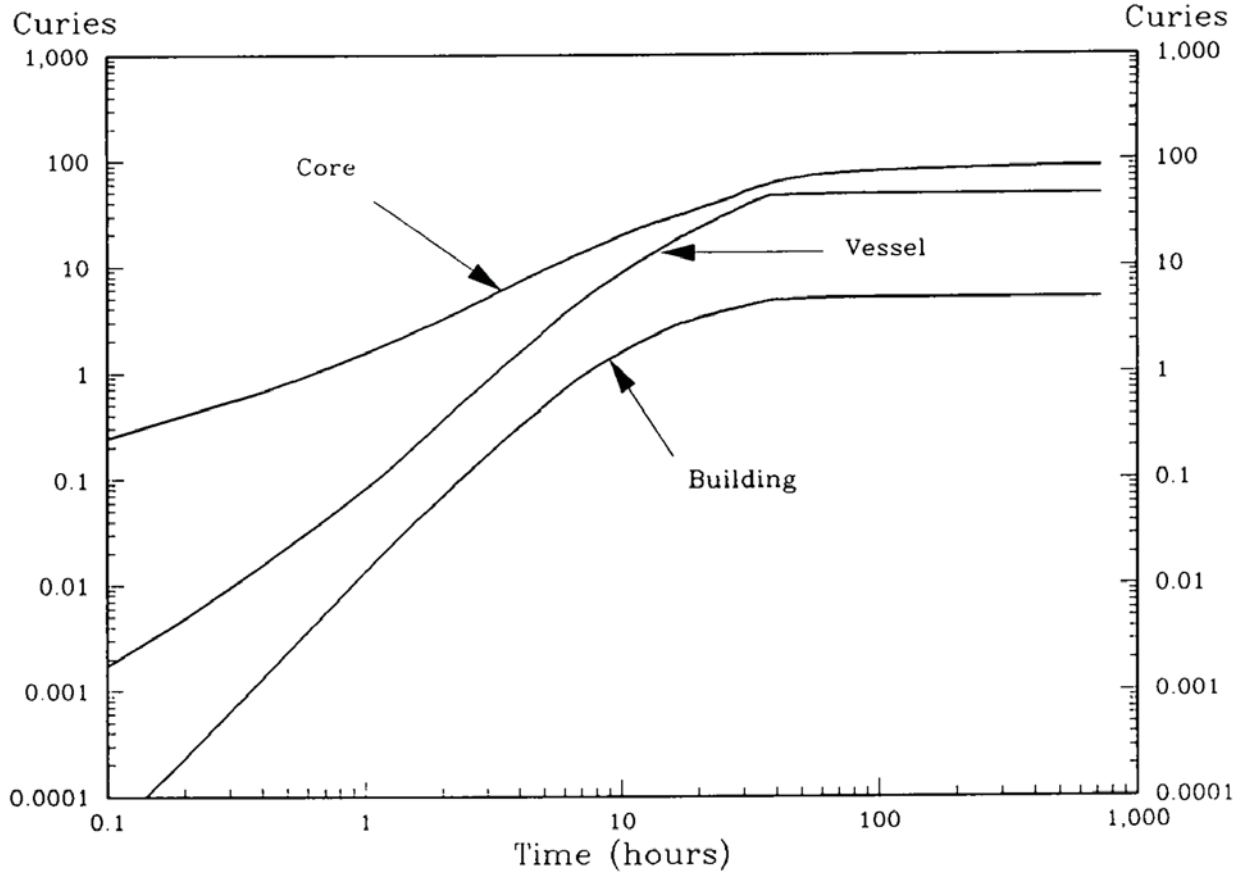

Figure 6-48. I-131 Release during SRDC-11 for 450 MW(t) MHTGR

6.2.2.2 Water Ingress plus Pressure Relief (SRDC-6)

This event is assumed to be initiated with an offset rupture of a steam generator tube and results in moderate water ingress into the primary loop. The steam mixes with the helium, which causes a significant increase in the primary coolant moisture concentration. Both the moisture monitors and the neutron flux controller are non-safety related equipment and are assumed to have failed. The moisture ingress causes an increase in core reactivity, which causes the reactor trip setpoint on high core power-to-flow ratio of 1.5 to be exceeded within a few seconds. Following the reactor trip, the feedwater pumps are ramped down to 15% of total flow, causing a similar reduction in primary coolant flow. Continued moisture ingress causes the high primary coolant pressure setpoint to be exceeded, which results in insertion of reserve

shutdown material into the core, shutdown of the main circulator, and isolation of the steam generator. However, the steam generator is assumed not to be dumped since the dump system is not safety related. The SCS circulator is also non-safety related and fails to start. These events initiate a high pressure conduction cooldown (HPCC) to the RCCS.

Steam reacts with the exposed kernels of failed particle and the small fraction of heavy metal in the form of contamination outside intact fuel particles. The steam also reacts endothermically with graphite to produce hydrogen and carbon monoxide. In terms of impact on the source term, hydrolysis of the exposed kernels is a key contributor to RN release from the core. For this event, the internal pressure within the reactor pressure vessel increases because of the steam ingress, hydrogen and carbon monoxide generation, and increasing temperatures. As shown in Figure 6-49, an analysis of this event for the 450 MW(t) MHTGR [Hoot 1991] predicted the pressure relief valve would cycle three times during the course of the accident, after which cooling and diminished moisture ingress prevented additional openings of the relief valve

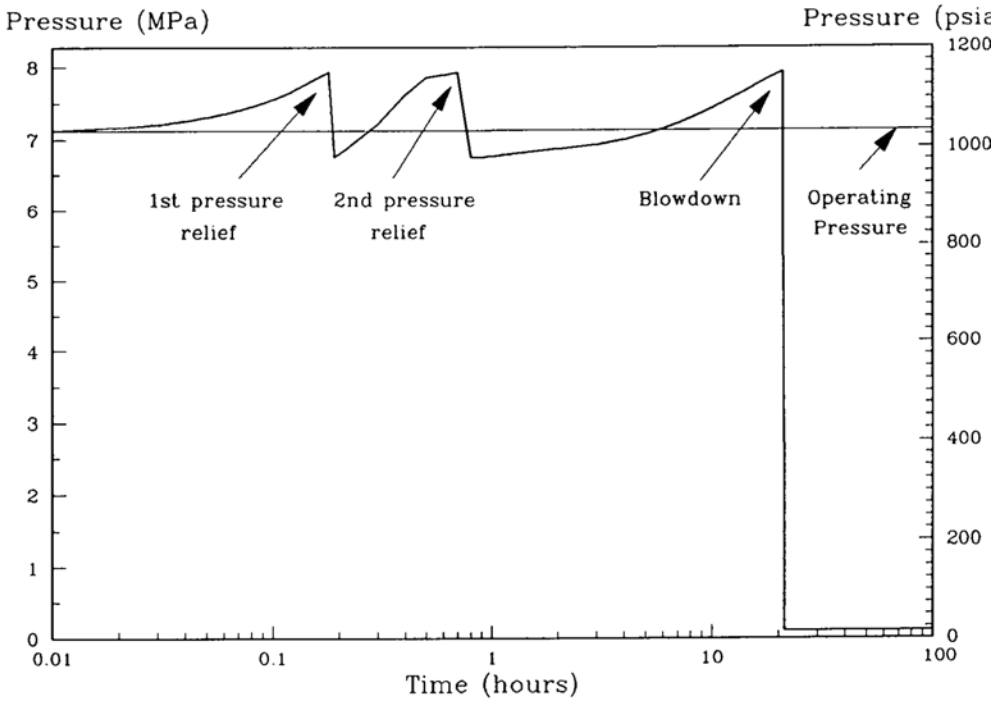

Figure 6-49. Primary Coolant Pressure Response during SRDC-6

To assess the maximum potential for RN release for this accident, the relief valve was assumed to fail open after the third cycle, approximately 21 hours after initiation of the accident. During this time period, a significant fraction of the exposed fuel kernels is predicted to have hydrolyzed as indicated in Figure 6-50. After the final pressure relief, the system depressurizes in about 13 minutes, after which the reactor undergoes a LPCC, with fuel temperature response similar

to that shown in Figure 6-47. Figure 6-51 shows the predicted release of I-131 from the core, vessel, and RB during this event for the 450 MW(t) MHTGR [Hoot 1991].

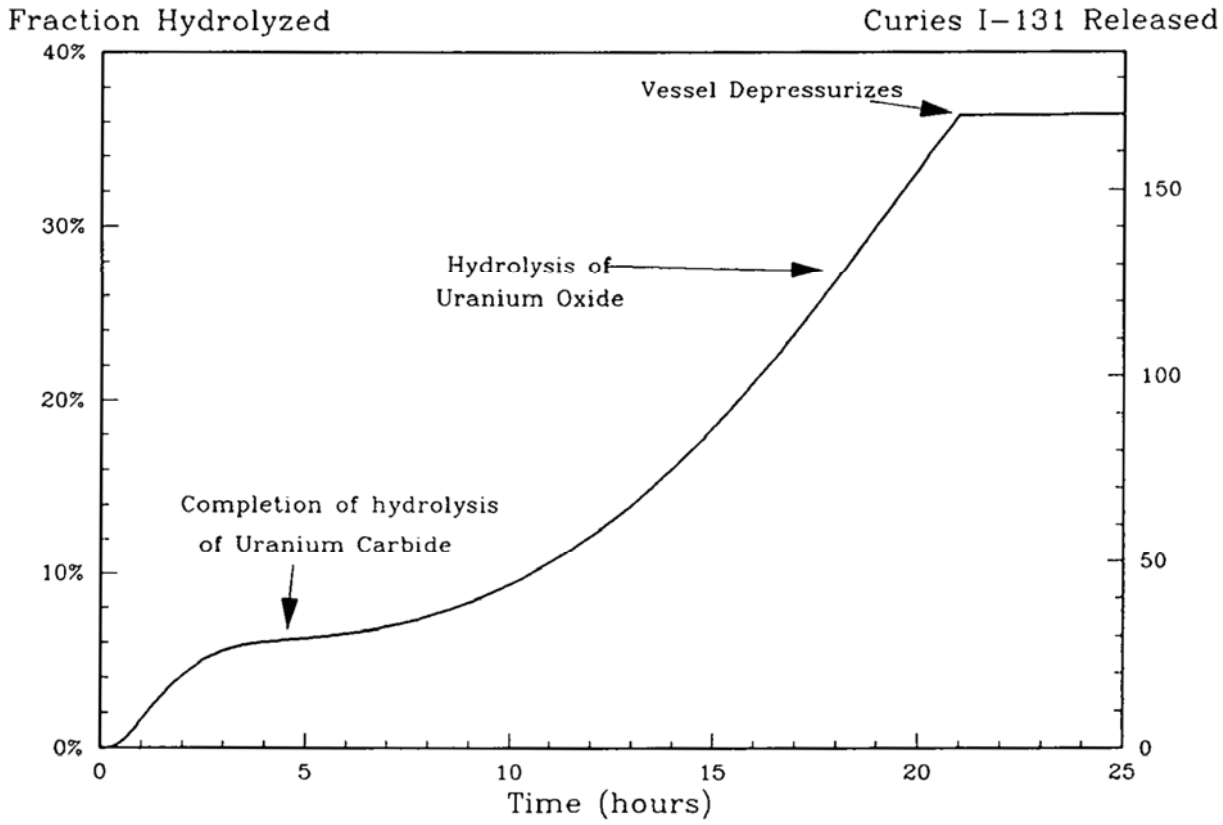

Figure 6-50. Hydrolysis of Exposed Fuel Kernels during SRDC-6 for 450 MW(t) MHTGR

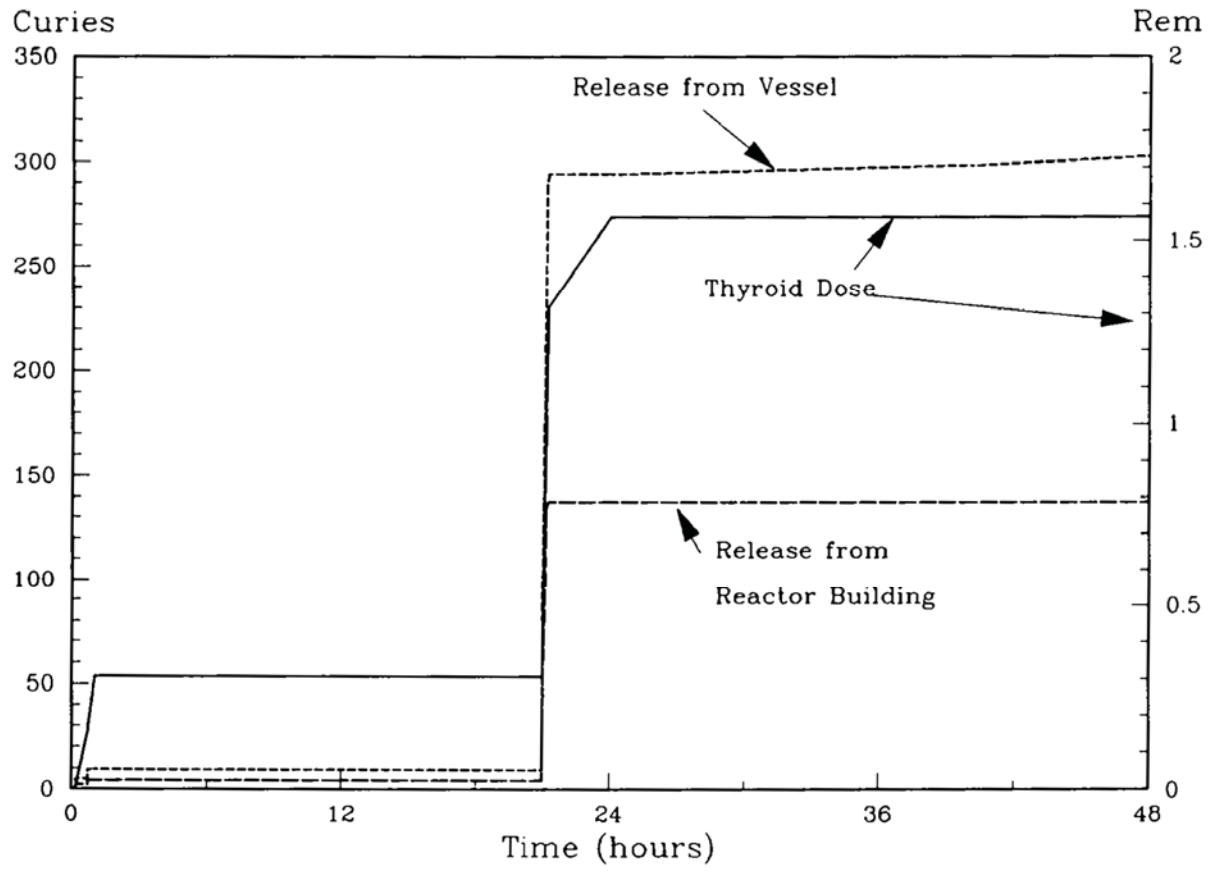

Figure 6-51. I-131 Release during SRDC-6 for 450 MW(t) MHTGR

6.2.2.3 Rapid Helium Depressurization (SRDC-10)

Rapid depressurization accidents (SRDC-10) receive little attention in [Richards 2008] evidently for two reasons. First, that study focused on various containment options for a steam-cycle MHR; however, the RB options considered were all low-pressure variants of the standard GA VLPC (i.e., a high pressure LWR-type containment building was not considered). Standard VLPCs are expected to provide little attenuation of the offsite RN releases during the initial (blowdown) phase of a rapid depressurization event.[47] Secondly, the delayed source term for rapid depressurization events leading to LPCC (SRDC-10) is bounded by the source term for slow depressurization events leading to LPCC (SRDC-11) for the reasons described above.

Rapid depressurization events are addressed in [Dilling 1993] which is essentially the basis for the source terms in [Richards 2008]. The results depend strongly upon the assumptions made regarding RN transport and weather. Using “Maximum Expected” iodine plateout inventories, best-estimate liftoff fractions (0.2%), and favorable weather, the PAG thyroid dose limit is met

[47] However, Westinghouse/PBMR did claim some RB retention during rapid depressurization events for certain RB designs [Wells 2008].

with large margins (two orders of magnitude) for various RB design options, including the standard GA VLPC. However, the PAG thyroid limit would be slightly exceeded using “Design” plateout inventories, conservative liftoff fractions (5%) and NRC Reg Guide 1.4 weather, as was done in the Functional Analysis (Appendix A) and in [PSID 1992]. The latter circumstance results by definition since the limits on I-131 release from the core for the 350 MW(t) steam-cycle MHTGR were derived such that the PAG thyroid dose limit would just be met with the aforementioned assumptions (Section 4 and Appendix A); and for a given core release fraction, the plateout inventories for a 450 MW(t) MHTGR are larger by the ratio of the power levels.

7 COMPARISON OF PREDICTED AND TARGET DECONTAMINATION FACTORS

The target RN decontamination factors presented in Section 4 are reviewed considering the predicted behavior of steam-cycle cores operating at 750 ^{o}C (Section 6.1) and the decontamination factors predicted for core designs analyzed as part of the CPA task [GA 2009b]. The emphasis is on the in-core RN retention barriers (kernels, coatings and graphite), but the predicted ex-core RN transport behavior under accident conditions (Section 6.2) is also reviewed.

7.1 Sensitivity Studies

The fuel performance and fission product release predictions reported in Section 6 for a 750 ^{o}C steam-cycle core, in Section 8 for cores with outlet temperatures of 850 ^{o}C and 950 ^{o}C and in the CPA report for a 900 ^{o}C outlet temperature [GA 2009b] are all intended to be best estimates. As discussed in previous review reports [e.g., Martin 1993], these predictions are based upon component models and material property data that, in general, have very large uncertainties (hence, the large number of fuel/fission product DDNs that have been identified). A large number of variation cases were run with SURVEY and TRAFIC-FD to determine how sensitive the predicted fuel performance and fission product release are to certain key material property data. In general, these sensitivity studies were performed for core outlet temperatures of 750 ^{o}C and 900 ^{o}C; the results are summarized in Table 7-1.

The issue of potential diffusive release of volatile fission metals from intact TRISO particles is of substantial importance. That Ag isotopes are diffusively released from intact TRISO particles at high temperature is widely accepted. As indicated in Table 7-1, the predicted amount of diffusive Ag release is highly dependent on the choice of diffusion coefficient. The FDDM/F Ag-in-SiC diffusion correlation results in a much larger core releases than the KFA correlation: 138x at 750 ^{o}C and 26x at 900 ^{o}C; based upon the data review in [Acharya 1994], the KFA correlation is judged to be more reliable. Nevertheless, the Ag-in-SiC diffusivity needs to be measured for US-made LEU UCO TRISO particles irradiated to full burnup (>20% FIMA).

The release of other volatile fission metals, especially Cs and Sr, from nominally intact TRISO particles is more controversial. FDDM/F states that only Ag (and H-3) are diffusively released from intact TRISO particles. In fact, some researchers have argued that Cs release from irradiated, nominally intact TRISO particles being heated at high temperatures can be used as an indicator of the structural integrity of the SiC; others have argued that Cs is diffusively released from “good” SiC at sufficiently high temperatures (e.g., see [Martin 1993] for competing arguments and references).

The diffusive release of Sr from intact TRISO particles is even more controversial. The Germans (KFA) claim that the Sr-in-SiC diffusivity is practically the same as the Ag-in-SiC diffusivity [Moormann 1987].[48] Given its high effectivity (rem/Ci), the allowable Sr release during normal operation and core heatup accidents is low. Fortunately (and perhaps surprisingly), the use of the KFA Sr-in-SiC diffusion correlation along with their Sr-in-UO_2 diffusion correlation does not give core-average Sr fractional releases that are dramatically larger than the current GA modeling assumption of 100% Sr release from failed particles and 0% Sr diffusive release from intact TRISO particles.

Additional sensitivity studies were performed to determine the potential impact of the German correlations for metal release from intact TRISO particles [Moormann 1987]. The fractional metal releases for various combinations of kernel and SiC diffusivities are plotted as a function of core outlet temperature (Case 7.9) in Figure 7-1. For Ag-110m, the release curve shown is for the FDDM/F UCO kernel diffusivity and the KFA SiC diffusivity per the recommendation of [Acharya 1994]. For Cs-137, two release curves are shown: (1) 100% release from failed particles and 0% release in intact particles (curve labeled “no diffusion”), and (2) KFA UO_2 kernel and SiC diffusivities. For Sr-90, three release curves are shown: (1) 100% release from failed particles and 0% release in intact particles (curve labeled “no diffusion”), (2) KFA UO_2 kernel and SiC diffusivities, and (3) FDDM/F UCO kernel diffusivity and KFA SiC diffusivity.

The predicted Ag-110m fractional release is the highest over the entire temperature range considered because of the high diffusive Ag release from intact TRISO particles and minimal Ag retention in matrix/graphite. For Cs-137, the inclusion of kernel retention is more important than the inclusion of diffusive release from intact TRISO particles. Matrix/graphite retention of Cs-137 is very significant at the lowest temperatures but drops off rapidly with increasing temperatures. In contrast for Sr-90, the inclusion of kernel retention is less important than the inclusion of diffusive release from intact TRISO particles. Matrix/graphite retention of Sr-90 is extremely important even the highest temperatures.

[48] In fact, Moormann has asserted that intact TRISO particles do not effectively retain Ag, Sr or Cs above ~1100 ^{o}C [Moormann 2008]. This assertion has been rejected by other German fuel specialists [e.g., Verfondern 2008].

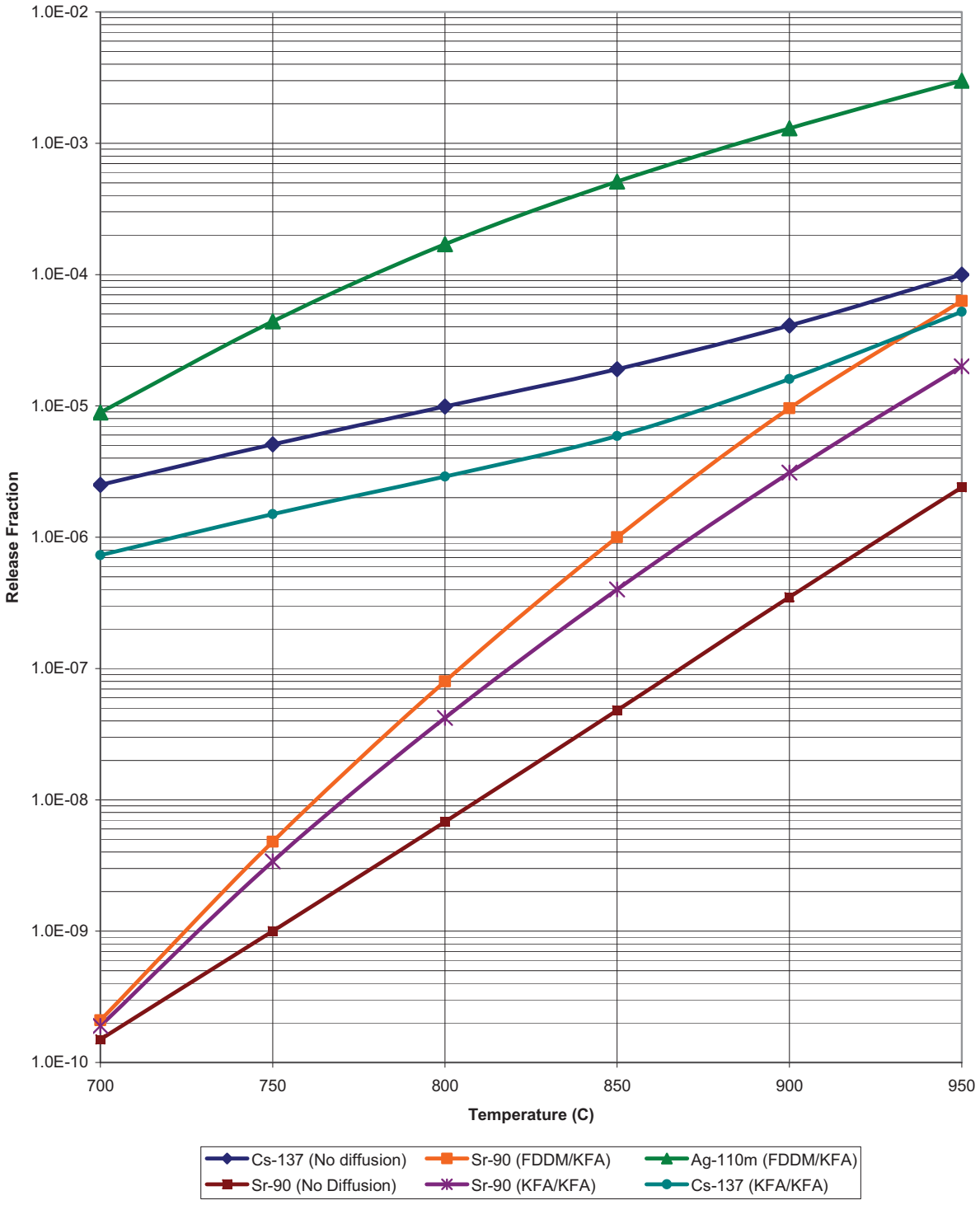

Figure 7-1. Effect of KFA Correlations on Predicted Metal Release

Table 7-1. Sensitivity of RN Release during Normal Operation to Transport Properties

Nuclide	Variation Parameter	Data Source	COT (°C)	Fractional Release			Comment
				Base Case	Variation Case	Change Factor	
Noble Gases. Base Case = FDDM/F models for hydrolyzed UCO particles							
Kr-88	4x $(R/B)_{failed}$	FDDM	900	9.2E-07	1.1E-06	1.2	Gas release dominated by HM contamination
I-131	4x $(R/B)_{failed}$	FDDM	900	2.2E-06	2.6E-06	1.2	Gas release dominated by HM contamination
Ag-110m. Base Case = FDDM/F models except for KFA correlation for Ag-in-SiC diffusivity							
Ag-110m	Diffusivity in SiC	FDDM	750	4.4E-05	6.1E-03	138	High sensitivity to Ag-in-SiC diffusivity
Ag-110m	Diffusivity in SiC	FDDM	900	1.3E-03	3.4E-02	26	High sensitivity to Ag-in-SiC diffusivity
Ag-110m	10x Diffusivity in graphite	FDDM	750	4.4E-05	4.7E-05	1.07	Little Ag retention by graphite @ COT=750C
Ag-110m	10x Diffusivity in graphite	FDDM	900	1.3E-03	1.3E-03	1.0	No Ag retention by graphite
Ag-110m	0,1x Diffusivity in graphite	FDDM	750	4.4E-05	2.6E-05	0.59	Minimal sensitivity to Ag-in-graphite diffusivity
Ag-110m	0,1x Diffusivity in graphite	FDDM	900	1.3E-03	1.0E-03	0.77	Minimal sensitivity to Ag-in-graphite diffusivity
Cs-137. Base Case = FDDM/F models except for no Cs retention in UCO kernels (large burnup dependence suspect)							
Cs-137	Diffusivity in UCO kernel	FDDM	750	5.1E-06	6.7E-08	0.013	Large burnup dependence of D_{UCO} suspect
Cs-137	Diffusivity in UCO kernel	FDDM	900	4.1E-05	4.5E-07	0.011	Large burnup dependence of D_{UCO} suspect
Cs-137	Diffusivity in UCO kernel	KFA	750	5.1E-06	1.5E-06	0.29	KFA UO_2 correlation; no burnup dependence
Cs-137	Diffusivity in UCO kernel	KFA	900	4.1E-05	1.1E-05	0.27	KFA UO_2 correlation; no burnup dependence
Cs-137	10x Diffusivity in graphite	FDDM	750	5.1E-06	1.4E-05	2.7	Graphite retention important @ COT =750 °C
Cs-137	10x Diffusivity in graphite	FDDM	900	4.1E-05	6.2E-05	1.5	Graphite less important @ COT=900 °C
Cs-137	0,1x Diffusivity in graphite	FDDM	750	5.1E-06	3.0E-07	0.059	Graphite retention important @ COT=750 °C
Cs-137	0,1x Diffusivity in graphite	FDDM	900	4.1E-05	8.8E-06	0.22	Graphite less important @ COT=900 °C
Sr-90. Base Case = FDDM/F models except for no Sr retention in UCO kernels (large burnup dependence suspect)							
Sr-90	D_{UCO}=FDDM; D_{SiC}=KFA	-	750	1.0E-09	4.8E-09	4.8	Intact TRISO release > kernel retention
Sr-90	D_{UCO}=FDDM; D_{SiC}=KFA	-	900	3.5E-07	9.6E-06	27.4	Intact TRISO release > kernel retention
Sr-90	D_{UO2}=KFA; D_{SiC}=KFA	KFA	750	1.0E-09	3.4E-09	3.4	Intact TRISO release > kernel retention

Nuclide	Variation Parameter	Data Source	COT (°C)	Fractional Release			Comment
				Base Case	Variation Case	Change Factor	
Sr-90	D_{UO2}=KFA; D_{SiC}=KFA	KFA	900	3.5E-07	3.1E-06	8.9	UO_2 retention > Intact TRISO release
Sr-90	10x graphite diffusion	FDDM	750	1.0E-09	1.9E-09	1.9	Little effect; Sr release desorption limited
Sr-90	10x graphite diffusion	FDDM	900	3.5E-07	4.2E-07	1.2	Little effect; Sr release desorption limited
Sr-90	0.1x graphite diffusion	FDDM	750	1.0E-09	7.8E-11	0.078	Sr diffusion barrier contributes to Sr retention
Sr-90	0.1x graphite diffusion	FDDM	900	3.5E-07	1.1E-07	0.31	Sr diffusion barrier contributes to Sr retention
Sr-90	10x matrix/graphite sorptivity	FDDM	750	1.0E-09	4.1E-11	0.041	Lower Sr desorption pressure, lower release
Sr-90	10x matrix/graphite sorptivity	FDDM	900	3.5E-07	1.6E-08	0.046	Lower Sr desorption pressure, lower release
Sr-90	0.1x matrix/graphite sorptivity	FDDM	750	1.0E-09	2.0E-08	20	Higher Sr desorption pressure, higher release
Sr-90	0.1x matrix/graphite sorptivity	FDDM	900	3.5E-07	3.3E-06	9.4	Higher Sr desorption pressure, higher release

7.2 Re-evaluation of Target Decontamination Factors

If a 600 MW(t) steam-cycle MHR were selected by the NGNP Project, the target RN decontamination factors would result in predicted source terms that nearly satisfy the requirement in [NGNP SRM 2009] to meet the lower limit PAGs at a 425-m EAB. In general, the thyroid doses are <2x higher than the 5-rem PAG limit which is to be expected because the power level, hence the RN inventories, would increase by 1.7x (600/350) and the target decontamination factors were chosen to just satisfy the 5-rem PAG limit for a 350 MW(t) plant.

As stated above, the NGNP Project is still in the conceptual design phase with major design selections yet to be made at this writing. While the GA team has made certain recommendations [Labar 2009], the NGNP Project has not officially chosen a plant power level, a core outlet temperature, or determined whether the steam generator will be located in the primary circuit. Given these circumstances, it appears premature to reallocate the RN decontamination factors simply because the thyroid doses are <2x higher than the 5-rem PAG limit. If such a reallocation were done now, the most effective reallocation would be to reduce the allowable in-service failure fractions and as-manufactured HM contamination by 1.7x to compensate for the increase in core power level.

While a reallocation of the RN decontamination factors is not recommended at the moment, it is appropriate to review the target decontamination factors in the context of the core performance analyses that have been done here and in the CPA task, and the sensitivity studies summarized in Section 7.1. Such a review has been done, and the results are summarized in Table 7-2. In this table, judgments are made as to which RN decontamination factors could be increased, decreased or left unchanged.

The contents of Table 7-2 are discussed below by release barrier. Four plant conditions are considered: (1) normal operation, (2) rapid depressurization (SRDC-10), (3) H_2O ingress plus pressure relief (SRDC-6), and (4) depressurized core conduction cooldown (SRDC-11); the three accident scenarios were described in Section 6.2.1. In addition to assessing how the decon factors might be reallocated, the key DDNs are identified and design features that could mitigate the source term are included. The implications for the fuel/fission product DDNs are elaborated in Section 9.

Unlike Section 4, the following subsections are ordered from the innermost release barrier outward (i.e., from the kernel outward) because the emphasis will be on the in-core release barriers.

7.2.1 RN Retention by Fuel Kernels

No credit is taken for Cs and Sr retention in the UCO kernels of particles with defective or failed SiC coatings or in exposed kernels because the extremely large burnup dependence of the FDDM/F correlations are judged to be highly suspect. It is expected that there will be

substantial kernel retention of Sr and, to lesser extent, of Cs under steam-cycle core conditions; however, Ag retention in the UCO kernel is expected to be modest.

It is critically important to obtain better data on I release from exposed UCO kernels under both dry and we core heatup conditions. Currently, core-average fractional release of I-131 from exposed kernels for SRDC-11 is predicted to be ~10%. If this value should prove to be too low, then the most effective solution would be to reduce the allowable in-service fuel failure during normal operation and core heatup accidents.

If the steam-cycle MHR design locates the steam generator in the primary circuit (which economic considerations will likely dictate), then water ingress plus pressure relief will likely be the bounding accident. As discussed in [Richards 2008 and Dilling 1993], the off-site dose consequences of SRDC-6 could be greatly reduced by including a high-efficiency filter in the pressure relief train that would remove a large fraction of the iodines and other condensable radionuclides in the effluent. With inclusion of such a filter, the importance of fuel hydrolysis would be much reduced.

7.2.2 RN Retention by Particle Coatings

An effective way of reducing the RN source term would be to reduce the allowable coating failure fraction during normal operation and postulated accidents. Based upon the fuel performance analyses performed to date, a ~2x reduction appears to be practical, especially under steam-cycle core conditions. The primary reason for this circumstance was the reduction of the allowable as-manufactured missing-buffer fraction from 5×10^{-5} for the steam-cycle MHTGR to 1×10^{-5} for the commercial GT-MHR. In addition, the amount of in-service SiC failure is quite low, consistently less than the as-manufactured SiC defect fraction even using the FDDM/F FP/SiC corrosion which is expected to be quite conservative (see Figure 6-10). As a consequence, the predicted exposed kernel fraction is typically $\sim 1 \times 10^{-5}$ (see Figure 6-12).

The main reason for not immediately decreasing the allowable in-service failure fraction during normal operation is that it would require that the NGNP/AGR fuel program irradiate successfully a larger number of fuel particles to obtain the requisite statistics. The reason for not decreasing the allowable incremental coating failure during core heatup accidents is even more compelling: at this writing there are no postirradiation heating data for high-quality, high-burnup LEU UCO fuel particles. Based upon the very positive German experience with heating lower burnup 8-10% FIMA UO_2 fuel, it is expected that LEU UCO will also perform well. Assuming that the planned postirradiation heating of high-quality UCO fuel from AGR-1 confirms this expectation, it would be possible to consider reducing the allowable failure during core heatup accidents in about two years.

7.2.3 RN Retention by Fuel Element Graphite

The predicted retention of fission metals in the fuel-compact matrix and fuel-element graphite is less than the target allocations, especially at the higher core outlet temperatures. The output

from the TRAFIC-FD code is such that it is not easy to determine precisely the amount of holdup in the matrix and graphite; the sensitivity studies are the best indicator. The Ag retention in matrix/graphite is practically insignificant. Decreasing the Ag diffusivity by 10x only decreases the core-average fractional release by 1.7x at 750 ^{o}C and by 1.3x at 900 ^{o}C. Inspection of Figure 6-22 indicates that the matrix/graphite reduces the Cs release into the coolant by 10-20x during the first two irradiation cycles but perhaps slightly less during the final three cycles. The Sr retention by matrix/graphite is highly temperature which can be seen from the temperature sensitivity study in Table 8-1. The matrix/graphite attenuation factor can be estimated by dividing total SiC failure fraction by the Sr fractional release; it varies from ~60,000x at 750 ^{o}C to ~83x at 950 ^{o}C.

It will be important for the NGNP/AGR fuel program to characterize the transport Sr and Cs in the new grade of fuel-element graphite that is selected to replace H-451 graphite which is no longer available. It will also important for the program to determine whether fission metals, especially Sr, that are retained in the graphite during normal operation are released during water ingress events as some scoping data appear to suggest.

7.2.4 RN Retention by Primary Coolant Pressure Boundary

The condensable radionuclides that deposit in the primary circuit during normal operation may be partially re-entrained during rapid depressurization accidents and during water ingress plus pressure relief events.

The target decontamination factor assumed a 5% fractional liftoff of plateout activity during SRDC-10. Based upon the measured liftoff fractions in the COMEDIE BD-1 test [Medwid 1993], it should be possible to justify a significantly lower liftoff fraction. In that in-pile loop test, four *in situ* blowdown tests were performed at progressively higher shear ratios, [49] and the maximum measured fractional liftoff at a shear ratio of 5.6 was 0.13% for I-131, 0.11% for Cs-137, and 0.74% for Sr-90 (the peak shear ratio during SRDC-10 is <1.1).

The washoff fractions used in the SRDC-6 analysis are highly uncertain since they are based upon a few scoping measurements. However, as stated above, the off-site dose consequences of SRDC-6, including the contribution from washoff, could be greatly reduced by including a high-efficiency filter in the pressure relief train that would remove a large fraction of the iodines and other condensables in the effluent.

One of the target decontamination factors applied in the Functional Analysis (Appendix A) and in [PSID 1992] seems problematic. As discussed above, it was assumed that releases of

[49] Shear ratio = the wall shear stress during blowdown divided by the wall shear stress during normal operation.

condensables during SRDC-11 will be attenuated by ≥ 30x by primary circuit removal mechanisms including in-vessel plateout and thermal contraction of the gas mixture in the vessel with the latter effect being the more important. This decontamination factor is dependent upon the detailed timing of the event sequence. Essentially, it assumes that the RV has been depressurized and that the mass of helium/air in the RV and the reactor cavity has begun to contract before the peak RN release rates from the core have been established. It is apparent that one could construct a different event scenario (e.g., an initially small primary coolant leak that becomes progressively larger as the primary circuit overheats) whereby the RN release rates from the core become significant before the RV is fully depressurized. In case of point, the predicted time history of the I-131 release during SRDC-11 for 450 MW(t) MHTGR (Figure 6-48) indicates very little attenuation by the reactor vessel.

7.2.5 RN Retention by VLPC

The safety analysis for the 350 MW(t) steam-cycle MHTGR in [PSID 1992] takes no credit for RN retention in the VLPC during LPCC events (e.g., SRDC-11) for unspecified reasons. The preliminary safety analysis for the commercial GT-MHR claims an order of magnitude attenuation of I-131 release in the VLPC during a LPCC [Bolin 1994]. Conceptually, it would seem easier to justify a 10x attenuation factor for VLPC than the 30x attenuation factor for the vessel (preceding subsection).

As discussed in Section 4.1.1, an experimental program has been proposed to characterize RN transport under the conditions predicted for the VLPC during specific MHR accident scenarios [Hanson 2008c]. MHRM

Table 7-2. Potential for Reallocation of RN Decontamination Factors

RN Retention Barrier	RN	Reallocation of RN Decontamination Factors (- / 0 / +)[50]				Key DDNs
		Normal	SRDC-10	SRDC-6	SRDC-11	
Kernels	Xe[51]	0	NA[52]	+	+	Effect of hydrolysis on Kr, Xe, Te & I release; I release during LPCC
	I	0	NA	+	+	
	Cs	+	NA	0	+	Kernel retention of Sr and Cs during normal operation and LPCC. Burnup dependence of diffusivity
	Ag	+	NA	-	-	
	Sr	++	NA	+	++	
Coatings	Xe	++	NA	++	++	Determine performance limits of TRISO particles. Determine feasibility of tighter limits on allowable coating failure during normal operation & HPCC/LPCC
	I	++	NA	++	++	
	Cs	++	NA	++	++	
	Ag	++	NA	++	++	
	Sr	++	NA	++	++	
Matrix/ Graphite	Xe	NA	NA	NA	NA	No significant graphite retention
	I	NA	NA	NA	NA	
	Cs	+	+	+	+	Characterize metal transport behavior in new fuel-block graphite.
	Ag	-	-	-	-	

[50] Scale (- / 0 / +) denotes (smaller RN retention factor/no change/larger RN retention factor) to be assigned as required.
[51] Applies to Kr isotopes as well as Xe isotopes.
[52] NA = not applicable; barrier not effective under these circumstances.

RN Retention Barrier	RN	Reallocation of RN Decontamination Factors (- / 0 / +)[50]				Key DDNs
		Normal	SRDC-10	SRDC-6	SRDC-11	
	Sr	++	++	++	++	Determine metal behavior in graphite during H_2O ingress.
Primary Coolant Pressure Boundary	Xe	0	NA	NA	NA	Improved sorption isotherms for condensables. Characterize liftoff during rapid depressurization and washoff during H_2O ingress + pressure relief.
	I	++	++	+	+	
	Cs	++	++	+	+	
	Ag	++	++	+	+	
	Sr	++	++	+	+	
Reactor Building	Xe	NA	NA	NA	NA	Characterize RN transport in VLPC during H_2O ingress + pressure relief and depressurized core conduction cooldown.
	I	NA	-	++	++	
	Cs	NA	-	++	++	
	Ag	NA	-	++	++	
	Sr	NA	-	++	++	
Design Mitigation Features		Improved control rod management to reduce power peaking	TBD	High efficiency filter in pressure relief train.	Purge system to minimize air ingress into core.	Characterize efficiencies of candidate filters, especially for I removal from He/steam mixtures.

8 IMPACT OF HIGHER CORE OUTLET TEMPERATURES ON RN CONTROL

The effect of higher core outlet temperatures on RN control was evaluated by performing a sensitivity study; the results are summarized in Table 8-1. This temperature sensitivity study complements the material property sensitivity study presented in Section 7.1.

In performing this temperature sensitivity study, there were two logical choices for the base case: (1) the steam-cycle base case presented in Section 6 of this report with T_{in} = 322 ^{o}C and T_{out} = 750 ^{o}C; or (2) the VHTR base case for the CPA task [Ellis 2009] with T_{in} = 540 ^{o}C and T_{out} = 900 ^{o}C. The second choice was judged to be more appropriate for the following reasons. The "reference" steam-cycle core design has a relatively high core temperature rise of 428 ^{o}C which is typical of steam-cycle cores (e.g., the 350 MW(t) MHTGR had a core temperature rise of 429 ^{o}C [Jovanovic 1989]).

For a steam-cycle plant, a low core inlet temperature is attractive for several reasons. First, it permits the use of proven LWR reactor vessel steels without the need for vessel cooling. Secondly, it permits a large log-mean temperature difference which reduces the size of the steam generator. Finally, it reduces the required circulator power. However, the price of a large core temperature rise is higher peak fuel temperatures for a given core outlet temperature since, as stated above, the temperature rise in a given coolant channel is proportional to the product of the core-average temperature rise and the sub-column peaking factor (i.e., the radial peaking factor).

For a direct-cycle GT-MHR with a typical core outlet temperature of 850 ^{o}C [Shenoy 1996] or a VHTR with a typical core outlet temperature of ≥ 900 ^{o}C [GA PCDSR 2007], a smaller core temperature rise is optimal. For these designs, the use of LWR reactor vessel steels without vessel cooling is impractical. In addition, these designs with their higher core outlet temperatures require design selections that minimize peak fuel temperatures. Given that core designs with core outlet temperatures >750 ^{o}C would most likely have smaller core temperature rises than a steam-cycle plant, the VHTR base case for the CPA task with T_{out} = 900 ^{o}C and a ΔT_{core} = 360 ^{o}C was chosen as the base case for the temperature sensitivity study. The SURVEY and TRAFIC-FD codes were also run for T_{out} = 700, 750, 800, and 950 ^{o}C and with the ΔT_{core} = 360 ^{o}C for each outlet temperature; results for T_{out} = 900 ^{o}C were already available from the CPA task. The results are summarized in Table 8-1.

The "reference" steam-cycle case presented in Section 6 is also included in Table 8-1. By inspection of the two T_{out} = 750 ^{o}C cases in the table, the considerable performance penalty of a significantly larger core temperature rise becomes apparent.

The scope-of-work in [Work Plan 2009] calls for an assessment of the fuel performance and fission product release for core outlet temperatures of 800 and 950 ^{o}C, and these calculations were performed with the results summarized in Table 8-1. The original intent was to elaborate the results for T_{out} = 800 ^{o}C and for T_{out} = 950 ^{o}C at this point of this report, However, inspection of Table 8-1 indicates that the FP release for T_{out} = 800 ^{o}C and ΔT_{core} = 360 ^{o}C is nearly the

same as for "reference" steam-cycle case of T_{out} = 750 °C and ΔT_{core} = 428 °C (for some parameters, the former case is even nominally better). Consequently, it was decided to elaborate the T_{out} = 850 °C and ΔT_{core} = 360 °C case rather than the T_{out} = 800 °C case here along with the T_{out} = 950 °C case. The most temperature-sensitive performance metrics – SiC failure fraction, Ag fractional release, Cs fractional release and Sr fractional release – are plotted as a function of core outlet temperature in Figures 8-1 through 8-4. In the temperature range and variables considered, the SiC failure fraction is the least temperature sensitive and the Sr fractional release is the most temperature sensitive.

Two additional cases with ΔT_{core} = 428 °C are also plotted on Figures 8-2 through 8-4: one with T_{out} = 750 °C (the "reference" steam-cycle design), and the other with T_{out} = 687 °C (the earlier MHTGR). The metal release penalty associated with a higher ΔT_{core} is evident from comparing the two T_{out} = 750 °C results. The benefits of a lower core outlet temperature (Section 6.1.5) with regard to reduced metal release are also evident by comparing the releases at T_{out} = 700 °C and T_{out} = 750 °C at ΔT_{core} = 360 °C and by comparing the releases at T_{out} = 687 °C and T_{out} = 750 °C at ΔT_{core} = 428 °C. The effect is quite dramatic for Sr-90 release.

The T_{out} = 850 °C case could be considered a typical direct-cycle gas-turbine MHR core design, and the T_{out} = 950 °C case could be considered a nominal VHTR core design (although some would question whether a plant design with T_{out} >~900 °C is currently viable). In the subsections that follow for these two cases, less information is presented than for the "reference" steam-cycle case in Section 6 here and for the VHTR base case in [Ellis 2009] for several reasons: (1) the fast fluence and burnup distributions are unchanged for all cases; (2) only the fuel temperature distributions are presented because the graphite temperature distributions are unremarkable and simply track on the fuel temperature distributions; and (3) only the results for the fissile particle are presented since they bound the results for the fertile particle by factors of several.

Table 8-1. Effect of Core Outlet Temperature on RN Release during Normal Operation

Case	Core Outlet Temperature[53] (°C)	Fuel Temperature (°C)		Failure Fraction			R/B		Cumulative Fractional Release		
		Time-Ave. Maximum	Peak	Fissile Exposed Kernel	Total SiC (includes defects)	In-Service SiC	Kr-88	I-131	Cs-137	Ag-110m	Sr-90
7.9SC[54]	750	1171	1460	1.2E-05	6.6E-05	8.3E-06	5.8E-07	1.6E-06	8.7E-06	3.2E-04	3.4E-08
7.9.A	700	1061	1313	1.0E-05	5.8E-05	4.4E-07	4.5E-07	1.4E-06	2.5E-06	8.9E-06	1.5E-10
7.9.B	750	1111	1355	1.0E-05	5.9E-05	1.4E-06	5.3E-07	1.6E-06	5.1E-06	4.4E-05	1.0E-09
7.9.C	800	1157	1401	1.0E-05	6.2E-05	4.7E-06	6.2E-07	1.8E-06	9.9E-06	1.7E-04	6.8E-09
7.9.D	850	1203	1442	1.1E-05	7.3E-05	1.5E-05	7.4E-07	1.9E-06	1.9E-05	5.1E-04	4.8E-08
7.9.E	900	1249	1488	1.2E-05	1.1E-04	4.7E-05	9.2E-07	2.2E-06	4.1E-05	1.3E-03	3.5E-07
7.9.F	950	1295	1529	1.6E-05	2.00E-04	1.4E-04	1.3E-06	2.6E-06	1.0E-04	3.0E-03	2.4E-06

[53] For "7.9SC" case, Tin = 322 °C and ΔT_{core} = 428 °C (Section 6); for all other cases (7.9.A - 7.9.F), ΔT_{core} = 360 °C
[54] "SC" = steam-cycle MHTGR core

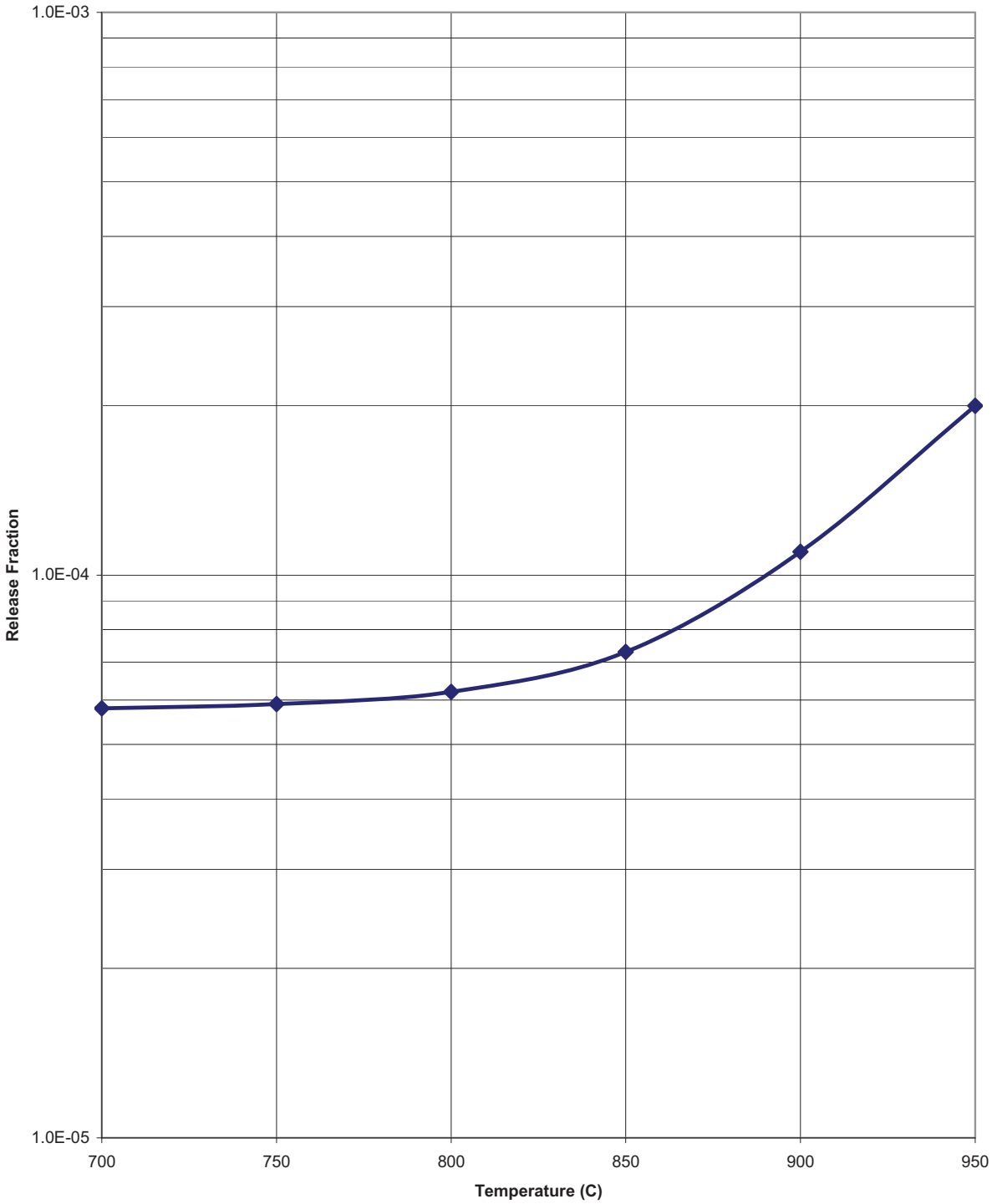

Figure 8-1. SiC Failure Fraction Versus Core Outlet Temperature

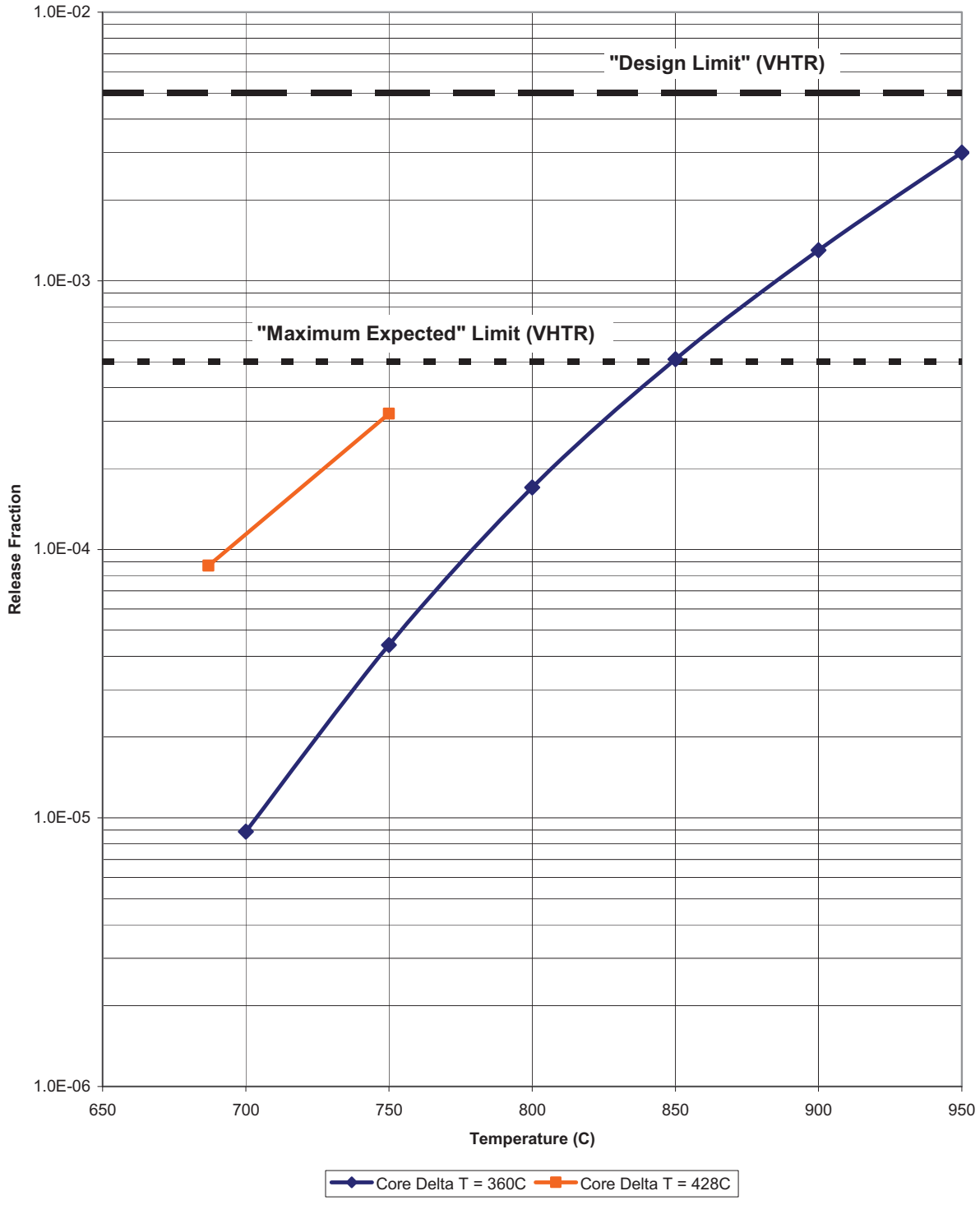

Figure 8-2. Ag-110m Cumulative Fractional Release versus Core Outlet Temperature

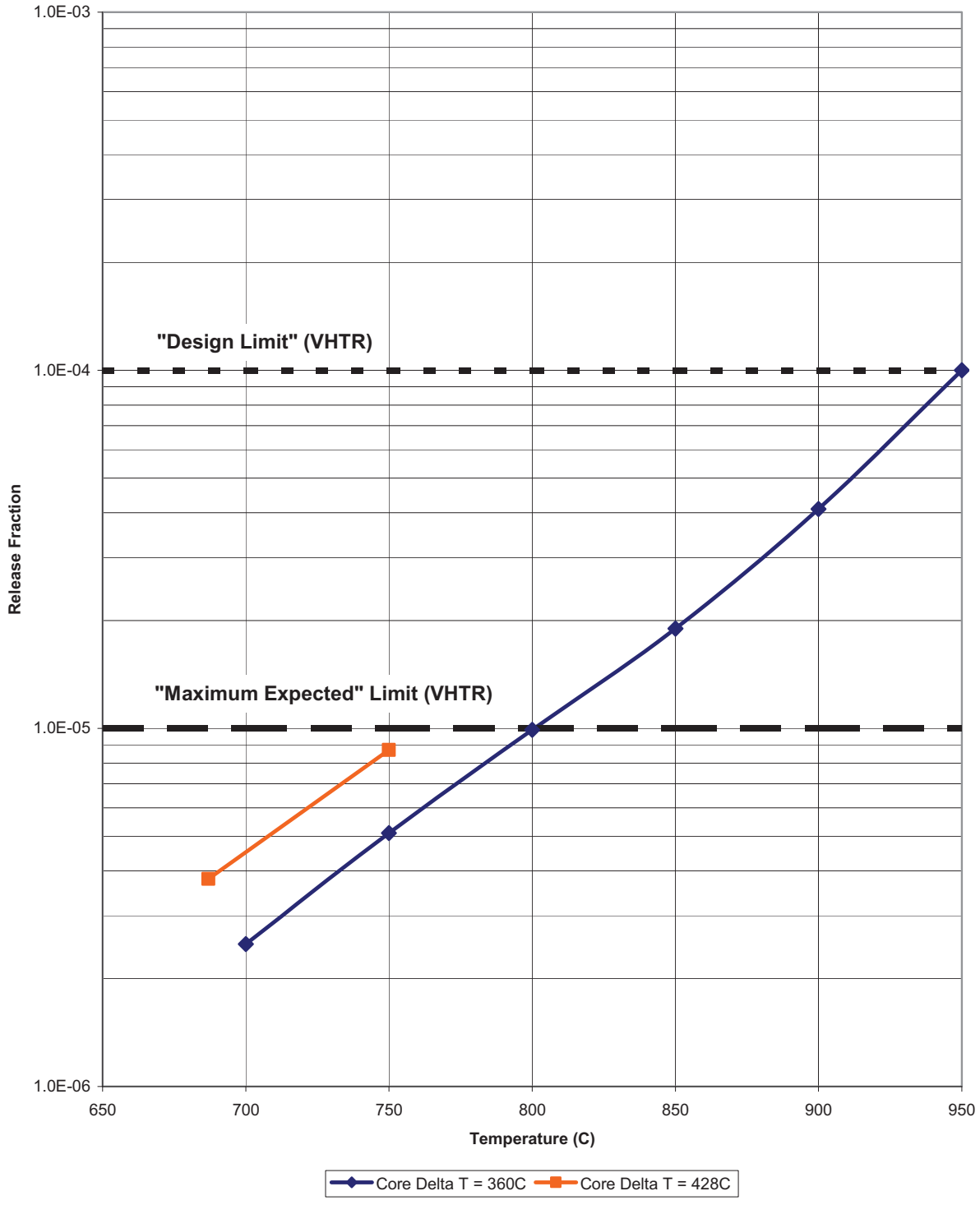

Figure 8-3. Cs-137 Cumulative Fractional Release versus Core Outlet Temperature

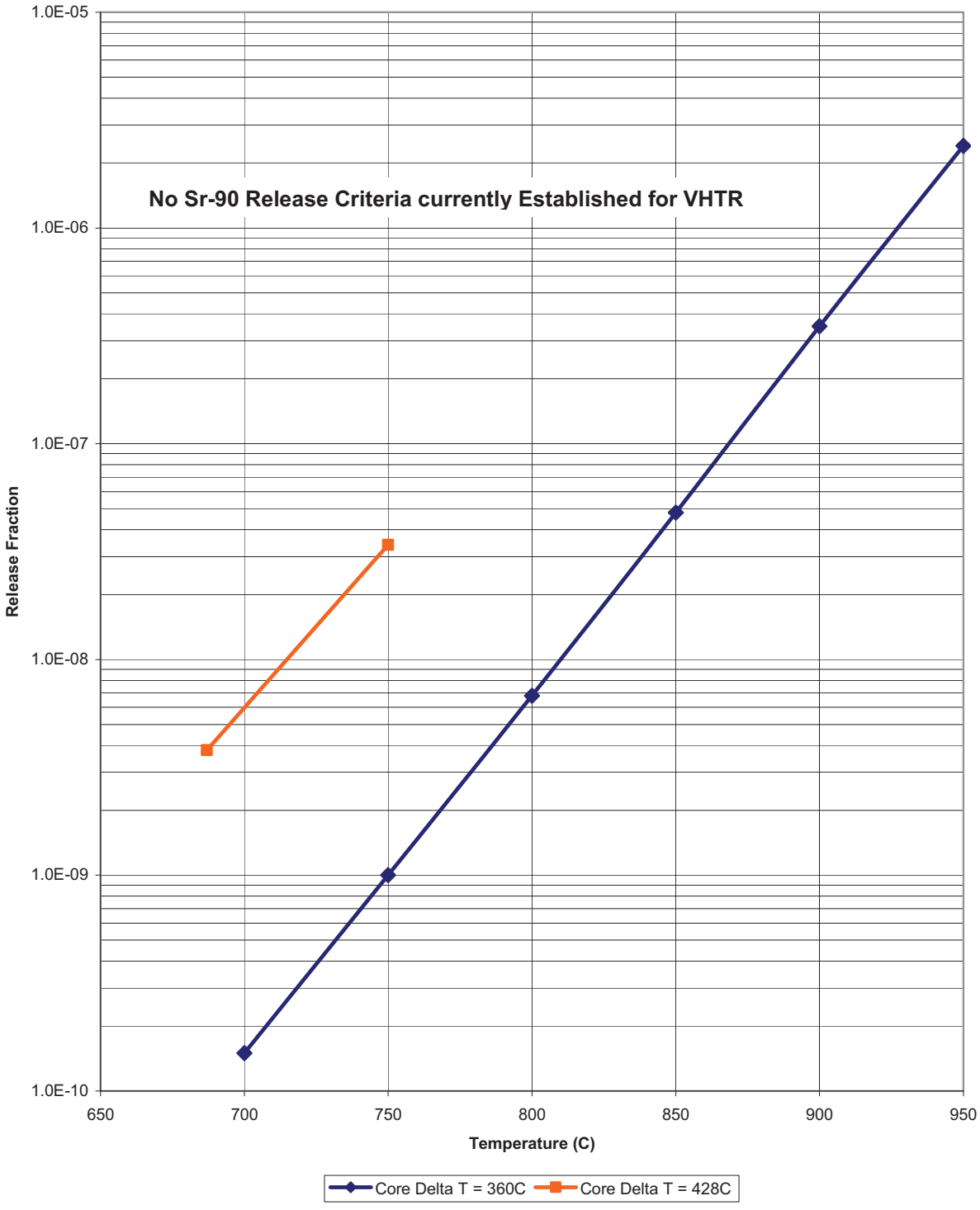

Figure 8-4. Sr-90 Cumulative Fractional Release versus Core Outlet Temperature

8.1 Predicted Core Performance at 850 °C Core Outlet Temperature

The predicted fuel performance and fission product release for Case 7.9 with T_{out} = 850 °C and ΔT_{core} = 360 °C are summarized below.

8.1.1 Temperature Distributions

Figures 8-5 and 8-6 give peak temperature distributions for fuel Segment 1; the plots are given for both the full-core volume and hottest 5% of the core. The corresponding maximum temperature for Segment 2 is slightly lower (1410 versus 1442 °C). However, the maximum time-average temperature is slightly higher in Segment 2 (1203 versus 1176 °C); the full-core volume and hottest 5% of the core for Segment 2 are shown in Figures 8-7 and 8-8, respectively. Such volume-distribution plots have been generated for both Segments 1 and 2, but neither set of plots has any unique features so the segment with the highest temperature is included here. The extreme peak fuel temperatures evident in Figures 8-5 and 8-6 are of concern, but they are limited to a relatively small fraction of the core and persist for only a short period of time. The maximum time-average fuel temperatures for Segment 1 and Segment 2 are all less than the design goal of <1250 °C.

Similar volume-distribution plots have also been generated for the fuel-element graphite, but they simply track on the fuel distribution plots so they are not included here.

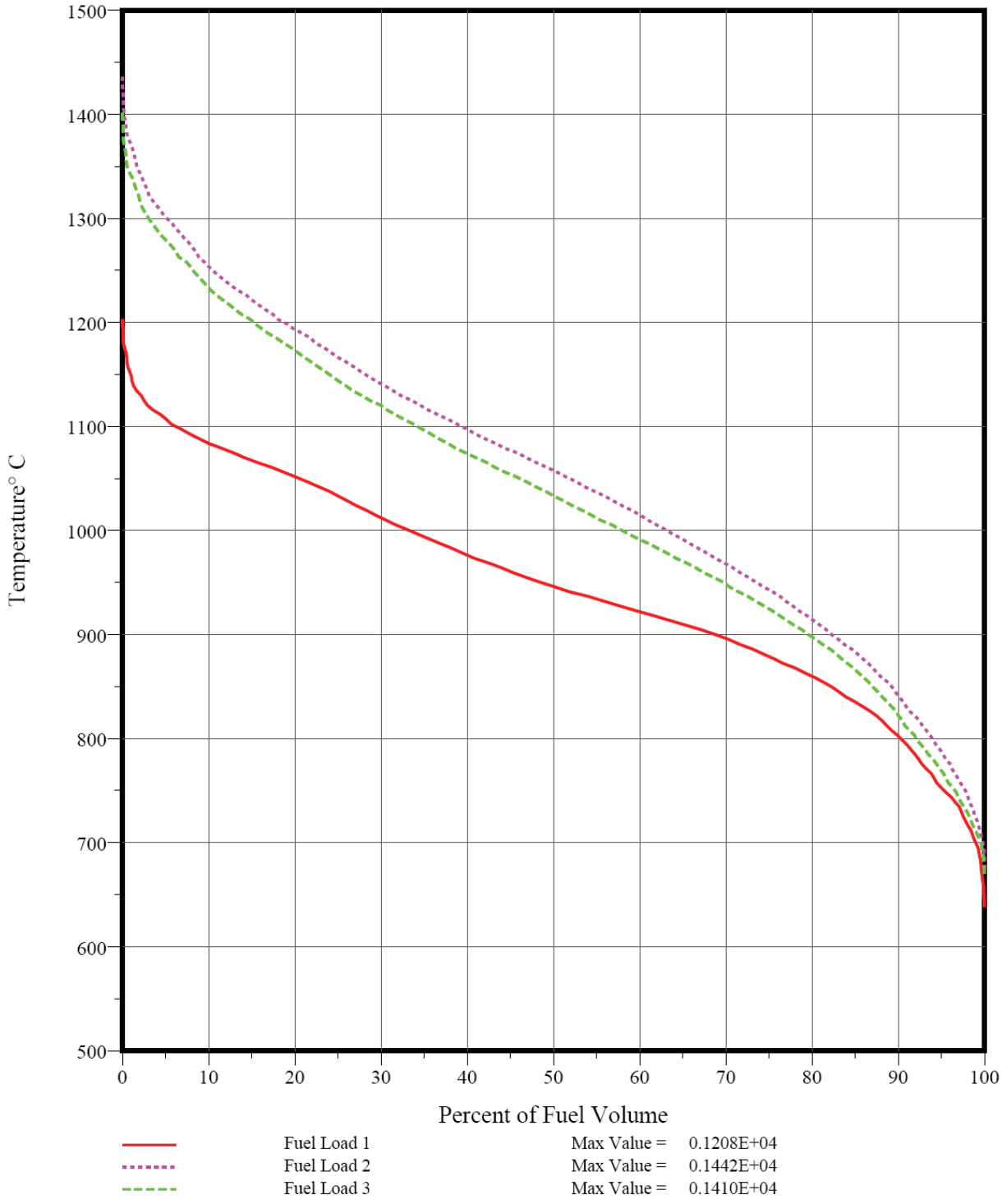

Figure 8-5. Peak Fuel Temperature Volume Distribution for Seg. 1 (T_{out} = 850C)

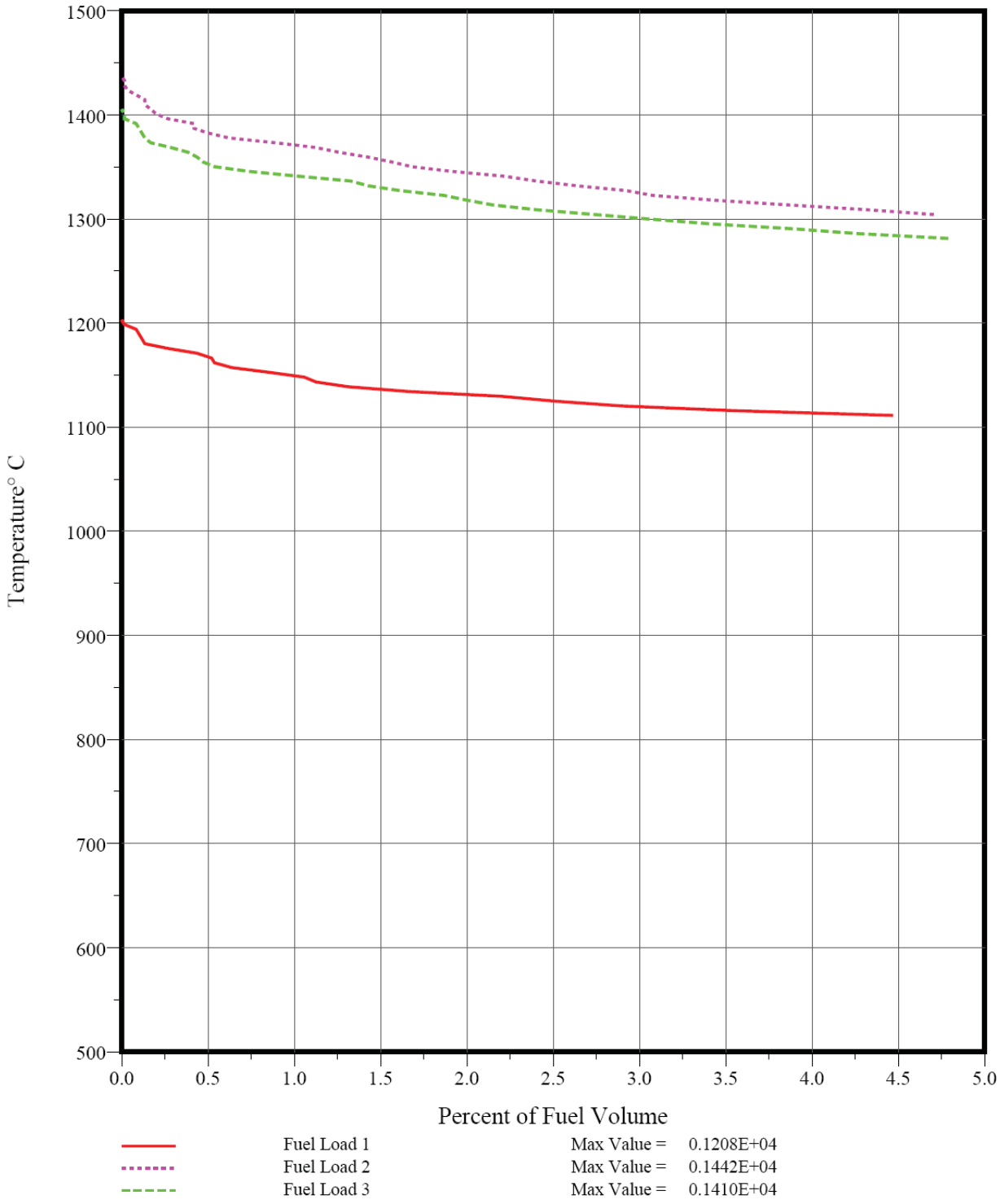

Figure 8-6. Peak Fuel Temperature Volume Distribution for Seg. 1 (0-5%) (T_{out} = 850C)

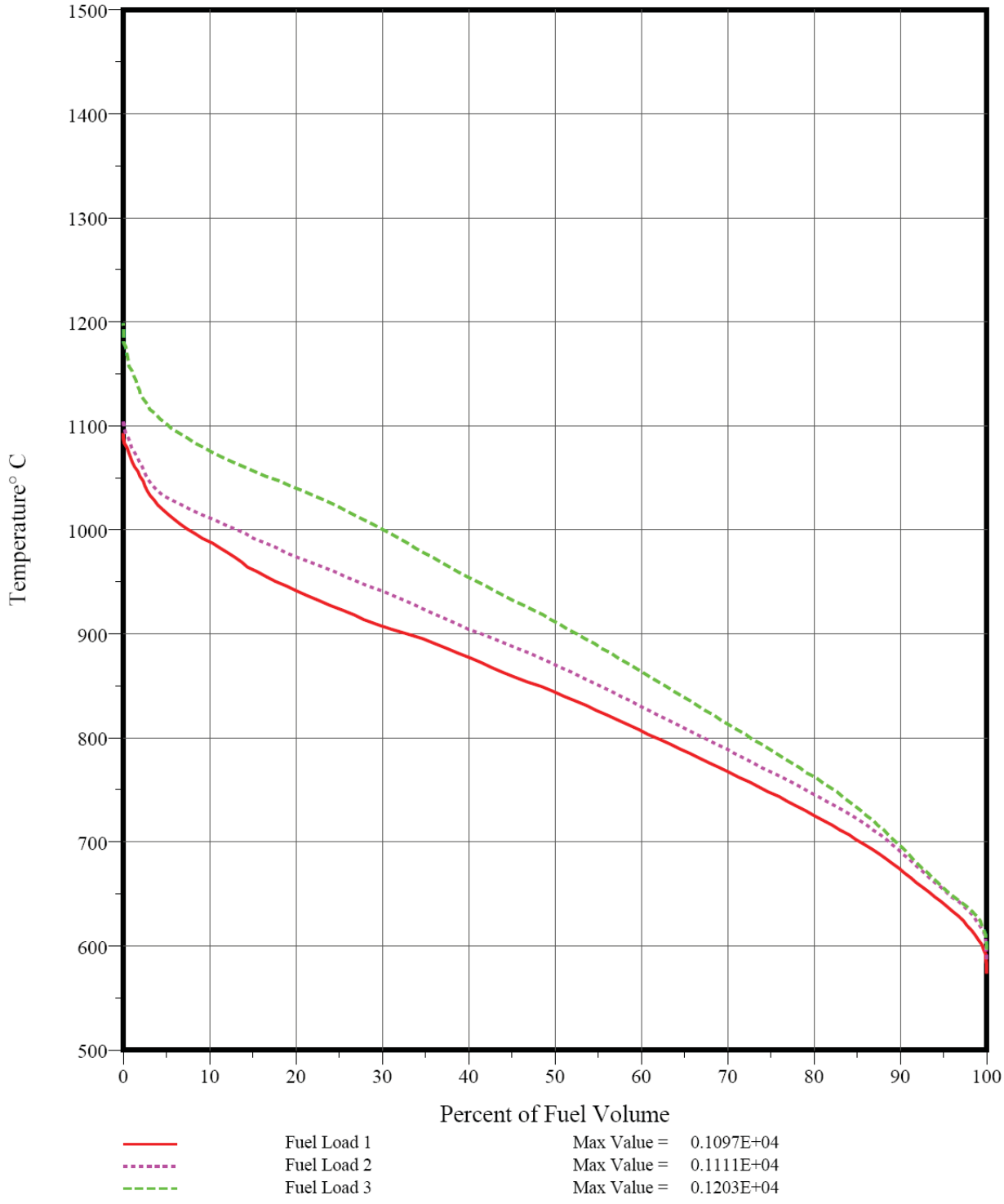

Figure 8-7. Time-ave. Fuel Temperature Volume Distribution for Seg. 2 (T_{out} = 850C)

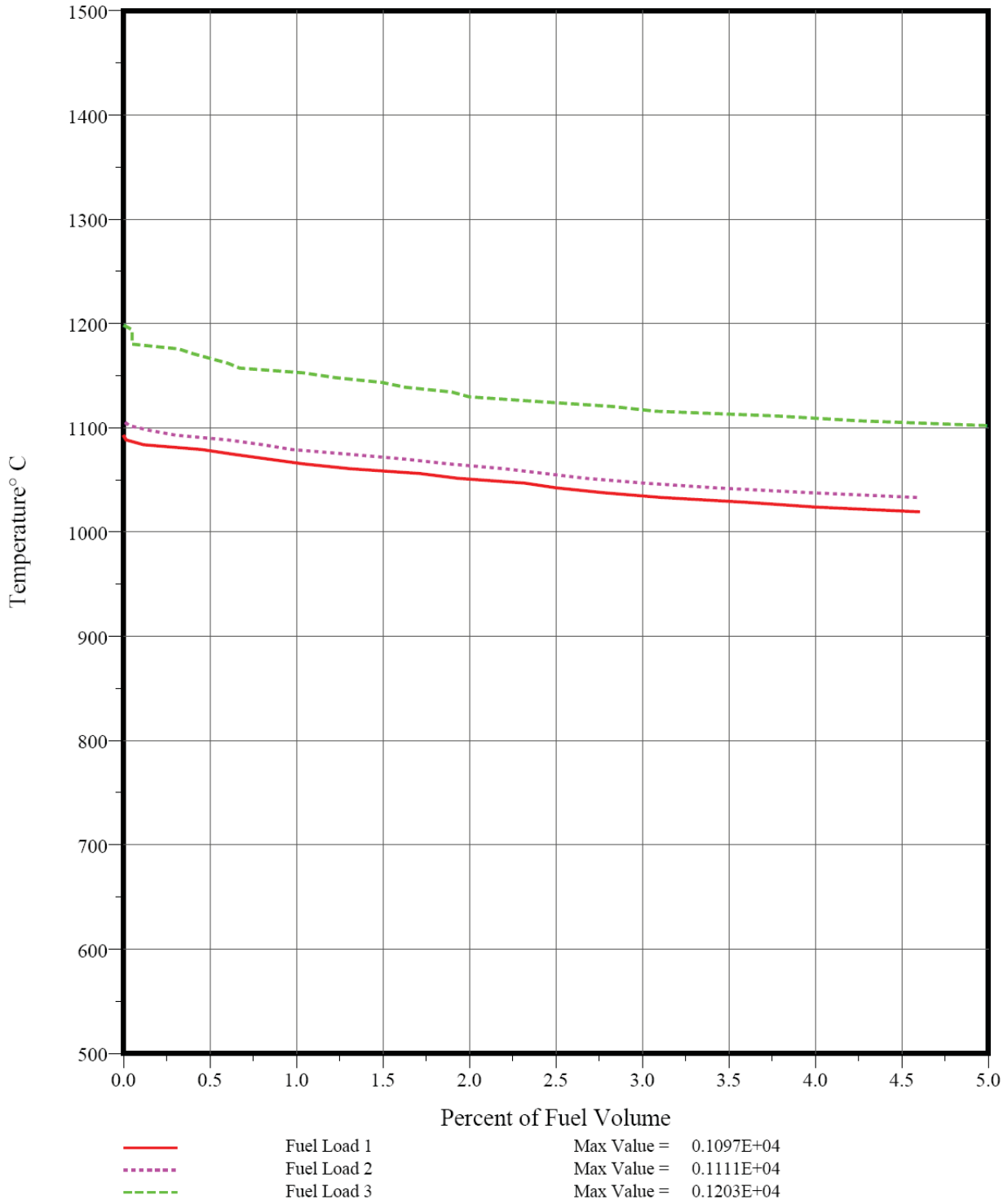

Figure 8-8. Time-ave. Fuel Temperature Volume Distribution for Seg. 1 (0-5%) (T_{out} = 850C)

8.1.2 Fuel Particle Failure

Based upon the burnups, fast fluences, and temperatures calculated by SURVEY/THERM, the fuel performance of Case 7.9 with T_{out} = 850 ^{o}C was calculated by SURVEY/PERFOR using the component models and material property data from FDDM/F.

The core-average SiC failure fraction as a function of operating time for the LEU fissile particle is shown in Figure 8-9. The value plotted on the ordinate is the sum of the as-manufactured SiC defect fraction and the in-service SiC failure probability as a result of FP/SiC reactions plus kernel migration plus thermal decomposition plus heavy-metal dispersion as result of a defective IPyC layer. The in-service SiC failure results from HM metal dispersion in the IPyC layer and FP/SiC reactions; kernel migration and SiC thermal decomposition are negligible. The predicted SiC failure fraction for the fertile particle is slightly lower for the fissile particle since the FP/SiC corrosion failure is burnup dependent (5.9×10^{-5} vs. 7.3×10^{-5}). The amount of in-service SiC failure peaks at the end of cycle 3 and is less than the as-manufactured SiC defect fraction in all cycles.

The maximum exposed kernel fraction calculated for the fissile and fertile fuel particles are about 1.2×10^{-5} and 3.5×10^{-6}, respectively; the fissile particle failure is shown in Figure 8-10. The initial value is very low because any exposed kernels in the as-manufactured fuel compacts would be counted as heavy-metal contamination. The contribution from PV failure of standard particles is insignificant because the failure probability is predicted to be negligible. The dominant sources of exposed kernels are therefore: (1) PV failure of particles with missing buffer layers, (2) PV failure of particles with defective or failed OPyC layers, and (3) OPyC failure on particles with defective or failed SiC layers. As stated above, 3% OPyC failure is predicted at a fast fluence of 2×10^{25} n/m^2. On a core-average basis, most of the fissile particles with missing buffers (~100%) are predicted to fail; however, a significant fraction of the fertile particles with missing buffers are predicted to survive (>80%).

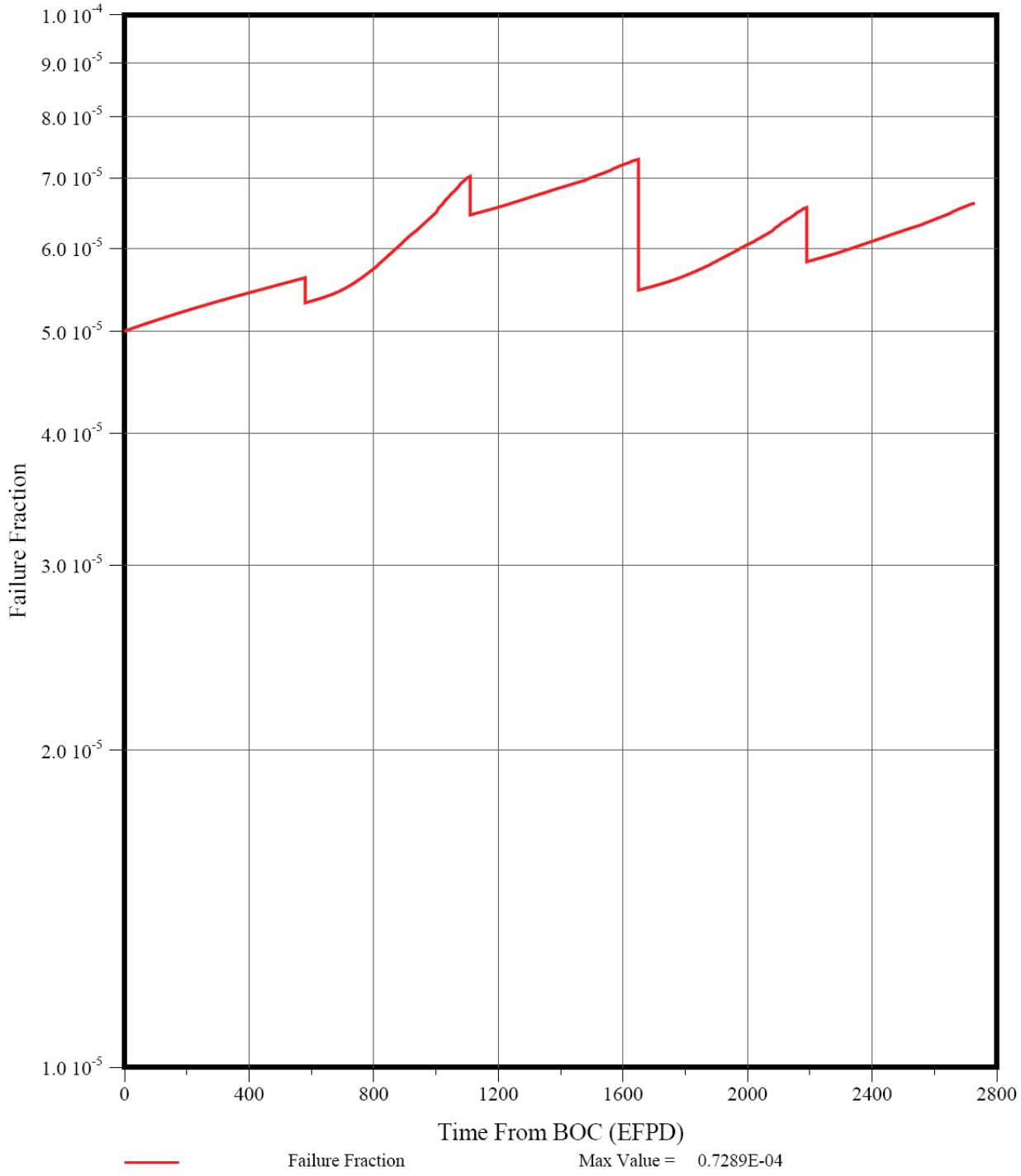

Figure 8-9. SiC Coating Failure Fraction for LEU UCO Fissile Particle (T_{out} = 850C)

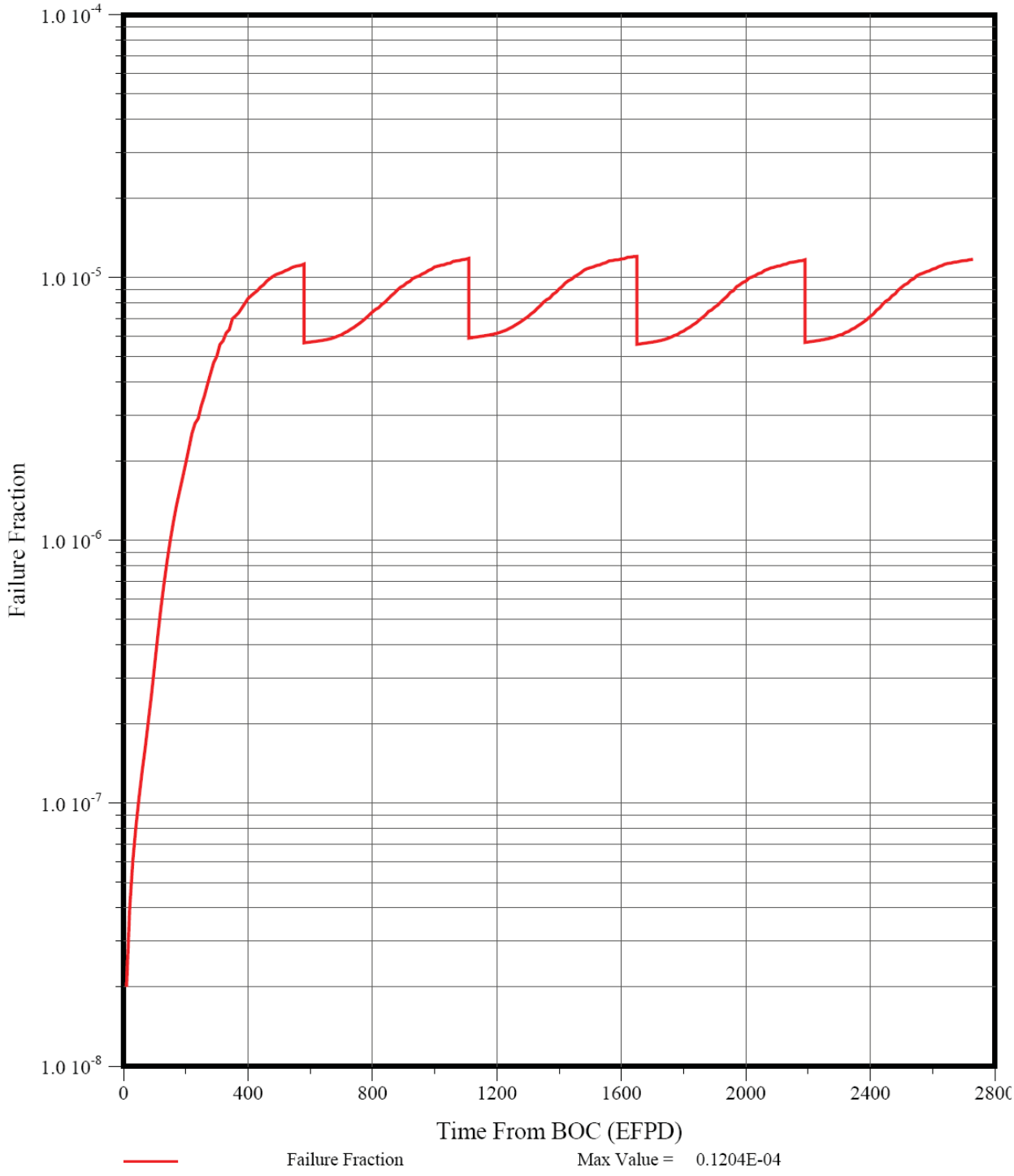

Figure 8-10. Exposed Kernel Fraction for LEU UCO Fissile Particle (T_{out} = 850C)

8.1.3 Gaseous Fission Product Release

The release rate-to-birth rate (R/B) ratios (equivalent to the fractional release for steady-state calculations such as these) for 2.8-hr Kr-88 and 8-day I-131 were also calculated by SURVEY/PERFOR using the FDDM/F fission gas release models for hydrolyzed UCO fuel. These R/Bs as a function of time are shown in Figures 8-11 and 8-12. The predicted fission gas release is dominated by the contribution from heavy-metal contamination. The contribution from failed particles is low because the predicted exposed kernel fraction is very low as discussed above (primarily a result of the tight specification on allowable missing-buffer particles). The only effective way of reducing these R/Bs would be to tighten the specification on heavy-metal contamination.

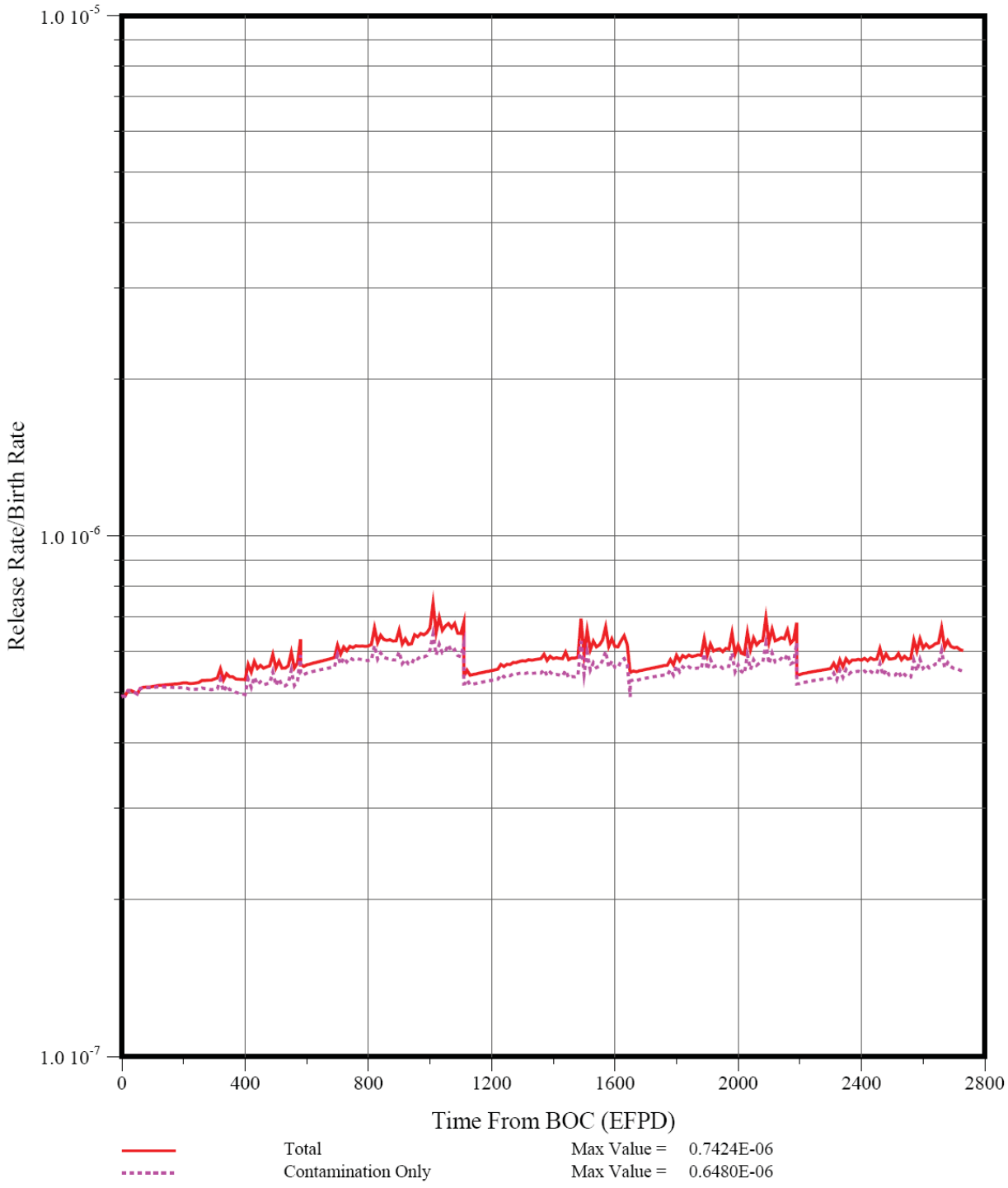

Figure 8-11. Core-Average R/B for Kr-88 (T_{out} = 850C)

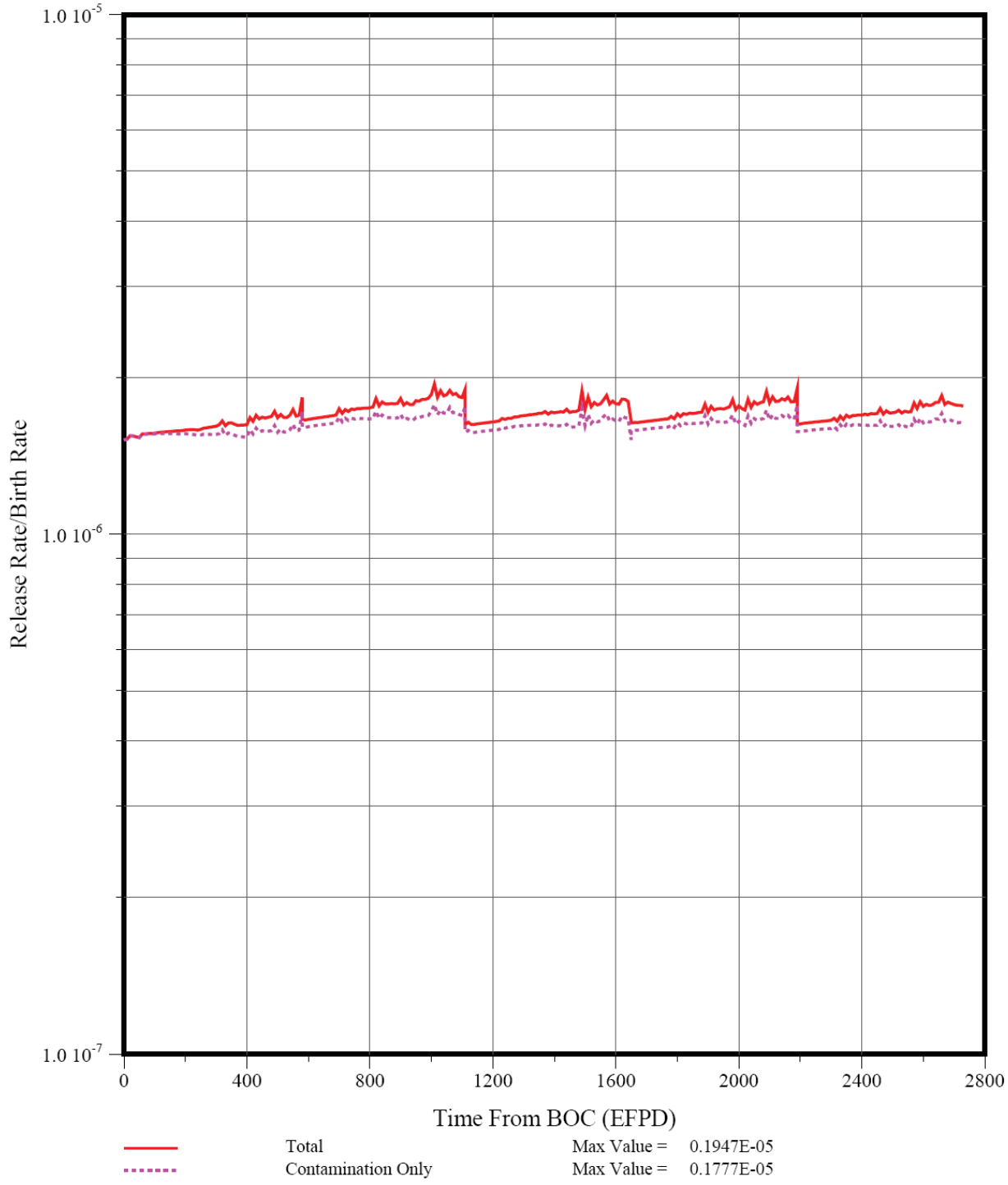

Figure 8-12. Core-Average R/B for I-131 (T_{out} = 850C)

8.1.4 Metallic Fission Product Release

The SURVEY/PERFOR results summarized above were supplied as input to the TRAFIC-FD code which was used to predict the releases of Ag-110m and Cs-137 from the core for Case 7.9 with T_{out} = 850 ^{o}C.

The predicted overall mass balance for 250-day Ag-110m is shown in Figure 8-13. The following "total" core (1/3 core because of symmetry) inventories are shown: (1) particle 1 (fissile), (2) particle (fertile), (3) matrix, (4) graphite, and (5) cumulative release into the coolant.[55] The cumulative fractional release of Ag-110m into the coolant is shown in Figure 8-14. The cumulative fractional release at any time point is defined as the cumulative release into the He coolant from time zero to that time point divided by the cumulative birth in the core from time zero to that time point with both release and birth inventories corrected for decay (the cumulative birth includes the birth in the fuel in the core at any given time plus the birth in any previously discharged fuel loads).

As observed for the "reference" steam-cycle case, there is little predicted Ag holdup in the matrix and graphite. The Ag fractional release, which is dominated by diffusive release from intact particles, predicts at the end of Cycle 2 during which the fuel temperatures were the highest. The predicted Ag fractional release for T_{out} = 850 ^{o}C is only slightly higher than for the "reference" steam-cycle case (5.1×10^{-4} vs. 3.5×10^{-4}) because of the higher fuel temperatures resulting from the larger core temperature rise for the latter.

[55] As stated previously, only the relative inventories reported in this section should be used directly (e.g., ratio of the inventory in the graphite to that in the particles). See footnote 25 for details.

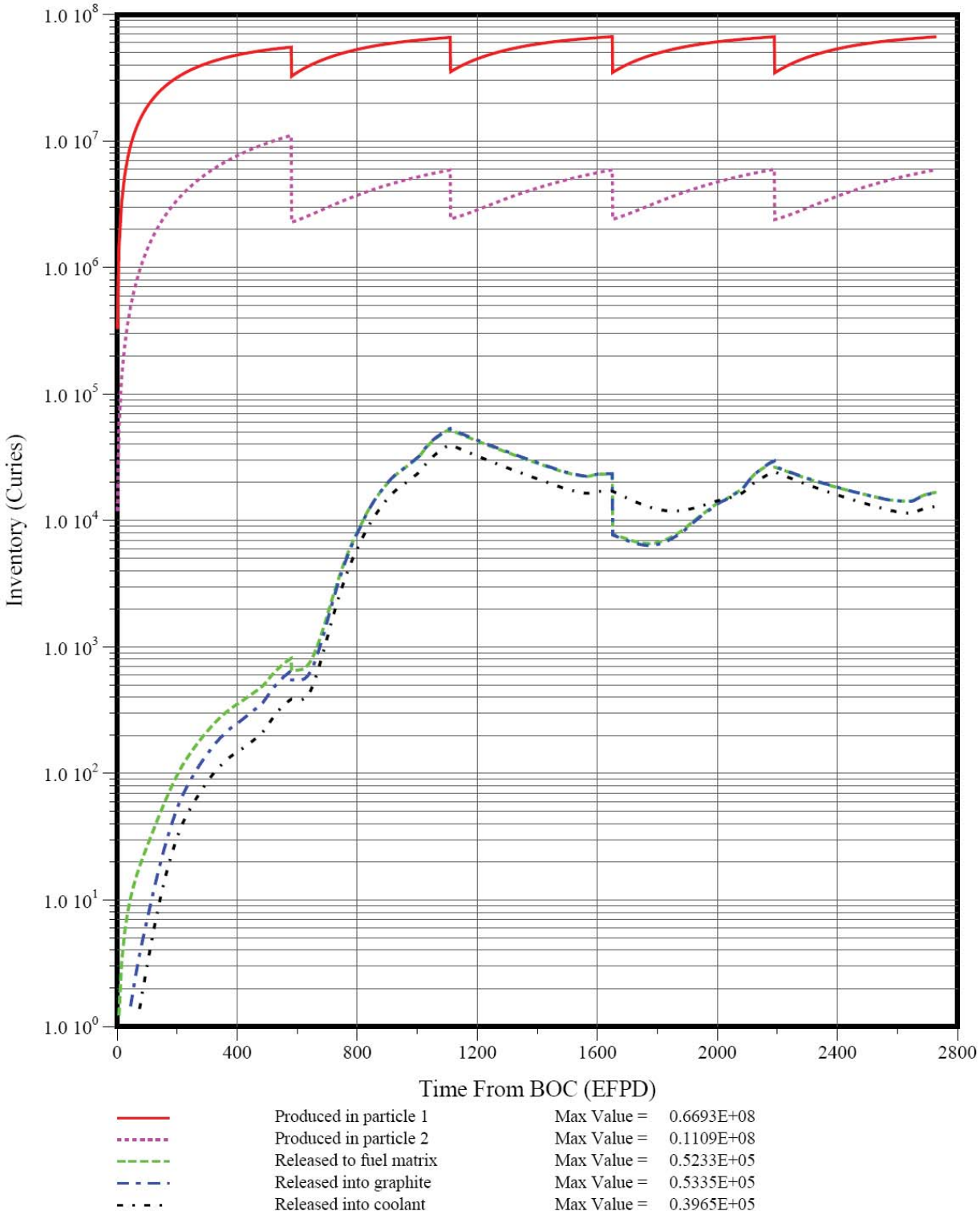

Figure 8-13. "'Full-core" Ag-110m Inventories by Core Material Region (T_{out} = 850C)

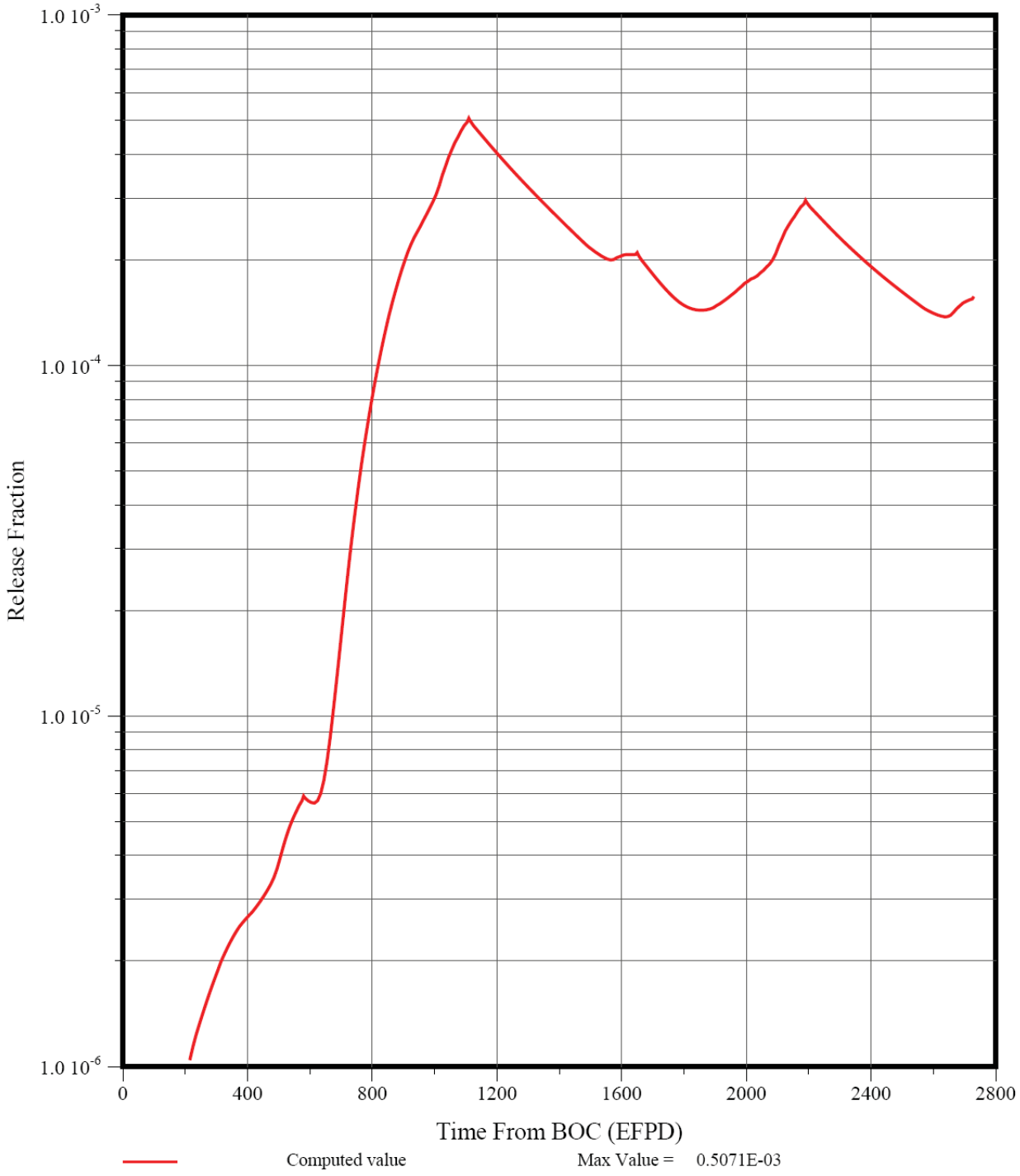

Figure 8-14. Cumulative Fractional Release of Ag-110m (T_{out} = 850C)

The corresponding predicted transport behavior of 30.1-yr Cs-137 is shown in Figures 8-15 and 8-16. As stated previously, the predicted behavior Cs-137 is generally similar though not identical to that of Ag-110m for two primary reasons. First, the half life of Cs-137 is much longer than that of Ag-110m (30.1 yr versus 0.68 yr) and much longer than an irradiation cycle; consequently, decay effects are insignificant during the five cycles analyzed. Secondly, there is no diffusive release from intact TRISO particles per the dictates of FDDM/F.[56]

In contrast to the predicted Ag behavior, there is significant Cs holdup by the matrix and graphite; the effect is most obvious in the first cycle. The core temperatures and, consequently, the SiC failure fractions and Cs release rates peak at the end of Cycle 2. Thus, during Cycle 3 and subsequent cycles, the fractional release of "new" Cs remains relatively constant, and the cumulative Cs release to the coolant is dominated by release during the first two cycles (in contrast to Ag-110m, this early Cs-137 release is not reduced because of its 30.1-yr half life).

The predicted Cs fractional release for T_{out} = 850 ^{o}C is ~2x higher than for the "reference" steam-cycle case (1.9×10^{-5} vs. 8.7×10^{-6}); again the benefit of the latter's 100 ^{o}C lower outlet temperature partially offset by its larger core temperature rise. As stated above, the predicted Cs release would likely be significantly reduced if the burnup-dependent FDDM/F correlation for Cs diffusion in UCO kernels were used; however, the use of that correlation is considered to be unjustified.

The predicted transport behavior of 29-yr Sr-90 is shown in Figures 8-17 and 8-18. The Sr behavior is similar to that of Cs except that there is much more holdup in the matrix/graphite. The fractional release of Sr-90 for T_{out} = 850 ^{o}C is only 1.4x higher than for the "reference" steam-cycle case (4.8×10^{-8} vs. 3.4×10^{-8}); once again the benefit of the latter's 100 ^{o}C lower outlet temperature partially offset by its larger core temperature rise.

[56] Per [FDDM/F 1987], Cs is not diffusively released from intact TRISO particles.

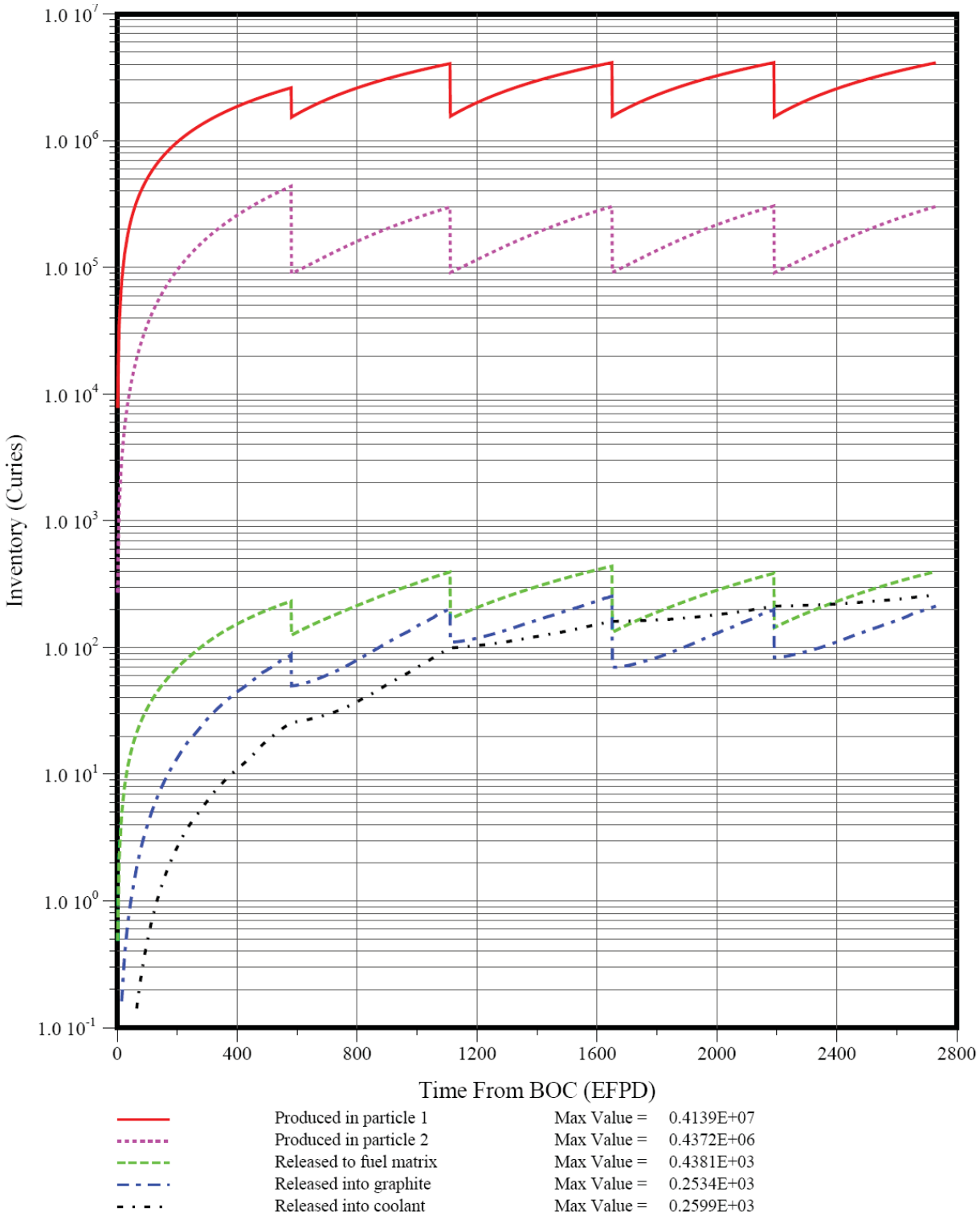

Figure 8-15. "'Full-core" Cs-137 Inventories by Core Material Region (T_{out} = 850C)

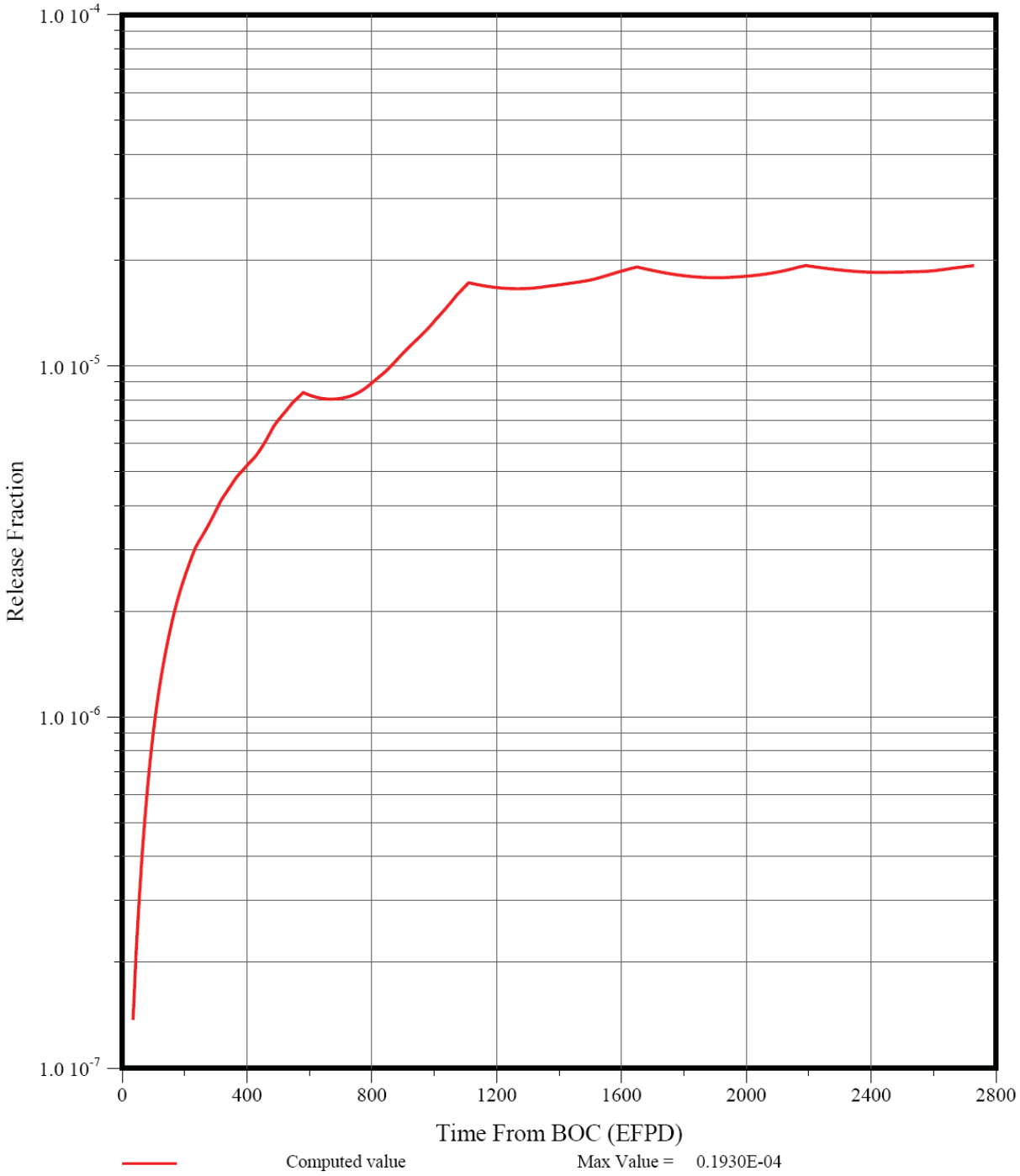

Figure 8-16. Cumulative Fractional Release of Cs-137 (T_{out} = 850C)

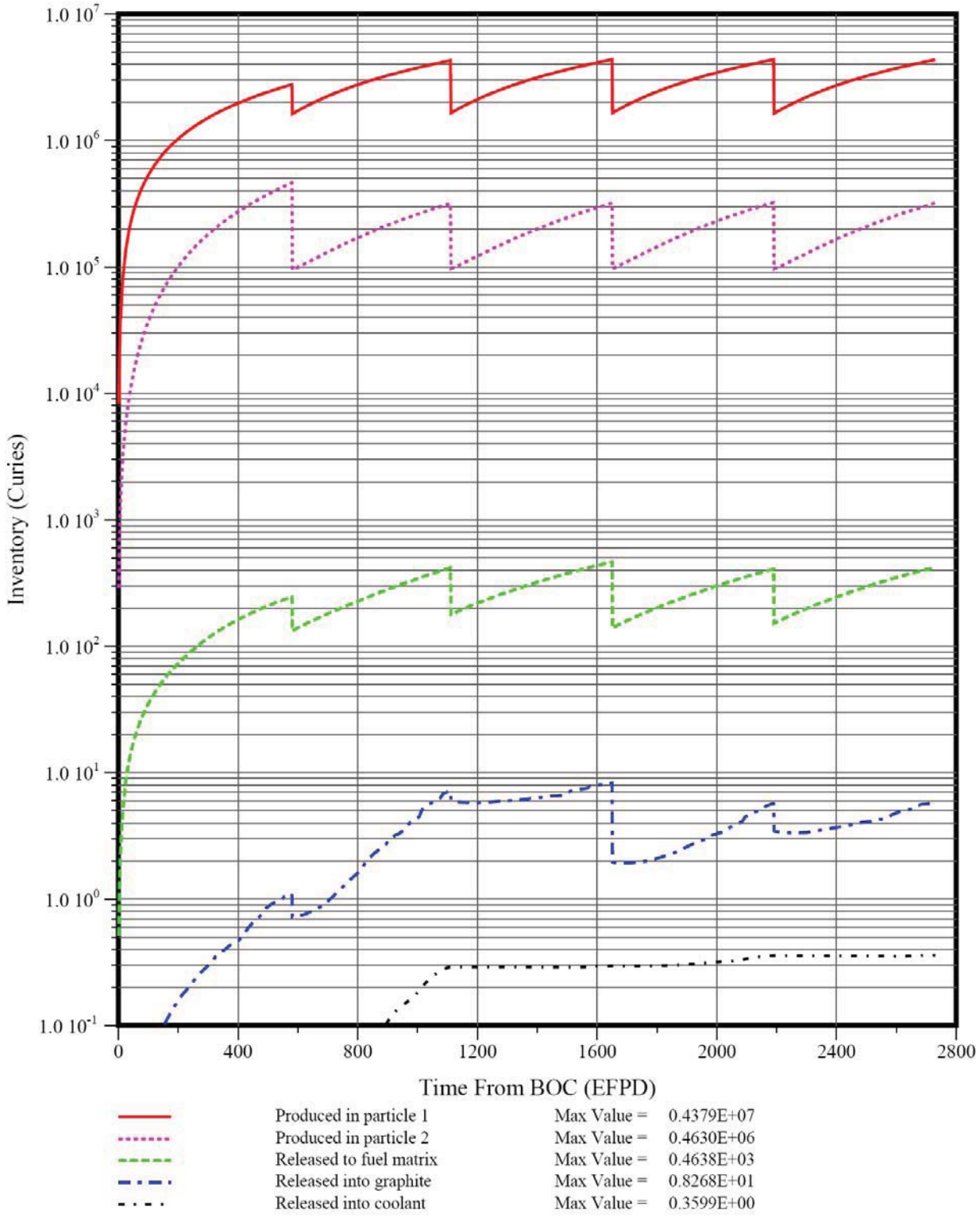

Figure 8-17. "'Full-core" Sr-90 Inventories by Core Material Region (Tout = 850C)

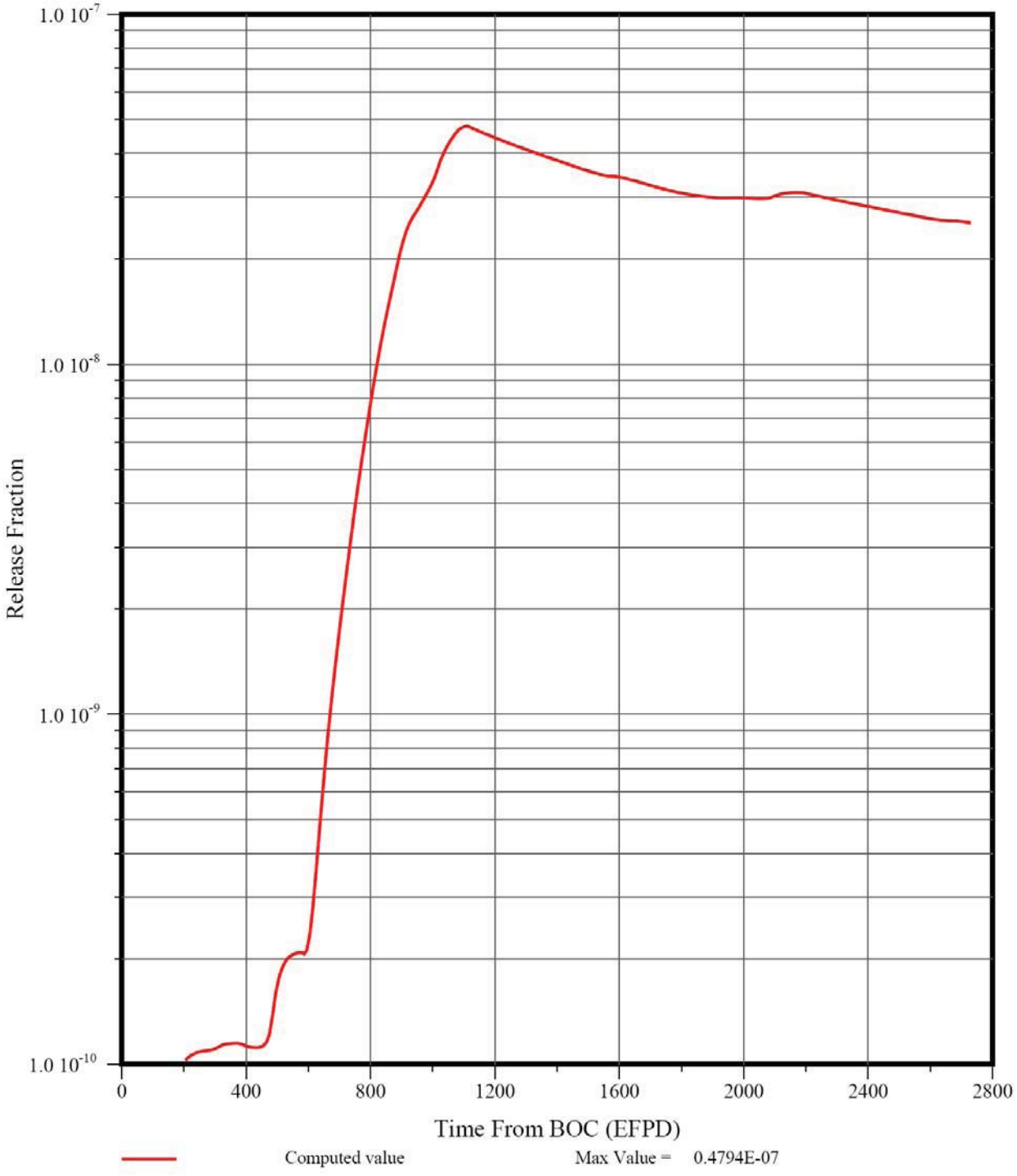

Figure 8-18. Cumulative Fractional Release of Sr-90 (Tout = 850C)

8.2 Predicted Core Performance at 950 °C Core Outlet Temperature

The predicted fuel performance and fission product release for Case 7.9 with T_{out} = 950 °C and ΔT_{core} = 360 °C are summarized below.

8.2.1 Fuel Temperature Distributions

Figures 8-19 and 8-20 give peak temperature distributions for fuel Segment 1 for the full-core volume and hottest 5% of the core, respectively. The corresponding maximum temperature for Segment 2 is slightly lower (1502 versus 1529 °C). However, the maximum time-average temperature is slightly higher in Segment 2 (1295 versus 1267 °C); the full-core volume and hottest 5% of the core for Segment 2 are shown in Figures 8-21 and 8-22, respectively. The maximum time-average fuel temperatures for Segment 1 and Segment 2 exceed the design goal of <1250 °C; however, as discussed previously, this temperature goal is only a crude rule-of-thumb which the present study has demonstrated is of limited value, especially for predicting the magnitude of volatile metal release.

Similar volume-distribution plots have also been generated for the fuel-element graphite, but again they simply track on the fuel distribution plots so they are not included here.

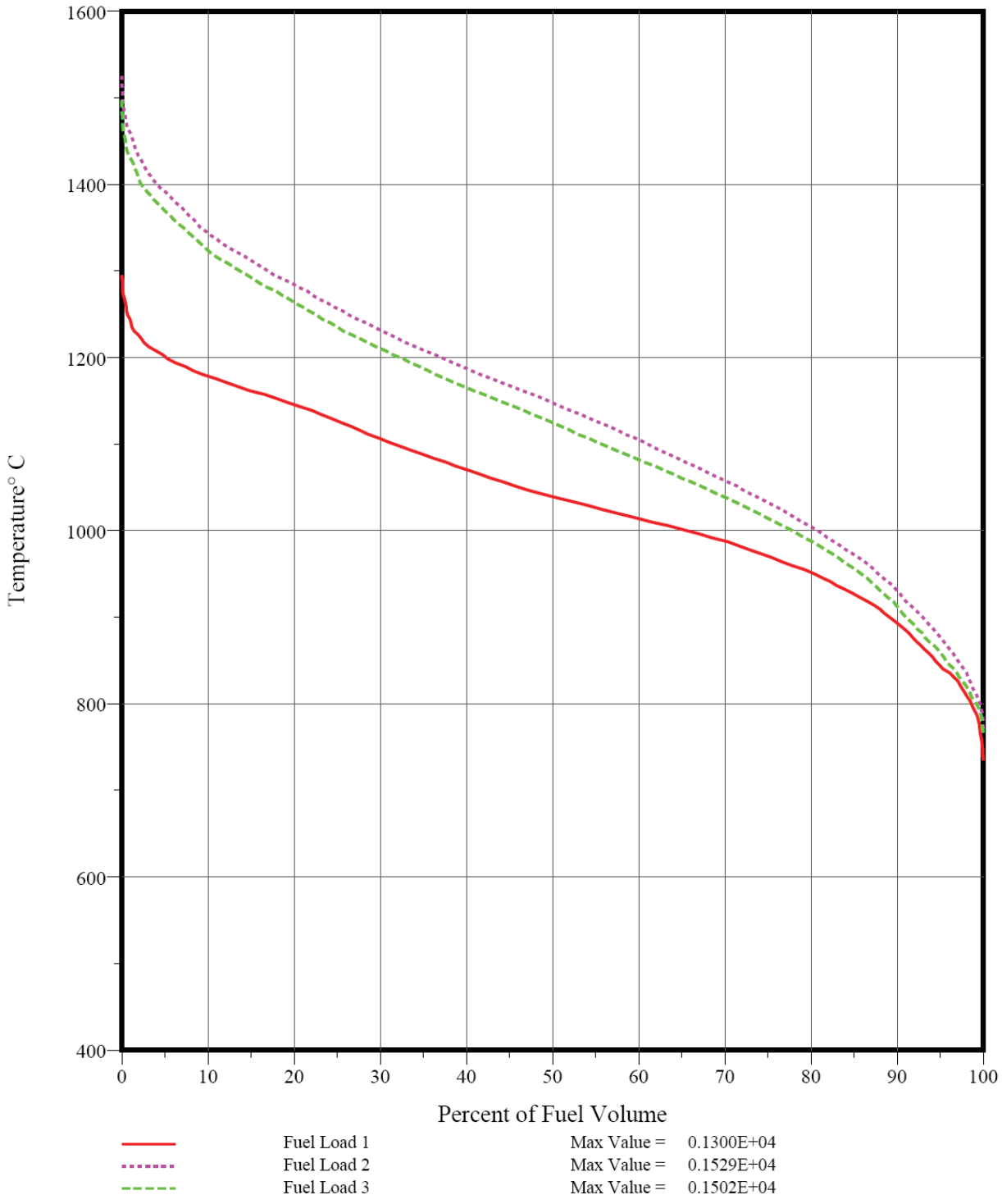

Figure 8-19. Peak Fuel Temperature Volume Distribution for Seg. 1 (T_{out} = 950C)

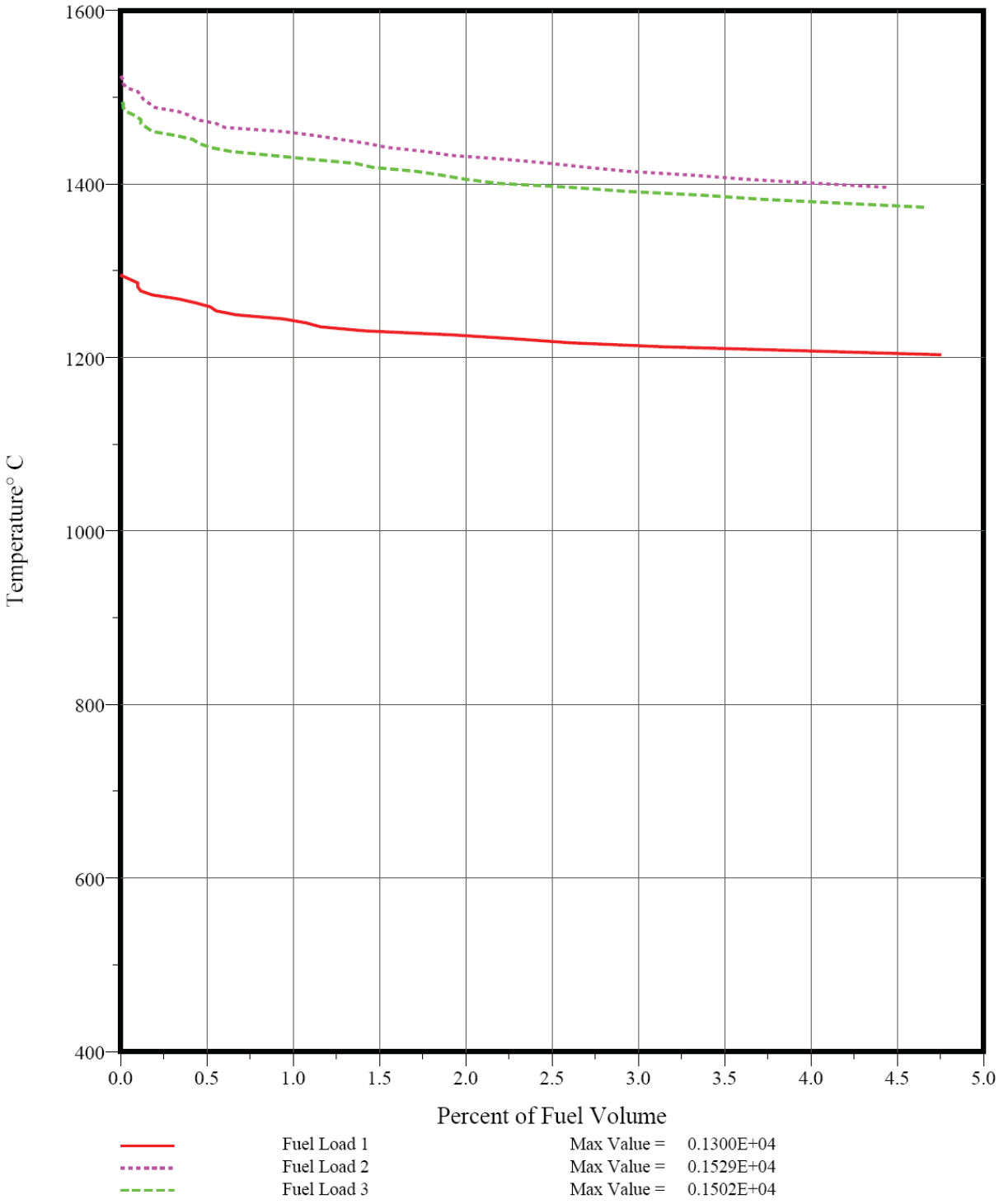

Figure 8-20. Peak Fuel Temperature Volume Distribution for Seg. 1 (0-5%) (T_{out} = 950C

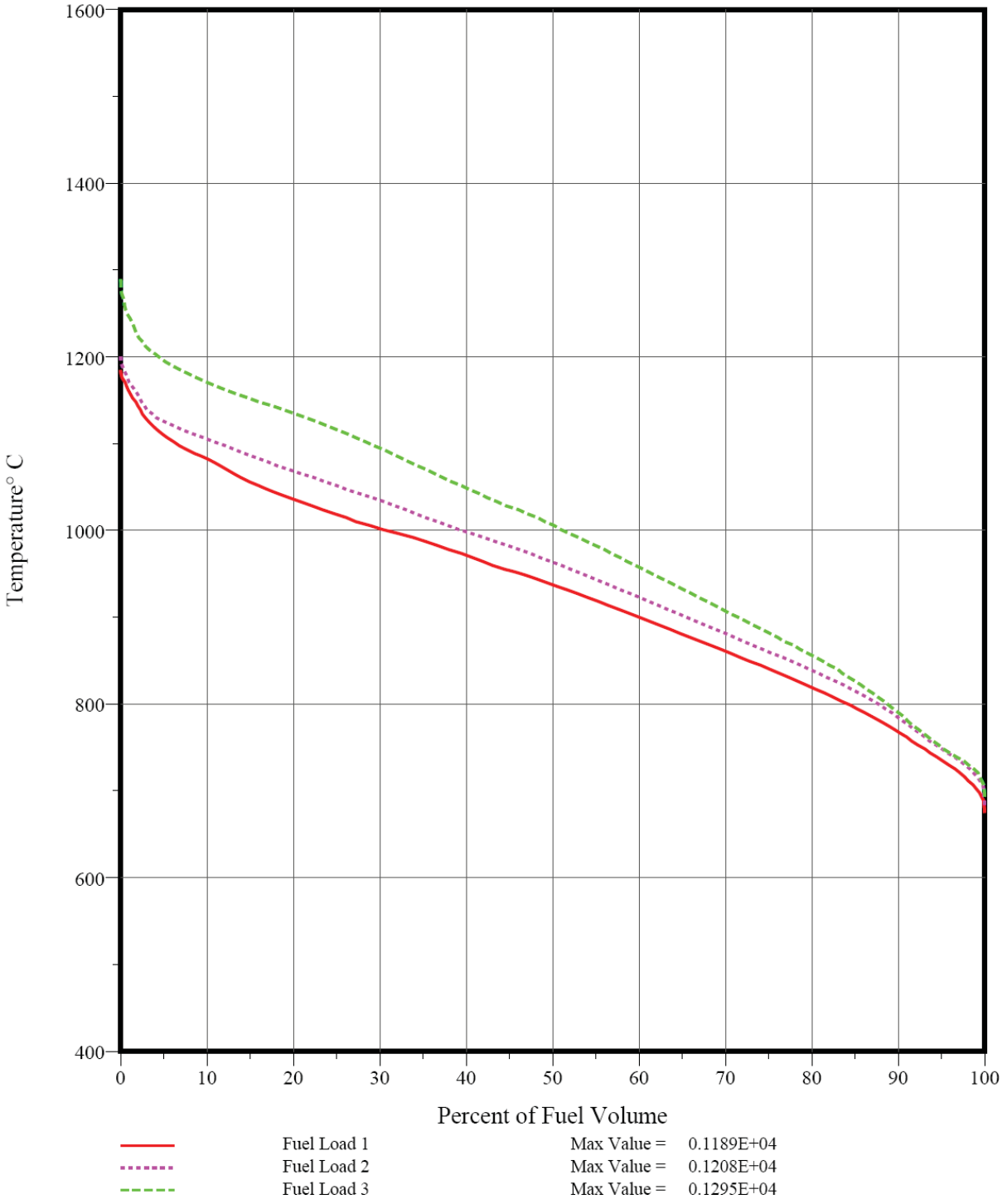

Figure 8-21. Time-Ave. Fuel Temperature Volume Distribution for Seg. 2 (T_{out} = 950C)

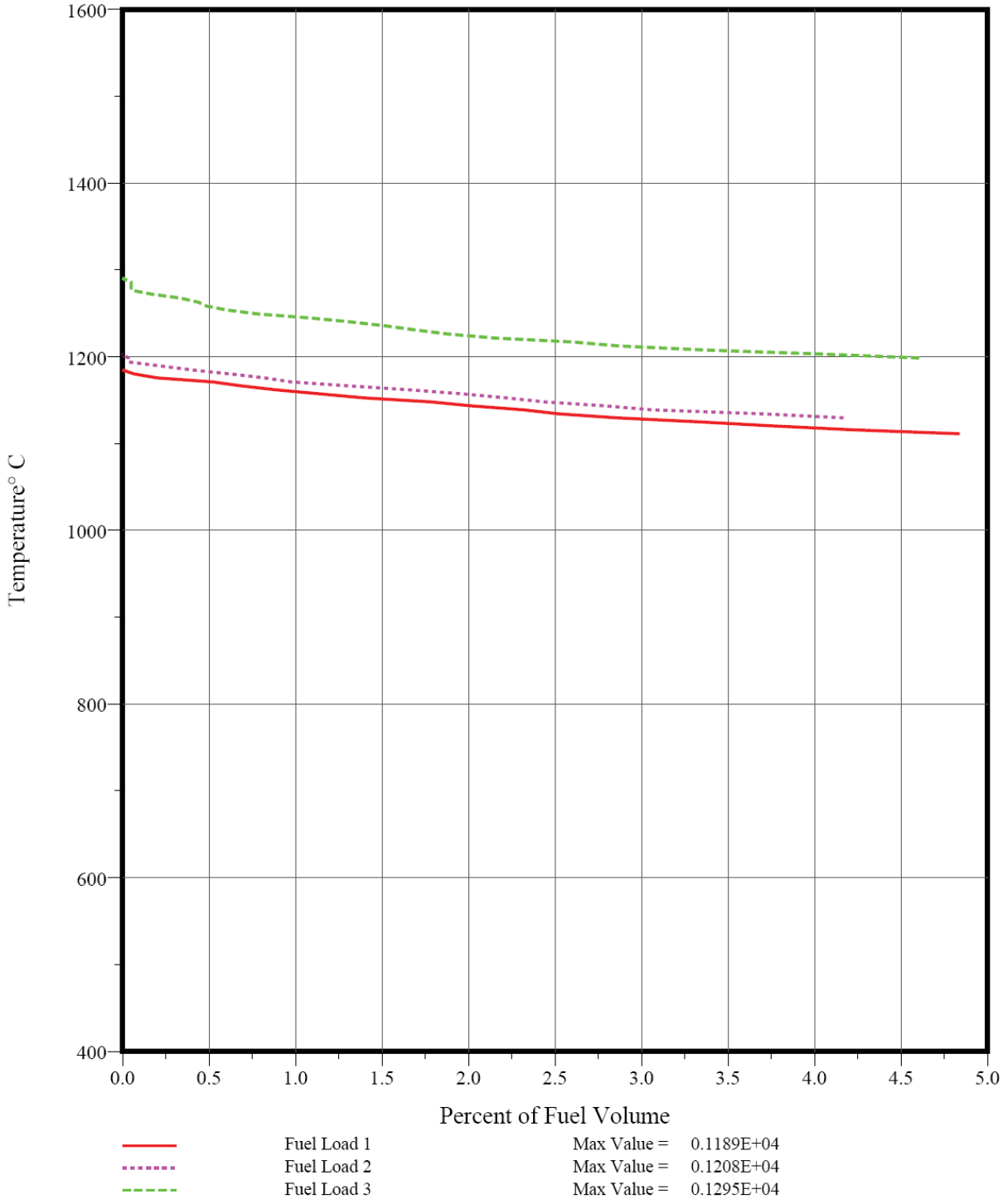

Figure 8-22. Time-Ave. Fuel Temperature Volume Distribution for Seg. 1(0-5%) (T_{out} = 950C)

8.2.2 Fuel Particle Failure

Based upon the burnups, fast fluences, and temperatures calculated by SURVEY/THERM, the fuel performance of Case 7.9 with T_{out} = 950 ^{o}C was calculated by SURVEY/PERFOR using the component models and material property data from FDDM/F.

The core-average SiC failure fraction as a function of operating time for the LEU fissile particle is shown in Figure 8-23. The in-service SiC failure results from HM metal dispersion in the IPyC layer and FP/SiC reactions; kernel migration and SiC thermal decomposition are still negligible. The predicted SiC failure fraction for the fertile particle is slightly lower for the fissile particle since the FP/SiC corrosion failure is burnup dependent (2.0×10^{-4} vs. 8.0×10^{-5}). At this extreme core outlet temperature, FP/SiC corrosion failure is the dominant source of SiC failure. The amount of in-service SiC failure peaks at the end of cycle 3, but it exceeds the as-manufactured SiC defect fraction in all cycles.

With a core outlet temperature of 950 ^{o}C, the performance limits of conventional TRISO particles are being approached. It should be noted that the results reported here are best-estimate results. If the uncertainties in the nuclear, thermal and fuel performance predictions were included, the additional amount of SiC failure would be substantial. In particular, there is a large uncertainty in the FP/SiC corrosion model, especially with regard to the time dependence of the reaction.

Despite the very high peak fuel temperatures for this case, the maximum exposed kernel fraction calculated for the fissile and fertile fuel particles are about 1.7×10^{-5} and 5.6×10^{-6}, respectively; the fissile particle failure is shown in Figure 8-24. The contribution from PV failure of standard particles remains negligible. The failure of MB particles continues to be the main source of exposed kernels. On a core-average basis, most of the fissile particles with missing buffers (~100%) are predicted to fail; however, a significant fraction of the fertile particles with missing buffers are still predicted to survive (>75%). However, the irradiation-induced OPyC failure of particles with failed SiC failure is becoming significant compared to MB particle failure.

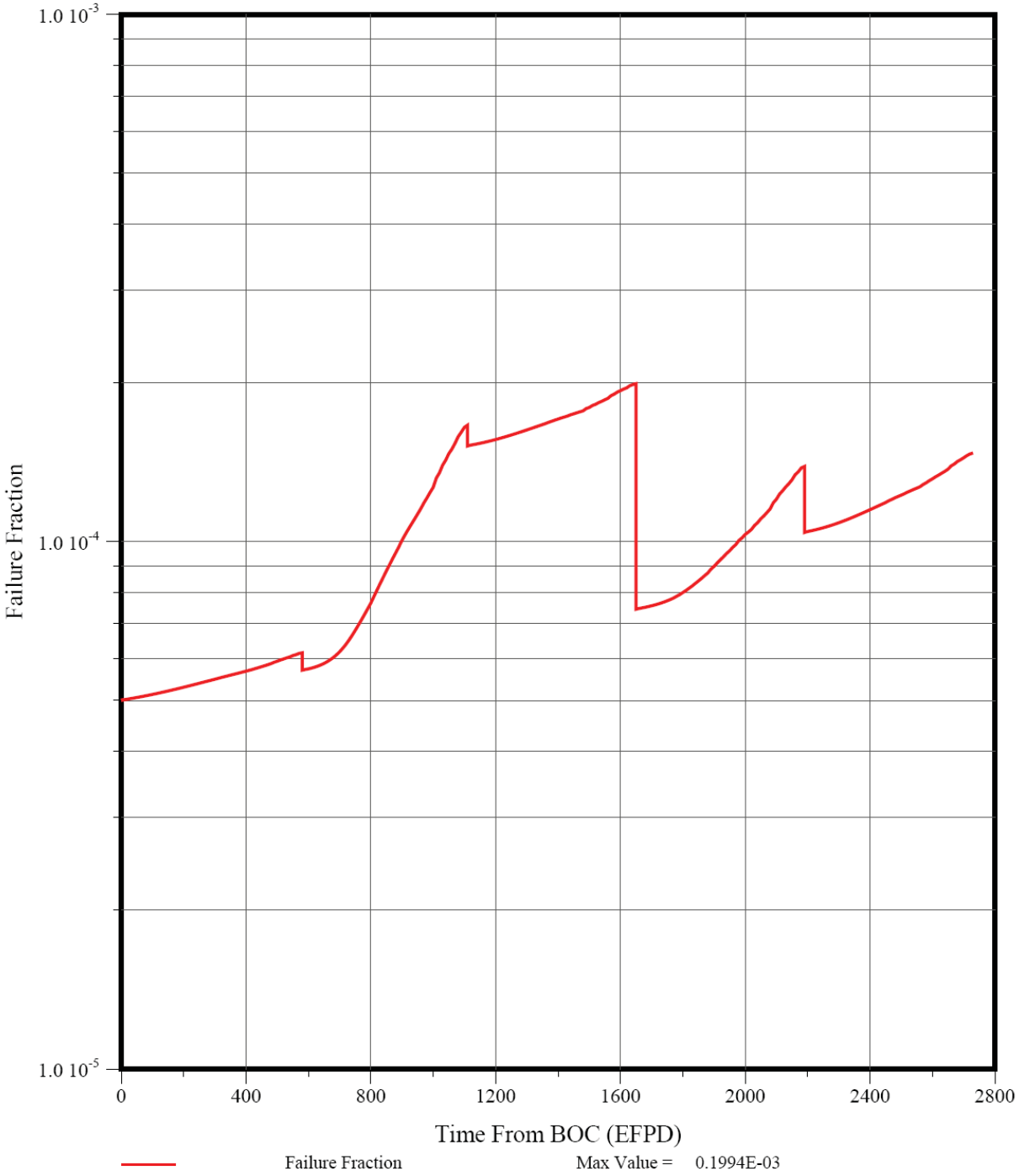

Figure 8-23. SiC Coating Failure Fraction for LEU UCO Fissile Particle (T_{out} = 950C)

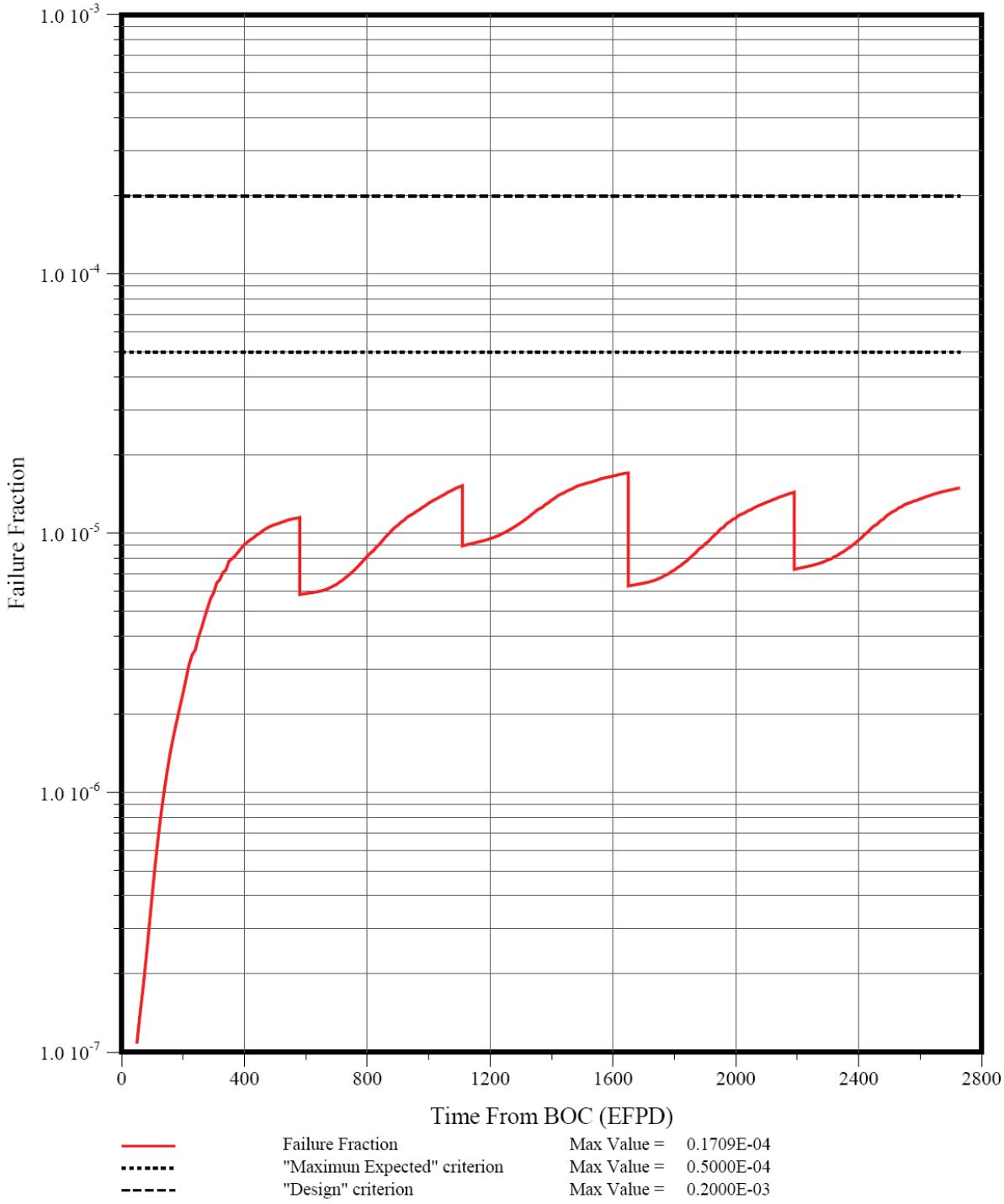

Figure 8-24. Exposed Kernel Fraction for LEU UCO Fissile Particle (T_{out} = 950C)

8.2.3 Gaseous Fission Product Release

The release rate-to-birth rate (R/B) ratios for 2.8-hr Kr-88 and 8-day I-131 were also calculated by SURVEY/PERFOR using the FDDM/F fission gas release models for hydrolyzed UCO fuel. These R/Bs as a function of time are shown in Figures 8-25 and 8-26. The predicted fission gas release is still dominated by the contribution from HM contamination although the relative contribution from failed particles has increased compared to the lower COT cases. It remains low because the predicted exposed kernel fraction is very low despite the very high fuel temperatures associated with COT = 950 ^{o}C. The only effective way of reducing these R/Bs would be to tighten the specification on HM contamination.

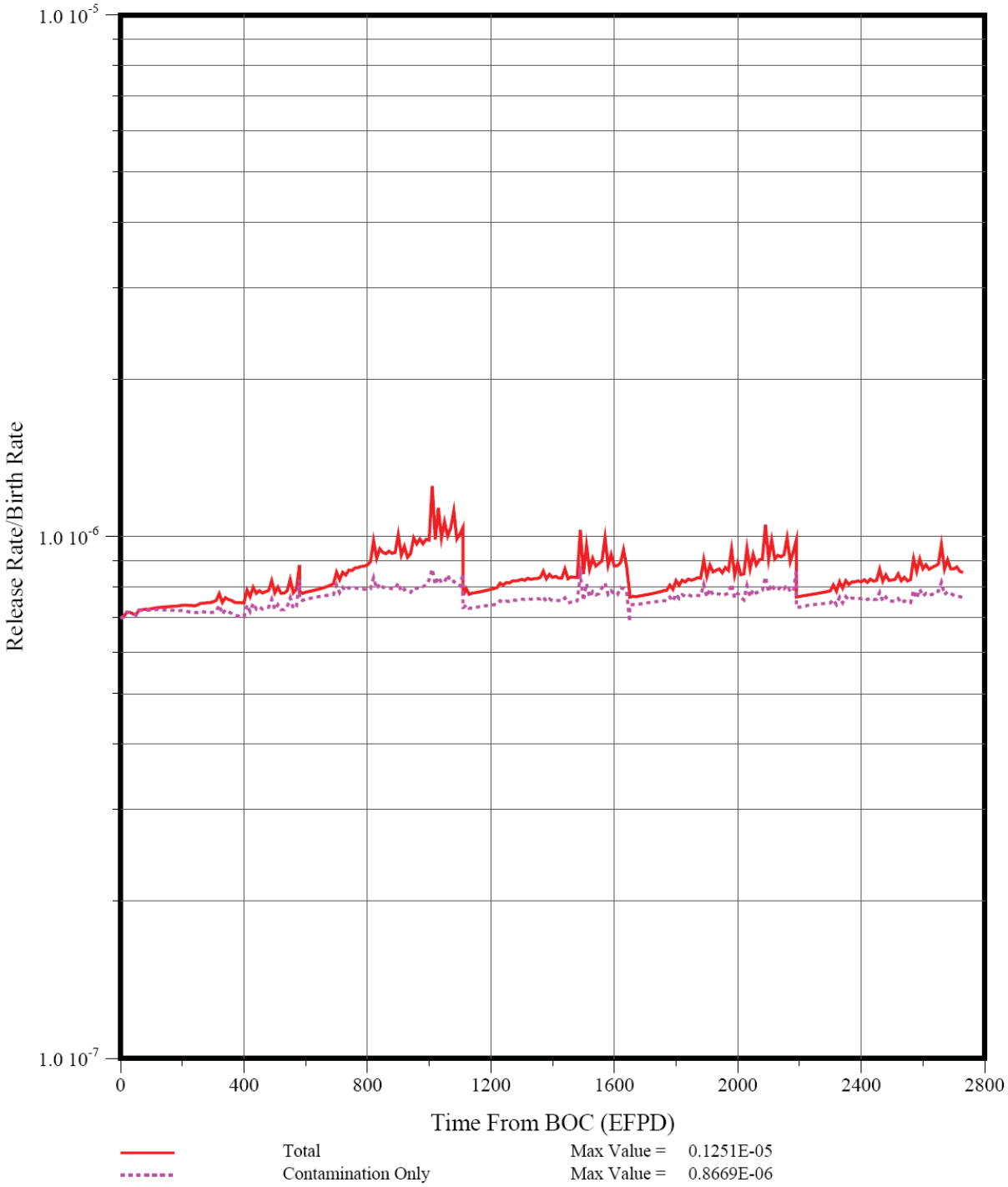

Figure 8-25. Core-Average R/B for Kr-88 (T_{out} = 950C)

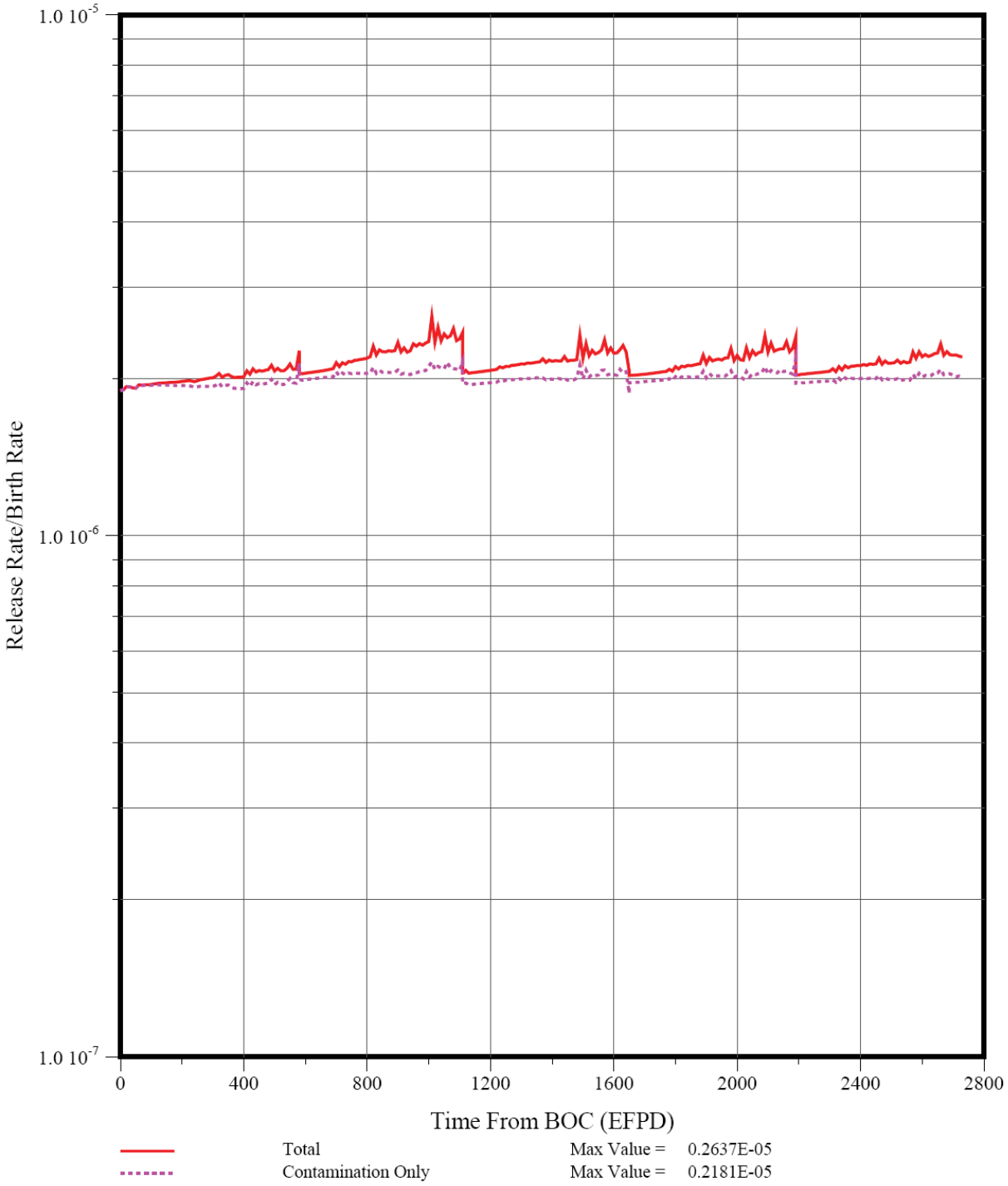

Figure 8-26. Core-Average R/B for I-131 (T_{out} = 950C)

8.2.4 Metallic Fission Product Release

The SURVEY/PERFOR results summarized above were supplied as input to the TRAFIC-FD code which was used to predict the fractional releases of Ag-110m, Cs-137, and Sr-90 for case 7.9 with T_{out} = 950 ^{o}C.

The predicted overall mass balance for 250-day Ag-110m is shown in Figure 8-27, and the cumulative fractional release of Ag-110m into the coolant is shown in Figure 8-28. With T_{out} = 950 ^{o}C, there is essentially no predicted Ag holdup in the matrix and graphite. The Ag fractional release, which is dominated by diffusive release from intact particles, peaks at the end of Cycle 2 during which the fuel temperatures were the highest. The predicted Ag fractional release for T_{out} = 950 ^{o}C is an order of magnitude higher than for the "reference" steam-cycle case (3.0×10^{-3} vs. 3.5×10^{-4}). Use of the FDDM/F Ag-in-SiC diffusivity correlation with T_{out} = 950 ^{o}C would result in at least another order of magnitude increase in the Ag fractional release (as an indication, see the result for T_{out} = 900 ^{o}C in Table 7-1). The predicted Cs fractional release is 3x higher than the provisional limit proposed for a VHTR which is surprisingly good for such a high COT.

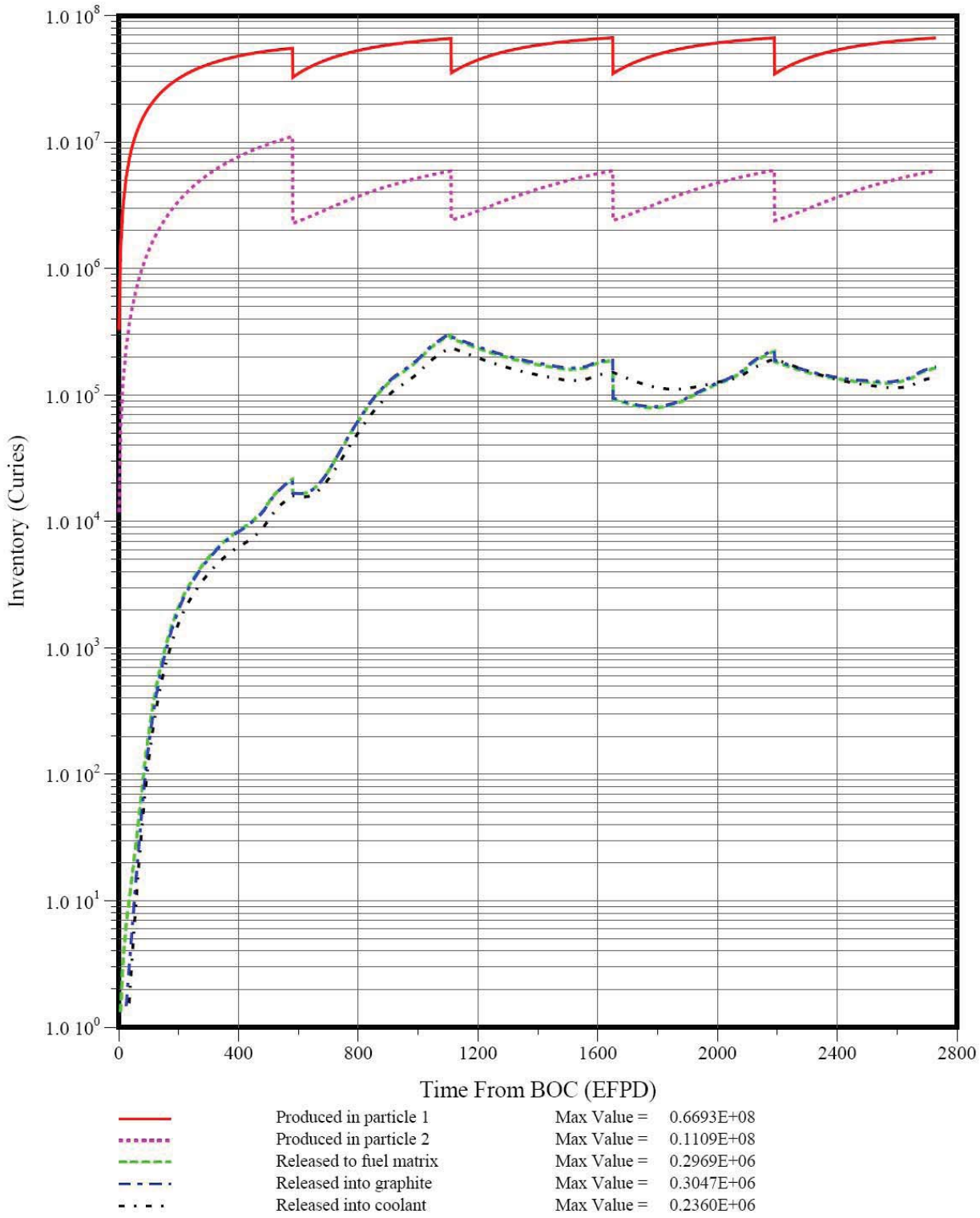

Figure 8-27. "'Full-core" Ag-110m Inventories by Core Material Region (T_{out} = 950C)

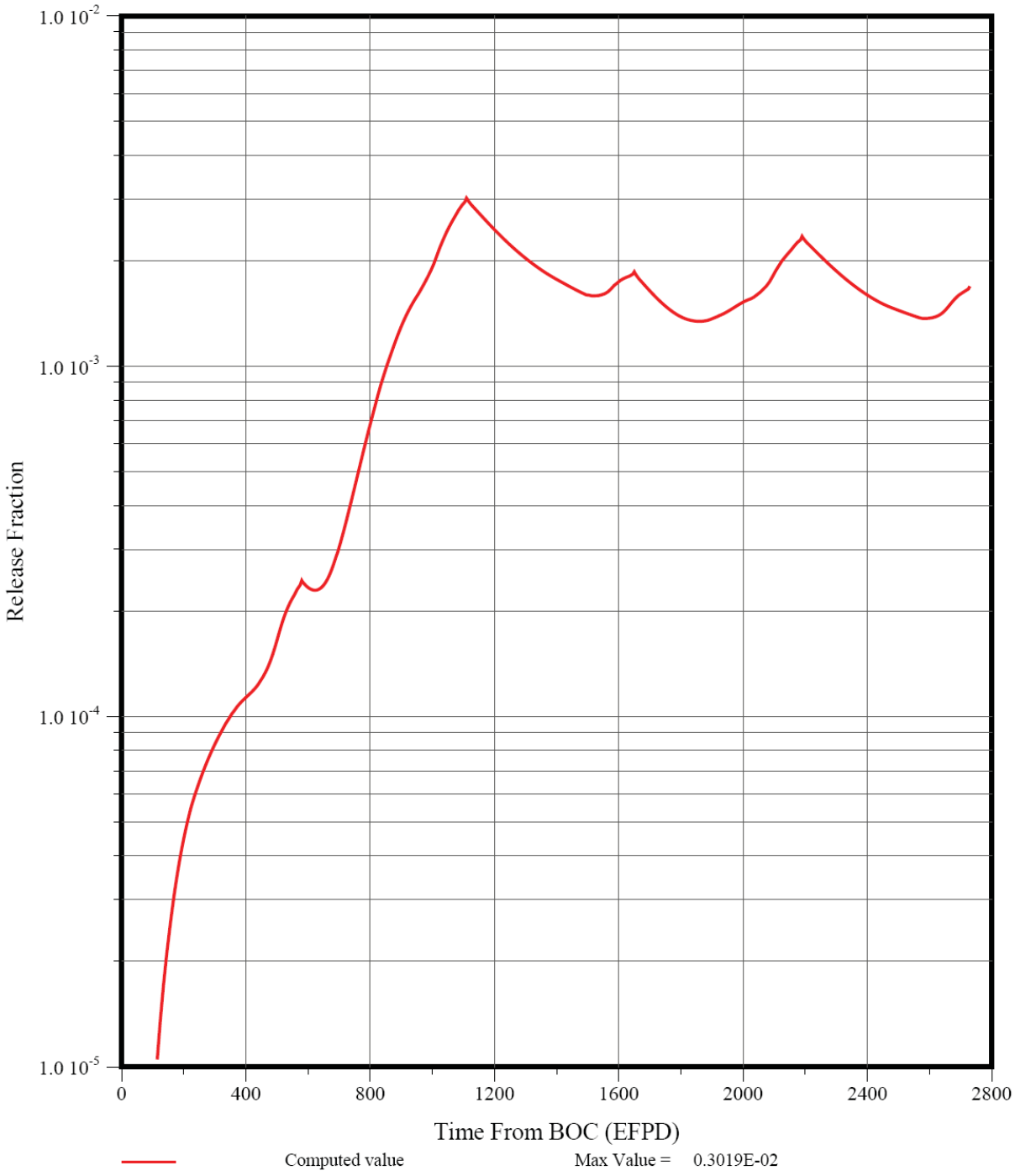

Figure 8-28. Cumulative Fractional Release of Ag-110m (T_{out} = 950C)

The corresponding predicted transport behavior of 30.1-yr Cs-137 is shown in Figures 8-29 and 8-30. In contrast to the predicted Ag behavior, there is still modest Cs holdup by the matrix and graphite; the effect is most obvious in the first cycle. The core temperatures and, consequently, the SiC failure fractions and Cs release rates peak at the end of Cycle 2. Thus, during Cycle 3 and subsequent cycles, the fractional release of "new" Cs remains relatively constant, and the cumulative Cs release to the coolant is dominated by release during the first two cycles. The predicted Cs fractional release for T_{out} = 950 ^{o}C is an order of magnitude higher than for the "reference" steam-cycle case (1.0×10^{-4} vs. 8.7×10^{-6}). The predicted Cs fractional release is 10x higher than the provisional limit proposed for a VHTR.

The predicted transport behavior of 29-yr Sr-90 is shown in Figures 8-31 and 8-32. The Sr behavior is similar to that of Cs except that there is more holdup in the matrix/graphite. The fractional release of Sr-90 for T_{out} = 950 ^{o}C is 71x higher than for the "reference" steam-cycle case (2.4×10^{-6} vs. 3.4×10^{-8}) indicating significantly less matrix/graphite retention. No Sr release limit has been proposed for a VHTR; however, the predicted Sr fractional release of 2.4×10^{-6} is very high by historical standards.

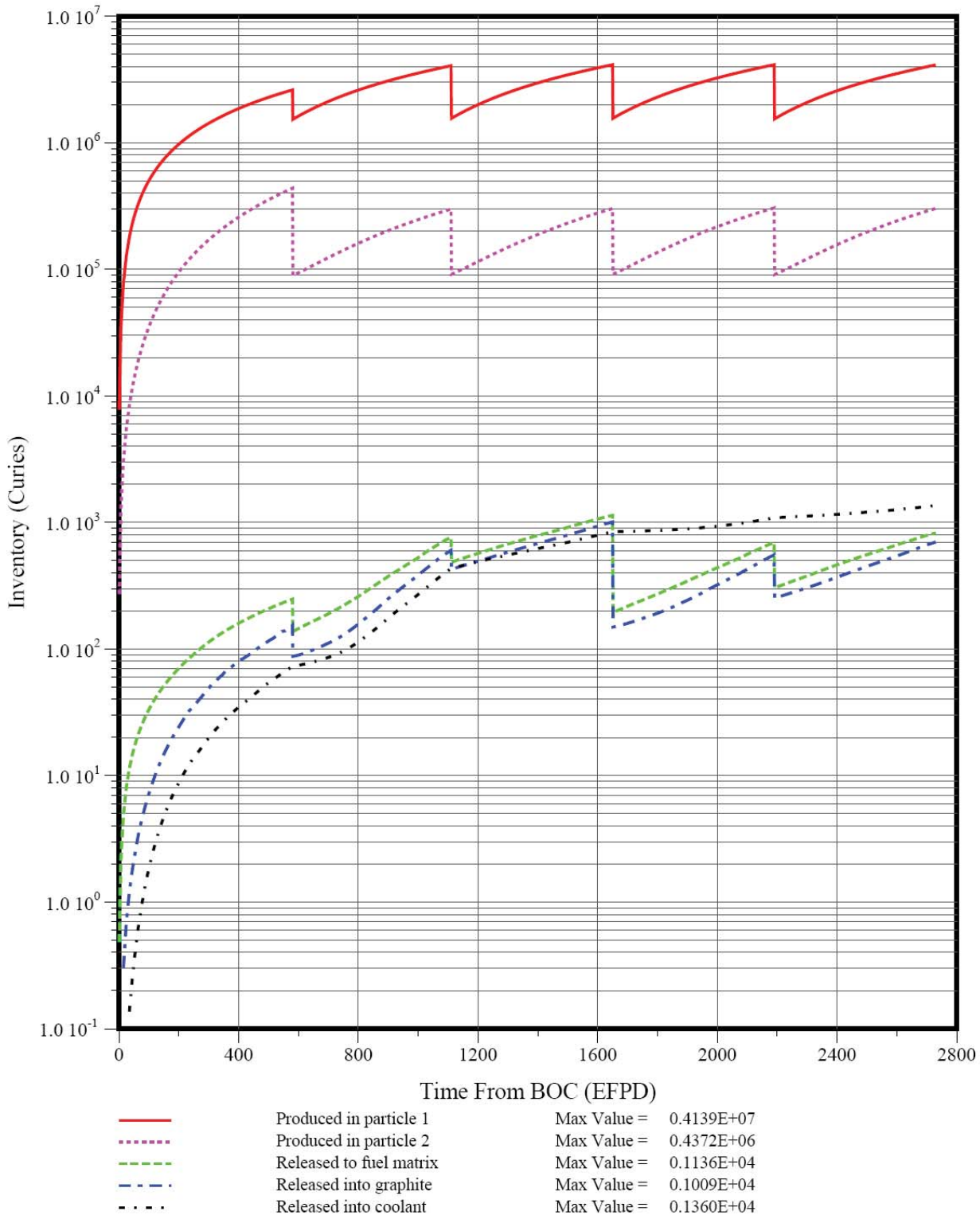

Figure 8-29. "'Full-core" Cs-137 Inventories by Core Material Region (T_{out} = 950C

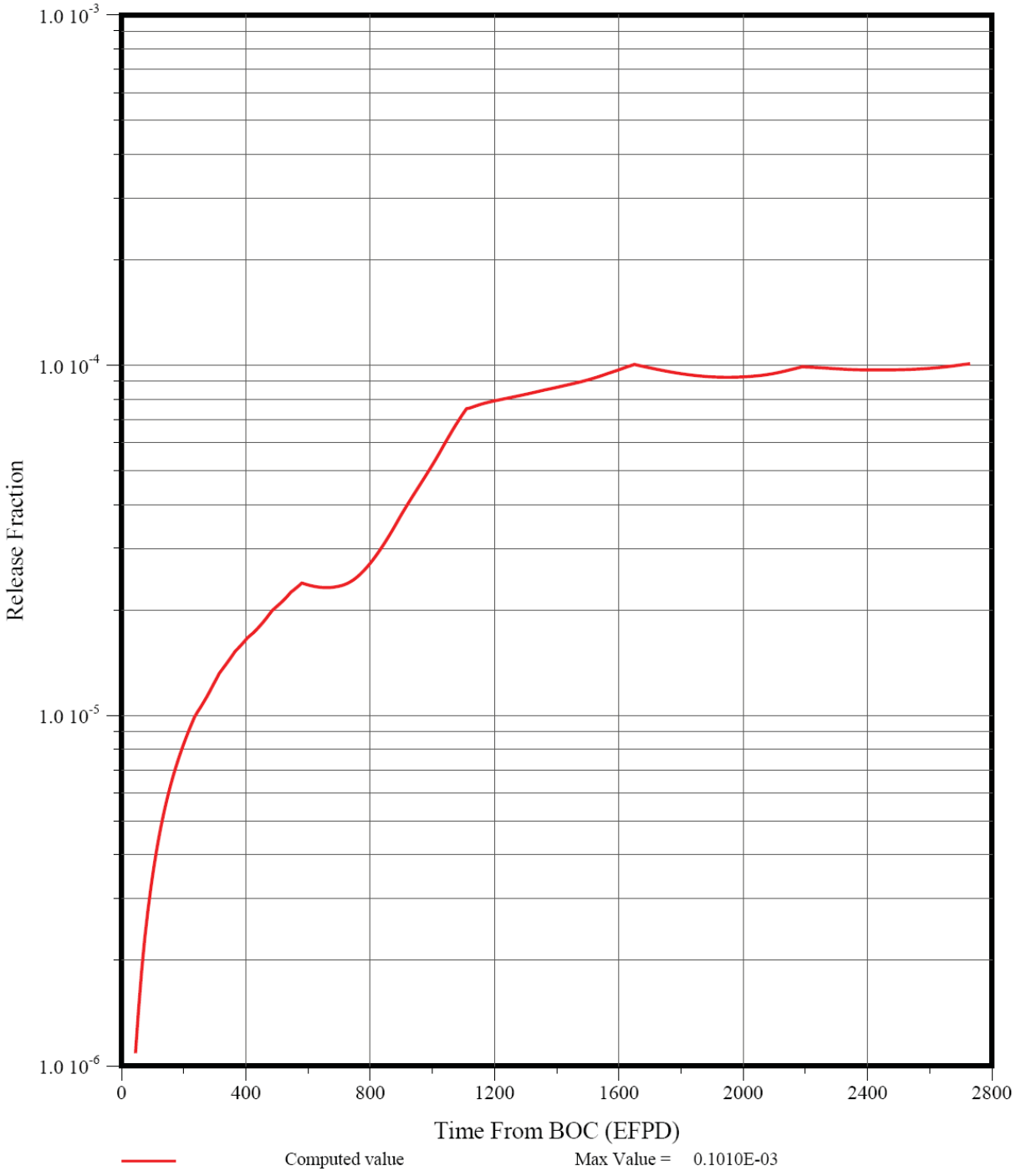

Figure 8-30. Cumulative Fractional Release of Cs-137 (T_{out} = 950C)

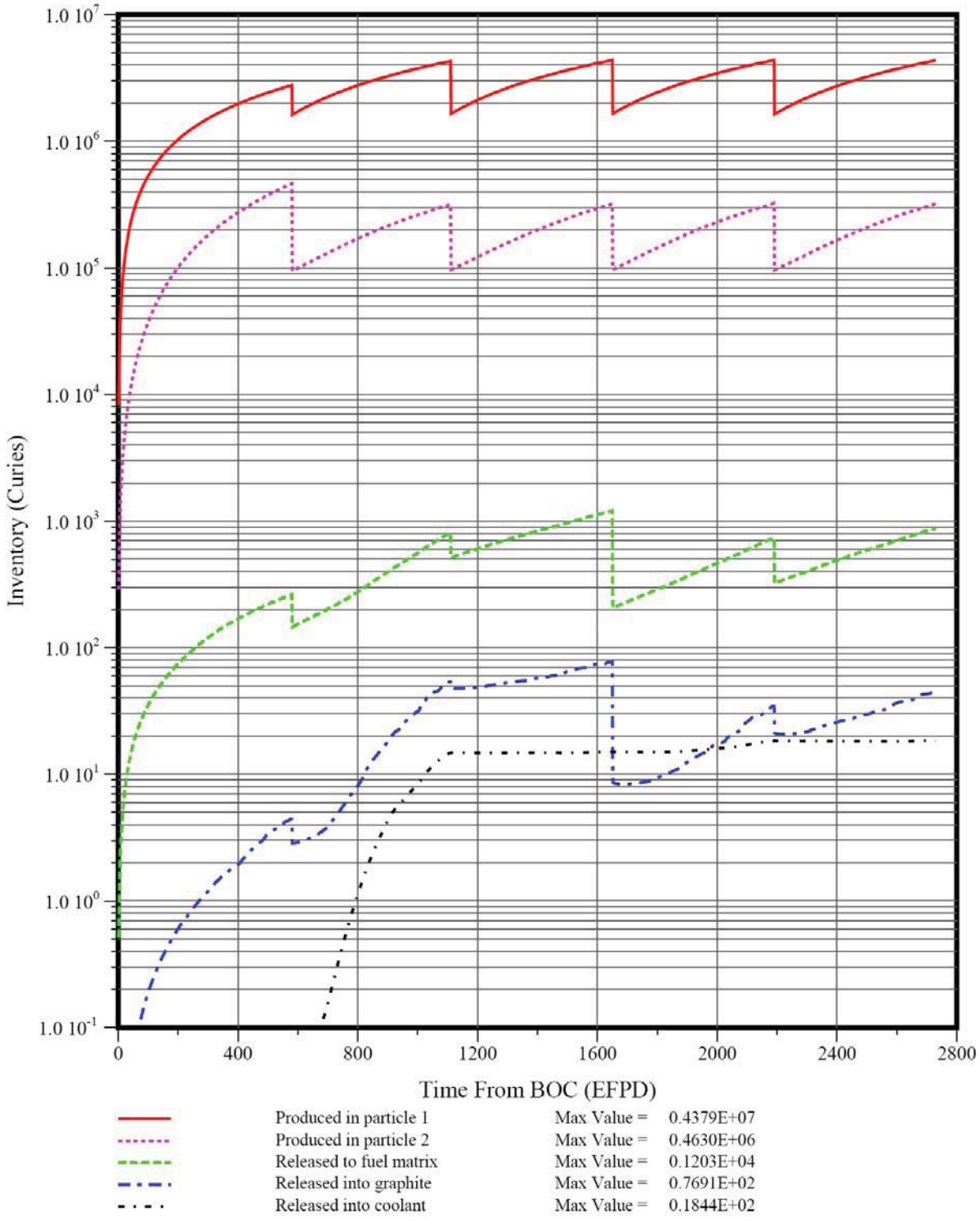

Figure 8-31. "'Full-core" Sr-90 Inventories by Core Material Region (Tout = 950C

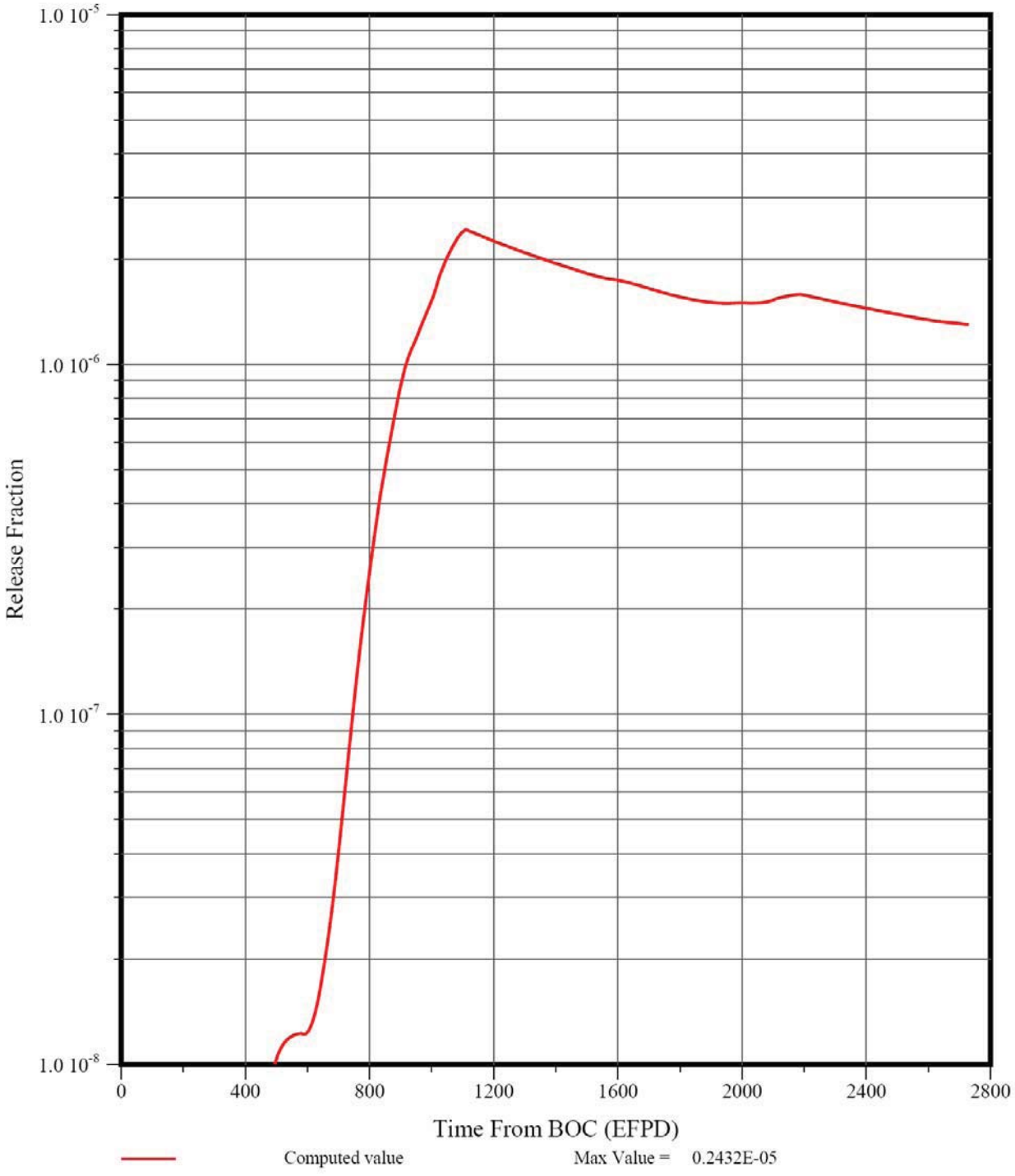

Figure 8-32. Cumulative Fractional Release of Sr-90 (Tout = 950C)

9 IMPLICATIONS FOR NGNP FUEL/FISSION PRODUCT DDNS

Two of the major reasons for preparing this report were: (1) to provide a logical basis to refine, and to revise as necessary, the fuel/fission product Design Data Needs that have been identified for the NGNP [Hanson 2008b], and (2) to provide direction to the NGNP/AGR fuel program to assure that its goals are responsive to the needs of the NGNP Project.

The implications for the NGNP fuel/fission product DDNs are summarized in Table 9-1. No new fuel/fission product DDNs were identified in the process of performing this task. The major conclusions and recommendation are summarized below.

9.1 Fuel Development

1. As the core outlet temperatures are increased and/or the core power density is increased to improve economics, higher fuel and graphite temperatures will result. Very low coating failure fractions are predicted even for core outlet temperatures up to 950 ^{o}C. Despite these low failure fractions, the predicted I-131 R/Bs are still at the "Maximum Expected" limit derived from the PAG thyroid dose limit for core outlet temperatures >~850 ^{o}C because of release from heavy-metal contamination. Likewise, the cumulative fractional release of Cs-137 exceeds the "Maximum Expected" limit for core outlet temperatures >~800 ^{o}C because of reduced Cs retention by the matrix/graphite. Given these trends, the feasibility of tightening the specifications on as-manufactured, HM contamination and SiC coating defects should be investigated.
2. The NGNP/AGR fuel program should have the goal of developing and qualifying fuel manufacturing processes that can meet the "Maximum Expected" fuel quality requirements (rather than the "Design" values) in Table 5-1 on a core segment basis with 95% confidence. The "Design" fuel quality requirements in Table 5-1, which are less stringent, should be applicable to individual fuel compact lots and must also be met at the 95% confidence level.
3. Even under steam-cycle core conditions, a small fraction of the fuel may experience temperatures >1400 ^{o}C, and there is significant uncertainty in the predicted fuel temperatures. Consequently, it is extremely important to perform a margin test as soon as possible (i.e., as is currently planned in one of the AGR-2 capsules). A more reliable fission product/SiC corrosion model is urgently needed, especially with regard to the time dependence.
4. Postirradiation heating tests need to be performed in atmospheres that are characteristic of air ingress and water ingress events rather than exclusively in pure dry helium.

9.2 Fission Product Transport

1. Based upon past experience with the 350 MW(t) steam-cycle MHTGR, large water ingress plus pressure relief will likely be the bounding accident for a steam-cycle MHR. The effects of hydrolysis at high water partial pressures need to be better quantified, and the release

rates of I-131 need to be measured directly. (Plans are currently being developed to include such testing in the NGNP/AGR Fuel Program.)

2. The release of I-131 from failed UCO particles under core heatup conditions needs to be measured as is planned in the NGNP/AGR Fuel Program.
3. The diffusivities of volatile fission metals (Cs, Sr and, to a lesser extent, Ag) in UCO kernels need to be determined as a function of temperature and burnup. The FDDM/F correlations are highly suspect. The planned AGR-3/-4 tests can, in principle, provide the requisite data; however, the tests must be designed such that: (1) the fuel temperatures are maintained nearly constant during the entire irradiation, and (2) the irradiated test fuel must have a broad range of burnups. One means of accomplishing both of these requirements would be to include natural UCO fertile particles in the test.
4. The diffusivities of Ag and Sr in the SiC coatings of US-made TRISO particles need to be measured. Intact UCO particles recovered from the AGR-1 test will provide the first opportunity for making such measurements; however, the process conditions for depositing SiC coatings appear to be evolving which adds uncertainty to the utility of any data derived from AGR-1 particles.
5. The transport properties of volatile metals (Cs, Sr, Ag) in the new fuel-element graphite selected to replace H-451 need to be characterized. The planned AGR-3/-4 tests can, in principle, provide the requisite data regarding the diffusive transport. However, separate laboratory measurements will be required to measure sorption isotherms; the effect of irradiation needs to be included since metal sorptivity increases with increasing fast fluence.
6. The reentrainment of plateout activity under dry and wet conditions needs to be better characterized. Both single-effects and integral tests have been proposed, but no experimental work has been funded to date.
7. The transport of radionuclides, especially iodines, in the VLPC under depressurized core conduction cooldown conditions needs to be characterized. Both single-effects and integral tests have been proposed, but no experimental work has been funded to date.
8. Despite the considerable programmatic challenges, integral tests in an in-pile loop are necessary to convincingly validate the design methods for predicting RN source terms.

Table 9-1. Implications for Fuel/Fission Product DDNs

DDN #	DDN Title	Implications of Present Study	Proposed Resolution
C.07.02	**Fuel Performance**		
C.07.02.01	Coating Material Property Data	Not directly applicable	
C.07.02.02	Defective Particle Performance Data	SiC defects are an important source of fission metal release under steam-cycle conditions	Evaluate practicality and cost penalty of tighter SiC defect specification.
C.07.02.03	Thermochemical Performance Data for Fuel	More reliable FP/SiC corrosion model needed, especially time dependence.	Perform margin test (T ≥ 1400 °C) in AGR-2 test. Perform lab tests with irradiated particles to determine time-dependence of FP/SIC corrosion reactions.
C.07.02.04	Fuel Compact Thermophysical Properties	Thermal conductivity of irradiated fuel compacts needs to be measured	Measure thermal conductivity of unirradiated fuel compacts and irradiated AGR-1 fuel compacts.
C.07.02.05	Normal Operation Fuel Performance Validation Data	High fuel temperatures (T ≥ 1400 °C) should be expected for “reference” steam-cycle MHR design.	Perform margin test (T ≥ 1400 °C) in AGR-2 test. Validate negligible PV failure of standard particles.
C.07.02.06	Accident Fuel Performance Validation Data	Effect of water and air on accident fuel performance urgently needed	Develop the capability to perform postirradiation heating tests in air and water as part of AGR-2 test.
C.07.02.07	Fuel Proof Test Data	None	
N.07.02.08	Irradiation Performance of LEU UO_2 (NFI extended burnup fuel))	Use of German 500-μm UO_2 as the fertile particle (natural or depleted U) in binary designs may be attractive.	Evaluate feasibility of using low-burnup UO_2 as fertile particle. Measure kernel migration in UO_2 particles irradiated in AGR-2.
N.07.02.09	Accident Performance of LEU UO_2 (NFI extended burnup fuel))	Use of German 500-μm UO_2 as fertile particle (natural or depleted U) may be attractive.	Measure CO content of UO_2 particles irradiated in AGR-2

DDN #	DDN Title	Implications of Present Study	Proposed Resolution
C.07.03	**Radionuclide Transport**		
C.07.03.01	Fission Gas Release from Core Materials	Large water ingress plus pressure relief may be bounding accident for steam-cycle MHR.	Develop the capability to perform postirradiation heating tests in air and water as part of AGR-2 test.
C.07.03.02	Fission Metal Effective Diffusivités in Fuel Kernels	Reliable correlations for fission metal diffusivities in UCO kernels, including the effect of burnup, are needed.	Proceed with AGR-3/-4 tests with "designed-to-fail" UCO particles. Design tests for a large range of burnups.
C.07.03.03	Fission Product Effective Diffusivities in Particle Coatings	Ag release highly dependent upon Ag-in-SiC diffusivity (and perhaps Sr release as well).	Include intact UCO TRISO particles as piggy-back samples in AGR-3/-4. Perform postirradiation heating tests on intact particles recovered from AGR-1.
C.07.03.04	Fission Product Diffusivities/Sorptivities in Graphite	Graphite critical barrier to Sr release, and important barrier to Cs release, especially under steam-cycle conditions.	Proceed with AGR-3/-4 tests. Design tests for a large range of temperature and fast fluence.
C.07.03.05	Tritium Permeation in Heat Exchanger Tubes	Not directly applicable; importance will depend upon plant mission.	See [Hanson 2007b]
C.07.03.06	Tritium Transport in Core Materials	Not directly applicable; importance will depend upon plant mission.	See [Hanson 2007b]
C.07.03.07	Radionuclide Deposition Characteristics of Structural Materials	Not directly applicable; determines initial conditions for depressurization and water ingress plus pressure relief accidents.	See [Hanson 2005]
C.07.03.08	Decontamination Protocols for Turbine Alloys	Not applicable	
C.07.03.09	Radionuclide Reentrainment Characteristics for Dry Depressurization	Fractional liftoff during depressurization accidents determines allowable iodine release from the core during normal operation.	Perform single-effect tests in out-of-pile loop (such tests are in AGR Plan but have not been funded to date).

DDN #	DDN Title	Implications of Present Study	Proposed Resolution
C.07.03.10	Radionuclide Removal Characteristics for Wet Depressurization	Fractional removal of I-131 by liquid water and/or steam contributes significantly to offsite doses during water ingress plus pressure relief accidents.	Perform single-effect tests in out-of-pile loop (such tests are in AGR Plan but have not been funded to date).
C.07.03.11	Characterization of the Effects of Dust on Radionuclide Transport	Not directly applicable; importance will depend upon concentration of dust in primary circuit. Significant dust concentrations would increase fractional liftoff during depressurization accidents.	Collaborate with JAEA for further characterization of the dust in HTTR. Perform single-effect tests in out-of-pile loop (such tests are in AGR Plan but have not been funded to date).
C.07.03.12	Fission Product Transport in a Vented Low-Pressure Containment	Retention of iodines in VLPC during depressurized core cooldown accidents important.	Add tests for characterization of RN transport in VLPC to AGR program [Hanson 2007a].
C.07.03.13	Decontamination Efficiency of Pressure Relief Train Filter	Filter in pressure relief train could greatly reduce offsite thyroid doses during water ingress plus pressure relief accidents.	Add characterization of candidate filter media to AGR Plan.
C.07.03.14	Fission Gas Release Validation Data	Validation of design methods for predicting source terms required for plant licensing.	Perform planned AGR-8 test. Conduct integral tests in in-pile loop (programmatically challenging).
C.07.03.15	Fission Metal Release Validation Data	Validation of design methods for predicting source terms required for plant licensing.	Perform planned AGR-8 test. Conduct integral tests in in-pile loop (programmatically challenging).
C.07.03.16	Plateout Distribution Validation Data	Not directly applicable; determines initial conditions for depressurization and water ingress plus pressure relief accidents.	Conduct integral tests in in-pile loop designed for *in situ* blowdown tests and water ingress tests (programmatically challenging).
C.07.03.17	Radionuclide "Liftoff" Validation Data	Validation of design methods for predicting source terms required for plant licensing.	Conduct integral tests in in-pile loop designed for *in situ* blowdown tests and water ingress tests (programmatically challenging).

DDN #	DDN Title	Implications of Present Study	Proposed Resolution
C.07.03.18	Radionuclide "Washoff" Validation Data	Validation of design methods for predicting source terms required for plant licensing.	Conduct integral tests in in-pile loop designed for in situ blowdown tests and water ingress tests (programmatically challenging). High-pressure tests only practical in in-pile loop.
N.07.03.19	Physical and Chemical Forms of RNs Released during Core Heatup	Current design methods assume radionuclides released in elemental form during core heatup accidents.	Add sampling train to furnaces to be used for postirradiation heating tests.
N.07.03.20	RN Sorptivities of VLPC Surfaces	Sorption of radionuclides on fixed surfaces in VLPC assumed to be major removal mechanism during core heatup accidents.	Add measurements of iodine sorptivities on VLPC materials of construction in laboratory apparatus to AGR program.
N.07.03.21	Qualification of Coatings with High Iodine Sorptivity	Not applicable	
N.07.03.22	Validation Data for Predicting RN Transport in VLPC	Validation of design methods for predicting source terms required for plant licensing.	Add simulated VLPC to in-pile RN transport loop.
N.07.03.23	Tritium Release from TRISO Particles	Not directly applicable; importance will depend upon plant mission.	See [Hanson 2007b]
N.07.03.24	Tritium Release from Control Materials	Not directly applicable; importance will depend upon plant mission.	See [Hanson 2007b]
	New DDNs		
	None	No new DDNs identified at this writing.	

10 REFERENCES

[1992 PAG] “Manual of Protective Action Guides and Protective Actions for Nuclear Incidents,” EPA-400-R-92-001, Environmental Protection Agency, May 1992.

Acharya, R. T., GA Internal Memorandum to D. L. Hanson, “Transport of Silver in Particle Coatings and Graphite,” 818:RTA:293:94, November 30, 1994.

[AGR Plan/2] “Technical Program Plan for the Next Generation Nuclear Plant/Advanced Gas Reactor Fuel Development and Qualification Program” INL/EXT-05-00465, Rev. 2, Idaho National Laboratory, July 2008.

Alberstein, D., P. D. Smith, and M. J. Haire, “Metallic Fission Product Release from the HTGR Core,” GA-A13258 (GA-LTR-20), General Atomic, May 1975.

Besmann, T. M., “SOLGASMIX-PV, A Computer Program to Calculate Equilibrium Relationships in Complex Chemical Systems,” ORNL/TM-5775, Oak Ridge National Laboratory, April 1977.

Bolin, J., L. Mascaro, and V. Tangirala, “GT-MHR Preliminary Safety Assessment Report,” DOE-GT-MHR-1 00230, Rev. 0, General Atomics, September 1994.

Cadwallader, G. J., “SORS/NP1 Code Description and User’s Manual,” CEGA-002092, CEGA Corporation, September 1993.

[CNSC], “Standards and Guidelines for Tritium in Drinking Water,” INFO-0766, Canadian Nuclear Safety Commission, January 2008.

Dilling, D., “450 MW(t) MHTGR Source Term and Containment Report,” DOE-HTGR-90321, Rev. 1, Bechtel National, Inc. and General Atomics, San Diego, CA, March 1993.

[DDN Procedure] “DOE Projects Division Program Directive #16: HTGR PROGRAMS - Design Data Needs (DDNs) Interim Procedure,” PD#16, Rev. 1, February 1986.

[DOE-HTGR-86089] ‘Site Personnel Dose Assessment Report Standard HTGR,” Rev. 1, Bechtel National, Inc., December 1989.

Eichenberg, T. W., “RADC Users Manual,” CEGA-002814, Rev. N/C, CEGA Corporation, September 1993.

Eckerman, K. F., et al., “Federal Guidance Report No. 13: Cancer Risk Coefficients for Environmental Exposure to Radionuclides,” EPA 402-R-99-001, Oak Ridge National Laboratory, September 1999.

Ellis, C., A. Baxter, and D. Hanson, ”Final Report – NGNP Core Performance Analysis, Phase 1,” 911160, Rev. 0, General Atomics, March 2009.

[EPRI 2001] “EPRI NMAC Maintainability Review of the International Gas Turbine Modular Helium Reactor Power Conversion Unit,” 1001231, Electric Power Research Institute, February 2001.

[EPRI 2002] “EPRI NMAC Maintainability Review of the Pebble Bed Modular Reactor Demonstration Plant,” 1003386, Electric Power Research Institute, May 2002.

[FDDM/F] Myers, B. F., "Fuel Design Data Manual," 901866, Issue F, General Atomics, August 1987 *(GA Proprietary Information)*.

[GA 2009a] Ellis, C., A. Baxter, and D. Hanson, “Interim Report – NGNP Core Performance Analysis, Phase 2,” Rev. 0, General Atomics, September 2009a.

[GA 2009b] “Final Report – NGNP Core Performance Analysis, Phase 2,” 911184, Rev. 0, General Atomics, September 2009b.

[GA SRM] Labar, M., D. Phelps, and J. Saurwein, “System Requirements Manual,” 911102, Rev. 0, General Atomics, March 2007.

[GA PCDSR] “NGNP and Hydrogen Production Preconceptual Design Studies Report,” 911107, Rev. 0, General Atomics, July 2007.

Haire, M.J., and D.W. McEachern, "Gaseous Radioactivity Levels in the Primary Coolant of an HTGR," GA-A12946 (GA-LTR-14), General Atomic, October 1974.

Hanson, D. L., "Plateout Criteria for the 2240 MW(t) HTGR SC/C," 907003, Rev. 1, GA Technologies, September 1983.

Hanson, D. L., GA Internal Memorandum to A. J. Neylan, “Revised Core Release Criteria for Commercial GT-MHR,” 818:DLH:143:94, Rev. 1, August 1, 1994.

Hanson, D. L., “Logic for Deriving Fuel Quality Specifications,” PC-000498, Rev. 0, General Atomics, March 2001.

Hanson, D. L., “Plate-Out Phenomena in Direct-Cycle High Temperature Gas Reactors,” 1003387, Electric Power Research Institute, June 2002b.

Hanson, D. L., and J. J. Saurwein, “Development Plan for Advanced High Temperature Coated-Particle Fuels,” PC 000513, Rev. 0, General Atomics, December 2003.

Hanson, D. L., “Requirements for an In-Pile Fission Product Transport Loop,” PC 000522, Rev. 0, General Atomics, December 2004.

Hanson, D. L., “Test Plan for Single-Effects, Fission Product Plateout and Liftoff Tests,” PC-000526, Rev. 0, General Atomics, April 2005.

Hanson, D. L., “TRITGO Code Description and User’s Manual,“ GA Document 911081, Rev. 0, General Atomics, February 2006a.

Hanson, D. L., “Review of Tritium Behavior in HTGRs,” PC-000535, Rev. 0, General Atomics, May 2006b.

Hanson, D. L., and J. M. Bolin, “Radionuclide Transport in a Vented Low-Pressure Containment,” PC-000541, Rev. 0, General Atomics, April 2007a.

Hanson, D. L., “Test Plan for Characterizing Tritium Transport in a VHTR,” PC-000550, Rev. 0, General Atomics, December 2007b.

Hanson, D., “NGNP Contamination Control Study,” 911117, Rev. 0, General Atomics, April 2008a.

Hanson, D. L., “Reconciliation of NGNP DDNs with NRC PIRTs,” Rev. 0, General Atomics, September 2008b.

Hanson, D. L., “Test Plan to Characterize Radionuclide Transport in a Vented Low-Pressure Containment,” Rev. 0, General Atomics, September 2008c.

Hoot. C. G., et al., “450 MW MHTGR Safety Consequence Assessment,” DOE-HTGR-90229, Rev. 0, General Atomics, San Diego, CA, September 1991.

[HTGR-85-022], “Procedures and Guidelines for Functional Analysis,” General Atomics, June 1985.

Jovanovic, V., "Radionuclide Design Criteria for the 2240 MW(t) HTGR SC/C," 906349, Rev. 3, April 1984.

Jovanovic, V., “Radionuclide Design Criteria for the MHTGR Primary Coolant Circuit,” 908095, Rev. 4, GA Technologies, June 1989.

Jovanovic, V., “Radionuclide Control for MHTGR,” DOE-HTGR-88245, Rev. 1, General Atomics, August 1989.

Labar M., and D. Carosella, “Nuclear Heat Supply System Point Design Study for NGNP Conceptual Design,” Report 911167, Rev. 0, General Atomics, April 2009.

Martin, R. C., “Compilation of Fuel Performance and Fission Product Transport Models and Database for MHTGR Design,” ORNL/NPR-91/6, Oak Ridge National Laboratory, October 1993.

Medwid, W., and A. Gillespie, “COMEDIE BD-1 Test Evaluation Report,” DOE-HTGR-88552, Rev. 0, General Atomics, October 1993.

Moormann, R., and K. Verfondern, “Methodik umfassneder probabilistischer Sicherheitsanalysen fuer zunkuenftige HTR-Anlagenkonzepte. Ein Statusbericht (Sand 1986); Band 3: Spaltproduktfreisetzung,” Juel-Spez-388/Bd. 3, Kernforschungsanlage Juelich, Mai 1987 *(in German)*.

Moormann, R., “A Safety Re-Evaluation of the AVR Pebble Bed Reactor Operation and its Consequences for Future HTR Concepts,” Proceedings of the 4th International Topical Meeting on High Temperature Reactor Technology (HTR2008), September 28-October 1, 2008, Washington, DC USA.

Munoz, S. P., “Fuel Product Specification [for the GT MHR],” DOE-GT-MHR-100209, Rev. 0, General Atomics, May 1994.

Myers, B. F., "Update of Fuel Performance Data and Models,” 908721, Rev. 0, GA Technologies, February 1986 (GA Proprietary Information).

Nabielek, H., et al., “Performance Limits of Coated Particle Fuel; Part III: Fission Product Migration in HTR Fuel,” DP-828 (Pt. 3), Dragon Project, June 1974.

[NGNP SRM] “Next Generation Nuclear Plant System Requirements Manual,” INL/EXT-07-12999, Rev. 2, Idaho National Laboratory, March 2009.

[NGNP TDP] Hanson, D. L., “NGNP Umbrella Technology Development Plan,” PC-000543, Rev. 0, General Atomics, July 2007.

Olsen, B. E., “Functional Analysis Worksheets - FAW's,” PC-000269, Rev. 0, GA Technologies, February 1988.

[PC-MHR] “MHTGR Plutonium Consumption Study Phase II Extension FY-94 Final Report,” GA/DOE-186-94, September 1994.

Pelessone, D., “PISA, A Coupled Thermal-Stress Code for the Mechanical Analysis of Irradiated Fuel Particles – User’s Manual,” CEGA-002550, Rev. 0, CEGA Corporation, August 1993.

Pfremmer, R. D., “Software Description and User’s Manual for GT-MHR Fuel Performance Code, SURVEY,” GA Document 911009/0, General Atomics, April 2002.

[PSID] “Preliminary Safety Information Document for the Standard MHTGR,” Volumes 1-6, HTGR-84-024, Amendment B, August 1992.

Reichert, P., “”URS-WD Informal Evaluations of Selection of Dose Conversion Factors for Use in the Determination of EPA PAG Compliant Source Terms,” Letter Report, April 13, 2009.

Richards, M. B., “Reactor Containment, Embedment Depth, and Building Functions Study,” 911128, Rev. 0, General Atomics, September 2008.

Shenoy, A. S., "GT-MHR Conceptual Design Description Report,” 910720, Rev. 1, General Atomics, July 1996.

Silady, F. A., “Closeout Report for the Gas Turbine-Modular Helium Reactor (GT-MHR) Program,” PC-000467, Rev. 0, General Atomics, September 1996.

[SOW-6795] “General Atomics FY09-2 Conceptual Design Work for the NGNP with Hydrogen Production,” Rev. 0, Idaho National Laboratory, January 12, 2009.

Tangirala, V. and W. Betts, “OXIDE-4 Software Design Description and User's Manual,” CEGA 001871, Rev. 0, CEGA Corporation, September1993.

[TECDOC-978] “Fuel Performance and Fission Product Behavior in Gas Cooled Reactors,” International Atomic Energy Agency, November 1997.

Tzung, F., “TRAFIC-FD, A Finite Difference Program to Compute Release of Metallic Fission Products from an HTGR Core: Code Theory and Users Manual,” CEGA-001904, CEGA Corporation, September 1992a.

Tzung, F., “COPAR-FD, A Finite Difference Program to Compute Release of Metallic Fission Products from Coated Particles: Code Theory and Users Manual,” CEGA-002098, Rev. N/C, CEGA Corporation, September 1992b.

Verfondern, K., and H. Nabielek, “Fission Product Release from HTGR Fuel under Core Heatup Accident Conditions,” Proceedings of the 4th International Topical Meeting on High Temperature Reactor Technology (HTR2008), September 28-October 1, 2008, Washington, DC USA.

Wells, P., and K. Fleming, “Reactor Building Functional and Technical Requirements and Evaluation of Reactor Embedment,” NGNP-NHS 100-RXBLDG, Rev. 0, Westinghouse Electric Company, September 2008.

[Work Plan] “NGNP Fuel Performance Requirements and Fuel Product Specification Basis Report,“ General Atomics, February 2009.

APPENDIX A.
FUNCTIONAL ANALYSIS FOR THE STEAM-CYCLE MHTGR

A.1. INTEGRATED APPROACH

Top-level radionuclide control requirements, such as offsite dose limits and occupational exposure limits, are defined by both plant regulators and (potential) users. Lower-level requirements are then systematically derived using a top-down functional analysis methodology. As part of the 350 MW(t) steam-cycle MHTGR program supported by DOE in the 1980s, an Integrated Approach was developed for establishing and defending a well-developed nuclear plant design [HTGR-85-022 1985].

As described in [PSID 1992], the Integrated Approach is a systematic systems engineering process utilized to develop the functions, requirements, and design selections to achieve all of the top-level regulatory criteria and the user requirements. The analysis tools include the use of functional analysis, reliability evaluations probabilistic risk assessments, trade studies, and engineering analyses.

A key element of the Integrated Approach is functional analysis. Functional analysis is a process of systematically ordering, from the top down, the many functions which must be achieved to meet the overall goals. Figure A-1 shows the starting point for the functional analysis, namely the four Goals identified to achieve safe, economic power:

Goal 1: Maintain Safe Plant Operation

Goal 2: Maintain Plant Protection

Goal 3: Maintain Control of Radionuclide Release

Goal 4: Maintain Emergency Preparedness

Goal 1 deals with scheduled operations such as energy production, plant shutdown for scheduled maintenance, ISI, etc. Goal 2 deals with unscheduled events, such as steam generator tube plugging, which impact plant investment and availability. Goal 3 deals with unscheduled events, such as primary coolant leaks, which may involve the release of radionuclides and hence may impact the health and safety of the public. Goal 4 establishes an emergency preparedness plan and procedures for public protection in the event of an accident. The fuel design must satisfy the requirements deriving from all of four top-level goals. In practice, the requirements derived from Goal 3 are bounding on the fuel design.

A.1.1 Functional Trees

Figure A-2 shows a typical expansion of a Goal, in this case Goal 3, Maintain Control of Radionuclide Release. As illustrated in this figure, each subsequent level of subfunctions is developed by examining the next upper level function and answering the question, “How is the function to be achieved?" In such a manner, a "tree" of increasing levels of detail is defined until a specific design selection results. The extensive functional trees developed for the steam-cycle MHTGR are documented in [FA Report 1988].

A.1.2 Functional Analysis Worksheets

Functional Analysis Worksheets (FAWs) are used as a road map to the development of a complete plant design. These FAWs present, in a prescribed format, the bounding requirements and design selections that satisfy the functions and provide a brief means of recording references that support the requirements, analyses, trade studies and design selections. In principle, FAWs are to be prepared for each of the boxes in the functional trees. Where necessary, particularly in the early design development phase, engineering judgment (EJ) may have to be listed as the basis for a requirement or as a reference for an Analysis/Trade Study leading to a design selection until a more appropriate reference can be cited. The Functional Analysis Worksheets that were generated for the steam-cycle MHTGR are collected in [Olsen 1988].[57] [Olsen 1988] does not contain a FAW for every box that is included in the functional trees [FA Report 1988]; somewhat surprisingly, it does not include any FAWs for Goal 4.

A sample FAW for Function 3.1.1.2, “Control Radiation Transport,” is reproduced below [Olsen 1988]. For this FAW, the “REQUIREMENTS” are to meet the PAGs at the EAB for a spectrum of accidents. A number of “ANALYSES/TRADE STUDIES” are invoked, including the Fuel Design Data Manual/Issue F (there is a master list of the references cited in the FAW in [Olsen 1988]). A number of “ASSUMPTIONS/COMMENTS” are made regarding the expected RN decontamination factors for the three classes of bounding accidents defined in Section 6.2.1: (1) rapid depressurization, (2) core conduction cooldown, and (3) water ingress plus pressure relief. The resulting “DESIGN SELECTIONS” are limits on RN release from the core during normal operation and on incremental RN releases from the core during core conduction cooldown and water ingress plus pressure relief events. The contents of FAW were summarized in Sections 4.1.1 through 4.1.3. (All of the information presented in Section 4 is elaborated in the various FAWs related to RN control.)

A.2 REFERENCES

[HTGR-85-022], “Procedures and Guidelines for Functional Analysis,” General Atomics, June 1985.

[FA Report 1988] “Functional Analysis Report, Standard Modular HTGR Plant,” DOE-HTGR-86002, Rev. 5, General Atomics, October 1988.

Olsen, B. E., “Functional Analysis Worksheets - FAW's,” PC-000269, Rev. 0, General Atomics, February 1988.

[57] Surprisingly, [FA Report 1988] and [Olsen 1988] do not cite each other.

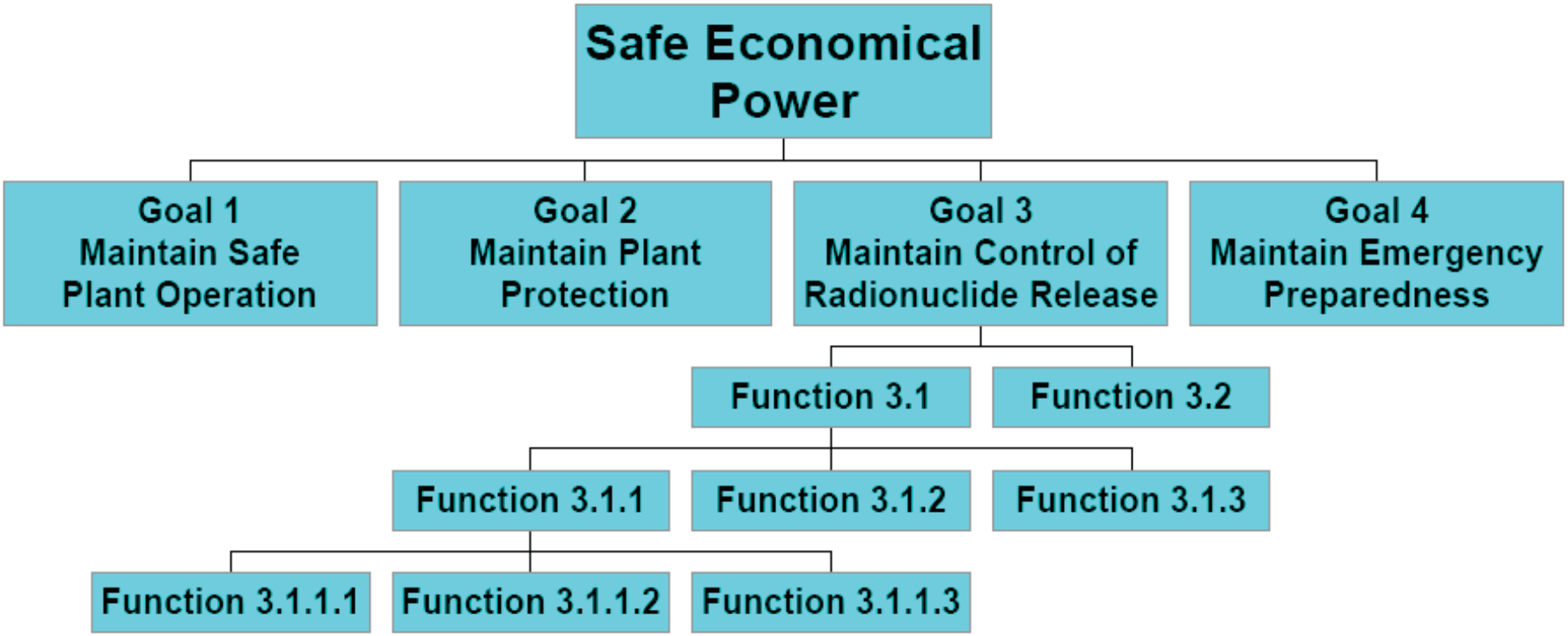

Figure A-1. Integrated Approach: Top-Level Goals

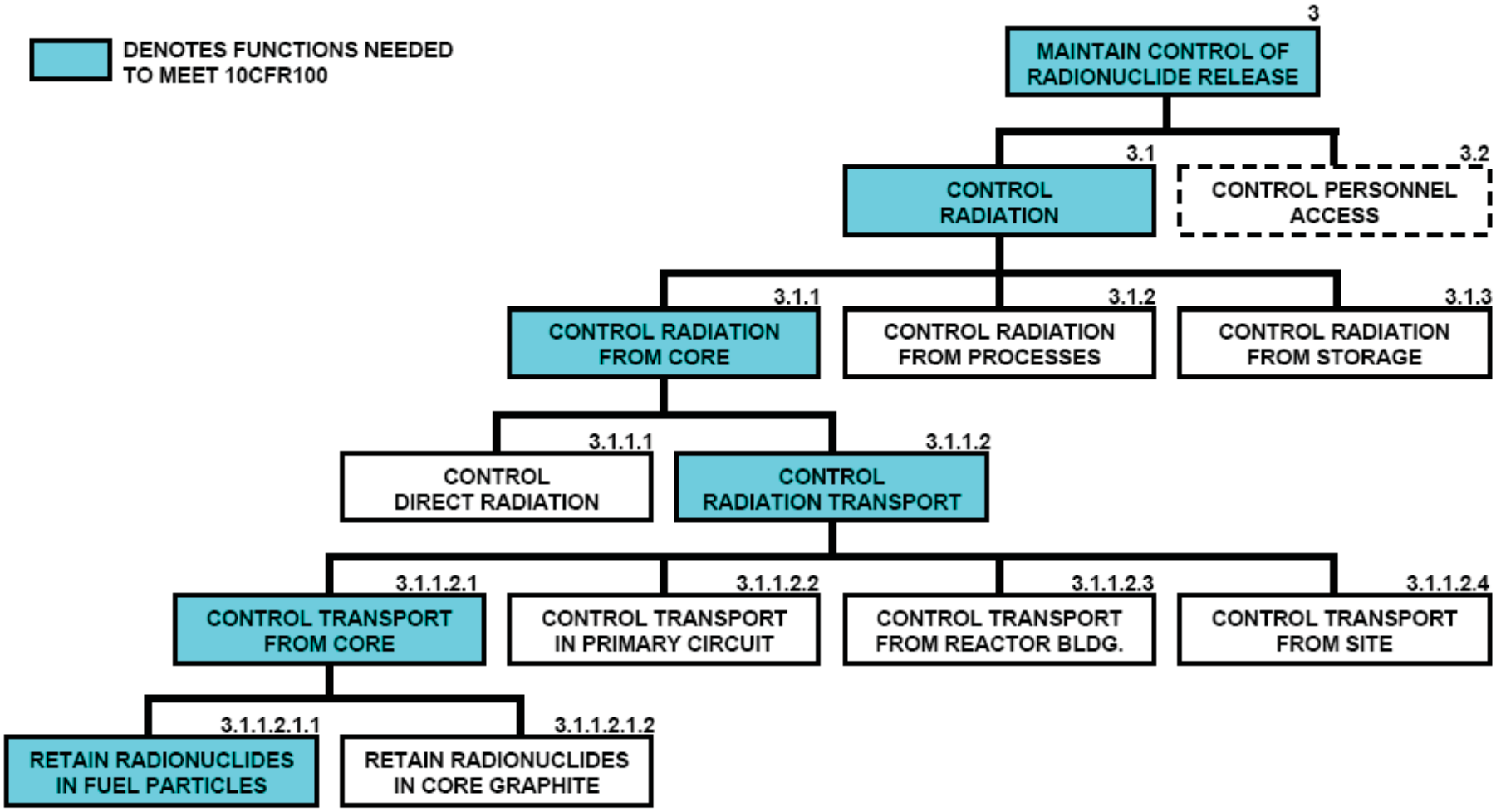

Figure A-2. Functional Tree: Goal 3. Maintain Control of RN Release

[190-8]

FUNCTIONAL ANALYSIS WORKSHEET

FUNCTION NO.: 3.1.1.2 DATE: 1/6/88 GA

FUNCTION: Control Radiation Transport PROJ: MHTGR

REFERENCE REQUIREMENTS (R)

F3.1 (DS1) 1. Limit radionuclide releases from plant during short-term (0-2 h) and long-term (0-30 day) accidents:

Nuclide	PAG (User) Limits (Ci) Short-Term	Long-Term	10CFR100 (Reg) Limits (Ci) Short-Term	Long-Term
Kr88	≤[170]	≤TBD	≤[3400]	≤TBD
Xe133	≤[TBD]	≤[2300]	≤[TBD]	≤[46,000]
I131	≤[2.6]	≤[29]	≤[78]	≤[870]
Sr90	≤[0.1]	≤[1.2]	≤[3]	≤[36]
Ag110m	≤TBD	≤TBD	≤TBD	≤TBD
Cs137	≤TBD	≤TBD	≤TBD	≤TBD

F3.1.1 (R1) 2. Sufficient reliability shall be provided to assure that the probability of exceeding the PAG limits in R1 above is $<5 \times 10^{-7}$ per plant year. (User)

F3.1.1 (R2) 3. Sufficient reliability shall be provided to assure that the probability of exceeding the 10CFR100 limits in R1 above (or appropriate fractions thereof) is $<1 \times 10^{-4}$ per plant year. (Reg.)

ANALYSES/TRADE STUDIES (A/TS)

Ref. 20 1. MHTGR radionuclide design criteria. (R1)

Ref. 476 2. Fuel Design Data Manual/Issue F. (R1)

Ref. 10 3. Decay heat removal evaluations. (R1, R)

Ref. 19 4. Safety Risk Assessment. (R1, R2)

Ref. 314 5. Accident radiological consequence analysis. (R1)

Ref. 124 6. BNI interim radiological dose evaluation for SV concepts. (R1)

Ref. 128 7. Fuel performance limits from top-level goals. (R1)

Ref. 316 8. Liftoff data base. (R1)

[190-9]

FUNCTIONAL ANALYSIS WORKSHEET

FUNCTION NO. 3.1.1.2 (continued)

Ref. 360 9. Licensing basis events for the MHTGR. (R2, R3)

Goal 1 & 2 Design Selections		Are Goal 1 & 2 Design Selections Adequate to Meet Goal 3 Requirements
G1-1	Table of allowable primary circuit activities during normal operation (Ci)	No
G1-2	Primary coolant system leak rate	Yes(?)
G2-1	Allowable incremental plateout from core conduction cooldown events	No

ASSUMPTIONS/COMMENTS (A/C)

1. Requirement 1 is restatement of the allowable Curies released from the plant for compliance with 10CFR100 and the PAG dose limits. (A/TS 7)

2. Safety risk for MHTGR is dominated by three classes of events: rapid depressurization, depressurized core conduction cooldown, and steam ingress plus pressure relief. (A/TS 4 through 8)

3. Plant release limits will be met by controlling the dominant sources of radionuclide release:

   a. Rapid depressurization (A/TS 1, 4, 6, 7, 8, 9)

      1) 100% of circulating activity and $\leq$5% of plateout activity will be released from primary circuit; no incremental core release. (A/TS 5)

      2) Design ($\geq$95% confidence) limits on circulating and plateout activity will be set accordingly. (A/TS 1)

      3) NRC will set comparable technical specifications. (A/TS 1)

      4) Building wake effects, etc. will attenuate offsite released by [1.5x] during blowdown. (A/TS 6)

[190-10]

FUNCTIONAL ANALYSIS WORKSHEET

FUNCTION NO. 3.1.1.2 (continued)

5) Radiological consequences of rapid depressurization dominated by release of I131 and Sr90; release of Cs and Ag inconsequential by comparison. (A/TS 6)

b. Core Conduction Cooldown (A/TS 2 through 7, 9)

1) Incremental release from core will be dominant source term.

2) Core releases of condensibles will be attenuated by $\geq$[30X] by primary circuit removal mechanisms.

3) Reactor building will attenuate release of condensible radionuclides, including iodines, to environment by [10X].

4) This is a design basis event so dose limits shall be met with $\geq$95% confidence.

5) For regulatory purposes, release characteristics are known well enough to calculate whether the releases would exceed 10CFR100 limits of fractions therefof at 95% confidence (for design basis or beyond design basis events).

c. Steam Ingress Plus Pressure Relief (A/TS 7, 9)

1) 100% of circulating activity will be released from primary circuit.

2) Incremental core release will result from incremental fuel hydrolysis.

3) $\leq$[50%] of the plateout activity will be removed from fixed surfaces by steam induced vaporization and washoff.

4) Condensible nuclides, including iodines, which are released from the core due to incremental fuel hydrolysis and graphite oxidation will be attenuated by $\geq$[100X] due to retention in dump tank water prior to environmental release.

a. Relief valve will reseal after 15% of gaseous volume is released; consequently, radionuclides in coolant as a result of washoff and incremental core releases, including iodines, will be attenuated by [7X].

[190-11]

FUNCTIONAL ANALYSIS WORKSHEET

FUNCTION NO. 3.1.1.2 (continued)

b. Reactor building will attenuate release of condensible radionuclides, including iodines, to environment by [10X].

5) This will be a design basis event, so dose limits shall be met with ≥95% confidence.

DESIGN SELECTIONS (DS)

A/TS 5, 7, 9 1. Provide above specified low probability of significant release by limiting core releases during accidents and by attenuating release with reactor vessel, reactor building, and site.

A/TS 5-9 2. Limit radionuclide release from core during normal operation such such that a ≤5% liftoff of I131 and Sr90 can be accommodated; retain limits on Cs and Ag release derived from Goals 1 and 2 considerations. Resulting limits on circulating and plateout activity during normal operation are (Ci):

	Circulating		Plateout	
Nuclide	P ≥ 50%	P ≥ 95%	P ≥ 50%	≥ 95%
H3	[0.2]	[0.7]	-	-
Kr88	[5.5]	[22]	-	-
Xe133	[2.5]	[10]	-	-
I131	[0.02]	[0.08]	[20]	[80]
Sr90	-	-	[0.32]	[3.2]
Ag110m	-	-	[7.3]	[73]
Cs137	-	-	[70]	[700]
Cs134	-	-	[13]	[132]

A/TS 5-9 3. Limit radionuclide release from core during conduction cooldown events (Ci)

	PAG (User) Limits	10CFR100 (Reg) Limits
Nuclide	P ≥ 95%	P ≥ [95%]
Kr88	≤TBD	≤TBD
Xe133	≤[2300]	≤[46,000]
I131	≤[13,050]	≤[3.9×10^5]
Sr90	≤[540]	≤[16,200]
Ag110m	≤TBD	≤TBD
Cs137	≤TBD	≤TBD

[190-12]

FUNCTIONAL ANALYSIS WORKSHEET

FUNCTION NO. 3.1.1.2 (continued)

A/TS 7 4. Limit incremental radionuclide release core* during short-term design basis events, such as steam ingress with direct release (Ci):

		PAG (User) Limits		10CFR100 (Reg) Limits	
	Nuclide	P ≥ 50%	P ≥ 95%	P ≥ 50%	P ≥ 95%
*	Kr88	≤TBD	≤[1168]	≤TBD	≤[23,780]
*	I131	≤TBD	≤[233]	≤TBD	≤[8150]

* *Allowable environmental release minus normal circulating activity and
* [50%] of normal plateout activity; attenuation factor 35 for condensibles.

P.O. BOX 85608 SAN DIEGO, CA 92186-5608 (858) 455-3000